An assessment of the utility of nerve- and vessel-related cranial characters for reconstructing primate phylogeny

Daniele Serdoz

University College London
2006

Submitted in partial fulfilment of the requirements of the Degree of Doctor of Philosophy

ProQuest LLC
789 East Eisenhower Parkway
P.O. Box 1346
Ann Arbor, MI 48106-1346

Abstract

Recent analyses have suggested that standard craniodental characters may be misleading regarding primate phylogenetic relationships. This has important implications for the study of human evolution because such characters dominate the datasets used to reconstruct the phylogenetic history of fossil primates. This project was designed to identify characters that will allow fossil primate relationships to be reconstructed more confidently. It is based on the finding that hominoid soft-tissue characters yield a phylogeny consistent with the strongly supported molecular phylogeny for these primates. If soft-tissue characters are phylogenetically informative then osteological characters associated with soft tissue may also be phylogenetically informative.

Information regarding the size, number, shape and position of cranial foramina and canals was collected on a sample of 30 *Gorilla gorilla*, 20 *Pan paniscus*, 30 *Pan troglodytes*, 48 *Homo sapiens*, 31 *Pongo pygmaeus*, 59 *Hylobates* plus three outgroups (*Cercopithecus, Colobus* and *Papio*). This information was coded into 112 characters using four different coding methods (Divergence coding, Segment coding, Baum's coding and Binary coding) and then subjected to parsimony and bootstrap analyses. The resulting phylogenies were compared to the well supported and widely accepted hominoid molecular phylogeny. Agreement between the morphology-based phylogenies and the consensus molecular tree would support the hypothesis that cranial characters related to nerves and vessels produce reliable phylogenies for the hominoids.

Seven of the 16 parsimony tests produced cladograms compatible with the consensus molecular phylogeny. In contrast, the bootstrap tests produced clades consistent with the molecular cladogram in all but one case. Thus, the parsimony tests only moderately supported the hypothesis while bootstrap tests strongly supported the hypothesis. Furthermore, the dataset composed of characters related to nerves and vessels performed significantly better than a dataset composed of standard craniometric variables in recovering the molecular relationships of the hominoids. Overall, these results suggest that primate foramina and canals may be a better focus for phylogenetic studies than standard craniodental characters.

It also emerged that the results of the parsimony analyses varied depending on the coding procedure adopted and on the composition of the outgroup. Divergence coding stood out as the most rigorous method and outperformed all other methods. In terms of outgroup choice, this study supports Colless (1985) suggestion that a number of taxa, or groups of taxa, should be used as outgroups in a phylogenetic analysis and then a consensus of the results should be drawn. Interestingly, bootstrap analyses seemed to be less affected by these factors and produced consensus cladograms that were consistent with each other and with the molecular tree.

Lastly, the effects of sexual dimorphism and non-phylogenetic character correlations were also investigated. The results indicated that both factors may have an effect on the outcome of phylogenetic analyses. These findings are discussed in the context of phylogenetic studies of fossil hominin material.

Acknowledgments

I would like to express my gratitude to my supervisors, Dr Mark Collard (University of British Columbia) and Dr Leslie Aiello (Wenner-Gren Foundation). Mark has been a constant source of motivation over the years through his work and enthusiasm. Despite the long distance, he has been present throughout the development of this project and he has provided invaluable insights on all aspects of this study. Leslie always made sure I kept focused and provided guidance and feedback on every chapter of this thesis. It was Leslie's course in palaeoanthropology that, six years ago, introduced me to this subject and inspired me to pursue a postgraduate program in anthropology. I feel very lucky to have worked with such inspiring teachers.

I am also grateful to all the museum curators that granted me access to the museum collections, and all the museum staff that patiently helped me organising my fieldwork: Paula Jenkins and Daphne Hill (NHM, London), Maggie Bellati (Duckworth Laboratory, Cambridge), Olavi Gröenwell (Swedish Natural History Museum, Stockholm), Olav Röhrer-Ertl (State Collection for Anthropology and Palaeoanatomy, Munich), Karin Isler (Anthropological Institute and Museum, University of Zurich-Irchel, Zurich), Wim Van Neer and Wim Vandelen (Royal Museum of Central Africa, Tervuren).

Many more people have provided support in many different ways. I would like to thank the following: Charlie Lockwood for many discussions about human evolution and phylogeny; Marc Jones for stimulating discussions about evolution since our undergraduate years, when we were flatmates; everyone at the London Evolutionary

Research Network (L.E.R.N.) for their enthusiasm; the Department of Anthropology at UCL, particularly Sophie Woodword, for the glamour, Sadie King, Sarah Gibbon, Patrick Laviolette and Isabelle DeGroote for being in the same boat; Chris Hagisavva, the IT wizard; the UCL Graduate School for their help and support; Mahir and the Starbucks posse (Clink Street branch) for all the free Tchai-tea lattes and chocolate cheesecakes while I was trying to make sense of this writing; my flatmates, Kat and Ste, and my best friends, Linda, David, Alex and Daniela, for their love and understanding. A very special thanks to Dr Fire 'Monster' Kovarovic, my partner in crime, for her loyal friendship, fun times ('You look like a princess!') and for sharing the good and bad times of the past four years.

Many artists, writers and directors have made my postgraduate life less painful through their work, especially during my fieldwork, when I was surrounded by hundreds of silent skulls! Among others: Alanis Morissette, Madonna, Red Hot Chilli Peppers, Janet Jackson, David Bowie, Britney Spears, J.K. Rowling, the creators of CSI, Sex and the City, and Will and Grace.

And last but not least, I am VERY grateful to my family for their continuing support, emotional and financial, at times when I questioned my own choices.

This work was funded by the UCL Graduate School Research Scholarship (3 years) and the Ruggles-Gates Fund for Biological Anthropology (Royal Anthropological Institute).

Table of Contents

Table of Figures

Table of Tables

Chapter 1. INTRODUCTION

1.1 The importance of estimating hominin phylogeny

In November 2004 a new hominin species from the island of Flores, Indonesia, was announced in *Nature* (Brown et al., 2004). This announcement sent both the scientific community and the mass media into a frenzy. The species, *Homo floresiensis*, lived on the island of Flores until at least 18,000 years ago (Morwood et al., 2004), raising the possibility that modern *Homo sapiens* coexisted with another human species until very recent times. Only two years earlier, another new hominin taxon, *Sahelanthropus tchadensis* (Brunet et al., 2002), was announced in *Nature* and caused excitement within the scientific community. This species was dated between 6 and 7 million years – a time that molecular evidence indicates as near the split between the chimpanzee and human lineages – becoming the oldest hominin species known. It was recovered from Chad, in central Africa, a largely unexplored region that is well removed from the areas that have traditionally yielded human fossils.

These are just two of a long series of fossil finds that have been added to the hominin hypodygm in the last few years. The announcements of new hominin fossils are generally followed by the definition of new species and the revision of the taxonomic status of older ones (Cela-Conde and Altaba, 2002). Currently, there is no consensus among palaeoanthropologists regarding the number of hominin species present in the fossil record (Curnoe, 2003). This number varies from around five to 23 (e.g. Table 1-1), with a median number of taxa in use of 14 (Curnoe and Thorne, 2003).

Table 1-1. Taxonomy of the tribe Hominini.

Genus	Species	Reference
Sahelanthropus	*S. tchadensis*	Brunet et al., 2002
Orrorin	*O. tugenensis*	Senut et al., 2001
Ardipithecus	*Ar. ramidus ramidus*	White et al., 1994
	Ar. ramidus kadabba	Haile-Selassie, 2001
Preanthropus	*Pr. afarensis*	Johanson et al., 1978
Australopithecus	*A. africanus*	Dart, 1925
	A. anamensis	Leakey et al., 1995
	A. bahrelghazali	Brunet et al.,1996
	A. rudolfensis	Alexeev, 1986, Wood and Collard, 1999
	A. habilis	Leakey et al., 1964, Wood and Collard, 1999
	A. garhi	Asfaw et al.,1999
Paranthropus	*P. aethiopicus*	Arambourg and Coppens, 1968
	P. robustus	Broom, 1938
	P. boisei	Leakey, 1959
Kenyanthropus	*K. platyops*	Leakey et al., 2001
Homo	*H. erectus*	Dubois, 1892, Mayr, 1944
	H. ergaster	Groves and Mazak, 1975
	H. floresiensis	Brown et al., 2004
	H. heidelbergensis	Schoetensack, 1908
	H. antecessor	Bermudez de Castro et al., 1997
	H. neanderthalensis	King, 1864
	H. sapiens	Linnaeus, 1758

The species and genera listed in this table are some of the groups commonly encountered in the fossil hominin literature.

For example, in their 2004 book "Bones, Stones and Molecules", Colin Groves and David Cameron adopted two very different taxonomic schemes for the Tribe Hominini. Groves included three genera in this taxon: *Pan*, *Orrorin* and *Homo*. The genus *Pan* (chimpanzee) comprised the two extant species *P. paniscus* (pygmy chimp) and *P. troglodytes* (common chimp). *Orrorin* comprised only one fossil species, *O. tugenensis*. The genus *Homo* comprised one extant species, *H. sapiens* (modern humans), and 20 fossil species. Cameron, instead, included seven genera within the hominin tribe: *Orrorin* (one fossil species), *Sahelanthropus* (one fossil species), the Garhi deme, *Australopithecus* (one fossil species), *Paranthropus* (three

fossil species), *Kenyanthropus* (two fossil species) and *Homo* (one extant and seven fossil species). In contrast, Curnoe and Thorne (2003) stated that, based on molecular evidence, chimps and humans should be congeneric (genus *Homo*, see also Page and Goodman, 2001), the number of fossil species in the human line should not exceed the number of five and they should all belong to the genus *Homo*.

Taxonomic dilemmas aside, the abundance of new fossil species in the human family has revealed that at any one time numerous hominin groups coexisted in Africa. On one hand this is revolutionising the way we look at patterns of human evolution (Lieberman, 2001; Wood, 2002; Mirazon Lahr and Foley, 2004). On the other hand, the addition of so many new species to the hominin tribe is reviving interest in the question of how these human ancestors were related to each other (Aiello and Collard, 2001; Gee, 2001; Wood, 2002). There are several reasons for this.

First, a robust phylogeny is the prerequisite for the formulation of hypotheses of ancestor/descendant relationships (Tattersall and Eldredge, 1977). Secondly, hypotheses that link environmental parameters (e.g. climatic and vegetational changes) to events in human evolution (e.g. the evolution of bipedalism and brain size) also rely on clear phylogenetic relations (Collard and Wood, 2000). Thirdly, information about species relationships can be useful in palaeobiogeographical studies. For example, Strait and Wood (1999) have recently used early hominin phylogenetic hypotheses to infer patterns of migration between south Africa, east Africa and the Malawi Rift. They found that the phylogenies were consistent with between four and seven hominin dispersal events, more than has been hypothesised before. Robust phylogenies are crucial for this type of inference.

In addition, comparative methods for studying primate adaptations – such as Independent Contrasts (Pagel, 1992) and Phylogenetic Autocorrelation (Gittleman and Kot, 1990) – also incorporate information about phylogeny. Comparative analyses assume that the data points used are independent. However, this is seldom the case because species possess similarities due to common ancestry in addition to similarities that evolved independently (Felsenstein, 1985; Harvey and Pagel, 1991; Purvis, 1995). Including information about phylogeny facilitates the identification of independent data points and helps minimize the effects of unquantifiable confounding variables (Harvey and Pagel, 1991; Nunn and Barton, 2001). For example, in studying the relationships between primate mating systems, body size and size dimorphism, Lindenfors and Tullberg (1998) had to take into account the fact that closely related species will tend to share similar mating systems, body size and pattern of dimorphism due to common ancestry. By incorporating a phylogeny developed by Purvis (1995) into their analysis they were able to correct for this confounding effect and to highlight the importance of sexual selection in the evolution of body size dimorphism. Computer simulations have also shown that comparative methods to study primate adaptations are sensitive to the accuracy and resolution of the phylogeny incorporated in the analyses (Purvis et al., 1994).

It follows that without a reliable phylogeny there is very little we can say about primate – and hominin – evolution. Unfortunately, there are a number of problems associated with the study of hominin phylogenetics (Curnoe, 2003; Hawks, 2004). First, as mentioned at the beginning of this chapter, the taxonomy of the hominin family is controversial. This is problematic because a clear taxonomy is one of the

fundamental assumptions of phylogenetic reconstruction (Lieberman et al., 1996; Curnoe, 2003). Secondly, the small number of fossil specimens available for the hominin hypodygm severely constrains sample sizes and therefore our knowledge of within-species variation (Trinkaus, 1990; Hawks, 2004). Thirdly, the fragmentary nature of the fossil material and the large proportion of missing data in the datasets used in phylogenetic studies seriously impair the quality of fossil hominin phylogenetic analyses. A fourth problem is the close relationship of the fossil taxa. If two species are very closely related it is unlikely that a character will be expressed largely as one state in one species and as another state in another species. Instead, each taxon will very likely be characterised by both states and these will only be expressed at different frequencies (Hawks, 2004). Other problems include methodological issues such as the poor or ambiguous definition of the character states used in phylogenetic reconstructions (Wiens, 2001), and non-phylogenetic correlations among characters (McCollum 1999; Lovejoy et al., 2001; Strait, 2001). These issues will be discussed in more details in the next chapters.

Lastly, the uncertainties over the factors that drive character evolution also introduce an error in phylogeny estimates. Many recent studies (e.g. Corruccini, 1994; Lieberman, 1999; Collard and Wood, 2000) have shown that current hypotheses of relationships for the hominins may not be accurate because the craniodental characters commonly used to infer primate phylogenetic relationships may not be reliable for this purpose. These studies generally attribute the inadequacy of primate craniodental morphology for phylogenetic inference to the widespread presence of homoplasy in the craniodental datasets (Hartman, 1989; Wood, 1991; Harrison, 1993; Collard and Wood, 2000; Viguier, 2002). Homoplasies are similarities that are not

due to common ancestry but that are shared by taxa because of other evolutionary processes, such as parallelism, convergence and reversal (Lockwood and Fleagle, 1999; Collard et al., in press); or because of the plastic nature of bone, the morphology of which is determined not only by a genetic code, but also by various environmental factors that act during ontogeny (Lieberman, 1996, 1997, 1999). Homoplasies are misleading about phylogeny because only heritable characters that appear in a common ancestor and that are acquired by all of its descendant species (i.e. homologies) are considered to be informative about phylogenetic relationships.

The implications of these findings are potentially profound: if the craniodental characters commonly used in hominin systematics are not reliable for phylogenetic inference then little confidence can be placed in current estimates of hominin relationships (Collard and Wood, 2000). It follows that new sets of characters of the primate skeleton need to be identified in order to be able to recover accurate and strongly supported phylogenetic hypotheses for fossil primates. The aim of the project reported here was to identify such characters and test their utility in the reconstruction of primate relationships.

One way of testing the phyletic utility of a set of morphological characters is to choose a group of extant taxa whose relationships are well-known from molecular studies. Apes and humans (superfamily Hominoidea) are an excellent group for this purpose because their relationships are known from a large number of molecular analyses (Ruvolo, 1997). The morphological dataset can then be used to generate phylogenetic hypotheses for the extant study-group using cladistic techniques. If the cladograms generated from the morphological characters are congruent with the

hominoid consensus molecular phylogeny, it can be concluded that the characters are reliable for phylogenetic inference. Conversely, if the cladograms are not congruent with the molecular phylogeny, it can be concluded that the characters are not reliable for estimating hominoid relationships. Several applications of this 'congruence' method are found in the palaeoanthopological literature (e.g. Hartman, 1989; Collard and Wood, 2000; Gibbs et al., 2000, 2002; Strait and Grine, 2004; Lycett and Collard, 2005; Nadal-Roberts and Collard, 2005) and these will be discussed extensively in the next chapter.

Here, the same principle is applied to a group of osseous characters related to soft-tissue structures (i.e. nerves and vessels). The reason behind the choice of this set of characters is the finding that soft tissue characters yield a strongly-supported and accurate phylogenetic tree for the extant hominoids (Gibbs et al., 2000, 2002). I reasoned that if soft-tissue traits carry a reliable phylogenetic signal, then it is plausible to think that osseous characters related to soft-tissue traits may also carry a clear phylogenetic signal. This project sets out to test this hypothesis by applying cladistic methods to a dataset that comprises characters of the skull associated with nerves and vessels in order to generate phylogenetic hypotheses for extant hominoid primates. These cladograms are then compared to the hominoid consensus molecular cladogram, which is strongly supported and therefore assumed to be correct. The rationale of this study is that congruence between the morphological trees and the molecular tree will indicate that nerve- and vessel-related characters are phylogenetically informative. Alternatively, disagreement between the two will suggest that cranial morphology alone is unable to recover the molecular relationships

of apes and humans. Either outcome will have very important implications for the study of primate, and in particular hominin, evolutionary history.

1.2 Structure of the thesis

This thesis is divided into eight chapters. The next chapter, Chapter 2, reviews the evidence in support of the hypothesis that standard craniodental characters are not reliable for recovering the phylogenetic relationships of the fossil hominins. It revisits the findings of recent phylogenetic analyses based on hominin craniodental material and highlights some of the problems associated with the use of this type of evidence in the reconstruction of primate evolutionary relationships. The results of two cladistic analyses based on hominoid soft-tissue data are also reported (Gibbs et al., 2000, 2002). The latter produced phylogenetic trees for the hominoids that were reliable and very strongly supported. The formulation of the main hypothesis of this project, namely that characters associated with nerves and vessels produce reliable phylogenies for the hominoids, was based on these findings. The biological and phylogenetic significance of soft tissue-related osseous characters is then discussed in the last part of Chapter 2.

One of the assumptions of this investigation is that the phylogenetic relationships of extant apes and humans are well known from molecular studies. Accordingly, Chapter 3 reviews the evidence in support of each branch of the hominoid consensus molecular cladogram. As explained in the previous section, the molecular phylogeny for the extant hominoids is strongly supported. For this reason, cladograms generated

for this group of primates from the morphological characters can be compared to the consensus molecular tree in order to make an assessment of the utility of osseous characters for phylogenetic inference.

The samples, characters and analytical methods used in the study are discussed in Chapter 4. Here, I describe in more detail the morphological characters used to generate phylogenetic hypotheses for the hominoids, with particular emphasis on how they were scored. I also carry out a character analysis to identify differences in the expression between the sexes and correlations among the characters. In the second part of the chapter, I introduce some basic concepts of cladistic analysis, including the use of outgroups to root the trees, the coding procedures adopted, parsimony and bootstrap analyses. The hypotheses tested in this project and the methodologies employed for this purpose are outlined at the end of Chapter 4.

The results of the tests are reported in the subsequent three chapters. Each chapter deals with one specific hypothesis and highlights the main findings of the tests. Chapters 5 and 6 report the results of the cladistic analyses carried out to test the main hypothesis of this project, working at the generic level first, and then at the specific level. Chapter 7 investigates the impact of sexual dimorphism on phylogenetic analysis.

In the final chapter of the thesis (Chapter 8) the findings of this study are summarised and discussed within the context of phylogenetic studies of fossil hominins, sexual dimorphism and methodological choices in cladistic analyses.

Chapter 2. BACKGROUND

2.1 Craniodental morphology and hominin phylogeny

Human and non-human primate palaeontologists usually rely on cranial, mandibular and dental traits to recognise extinct species, and to infer their evolutionary relationships (e.g. Rosenberger et al., 1985; Wood and Chamberlain, 1987; Skelton and McHenry, 1992; Wood, 1992a, 1992b; Benefit and McCrossin, 1997; Bermudez de Castro et al., 1997; Strait et al., 1997; Asfaw et al., 1999; Kohler and Moya-Sola, 1999; Curnoe, 2001; Haile-Selassie, 2001; Strait and Grine, 2004; Cameron and Groves, 2004). The primary reason for this is that craniodental remains make up the largest part of the primate fossil record, and for some hominin taxa it is the only type of evidence available. Particular emphasis has been given to dental traits because dental enamel is more durable than bone and therefore more commonly preserved in the fossil record (Wood, 2000).

This chapter will begin with a discussion of current phylogenetic hypotheses for the hominins derived from commonly-used craniodental characters. I will then examine the reliability of craniodental traits for recovering primate phylogenies and discuss reasons why they might not be as reliable as is usually assumed. Lastly, I will consider alternative sources of phyletic information that may be a better focus for phylogenetic studies than standard craniodental characters.

2.1.1 Hominin phylogenetic relationships

The term hominin herein describes humans and all the fossil taxa more closely related to humans than to the other hominoids. Despite the many studies that have been carried out in recent years, no agreement has yet been reached on the phylogenetic relationships of the members of the hominin tribe and the question of how hominins are related remains mostly unanswered (Wood and Collard, 1999; Cameron and Groves, 2004). Hominin craniodental cladistic analyses have yielded contrasting and weakly supported phylogenies (Skelton et al., 1986; Chamberlain and Wood, 1987; Wood and Chamberlain, 1987; Stringer, 1987a, 1987b; Skelton and McHenry, 1992; Wood, 1991, 1992a; Lieberman et al., 1996; Strait et al., 1997; Curnoe, 2001; Haile-Selassie, 2001; Strait and Grine, 1998, 1999, 2004; Cameron and Groves, 2004). The results of these analyses typically fall into one or more of the following categories: 1) craniodental datasets produce equally parsimonious solutions that support contrasting hypotheses of relationships (e.g. Strait et al., 1997); 2) the minimum length trees recovered in the parsimony analyses are only slightly shorter than less parsimonious ones and their topologies support very different phylogenetic hypotheses (e.g. Lieberman et al., 1996); and 3) analyses based on different character sets (or subsets) produce major taxonomic rearrangements (e.g. Lieberman et al., 1996). In this section I report on the results of a number of phylogenetic studies that have been carried out in recent years, presented in a chronological order. I have limited my account to the last 20 years because it was during this time period that most of the phylogenetic hypotheses crucial to the understanding of the problems highlighted in this study were formulated. Furthermore, it was only in recent years that a more rigorous and computer-assisted approach to cladistic analysis was adopted.

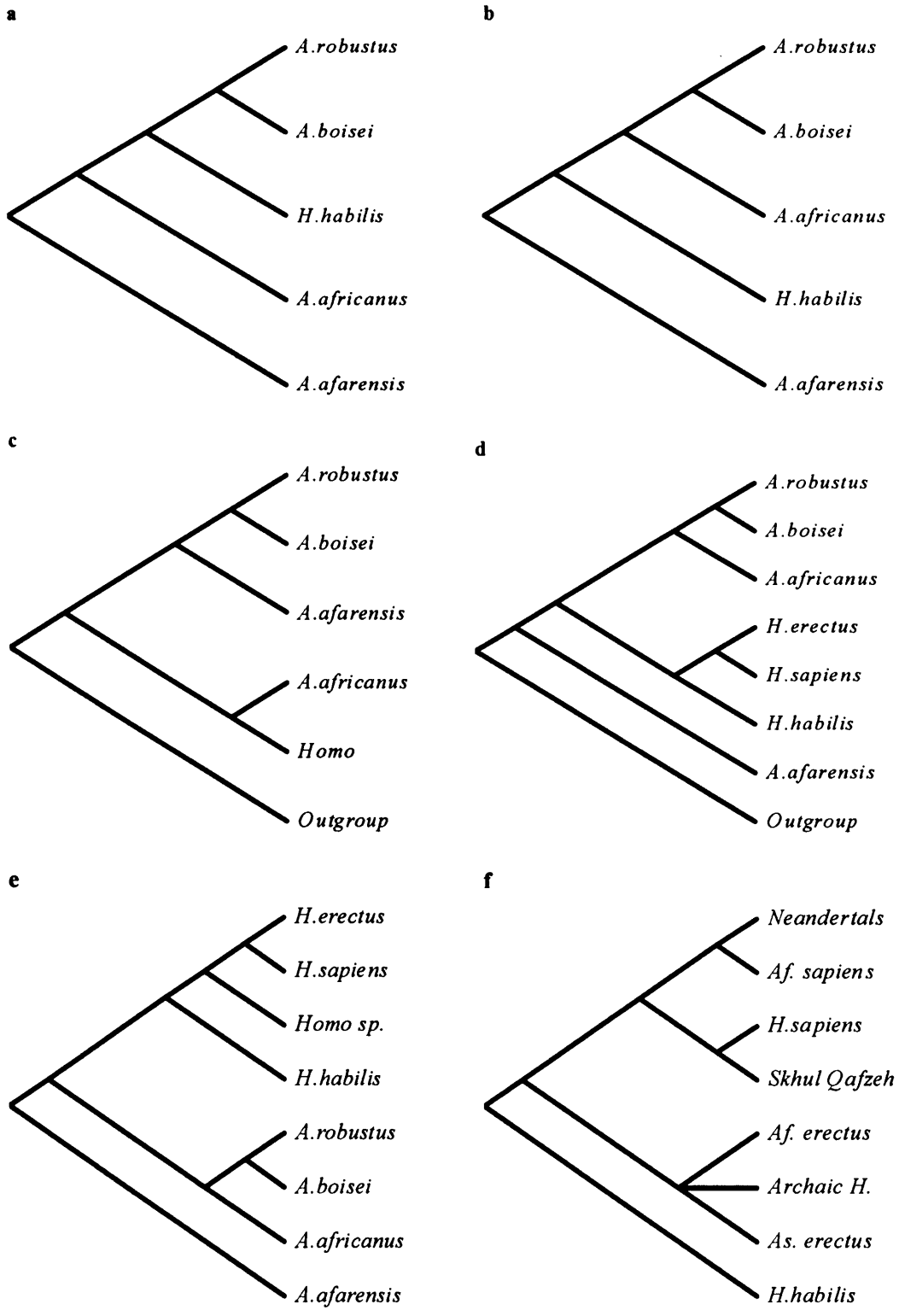

Figure 2-1. Results of recent hominin phylogenetic analyses.
Most parsimonious cladograms generated by recent cladistic analyses of hominin craniodental materials. (a,b) Skelton et al., 1986; (c) Wood and Chamberlain, 1987; (d) Chamberlain and Wood, 1987; (e) Stringer, 1987a; (f) Stringer, 1987b; (g) Skelton and McHenry, 1992; (h) Lieberman et al., 1996; (i) Collard and Wood, 1999; (j) Strait and Grine, 2004; (k) Cameron and Groves, 2004.

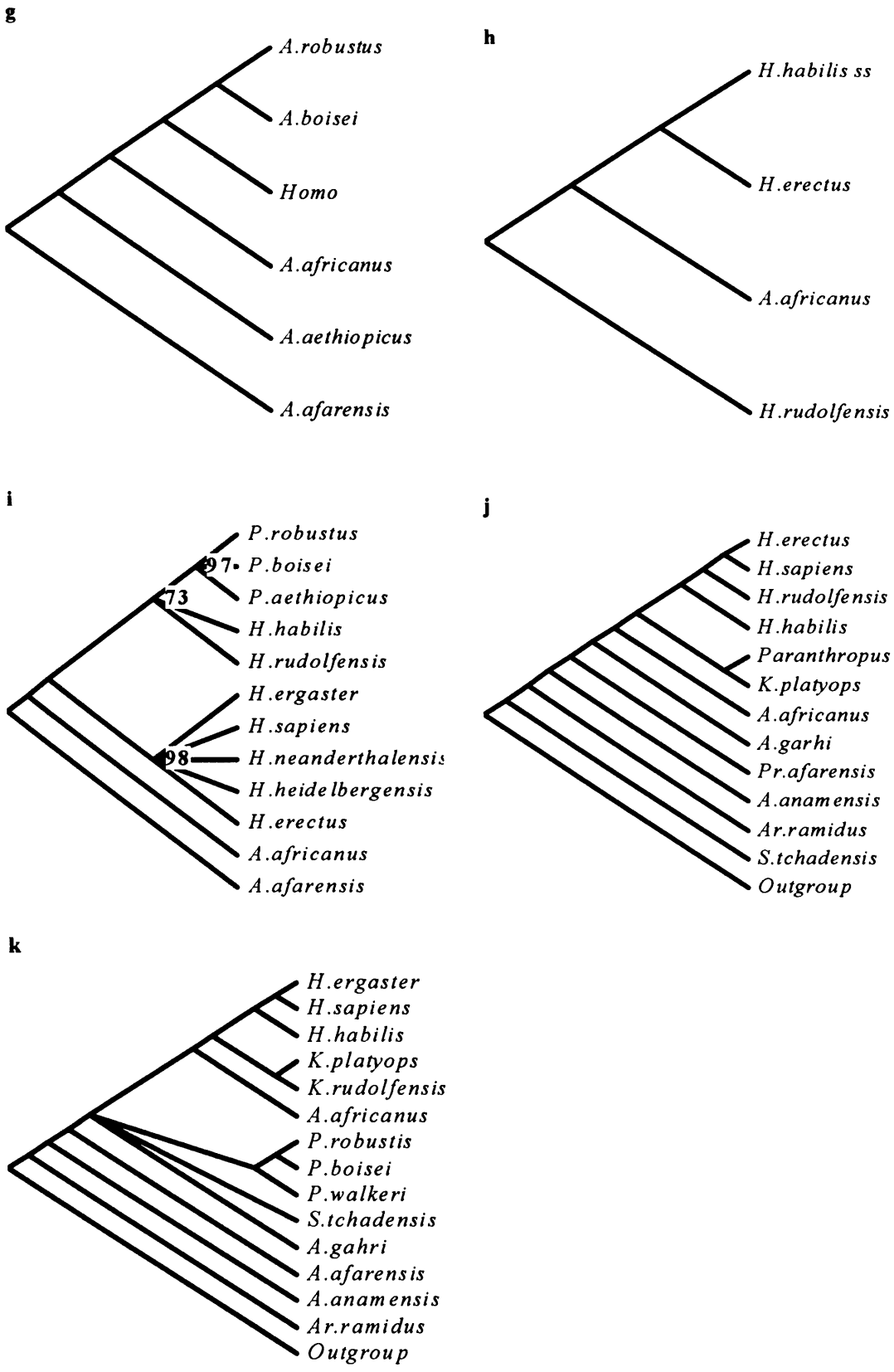

Figure 2-1, continued. Results of recent hominin phylogenetic analyses.

In 1986 Skelton et al. published an extensive phylogenetic study of four early hominin taxa – *A. afarensis*, *A. africanus*, *H. habilis* and the 'robust' australopithecines – based on 69 characters, grouped into 12 character complexes. Their analysis returned two solutions that differed only slightly in the level of internal consistency of the characters. However, these trees supported very different phylogenetic hypotheses. The first solution (Figure 2-1a) was consistent with 65% of the characters examined and placed *A. afarensis* at the base of the tree whilst *A. africanus* was the sister-group of a clade that comprised *H. habilis* and the 'robust' australopithecines. The second solution (Figure 2-1b) was consistent with 64% of the characters and placed *H. habilis* next to a clade formed by *A. africanus* and the 'robust' australopithecines. This small difference in the level of support for the two topologies did not allow the authors to confidently choose one solution over the other. Although *A. afarensis* was placed consistently at the base of this clade, the relationships among *A. africanus*, *H. habilis* and the 'robust' australopithecines remained ambiguous.

The following year Wood and Chamberlain (1987) carried out a parsimony analysis using a dataset of 39 craniodental traits recorded on a number of hominin taxa – *A. africanus*, *A. afarensis*, *A. robustus*, *A. boisei* and *Homo* – and extant outgroups. They found a single most parsimonious tree (Figure 2-1c) in which *Homo* was the sister clade of *A. africanus*, and, in a separate clade, *A. afarensis* was the sister group of the 'robust' australopithecines (*A. robustus* and *A. boisei*). This tree was only three steps more parsimonious than the next-best solution, in which *A. africanus* was the sister taxon of the *A. afarensis*/'robust' australopithecine clade to the exclusion of *Homo*. Wood and Chamberlain also reanalysed Skelton et al.'s (1986) dataset using the phylogenetic software PAUP (Swofford, 1998) and found that in fact the most

parsimonious solution based on this dataset placed *A. afarensis* at the base of the tree and *H. habilis* next to a clade formed by *A. africanus* and the paranthropines (Figure 2-1b). Clearly, Wood and Chamberlain's and Skelton et al.'s datasets produced cladograms that supported very different phylogenetic hypotheses for these groups of hominins. Wood and Chamberlain (1987) went on to emphasise how the results of these parsimony analyses were affected by the initial choice of the characters.

In the same year, Chamberlain and Wood (1987) recovered a single most parsimonious tree from a set of 90 hominin craniometric variables recorded on seven hominin species and a sample of extant primates that were used as an outgroup. The shortest tree (Figure 2-1d) supported a phylogenetic hypothesis in which the genus *Homo* was monophyletic and, within this group, *H. habilis* (*sensu lato*) was the sister-taxon of a clade formed by *H. sapiens* and *H. erectus*. A separate clade contained the 'robust' australopithecines and *A. africanus*. In this clade the 'robust' australopithecine species, *A. robustus* and *A. boisei*, shared an ancestor not shared with *A. africanus*. *A. afarensis* was placed as the sister-group of all other hominins. Again, this solution was only slightly more parsimonious than other cladograms that differed in the position of *A. africanus* and of the 'robust' australopithecines. The relationships among the later *Homo* species, and the monophyletic relationship of the 'robust' australopithecines were consistent in all the solutions. Interestingly, the analysis was sensitive to the taxonomic classification of the specimens assigned to early *Homo*. When Chamberlain and Wood adopted different classifications of these specimens, major topological rearrangements were produced within the cladograms, resulting in both the genus *Homo* and the genus *Australopithecus* to be paraphyletic.

This underscores the fact that a clear taxonomy for the hominin is central in phylogenetic reconstruction.

Stringer (1987a) examined the relationships of eight hominin taxa – *A. afarensis*, *A. africanus*, *A. boisei*, *A. robustus*, *H. erectus*, *H. habilis*, *H. sapiens* and *Homo sp.* His most parsimonious tree (Figure 2-1e) suggested that *A. afarensis* is the sister group of all other hominins; that *A. africanus* forms a clade with *A. robustus* and *A. boisei*; and that all the *Homo* taxa form a monophyletic group. Within the latter, *H. erectus* and *H. sapiens* shared a common ancestor not shared with early *Homo* species, of which *H. habilis* was the most ancestral taxon. These relationships were consistent with those recovered by Chamberlain and Wood (1987).

In another study Stringer (1987b) focused on the species-level relationships within the genus *Homo*. This analysis concentrated on 11 characters scored on nine taxonomic groups belonging to the genus *Homo*. It returned three most parsimonious trees. The strict consensus of these three solutions (Figure 2-1f) placed *H. habilis* at the base of the cladogram. The first clade to branch off was a trichotomy that comprised early African *H. erectus*, Asian *H. erectus* and, unexpectedly, early archaic *H. sapiens*. The second clade to branch off contained *H. sapiens*, the Skhul-Qafzeh sample, Neanderthals and late African archaic *H. sapiens*. In this clade, modern humans and the Skhul-Qafzeh sample formed a single clade next to Neanderthals and the late African archaic *H. sapiens*.

The relationships among two robust autralopithecine taxa, *A. robustus* and *A. boisei*, were investigated by Wood (1988). He employed three datasets from previous

phylogenetic studies to generate minimum-length trees using PAUP. The first dataset included 40 cranial characters recorded on the two robust species, plus *A. afarensis*, *A. africanus* and KNM-WT17000. The second dataset included 39 characters recorded on *A. afarensis*, *A. africanus*, the two robust australopithecine species and *Homo*. The last dataset included 90 cranial characters from the same five hominin taxa. All datasets generated most parsimonious solutions that supported monophyly of *A. robustus* and *A. boisei*. However, the most parsimonious trees recovered from the first and the third datasets were only slightly shorter than the less parsimonious solutions that supported a paraphyletic relationship for the robust australopithecines. Also, when the robust australopithecines were paraphyletic, the values of the consistency indices associated with these topologies were comparable to the values associated with the most parsimonious trees, indicating a similar level of homoplasy in the datasets. Wood (1988) stated that although common ancestry for *A. robustus* and *A. boisei* was supported by his analysis, it was still possible for many of the characters in the datasets to have evolved independently in the two taxa.

In the early 1990's, Wood (1991) used 90 cranial variables to review the taxonomy and phylogenetic relationships of nine hominin taxa – *A. afarensis*, *A. africanus*, *A. robustus*, *A. boisei*, *H. rudolfensis*, *H. habilis*, *H.* aff. *H. erectus*, *H. erectus* and *H. sapiens*. The most parsimonious cladograms suggested that *A. afarensis* was the most primitive of the hominin species examined. It also suggested that the 'robust' australopithecines formed a monophyletic group but, similar to previous studies, the position of *A. africanus* could not be clearly resolved. Wood reached similar conclusions in a later study which reviewed a set of characters from the cranium (140), mandible (28) and dentition (173) for the same hominin species (Wood,

1992a). In this study, the author concluded that the similarities between the paranthropines and *H. rudolfensis* are likely to be the result of homoplasy and he emphasised how homoplasy is a widespread phenomenon in the hominin fossil record.

Also in 1992, Skelton and McHenry published an analysis based on a craniodental dataset consisting of 77 traits (Skelton and McHenry, 1992). Their preferred tree also placed *A. afarensis* at the base of the hominin clade (Figure 2-1g). The 'robust' australopithecine species *A. aethiopicus* was the next to branch off the cladogram followed by *A. africanus* and finally a clade that comprised *Homo* and the other two 'robust' australopithecine species, *A. robustus* and *A. boisei.* Within the latter, *A. robustus* and *A. boisei* shared an ancestor not shared with *Homo.* This study also found that subsets of characters representing different anatomical or functional regions produced significantly different phylogenies (also noted by Skelton et al., 1986; Wood and Chamberlain, 1986; Lieberman et al., 1996). The authors pointed out that a problem in phylogenetic reconstruction may be the bias of current datasets towards characters from one or few functional regions, in particular the masticatory apparatus, that are prone to a high level of homoplasy. According to Skelton and McHenry, these characters are over represented in the hominin data matrices, thus driving the cladistic analyses and producing erroneous trees (a view also supported by Skelton and McHenry, 1998). However, this idea has not been supported by other studies (Strait and Grine, 1998; Collard and Wood, 2001). For example Strait and Grine (1997) reported that the omission of 30 characters related to the masticatory apparatus from a dataset of 60 craniodental traits did not affect the topology of the most parsimonious cladograms generated for nine fossil hominin species using the

complete datataset. This result is inconsistent with the prediction of Skelton and McHenry's (1992) hypothesis: if the characters related to mastication were highly homoplasious and drove the cladistic analysis, the omission of these traits – which made up half of Strait and Grine's (1997) dataset – from the analysis would be expected to produce a topological rearrangement.

An important investigation of the reliability of previous hominin phylogenetic studies was carried out by Corruccini (1994). Five of the craniodental datasets discussed above (Skelton et al., 1986; Wood and Chamberlain, 1986; Chamberlain and Wood, 1987; Wood, 1992a; and Skelton and McHenry, 1992) were used to generate dendrograms by means of an alternative 'clado-phenetic' approach based on dissimilarity coefficients as a measure of phylogenetic affinity. Corruccini also employed bootstrapping techniques to assign a level of confidence to each of the clades recovered. The conclusion he reached from his analyses was that the five datasets were unable to confidently resolve the phylogenetic relationships among the hominins although a clear separation could be placed between the australopithecines and *Homo*.

Next, Lieberman et al. (1996) used 48 standard cranial, dental and mandibular traits in a cladistic study of early *Homo* species aimed at examining the evolutionary positions of *H. habilis sensu stricto* and *H. rudolfensis*. The topology of the most parsimonious cladogram (Figure 2-1h) placed *H. habilis sensu stricto* and early African *H. erectus* in a clade next to *A. africanus*. This group was then joined by *H. rudolfensis*. The next three solutions were only three steps less parsimonious and supported quite different phylogenetic hypotheses. Lieberman et al. also bootstrapped the dataset to assign a

level of statistical support to each clade. The analysis recovered one strongly supported clade formed by *H. habilis sensu stricto* and *H. erectus* (100%), but was unable to confidently resolve the relationships of the other hominins. The authors noted that grouping characters by functional regions or using random subsets of the characters produced major topological rearrangements in the cladograms and generated conflicting trees. For these reasons, they concluded that little confidence could be placed in the results obtained from their analyses.

One of the most cited papers on hominin phylogenetics was published in 1997 by Strait, Grine and Moniz. These authors analysed 60 hominin craniodental traits and generated cladograms for nine fossil taxa – *A. afarensis*, *A. africanus*, *A. aethiopicus*, *A. robustus*, *A. boisei*, *H. habilis*, *H. rudolfensis*, *H. ergaster* and *H. sapiens* – and two outgroup taxa – *Gorilla gorilla* and *Pan troglodytes*. Eight parsimony analyses were conducted on the dataset to assess how methodological choices (e.g. presence/absence of missing data, characters ordered/unordered, characters variable/non-variable) affect the outcome of phylogenetic studies. The results of these analyses again strongly supported a 'robust' australopithecine clade but remained ambiguous over the position of *A. africanus* and *H. habilis*. In particular, although most topologies indicated *A. africanus* as the sister group of a clade formed by *Homo* and *Paranthropus*, in one analysis an equally parsimonious tree placed *A. africanus* as the sister taxon of the robust species. *A. afarensis* was consistently placed at the base of the hominin clade. The relationships among the members of the genus *Homo* and of the genus *Paranthropus* could not be clearly resolved.

In 1999, Wood and Collard published an influential study of the taxonomic and phylogenetic significance of the genus *Homo*. Part of this paper investigated the reliability of six hominin cladistic analyses that used craniodental traits to infer phylogenetic relationships. Of the six studies, only three had produced most parsimonious cladograms in which all *Homo* species formed a monophyletic group (Wood, 1991, 1992b; Strait et al., 1997). To evaluate the support for the *Homo* clade in these three datasets, Wood and Collard carried out two analyses. The first analysis found that removing *H. rudolfensis*, *H. habilis* and *H. ergaster* from these phylogenies and placing them as sister-groups of the australopithecines had little effect on the goodness-of-fit statistics associated with the most parsimonious cladograms (length, consistency index and retention index). In the second analysis, Wood and Collard bootstrapped the character matrices used in these three studies. The majority-rule consensus cladogram for 12 hominin species featured three main clades (Figure 2-1i) at the 70% confidence limit (Hillis and Bull, 1993). The first clade (97% bootstrap value) comprised a trichotomy formed by the three species of 'robust' australopithecines. The second clade comprised five species belonging to the genus *Homo*. Although this branch found strong statistical support (98% bootstrap value) the relationships within the clade were not resolved. Finally, the third clade comprised the paranthropines plus two early *Homo* species. This branch found a relatively lower level of support (73%) and indicated that the relationships of early *Homo* species to each other and to all other hominin taxa are uncertain. Hence, Collard and Wood's results showed that on one hand very different topological arrangements can find similar level of character consistency, as shown by the goodness-of-fit statistics associated with the hominin cladograms; and on the other hand, as highlighted by the bootstrap test, there is little we can confidently say about the relationships among

hominin species, except that the 'robust' australopithecines and later *Homo* species form two monophyletic groups, and that *A. afarensis* is the sister taxon of a clade formed by later hominin species.

Curnoe (2001) later reached similar conclusions. He carried out six cladistic analyses using 47 characters scored for 10 hominin groups. The analyses varied in the number of traits included in the datasets and in the assumptions about character state evolution (i.e. ordered/unordered). The trees obtained differed markedly from each other, underlining the sensitivity of phylogenetic analyses to methodological choices such as dataset composition and the ordering of the character states. Curnoe (2001) concluded that the range of topologies recovered in his analyses indicated that the phylogenetic relationships of early hominins could not be considered resolved. In a follow-up paper, Curnoe argued that all published cladistic analyses of hominin relationships fail to meet "standard quality criteria" (Curnoe, 2003: 225) in terms of methodological choices, pointing out that for this reason none of the cladograms yielded by recent cladistic studies can be considered reliable.

More recently, Strait and Grine (2004) produced a phylogeny based on 198 craniodental characters recorded on a sample of 13 fossil – *Ar. ramidus*, *A. anamensis*, *A. africanus*, *A. garhi*, *Pr. afarensis*, *H. habilis*, *H. rudolfensis*, *H. ergaster*, *K. platyops*, *P. aethiopicus*, *P. robustus*, *P. boisei* and *S. tchadensis* – and 5 extant hominoid groups – *Homo*, *Pan*, *Gorilla*, *Pongo* and *Hylobates*. The resulting most parsimonious tree (Figure 2-1j) supported a basal position for *S. tchadensis* within the hominin clade. The first taxon to branch off from the hominin lineage was *Ar. ramidus* followed, in order, by *A. anamensis*, *A. afarensis* and *A. garhi*. *A.*

africanus was placed next to a clade formed by two main branches: the first comprised *K. platyops* and the paranthropines; the second contained species belonging to the genus *Homo*. Within the latter, *H. habilis* was the sister group of a clade formed by *H. rudolfensis* and a branch containing *H. erectus* and *H. sapiens*. When craniometric characters were excluded from the cladistic analyses, three most parsimonious trees were found (Strait and Grine, 2004). The strict consensus differed from the previous solution in that it was unable to resolve the position of *K. platyops* relative to the paranthropines and *Homo*, and the position of *H. habilis* and *H. rudolfensis* within the *Homo* clade. These hypotheses of relationship did not find strong statistical support (Strait and Grine, 2004). A bootstrap test only recovered three hominin clades significant at the 70% confidence level: the *Paranthropus* clade (100%), a clade formed by *H. ergaster* and *H. sapiens* (86%), and a clade formed by *Paranthropus*, *Homo*, *A. africanus* and *K. platyops* (85%). The number of clades recovered in the bootstrap analysis increased when *K. platyops* was excluded from the analyses due to the large number of missing data for this taxon. In this case, the *Homo* clade was also recovered (77%), as well as a clade formed by *Homo* and *Paranthropus* (78%). *A. africanus* was placed as the sister group of a clade formed by *Homo* and *Paranthropus* in 94% of the bootstrap replicates. The position of *A. garhi* as the sister group of *A. africanus*, *Paranthropus* and *Homo* also found some support (71%). *Pr. afarensis* was placed next to the clade formed by *A. garhi*, *A. africanus*, *Paranthropus* and *Homo* (78%). Thus, the results of Strait and Grine's parsimony and bootstrap analyses were strongly affected by ingroup composition and dataset composition, a finding in line with previous studies.

The same year, Cameron and Groves (2004) published the most extensive hominin cladistic study to date in terms of number of fossil groups included in the analysis. This analysis was based on 92 craniodental characters taken from the recent literature recorded on 16 fossil and four extant hominid taxa. The fossil groups included Miocene hominoid taxa (*Kenyapithecus*, *Dryopithecus*, *Graecopithecus* and *Sahelanthropus*) and Plio-Pleistocene hominin species belonging to the genera *Praeanthropus*, *Ardipithecus*, *Australopithecus*, *Kenyanthropus* and *Paranthropus*. The extant genera comprised *Homo*, *Pan*, *Gorilla* and *Pongo*. The parsimony analysis of all 92 characters recovered eight most parsimonious solutions. The strict consensus of these solutions (Figure 2-1k) supported a basal position for *Ar. ramidus* among the hominins followed, in order, by *A. anamensis* and *Pr. afarensis*. Next, four clades were arranged in a polytomy: the first clade comprised *Sahelanthopus*, the second comprised *A. garhi*, the third comprised the paranthropines and the fourth comprised *A. africanus*, *Homo* and *Kenyanthropus*. The 'robust' australopithecines formed a monophyletic group in which *P. aethiopicus* (in this paper referred to as *P. walkeri*) was the sister group of a clade formed by *P. robustus* and *P. boisei*. And *A. africanus* was placed next to a clade formed by *K. platyops* and *K. rudolfensis* (note the different taxonomy adopted by these authors) on one side and three *Homo* species in a separate clade. Within the latter *H. sapiens* and *H. ergaster* were sister taxa to the exclusion of *H. habilis*. When this dataset was bootstrapped, only three clades were recovered at the 70% confidence level: the clade formed by *H. ergaster* and *H. sapiens* (88%), the clade formed by the three paranthropines species (91%) and, within the latter, the clade formed by *P. robustus* and *P. boisei* (83%). The number of characters was then reduced to 52 (i.e. only those characters present in either *S. tchadensis* or *K. platyops* were included in the analyses) and the number of most

parsimonious solutions found in the parsimony analysis increased to 20. The strict consensus of these trees agreed with the previous solution except that in this cladogram the position of *Preanthropus* and *A. anamensis* remained unresolved. Overall the results of their analysis confirmed the findings of some previous studies, namely that the genus *Australopithecus* as currently defined is a paraphyletic group, and that the genera *Homo* and *Paranthropus* are both monophyletic. The relationships among the other hominid taxa did not find any statistical support.

In summary, all the studies described in this section indicate that: 1) the evolutionary relationships among early hominins are still unresolved, as shown, for example, by the disagreement between the topologies recovered from different datasets; and 2) little confidence can be placed in the results yielded by these analyses as demonstrated, for example, by the application of bootstrapping techniques. Why are we unable to produce clear and reliable phylogenies for the hominins? Several explanations have been put forward. Curnoe (2003) asserted that the single largest source of error for cladistics and human phylogenetic reconstruction is the uncertainty over the number and composition of fossil human species. A clear taxonomy is in fact one of the underlying assumptions of cladistic analysis (Wood, 2002; Curnoe, 2003) and can strongly influence phylogenetic analyses as indicated by the results of several studies (e.g. Chamberlain and Wood, 1987). More recently Hawks (2004) showed that the small and fragmentary nature of fossil hominin samples is such that it would not allow the recovery of a true phylogeny for the hominins even if other important parameters that are known to affect cladistic analyses were controlled for, i.e. if characters were clearly scored and independent, and if a selection-free model for

character evolution was contended. Rhetorically, the solution to this problem is to unearth more fossil specimens to increase the size and quality of the hominin samples.

It has also been proposed that primate craniodental characters commonly used in evolutionary studies may themselves not be reliable for recovering the phylogenetic relationships of the fossil hominins (Hartman, 1988; Harrison, 1993; Corruccini, 1994; Lieberman, 1996; Collard and Wood, 2000). The validity of current methodologies used to reconstruct evolutionary relationships among extinct organisms – and specifically the utility of morphological character sets for recovering phylogeny – can be tested by applying the same methodologies to a group of extant organisms, the phylogeny of which is known from independent lines of evidence (e.g. molecules). Using this approach, morphology-based phylogenies can be judged against the 'true' phylogeny of the group and this way the reliability of the character sets employed can be evaluated. Because of the deep understanding we have of the evolutionary history of the superfamily Hominoidea based on molecular data, this group is an excellent starting point to explore any limits there may be to the utility of craniodental cladistics for phylogenetic inference (Hartman, 1988; Pilbeam, 1996; Collard and Wood, 2000, 2001; Gibbs et al., 2000, 2002). The hominoids also include the closest relatives of the human family, which makes comparative studies between the two groups even more relevant to the study of hominin evolution.

2.1.2 Reliability of primate craniodental datasets for phylogenetic inference

A number of recent studies have suggested that primate craniodental data may not be a reliable source of phylogenetic information because these characters are strongly

prone to homoplasy. The term 'homoplasy' refers to similarities between two taxa that are due not to common ancestry but to other evolutionary processes such as parallelism and convergence (Lockwood and Fleagle, 1999; Collard and Wood, 2001). These studies include Hartman's (1988) cladistic analysis of hominoid molar occlusal morphology. The dataset used in this study generated a number of trees of which all but one agreed in placing *Homo* and *Pongo* in a single clade. The other tree placed *Homo* and *Gorilla* in a clade next to *Pan*. Both topologies were inconsistent with the molecular phylogeny for the hominoids demonstrating the presence of homoplasy in the dataset used. Hartman concluded that although dental morphologies are certainly evolutionary related, their phylogenetic signal has been almost completely obscured by the functional requirements of diet. In particular, he emphasised that dental features shared by humans and orangutans are likely to be indicative of similar diets rather than common ancestry. A similar conclusion was later reached by Harrison (1993) in his study of East African Miocene catarrhine relationships. Using molar and lower facial traits, Harrison reflected that the topology produced by his cladistic analysis was likely to be caused by 'common adaptive patterns due to similar diets and allometric constraints', rather than the natural phylogeny of the group.

Corruccini (1994) also applied a 'dissimilarity coefficient' analysis on two datasets for extant apes and humans: one from Groves and Paterson (1991) and one from Martin (1986). Groves and Paterson's data matrix comprised 113 characters for *Homo sapiens*, *Pan troglodytes*, *Gorilla* and *Pongo*. A bootstrap analysis recovered an African ape group first (74%). This was joined by *Homo* (74%), and then by *Pongo* (100%). Martin's dataset consisted of 73 traits for the same species plus

Australopithecus and *Sivapithecus*. The bootstrap analysis found very strong support for three groups: *Pongo* and *Sivapithecus* (100%), *Gorilla* and *Pan* (100%), *Homo* and *Australopithecus* (100%). The relationships among these three groups were not resolved. Both analyses suggested that *Pan* and *Gorilla* are more closely related to each other than either is to *Homo* and thus confirmed that the relationships among *Homo, Pan* and *Gorilla* cannot be resolved using craniodental data.

A particularly relevant piece of work on this issue was carried out by Collard and Wood (2000). They analysed craniodental evidence from two groups of extant primates, hominoids and papionins. They used two sets of data, one qualitative and one quantitative. The phylogenies generated from their analyses were incompatible with the well-supported consensus molecular cladograms for these groups. Importantly, some of the morphological clades also found a high level of statistical support when the datasets were bootstrapped. Collard and Wood concluded that not only are standard primate craniodental traits of limited use for phylogenetic reconstruction but they can also be misleading since they produce strongly-supported 'false-positive' clades. Therefore, they reasoned that phylogenies generated for the hominins based only on this type of evidence cannot necessarily be relied upon. Additional analyses on the same datasets also showed that Collard and Wood's (2000) conclusions were independent of methodological choices such as body size correction techniques, non-phylogenetic character correlation and outgroup composition (Nadal-Roberts and Collard, 2005).

Three additional papers confirmed these findings for other groups of primate: galagos (Masters and Brothers, 2002), tamarins (Ackerman and Cheverud, 2002) and lemurs

(Viguier, 2002). A cladistic analysis of 21 galagonid species using 36 parsimony informative craniodental characters found high levels of homoplasy in the dataset and yielded a phylogenetic hypothesis that disagreed with those obtained from a behavioural dataset and a molecular dataset (Masters and Brothers, 2002). The authors proposed that a consensus between different lines of evidence (e.g. soft tissue, postcranial and molecular data) should be sought in order to evaluate the level of support for different clades. Interestingly, they also found that the resulting topology varied with outgroup composition. The trees produced when lorises were adopted as outgroups differed from those produced using cheirogaleids; these two solutions also differed from the cladogram obtained when both outgroups were included in the analyses at the same time.

Patterns of cranial morphology in tamarins were also used to investigate evolutionary process in primates (Ackerman and Cheverud, 2002). Using quantitative genetics theory this study found that the pattern of morphological variation across the whole genus *Saguinus* (tamarins) did not match the one expected under the assumption of evolution by random genetic drift, indicating the presence of selective forces acting on cranial morphology within the genus. In contrast, within each of the two major tamarin clades, i.e. large-bodied and small-bodied tamarins, the pattern of variability was consistent with the predictions of the genetic drift model. The authors noted that tamarin species that are phylogenetically very close to each other in fact differ considerably in their cranial morphology. Hence, Ackerman and Cheverud (2002) concluded that due to the processes of differentiation acting on these taxa, similarity in cranial morphology is not a good indicator of phylogenetic proximity for this group of primates.

Lastly, Viguier (2002) studied the cranial morphology of *Lemur catta* and of five species that belong to the genus *Eulemur* in order to assess whether the morphological differences across lemur skulls are constrained by the environment and/or by the group's phylogenetic history. Procrustes residuals were analysed by principal component analysis and the scatter-plots interpreted against the geographical distributions of taxa to determine whether morphology was correlated with geography. A morphological distance tree was computed and compared with various published cladograms to test for any correlation between morphology and phylogeny. The results of this study found that morphological differences between taxa were correlated with geographical distribution and not with phylogeny. Viguier concluded that the morphological disparity of lemur skulls is associated with a high degree of homoplasy probably as a result of ecological constraints. This conclusion also found support from a previous study (Yoder, 1994) in which morphological and molecular cladograms were compared for a number of strepsirhine taxa in order to investigate the position of Malagasy primates within this group. Mitochondrial DNA evidence strongly supported the notion that Malagasy primates (cheirogaleids and other lemuriforms) form a monophyletic group. In contrast, the morphological analyses – based on 51 craniodental characters, 23 postcranial characters, nine soft-tissue characters and three behavioural characters – produced phylogenetic hypotheses in which support for monophyly of Malagasy primates was extremely weak. Yoder (1994: 35) stated that "strepsirhine morphology is extremely homoplasious" and therefore a poor indicator of phylogeny.

It has also been suggested that some cranial regions (specifically the masticatory apparatus) are more prone to homoplasy than others and characters from these regions dominate current dataset for the hominins, producing unreliable cladograms (Skelton et al., 1986; Skelton and McHenry, 1992; Lieberman 1995; Lieberman et al., 1996). Collard and Wood (2001) tested the hypothesis that characters of the masticatory apparatus are less reliable for phylogenetic inference because they show higher levels of homoplasy compared to other cranial complexes. They generated cladograms for extant hominoids and papionins from four different datasets, each of which was dominated by characters from one of four cranial regions – face, cranial vault and base, palate and upper dentition, mandible and lower dentition. Then, they compared these cladograms to the strongly supported molecular trees for both primate groups. Collard and Wood found that none of the regional datasets recovered the molecular relationships of these primates and all showed equal levels of homoplasy. Specifically, the datasets that comprised characters from the palate and upper dentition, and mandible and lower dentition (i.e. the characters related to mastication) were no less reliable than the other datasets for inferring hominoid and papionin phylogenetic relationships.

Three points emerge from these investigations. First, there is a considerable level of homoplasy in the trees generated from primate cranial morphology. Homoplasy is not a simple monofactorial variable and it is likely to be the results of a complex interaction of different parameters that obscure the phylogenetic signal for this taxonomic group (Lieberman, 1999; Lycett and Collard, 2005). Second, this problem is not limited to a single primate group, but it is widespread within this order (e.g. hominoids, papionins, galagos, tamarins and lemurs). Third, homoplasy does not

seem to affect any particular region of the skull (e.g. dentition or masticatory apparatus). Rather, all regions of the skull appear to be equally prone to homoplasy. These findings have significant implications for studies of fossil primates, and therefore the hominins, since, as mentioned earlier, these studies are invariably based on craniodental datasets. If primate craniodental morphology is not reliable for phylogenetic inference, then caution should be taken when inferring phylogenies for extinct hominins based solely on this type of evidence.

A very different view was recently put forward by Strait and Grine (2004) who averred that the inclusion of fossil taxa within the hominoid ingroup can help recover the correct relationships among extant apes and humans using craniodental characters. The dataset used in their analyses comprised 198 standard craniodental traits and included both traditional morphological traits and craniometric traits. These were recorded on a sample of 13 fossil hominin species and five extant hominoid species. Two cercopithecoid taxa were also incorporated in the study as outgroups, *Colobus* and *Papio*. The results of their analyses can be summarised as follows. When only extant apes and humans were included in the tests, the cladograms produced were inconsistent with the consensus hominoid molecular phylogeny. Bootstrap analyses did not recover any significant clade at the 70% confidence level when all 198 characters were used. Two clades were recovered when craniometric characters were excluded from the analysis: a weakly supported clade formed by *G. gorilla* and *P. pygmaeus* (70%), and a strongly supported great ape and human clade (96%). When the fossil hominin taxa were incorporated in the analyses, the most parsimonious trees supported a topology in which *P. troglodytes* was the sister taxon of a clade formed by all the fossil hominins and modern humans. This group was joined by *G. gorilla* to

form the African ape and hominin clade, and then by *P. pygmaeus* to form the great ape and hominin clade. When the dataset was bootstrapped, only four clades were statistically significant at the 70% confidence level: a clade that comprised *H. ergaster* and *H. sapiens* (86%); the paranthropine clade (100%); a clade formed by *A. africanus*, *K. platyops*, the paranthropines and the *Homo* clade (85%); and finally the clade formed by the great apes and hominins (94%). Strait and Grine (2004) concluded that their results refuted the hypothesis that craniodental characters lack phylogenetic utility or are less reliable than other types of morphological data for recovering hominoid phylogenetic relationships (Collard and Wood, 2000). As a consequence of this, they stated that current phylogenetic hypotheses for the hominins are not futile and therefore should not be distrusted.

These statements were not supported by the work of Finarelli and Clyde (2004) who recently revisited the question of hominoid phylogeny using morphological cladistic and stratocladistic methods. The dataset used in the cladistic analysis included 200 morphological (craniodental and postcranial) characters collected on a sample of 13 fossil and 5 extant hominoid genera. The fossil groups encompassed taxa across the entire superfamily Hominoidea and not just the hominins (i.e. they also included Miocene apes, such as *Graecopithecus* and *Kenyapithecus*). The results did not produce unambiguous phylogenetic hypotheses for the hominoids, even if many fossil taxa were incorporated in the analyses. Four most parsimonious cladograms were recovered. Three of the shortest trees supported a close relationship between *Gorilla* and *Pan* to the exclusion of *Australopithecus*, and one tree supported a sister group relationship between *Australopithecus* and *Pan* to the exclusion of *Gorilla*. The clades were highly unstable and none of them found bootstrap support at the 70% confidence

level. Finarelli and Clyde (2004) concluded that the uncertainties in the phylogeny of the hominoids are dictated by the poor preservation of fossil taxa and the high levels of homoplasy in the datasets.

It should also be noted that Strait and Grine's (2004) paper did not take into account the results of Collard and Wood's (2000) analyses of craniometric variables for another group of primates for which the molecular relationships are strongly supported, the papionins. By repeating on a papionin dataset the analyses that they carried out in the same paper on the hominoid dataset, Collard and Wood found that the morphology-based cladograms disagreed with the papionins consensus molecular cladogram. Again, they concluded that craniometric characters are not reliable for recovering primate phylogenetic relationships.

As discussed at the beginning of this section, homoplasy arises from various different evolutionary processes (Lockwood and Fleagle, 1999; Collard et al., in press) such as parallelism, convergence and reversals. It has been proposed that homoiologies – morphological similarities primarily due to epigenetic factors – are also a major source of homoplasy in the hominid skull, especially in the regions affected by mastication-related strain (Lieberman, 1995, 1997, 1999; Lieberman et al., 1996), and that their presence greatly affects our ability to generate reliable estimates of phylogeny for the hominids. This 'homoiology hypothesis' is based on the observation that hominid phylogenetic analyses are largely based on evidence from the cranial skeleton and that the latter is significantly influenced by internal stimuli (e.g. tissue-tissue interactions, circulating hormones) as well as external stimuli (e.g. mechanical loading) (Lieberman, 1995, 1997, 1999; Lieberman et al., 1996). For

example, Lieberman (1996) found that in two mammalian groups, pigs and armadillos, cranial vault thickness (CVT), a character often used in hominin phylogenetic analyses (e.g. Stringer, 1987b; Frayer et al., 1993), is a consequence of systemic cortical bone growth that can be induced by non-genetic stimuli, such as exercise. In a very illuminating paper from 1997, Lieberman reviewed the genetic and epigenetic processes involved in bone development, and discussed the implications of the multifactorial nature of bone growth for behavioural and phylogenetic studies of fossil hominins. Lieberman stated in this paper that bone is not an ideal source of information for making phylogenetic inferences from fossil humans because it is a very dynamic tissue and highly affected by environmental stimuli (Lieberman, 1996, 1997). Lieberman also stated that phylogenetic inference should be based on characters of the bones that are less affected by environmental stimuli – like characters of the cranial base (Lieberman, 1997) – whilst other traits may be more informative about the habitual behaviour of an organism. Corroborative evidence for this hypothesis can be found in the fact that unlike primate craniodental characters, soft-tissue characters, which are thought to be less influenced by epigenetic factors than hard-tissue characters (Collard et al., in press), produce more reliable estimates of the relationships among higher primate species and genera (Gibbs et al., 2000, 2002).

The homoiology hypothesis was recently evaluated by Collard et al. (in press) and Lycett and Collard (2005). The first study tested the homoiology hypothesis using data from the extant hominoids whilst the second concentrated on another group of primates, the extant papionins. Both studies agreed that homoiology is not a major source of homoplasy for primates and therefore the inability to produce reliable

phylogenetic hypotheses for the hominins cannot be attributed to this factor. Instead, the authors stressed that the question of hominin homoplasy is a "complex and multifaceted" problem. These findings were also supported by the results of a study in which cladograms generated from a dataset that included characters of the basicranium – which supposedly are less affected by epigenetic influences and therefore more reliable for phylogenetic inference (Lieberman, 1996, 1997, 1999) – did not differ substantially from the cladograms generated from other parts of the cranium (Lieberman et al., 1996, 2000).

Another explanation why craniodental cladistics has not produced clear and reliable phylogenies for the fossil hominins is that large craniodental datasets violate one of the fundamental assumptions of the cladistic method, namely that the characters have arisen independently of each other (Lovejoy et al., 1999; McCollum and Sharpe, 2001). McCollum (1999) recently opined that most of the 20 traits commonly identified as synapomorphies of the paranthropines are in fact developmental by-products of a large postcanine dentition and a small anterior dentition. She used facial growth models to demonstrate that this suite of characters is developmentally integrated. On this basis she concluded that despite the morphological similarities among the paranthropines, their phylogenetic relationships cannot be resolved using the non-independent features commonly incorporated into cladistic analyses and without a greater understanding of the developmental basis of variation in craniodental morphology (McCollum, 1999; McCollum and Sharpe, 2001).

This concept was also reprised by Lovejoy et al. (1999, 2002) who recently argued that current cladistic methods are not able to resolve the phylogeny of the hominins

because the traits used to recover phylogenies do not include information on the morphogenesis of skeletal forms. Instead, hominid datasets rely on large lists of traits that are incorrectly assumed to be separately heritable units simply because they can be separately observed and analysed. This process results in the atomisation of morphologies into suites of developmentally and functionally correlated characters (Lovejoy et al., 1999, 2002).

The issue of character non-independence is a complex one. Collard and Wood (2001:170) contended that "too little is known about the issue of character correlation at the moment to use it as a justification for abandoning the use of multiple craniodental characters in cladistic analyses of hominids and other primates". For example, although hypotheses of functional and morphological integration predicted high levels of correlations among variables of the hominin cranial base, Strait (2001) found very low levels of correlation among these characters. This result was consistent with the outcome of a previous study that found a group of discrete cranial variables not to be significantly correlated in humans (Benfer, 1970). Recent fossil findings (e.g. Leakey et al., 2001) have also shown that craniodental characters widely assumed to be correlated (e.g. molar size and anterior positioning of the zygomatic arch) need not be so. Furthermore, Nadal-Roberts and Collard (2005) have shown that although non-phylogenetic correlation may be present in craniometric datasets, correlation-corrected datasets are not better at recovering the molecular relationships of extant hominoids. They argued that the evidence seems to indicate that character correlation is unlikely to be a major source of error in phylogeny estimates. However, the issue here is the lack of appropriate methodologies for the accurate recognition of non-phylogenetic correlations among characters.

In summary, the findings reported in this section have significant implications for phylogenetic analyses of fossil hominin material since these studies are regularly based on craniodental datasets. If standard craniodental characters are not reliable for phylogenetic inference then new sources of phyletic information need to be sought. This quest for phylogenetically informative characters is the theme of the next section of this chapter.

2.2 Phylogenetic value of soft tissue-linked osseous traits

2.2.1 The quest for phylogenetically informative characters

Different approaches have been proposed to overcome the problems imposed by the use of craniodental morphology. The integration of different types of data in cladistic analyses has recently been suggested by some authors (Collard and Wood, 2000; Masters and Brothers, 2002) and contested by others (Pilbeam, 2000). These may include postcranial data (Collard et al., 2001; Collard and Elton, 2002; Finarelli and Clyde, 2004), behavioural data (Banks and Collard, 2004), stratigraphic data (Fox et al., 1999; Finarelli and Clyde, 2004) and genetic data (Barriel, 1994; Yoder, 1994). The application of distance methods combined with geometric morphometric techniques has also been successful in recovering the phylogeny of the extant apes from the morphology of the temporal bone (Lockwood et al., 2004). Wood (2000) proposed that characters that are known to be only minimally affected by epigenetic

factors (e.g. enamel formation, middle and inner ear structures) should be more carefully scrutinised. Ideally, if the character is to carry a reliable phylogenetic signal, genetic heritability – i.e. the proportion of phenotypic variance of a trait explained by the genetic variance – should be very high (Lieberman, 1999). Unfortunately this is not always the case for osteological characters because, as discussed earlier, bone morphogenesis is very sensitive to environmental factors (Lieberman, 1996, 1997). Moreover, knowledge of the heritability value of a trait relies heavily on familial studies, which are not easy to carry out because suitable skeletal samples are not always available for this purpose (Hauser and De Stefano, 1989).

A greater knowledge about the processes underlying bone morphogenesis may also help discern between phylogenetically-informative and phylogenetically-misleading traits (Lieberman, 1995, 1996, 1997, 1999; Lieberman et al., 1996; Penin et al., 2002) and to detect intrinsic biases in the data matrices used to recover phylogenies due to morphological integration (Lovejoy et al., 1999, 2002; McCollum, 1999; McCollum and Sharpe, 2001). Interestingly, Collard and O'Higgins (2001) and O'Higgins and Collard (2002) found a consistency between the strongly supported molecular phylogeny of the papionins, which is thought to be accurate (Collard and Wood, 2000), and the relative importance of ontogenetic scaling and divergence between male and female growth trajectory to the determination of sexual dimorphism. They stated that this concordance may suggest that "the processes by which the skeletal similarities and differences among primate taxa arise are more phylogenetically informative than the skeletal similarities and differences themselves" (O'Higgins and Collard, 2002: 268).

Where can we look for phylogenetically informative characters? Gibbs et al. (2000, 2002) have recently investigated the reliability of primate soft-tissue traits (e.g. muscles, arteries and nerves) for phylogenetic inference. They gathered data from the literature about soft-tissue structures in the extant apes, and coded it into 171 characters to be used in a cladistic analysis. The parsimony analysis generated a single shortest cladogram that coincided with the consensus molecular cladogram for the hominoids. A bootstrap analysis also generated a cladogram compatible with the molecular tree and provided very high support for each clade. These results are important because, as the authors pointed out, they are the first morphological data to generate a statistically significant phylogeny congruent with the hominoid consensus molecular cladogram. This indicates that, unlike standard craniodental characters, hominoid soft-tissue characters may be reliable for phylogenetic inference.

Why do soft-tissue traits produce more accurate phylogeny estimates for the hominoids than craniodental osseous characters? Lieberman (1999) listed seven criteria for selecting phylogenetically informative characters. Characters should be: 1) natural units; 2) discrete and/or quantifiable; 3) more variable between species than within species; 4) derived with respect to a common ancestor; 5) uncorrelated; 6) highly heritable; 7) and homologous. Homologous soft-tissue traits are relatively easy to identify and to score (Pilbeam and Young, 2004). They are "discrete and natural morphogenetic units" and they are not under strong epigenetic effects (Pilbeam, 2000; Pilbeam and Young, 2004; Collard et al., in press). Therefore soft-tissue traits meet five of the requirements of phylogenetically-informative characters as they were enumerated by Lieberman (n. 1, 2, 4, 6, 7). Not much can be said about character correlations, and within-species *versus* between-species variation because

comparative soft-tissue studies for most non-human primate taxa are based on a very limited number of specimens (Gibbs et al., 2000, 2002).

Soft tissue is very rarely preserved in the fossil record and it is very unlikely that in the near future this type of data will find application in analytical studies of extinct primate relationships. However, soft tissue often leaves marks and impressions on bones (e.g. grooves), or is associated with specific osteological structures (e.g. foramina). If soft-tissue traits carry a strong phylogenetic signal, it seems worth considering the possibility that skeletal characteristics associated with soft-tissue structures may also carry a reliable phylogenetic signal. This project will explore this possibility by identifying a suite of soft tissue-linked cranial structures and testing their phylogenetic utility using cladistic methods.

There are several types of features that can be taken into consideration for this purpose. Muscles leave marks at their sites of origin and insertion. Many of these can be clearly identified and a few have been previously incorporated into phylogenetic analyses. For example, Skelton et al. (1986) included in their data matrix the size of the posterior part of the temporalis muscle relative to the anterior part, and the height of the origin of the masseter muscle; Groves (1986) included the site of insertion of the digastric and of the genioglossal (relative to the inferior transverse torus); and Begun et al. (1997) included the groove produced by the *flexor hallucis longus*. Many bony projections on the skeleton are sites of attachment of tendons and cartilages. These have been the subject of several comparative studies within the hominoids. For example, the nasal spine is the anterior site of attachment of the nasal septal cartilage. A true spine has been traditionally regarded as an autapomorphy of the *Homo* clade.

However more recently the trait has also been described in *Pan paniscus* (Braga, 1996b) and other variants have been observed in extant apes and fossil hominins (Eckhardt and von Zieten, 1992). Another example is the styloid process, a trait produced by secondary ossification of cartilaginous elements. Traditionally regarded as a specialisation of humans, Braga (1993) also reported its occurrence in apes where it appears frequently in the orangutan. Lastly, the preglenoidal tubercle commonly found in *Homo erectus* specimens is thought to be the insertion point of the short tendinous bunches of the lateral pterygoid muscle (Zeitoun, 1996). This character is not observed in the African apes and in early hominins although it is present in modern humans in very low frequencies.

Probably the most distinctive and obvious soft tissue-linked cranial structures are those associated with the passage of cranial nerves and vessels: this is the set of characters on which I will be concentrating in this project. Some of these traits have already been the focus of several evolutionary studies in the palaeoanthropological literature. The impressions left by the middle meningeal arteries on the intracranial surfaces of the temporal and parietal bones are clearly visible in extant and fossil species (Falk, 1993) and, together with endocasts of hominin brains, these impressions have allowed the investigation of the pattern of cranial blood drainage in hominins (Falk and Conroy, 1983; Falk, 1986; Tobias and Falk, 1988; Braga and Boesch, 1997a, 1997b). Msuya and Harrison (1996) recently examined the evolutionary significance of the number of circumorbital – infraorbital, zygomatico-facial and supraorbital – foramina and reported on their variability in 38 species of primates. A few characters related to cranial foramina have also been included in hominoid and fossil hominin cladistic analyses. For example, Skelton et al. (1986)

incorporated the position/orientation of the foramen magnum and the position/direction of the mental foramen in their fossil hominin phylogenetic analysis. Likewise, Groves' (1986) analysis of great ape relationships included the size/direction of the incisive canal and the position of the infraorbital foramen.

However, a systematic and comprehensive study on the phylogenetic value of these structures has never been carried out. This project sets out to carefully describe these characters and test their usefulness for reconstructing hominoid phylogenetic relationships with cladistic methods. The next part of this chapter will review our current knowledge about the aetiology of these traits in order to contextualise their phylogenetic significance.

2.2.2 Nerve- and vessel-related variation

The term 'nerve- and vessel-related' traits will be used throughout this study to designate any of the skeletal features of the primate cranium that mark the presence and/or the passage of nerves or vessels. Such features include bony foramina and canals that transmit nerves and vessels intra- and extra-cranially; grooves (or sulci) marking the passage of nerves and vessels on the surface of various cranial bones. They also include some hyperostotic and hypostotic variants (see below) associated with the aforementioned features, such as bony bridges that grow around vessels and nerves (e.g. the mylohyoid bridge on the mandibular ramus) or that separate different nerves and vessels within a foramen (e.g. hypoglossal canal division).

From a literature search through Gray's Anatomy (1999 edition) and Nomina Anatomica (1989), I found that there are over 80 described osseous foramina and canals in the human skeleton. Comparative data for primates, and in particular apes, is sparse. There is also a deficiency of data on normal variation in humans in the anatomical literature (Berge and Bergman, 2001) even though this type of information is invaluable for researchers and clinicians. For example, enlarged parietal foramina have been associated with a number of skeletal anomalies (Luker et al., 1998) as well as mental disorders such as the Potocki-Shaffer syndrome (Hall et al., 2001). Recently Berge and Bergman (2001) carried out a survey of the variation of the foramina of the skulls in a sample of 100 dry human skulls. They studied 27 paired foramina, two unpaired foramina and the length of the infraorbital canal. For all these structures they noted the average size/length and the size range, the variation in symmetry and they compared their results to the findings of previous studies. The authors emphasised that the availability of this type of information is becoming more and more important considering the increasingly important role of radiological techniques such as MRI (Magnetic Resonance Imaging) and CT (Computed Tomography) in the diagnosis of pathological conditions, in particular of the skull foramina.

Data on nerve- and vessel-related traits are usually included in studies of skeletal 'anomalies' or non-metric variation in human and primate populations. Non-metric variation can be recognised and scored like any other type of variation except in this case it cannot be measured. This type of variation is generally scored as present or absent although a degree of expression of the trait can also be evaluated by means of scales (Berry, 1967). Non-metric variants are also referred to as discrete, discontinuous, epigenetic or quasi-continuous. They are usually classified in three

groups: hypostotic variants, hyperostotic variants and foramina (Hauser and De Stefano, 1989; Braga, 1995, 1996a; Hanikara and Ishida, 2001a, 2001b, 2001c, 2001d). Hypostotic variants represent a fetal or immature stage of development that persists into adulthood (e.g. confluence of foramen ovale and spinosum). In this case osseous development is incomplete. As Hauser and De Stefano (1989) point out, because hypostotic features develop at different rates and different times, they are not the result of a single developmental event but each results from an independent process. Since they are associated with heterochronic processes these traits can be useful for the study of ontogeny and phylogeny (Braga, 1995). Hyperostotic variants are those due to the secondary ossification of cartilaginous or ligamentous anatomical elements (e.g. hypoglossal canal division, mylohyoid canals, pterygospinous bridging) and they are expressed as excess of bone growth. Many authors have insisted on the high heritability of both hypostotic and hyperostotic variants, whilst the number of foramina seems to be a less heritable trait (Ansorge, 2001). For example, Hauser and De Stefano (1989) reported low heritability values for the trait 'absence of the zygomatico-facial foramen' and for the trait 'ethmoid foramen extra-sutural', but a significant heritability value for the trait 'absence of parietal foramina'.

Most of our knowledge on the inheritance of non-metric variants comes from animal studies, in particular from mice (e.g. Gruneberg, 1952, 1963). Although the mechanism of phenotypic expression for each of the characters is still not fully understood, there is evidence from these studies that these types of variants are the result of genetic determination. The expression of non-metrical variants is thought to be the result of a number of alleles at different loci acting additively (multifactorial inheritance). These alleles control an underlying continuous variable that is expressed

only if it reaches a threshold value. Below this critical value the trait is not expressed. In addition to this, there is the environmental context in which the trait develops. This includes factors like maternal age, parity and size (Berry and Berry, 1971). The result is the manifestation of two phenotypes, presence or absence. In this sense the term 'quasi-continuous variants' has been used by some authors (e.g. Gruneberg, 1952) to describe the discontinuous nature of these otherwise continuous traits. In mice many of these characters do not have any adaptive value and their variation is thought to be affected by selectively neutral genes (Berry and Berry, 1971). Although some authors insist that they seem relatively unaffected by external factors such as diet (Anderson, 1967), others are more cautious and emphasise the difficulty in discerning the effects of environmental and genetic factors on their expression from skeletal samples (Hauser and De Stefano, 1989; Braga, 2001).

Many of the variants studied in the mouse are also observed in *H. sapiens* where they are phenotypically analogous (Berry and Berry, 1967). What we know about their inheritance in *H. sapiens* agrees with what we know for the mouse. Therefore there is reason to believe that the mode of inheritance of these traits in the two species is similar (Berry, 1967). However, direct evidence is weak since we lack the primary family and twin material that would allow such kind of study (Hauser and De Stefano, 1989). Most of the evidence for a genetic basis for these traits in humans comes from their association with inherited syndromes and the different frequencies for these traits in populations with different genetic compositions. As Berry (1967) pointed out, the probability of finding a trait in a population with a fairly fixed gene pool will be in itself fixed within limits and therefore the population incidence of a traits will become a real property of that population. Hence, non-metric traits become legitimate genetic

markers. However, Thoma (1981) reported an irregular pattern of quasi-continuous variation among some human populations, and warned that studies that incorporate this type of evidence should complement, not replace, metric and genetic information.

Hanihara and Ishida (2001a, 2001b, 2001c, 2001d) have recently published a series of papers in which they carried out a systematic analysis of the frequency variations of 20 discrete cranial traits in 81 major human populations throughout the world. They discussed separately supernumerary ossicles (2001a), hypostotic variations (2001b), hyperostotic variations (2001c), and vessel- and nerve- related variations (2001d). They concluded from their studies that it is very difficult to quantify the relative role of genetics and environment in the occurrence of the traits they discussed. They also argued that the pattern of frequency distributions across human populations suggests – at least in part – genetic drift as a possible cause of the variation among discrete cranial traits reinforcing evidence for a non-adaptive value of these traits. The class of traits labelled as nerve and vessel-related variants (Hanihara and Ishida, 2001d) comprised four foramina and canals (patent condylar canal, supraorbital foramen, accessory infraorbital foramen and accessory mental foramen). They included other characters related to nerves and vessels but, in their survey, they classified them as either hypostotic traits (ovale-spinosum confluence) or hyperostotic traits (median palatine canal, hypoglossal canal bridging, jugular foramen bridging, mylohyoid bridging).

The last issue that I want to mention concerns character correlation. In mice many non-metric variants are uncorrelated and therefore they are thought to be controlled by different parts of the genome (Berry, 1967). However, too few studies of non-metric

correlation have been carried out. Benfer (1970) applied multivariate analyses to a group of seven cranial characters in humans (parietal foramina, five circumparietal accessory ossicles, pattern of fronto-temporal suture) and concluded that these traits are independent of each other both within and across geographical groups. Hauser and De Stefano (1989) reviewed the evidence for inter-trait associations and also concluded that the evidence is either inconsistent or points to independence. Those characters that are produced by a common underlying process may be correlated in their expression – although this is not necessarily the case (Hauser and De Stefano, 1989). All of the other characters are largely independent of each other.

The phylogenetic value of non-metric variants was emphasised by Braga (2001:188) who stated: "the evidence from discrete trait analysis [...] agrees with the molecular evidence and clearly defines the relationships among extant taxa". Due to the uncertainty regarding the regulation of morphological similarities by homologous genotypes, some authors have expressed scepticism about cross-species comparisons using these traits (Berry and Berry, 1971). However others have endorsed it within the Hominoidea, based on the increasing evidence for genetic conservation among the members of this group (Thoma, 1977). Thoma (1978, 1979) used the frequency values of 31 quasi-continuous variants to estimate divergence values for humans and great apes. From his statistical analysis, using similarity coefficients, he found that *Pan paniscus* was the closest ape to humans whilst *Pongo pygmaeus* was the most different.

In summary, nerve- and vessel- related traits possess most of the seven criteria listed by Lieberman (1999) for selecting phylogenetically informative characters. They are

natural units of the primate skull (criterion 1). They can be easily described and quantified (criterion 2). Although correlations between some of these traits are to be expected, there is evidence that generally discrete traits are uncorrelated (criterion 5). They are heritable and there is some evidence that they are not majorly influenced by environmental factors (criterion 6). Homology can also be easily established in different species (criterion 7). Lastly, some studies (e.g. Msuya and Harrison, 1997; Braga, 2001) have shown trends from ancestral to more derived conditions in primates (criterion 4). The data concerning within- versus between-species variation (criterion 3) is still poor for many variants although high levels of overlapping intra-specific variation is to be expected for closely related species such as the hominoids (Hawks, 2004). A final notable characteristic is that these traits do not seem to be under strong selective pressures but rather their population genetics seems to be controlled by random drift.

2.3 Summary

In this chapter I have reviewed the evidence in support of the hypothesis that standard craniodental morphology is not reliable for recovering the phylogenetic relationships of hominoid primates. This is particularly problematic for the study of the evolutionary history of fossil primates, and in particular the hominids, because these studies are invariably based on craniodental evidence. As discussed in the first part of the chapter, this may be the underlying reason why we still do not have a clear phylogeny for the fossil hominins. I have also discussed the reasons why craniodental morphology may not be suitable for phylogenetic studies. Craniodental datasets

include many homoplasious characters that are not informative about phylogeny. On the contrary, homoplasious characters are misleading regarding primate relationships.

I then went on to describe how a recent analysis based on soft tissue characters yielded a strongly-supported and accurate phylogenetic tree for the extant hominoids. From this finding, I formulated the hypothesis that if soft-tissue traits carry a reliable phylogenetic signal, then it is plausible to think that osseous characters related to soft-tissue traits may also carry a clear phylogenetic signal. This project sets out to test this hypothesis by applying cladistic methods to a dataset that comprises characters of the skull associated with nerves and vessels in order to generate phylogenetic hypotheses for extant hominoid primates. These cladograms will then be compared to the hominoid consensus molecular cladogram, which is strongly supported and therefore assumed to be correct (the evidence in support of each molecular clade will be thoroughly reviewed in the next chapter). The rationale of this study is that congruence between the morphological trees and the molecular tree will indicate that nerve- and vessel-related characters are phylogenetically informative. Conversely, disagreement between the two will lend support to the hypothesis that cranial morphology alone is unable to recover the molecular relationships of apes and humans. Either outcome will have very important implications for the study of primate, and in particular hominid, evolutionary history.

Chapter 3. EXTANT HOMINOID RELATIONSHIPS

3.1 Introduction

The primary goal of this project is to test the hypothesis that cranial characters related to nerves and vessels produce reliable phylogenies for the extant hominoid genera. In order to do so, phylogenetic hypotheses for the hominoids will be generated using cladistic methods from a dataset that comprises a large number of osseous characters related to nerves and vessels. The cladograms produced from this dataset will then be compared with the hominoid consensus molecular tree, which is widely thought to be accurate. Agreement between the morphology-derived phylogenies and the molecular tree will support the hypothesis. Disagreement between the two, on the other hand, will falsify the hypothesis.

In this chapter I will focus on the core assumption of this project, namely that the phylogenetic relationships of the extant hominoids are sufficiently strongly supported by molecular data to warrant assuming that they are known for the purposes of further analysis. I shall begin by providing an overview of the extant hominoids' taxonomy and biogeography, and then discuss published work on their phylogenetic relationships. Specifically, I will discuss the morphological and molecular evidence in support of (or against) each of the strongly supported molecular clades, with particular emphasis on the affinities among African apes and humans. At the end of the chapter, I shall also describe briefly the systematics of the three outgroup taxa included in this study to root the cladograms: *Cercopithecus*, *Colobus* and *Papio*.

Table 3-1 Taxonomy of the extant hominoids.

Superfamily Hominoidea
Family Hylobatidae
Genus *Hylobates*
Species *H. (Symphalangus) syndactylus*
Species *H. lar*
Species *H. hoolock*
Species *H. moloch*
Species *H. concolor*
Species *H. agilis*
Species *H. muelleri*
Species *H. albibarbis*
Species *H. pileatus*
Species *H. klossii*
Species *H. hainanus*
Species *H. leucogenys*
Species *H. siki*
Species *H. gabrielle*
Family Hominidae
Subfamily Ponginae
Genus *Pongo*
Species *P. pygmaeus*
Subfamily Homininae
Tribe Gorillini
Genus *Gorilla*
Species *G. gorilla*
Tribe Panini
Genus *Pan*
Species *P. troglodytes*
Species *P. paniscus*
Tribe Hominini
Genus *Homo*
Species *H. sapiens*

This table presents the classification of the extant hominoids adopted in this project. It reflects the phylogenetic relationships among the members of this group, as understood from the molecular data.

3.2 Taxonomy and biogeography of the extant hominoids

The extant apes and humans are grouped within one superfamily, the Hominoidea (Gray, 1825). Within this taxon (Table 3-1), two families are recognised: the Hylobatidae (Gray, 1870), or lesser apes (gibbons and siamangs), and the Hominidae (Gray, 1825), or great apes and humans. Following Groves (2001), the family Hominidae is subdivided into two subfamilies. One, the Ponginae, contains a single extant genus, *Pongo* (the orangutan). The subfamily Homininae, on the other hand, contains three genera: *Gorilla* (the gorilla), *Pan* (the chimpanzee) and *Homo* (humans).

3.2.1 Genus *Hylobates* (Illiger, 1811): gibbons.

Hylobates is the only genus in the family Hylobatidae. Gibbon species are distributed throughout most of mainland South East Asia and also on several of the islands of the continental shelf. They are distinguished mainly on pelage and vocalisations.

Groves (2001) recognised 14 species (Table 3-1), which he allocated to four subgenera: *Hylobates* (the lar-group gibbons), *Bunopithecus* (the hoolock gibbons), *Symphalangus* (the siamang) and *Nomascus* (the crested gibbons). The subgenus *Hylobates* (Illiger, 1811) comprises seven species (Table 3-2). There is currently only one extant species in the subgenus *Bunopithecus* (Matthew and Granger, 1923): *Hylobates (Bunopithecus) hoolock* (Harlan, 1834), the hoolock gibbon. The subgenus *Symphalangus* (Gloger, 1841) also includes only one species: *Hylobates*

(Symphalangus) syndactylus (Raffles, 1821), the siamang. Recently, it has been proposed that, because of the long divergence time between gibbons and siamang (8Myr), the siamang should be placed in a separate genus (Goodman et al., 2002). Lastly, the subgenus *Nomascus* (Miller, 1933) comprises five species (Table 3-3).

Table 3-2. Taxonomy of the lar-group gibbons (subgenus *Hylobates*)

Species name	Common name
Hylobates (Hylobates) lar (Linnaeus, 1771)	Lar gibbon or white-handed gibbon
Hylobates (Hylobates) agilis (Cuvier, 1821)	Agile gibbon
Hylobates (Hylobates) albibarbis (Lyon, 1911)	Bornean white-bearded gibbon
Hylobates (Hylobates) muelleri (Martin, 1841)	Müller's Bornean gibbon
Hylobates (Hylobates) moloch (Audebert, 1797)	Silvery gibbon
Hylobates (Hylobates) pileatus (Gray, 1861)	Pileated gibbon
Hylobates (Hylobates) klossii (Miller, 1903)	Kloss gibbon or Bilou

Data from Groves (2001).

Table 3-3. Taxonomy of the crested gibbons (subgenus *Nomascus*).

Species name	Common name
Hylobates (Nomascus) concolor (Harlan, 1826)	Concolor gibbon or black crested gibbon
Hylobates (Nomascus) hainanus (Thomas, 1892)	Hainan gibbon
Hylobates (Nomascus) leucogenys (Ogilby, 1840)	Northern white-cheeked gibbon
Hylobates (Nomascus) siki (Delacour , 1951)	Southern white-cheeked gibbon
Hylobates (Nomascus) gabriellae (Thomas, 1909)	Red-cheeked gibbon

Data from Groves (2001).

3.2.2 Genus *Pongo* (Lacépède, 1799): orangutans.

The genus *Pongo* contains only one species, *Pongo pygmaeus* (Linnaeus, 1760), which is found in the jungles of North Sumatra (Sumatran orangutans) and in Borneo (Bornean orangutans). Studies on the Bornean and Sumatran orangs have emphasised differences in cranial, dental and molecular characteristics (Groves, 1986; Braga, 1995; Uchida, 1998; Röhrer-Ertl, 1999). On the basis of these differences, Groves (2001) recognises two separate species of *Pongo* (*P. pygmaeus* and *P. abelii*).

In this project I follow the traditional taxonomy of this group in which the Bornean and Sumatran orangs are classified as subspecies of *Pongo pygmaeus* (Groves, 1986; 1989; Novak, 1999; Röhrer-Ertl, 1999). *Pongo pygmaeus pygmaeus* (Linnaeus, 1760) is the Bornean orangutan (or Maias). It is found on the island of Borneo although it

seems to be absent in the southeast of the island (Novak, 1999; Groves, 2001). *Pongo pygmaeus abelii* (Lesson, 1827) is the Sumatran Orangutan (or Mawas). It is found in Sumatra north of the latitude of Danau Toba (Novak, 1999; Groves, 2001).

3.2.3 Genus *Gorilla* (I. Geoffroy, 1853): gorillas.

The genus *Gorilla* contains a single species, *Gorilla gorilla*. Recent morphological and molecular studies have shown that two types of gorillas, the eastern and western types, possess many distinctive traits (Braga, 1995; Garner and Ryder, 1996; Uchida, 1998). For this reason some taxonomists (e.g. Groves, 2001; Patterson and Matevia, 2001) now recognise two species of gorillas, *Gorilla beringei* (the eastern gorilla) and *Gorilla gorilla* (the western gorilla). The eastern gorillas can be further subdivided into three subspecies (*G. beringei graueri*, *G. b. beringei*, *G. b. sp.*?). Two subspecies, instead, are generally recognised within the western gorillas (*G. gorilla diehli* and *G. g. gorilla*).

In this project, I follow the traditional taxonomic scheme in which only one gorilla species is recognised, *Gorilla gorilla* (Savage, 1847). This species is subdivided into three subspecies (Groves, 1989):

1. *G. g. gorilla* (the Western gorilla) is found in southeastern Nigeria, southern Cameroon, Río Muni, Gabon, Congo, Cabinda, Mayombe, southernmost Central African Republic, and an isolate community in northern Congo-Zaire.
2. *G. g. beringei* (the Eastern Mountain gorilla) is found in Uganda, Rwanda and Congo-Zaire.

3. *G. g. graueri* (Eastern Lowland gorilla) lives in eastern Congo-Zaire, including the lowlands east of the Lualaba and the Mitumba Range from Mount Tshiaberimu south to the Itombwe Mountains near Fizi.

3.2.4 Genus *Pan* (Oken, 1816): chimpanzees.

Two species are recognised within this genus.

P. troglodytes (Blumenbach, 1799), the common chimpanzee, occupies the African tropical forest from Senegal to the Congo River in the west, across to the east in southeastern Congo-Zaire, southern Sudan, western Uganda, Rwanda, Burundi, and Tanzania, extending east of the northern half of Lake Tanganyika (Novak, 1999; Groves, 2001). Three subspecies are traditionally recognised within *P. troglodytes* (Groves, 1986, 2001):

1. *P. t. troglodytes* (Blumenbach, 1799) spreading from the Congo River mouth north into Cameroon, into Nigeria east of the River Niger, and into the Central African Republic east to the river Oubangui; but the boundaries with the other subspecies are unclear.
2. *P. t. verus* (Schwarz, 1934) ranging from Senegal to the Volta or the Dahomey Gap; the eastern boundary is traditionally given as the Niger River.
3. *P. t. schweinfurthii* (Giglioli, 1872) found in Congo-Zaire, north of the river Congo and east of the River Lualaba, into Sudan, Uganda, Rwanda, Burundi, and Tanzania.

The other species of chimps, *P. paniscus* (Schwarz, 1929), the pygmy chimpanzee or Bonobo, is found in the humid forests of the Congo-Zaire (below 1500m), south of the great bend of the Congo River, delimited in the south by the Kasai river and in the east by the river Lualaba (Dupain and Van Elsacker, 2001; Groves, 2001).

Recent molecular work has lead many scientists to believe that *Pan* should be included within the genus *Homo* (e.g. Goodman et al., 1998, 2002; Curnoe and Thorne, 2003; Wildman et al., 2003) based on their similar genomes and their recent divergence time. Goodman et al. (1998, 2002) and Page and Goodman (2001), for example, have recently challenged the traditional classification of apes and humans by reducing the Superfamily Hominoidea to family Hominidae, and grouping all living hominids within the subfamily Homininae. In this classification, the genus *Homo* includes the subgenus *H. (Pan)*, which comprises common and pygmy chimpanzees, and the subgenus *H. (Homo)* for humans. Their argument is based on the observation that humans and chimpanzees share more than 98.3% of fast-evolving, non-coding nuclear DNA and possibly more than 99.5% of coding DNA. They claim that such high genetic affinity is never found between species that belong to different genera, but only between congeneric species (Goodman et al., 1989, 1998).

3.2.5 Genus *Homo* (Linnaeus, 1758): humans.

This genus contains only one extant species: *Homo sapiens* (Linnaeus, 1758), or modern humans. Humans are distributed worldwide.

3.3 Phylogenetic relationships of extant hominoids

The five extant genera described in the previous part of this chapter – *Hylobates, Pongo, Gorilla, Pan* and *Homo* – form a monophyletic group (superfamily Hominoidea) within Primates. Some of the morphological similarities commonly cited in the literature as synapomorphies of this group are listed in Table 3-4. In this section I shall discuss the molecular evidence in support of (or against) each of the clades present in the hominoid consensus molecular tree (described below), with particular emphasis on the relationships among African apes and humans. I will also compare this information with the evidence from morphological data (bone and soft-tissue) and contrast the results obtained from these two different types of evidence.

The consensus molecular cladogram for the hominoids features three major clades:

1. A great ape and human clade: (*Pongo*, *Gorilla*, *Pan*, *Homo*) to the exclusion of *Hylobates*.
2. An African ape and human clade: (*Gorilla*, *Pan*, *Homo*) to the exclusion of *Pongo*.
3. A chimpanzee and human clade: (*Pan, Homo*) to the exclusion of *Gorilla*.

3.3.1 Great ape and human clade

There is little disagreement on the position of hylobatids within the hominoids. Virtually all morphological and biomolecular studies agree in recognising the Hominoidea as a monophyletic group, in which *Hylobates* is the basal taxon, sister-

group of a clade that comprises *Pongo*, *Gorilla*, *Pan* and *Homo* (morphological evidence: Andrews and Cronin, 1982; Ciochon, 1983; Andrews, 1985, 1987, 1992; Groves, 1986, 1987, 1989; Andrews and Martin, 1987; Pilbeam, 1996; Shoshani et al., 1996; Gebo et al., 1997; Rae, 1997. Molecular evidence: Sarich and Wilson, 1967; Sarich, 1971; Sibley and Ahlquist, 1984, 1987; Caccone and Powell, 1989; Sibley et al., 1990). A number of morphological synapomorphies have been identified for the great ape and human clade (Table 3-5). Only few phenetic analyses (e.g. Oxnard, 1984; Corruccini, 1992, 1994) have failed to unequivocally recover the basal position of *Hylobates* within the hominoids.

Table 3-4. Synapomorphies of the extant hominoids.

Characters	Reference
Differential usage of forelimb, with potential for raising arms above head, for extending forelimb at elbow and for rotation.	Andrews, 1992
Greater flexibility of wrist and opposable thumb	Andrews, 1992
More erect posture during locomotion and feeding	Andrews, 1992
Broadening of thorax and loss of tail	Andrews, 1992
Greater mobility of hip and ankle joints	Andrews, 1992
Broad spatulate central incisors	Andrews, 1992
Low crowned premolars with no honing facet	Andrews, 1992
Relatively broad molars with rounded cusps	Andrews, 1992
Presence of a vermiform appendix	Groves, 1989
Interstitial placental implantation	Groves, 1989
Sperm mitochondria with few gyres	Groves, 1989

This table lists some of the shared morphological features commonly listed in the literature as synapomorphies of the extant apes and humans.

Recent DNA analyses that support this clade include parsimony (Bailey et al., 1992) and maximum-likelihood analyses (Goodman et al., 1994) of the ε-globin gene and non-coding sequences of the γ-globin and φη-globin genes; and parsimony and maximum-likelihood analyses of a non-coding DNA intron sequence of the serum

albumin gene and intergenic and flanking regions of the linked γ^1- and γ^2- globin gene sequences (Page and Goodman, 2001). Notably, the latter study found a very strong statistical support for this clade (100% bootstrap value). Gibbon chromosomes are also markedly different from those of great apes and humans (Marshall and Sugardjito, 1986).

Table 3-5. Synapomorphies of the great ape and human clade.

Characters	Reference
Skull with enlarged maxillary sinuses	Andrews, 1992
Orbits higher than broad	Andrews, 1992
Increased alveolar prognathism with elongated premaxilla	Andrews, 1992
Facial lengthening with elongation of nasal bones and narrow incisive foramen	Andrews, 1992
Increase in size of incisors relative to molars	Andrews, 1992
Robust and enlarged premolars relative to molar teeth, accompanied by a reduction in upper premolar heteromorphy	Andrews, 1992
Reduced molar cingula	Andrews, 1992
Robust mandible featuring a large inferior transverse torus	Andrews, 1992
Distal humerus with deep sulci either side of lateral trochlear keel	Andrews, 1992
Shortened and robust canines	Groves, 1989
Presence of upper third premolar metaconid	Groves, 1989
Reduced body hair	Groves, 1989
Reorganisation of carpal bones	Groves, 1989
Loss of ischial callosities	Groves, 1989

This table illustrates some of the morphological features shared by great apes and humans, and commonly cited in the literature as synapomorphies of this clade.

3.3.2 African ape and human clade

Many phenetic and cladistic studies (e.g. Andrews and Cronin, 1982; Ciochon, 1983; Andrews, 1985, 1987, 1988, 1992; Groves, 1986, 1987, 1989; Andrews and Martin, 1987; Groves and Paterson, 1991; Begun, 1992, 1994; Shoshani et al., 1996; Page and

Goodman, 2001) have supported the orangutan as the sister-taxon of African apes and humans. Morphological similarities among *Homo*, *Pan* and *Gorilla* that are thought to be synapomorphies are shown in Table 3-6.

Table 3-6. Synapomorphies of the African ape and human clade.

Characters	Reference
Fusion of the *os centrale* to scaphoid	Andrews,1992
Enlarged and continuous supraorbital torus	Andrews,1992
Presence of a frontal sinus	Groves,1989
Developed postorbital sulcus	Begun,1994
Greater middle ear depth	Groves,1986
Increased klinorhynchy	Andrews,1992
Elongated nasoalveolar clivus of the premaxilla with narrowing of the incisive foramen	Begun,1994
Higher humeral torsion	Begun,1994
Robust metatarsal shafts	Begun,1994
Large middle phalanges	Begun,1994
Presence of an ear-lobe	Groves,1989
Large axillary organs	Groves,1986
Broad uterus	Groves,1986
Low proportion of type I aorta	Groves,1986
Eccrine glands abundant over body	Groves,1986
Apocrine glands sparsely distributed over body	Groves,1986

The characters listed in this table are some of the morphological traits shared by African apes and humans, and commonly cited in the literature as synapomorphies of this clade.

Two alternative taxonomic arrangements have been proposed in the past for the great apes and humans. One featured a clade containing *Pongo*, *Gorilla* and *Pan* to the exclusion of *Homo* (Ponginae Hypothesis, Kluge, 1983; Figure 3-1a); the second featured two clades, one containing *Homo* and *Pongo* and the other containing *Gorilla* and *Pan* (Red Ape Hypothesis, Schwartz, 1984a, 1984b, 1986, 1987; Figure 3-1b).

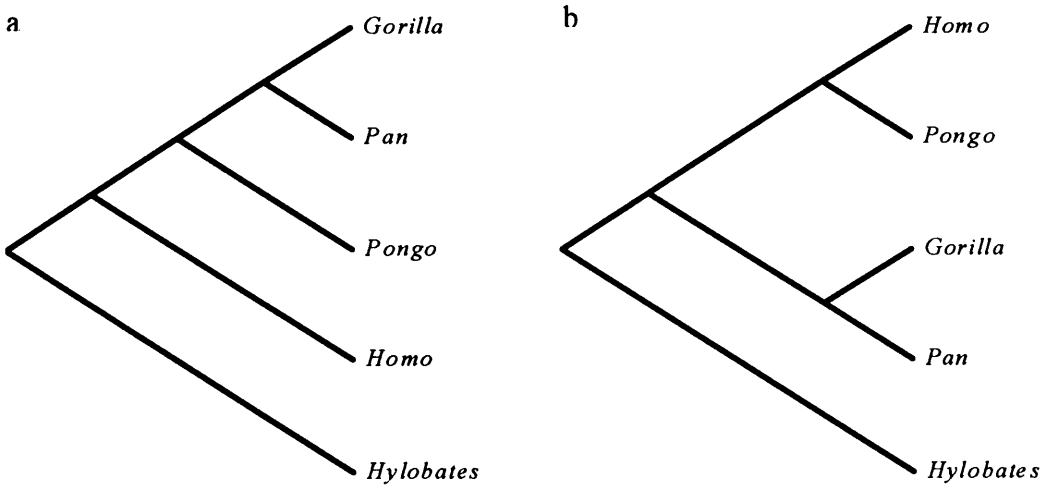

Figure 3-1. The Ponginae Hypothesis and the Red Ape Hypothesis.
These cladograms illustrate two taxonomic arrangements proposed for the great apes and humans. The Ponginae Hypothesis (a) supports a close relationship of all great apes to the exclusion of humans. The Red Ape Hypothesis (b) instead emphasises a close affinity between humans and orangutans to the exclusion of the African apes.

The Ponginae Hypothesis was put forward on the basis of 11 characters shared by the great apes (Kluge, 1983). However, Andrews (1987) demonstrated that only three of these characters could in fact be considered synapomorphies, the others being primitive retentions, allometric correlates of body size or parallel features. The Red Ape Hypothesis, instead, was based on 15 characters shared by humans and orangutans. Andrews (1987) accepted only four of these traits as potential synapomorphies and showed that the others were symplesiomorphic, ambiguous or of doubtful phylogenetic value. Hence, these two hypotheses were rejected on the basis that the characters used to support them were too few compared to the 12 synapomorphies that Andrews listed in support of an African ape and human clade.

Gorilla, *Pan* and *Homo* also share a number of biomolecular apomorphies not shared with *Pongo*. These have been emphasised in numerous reports (e.g. Zuckerkandl et

al., 1960; Goodman, 1962, 1963; Sarich and Wilson, 1967; Sarich, 1971; Sibley and Ahlquist, 1984, 1987; Sibley et al., 1990; Caccone and Powell, 1989). More recently, support has been gained from studies of orthologous DNA sequences, such as the β-globin genes (Goodman et al., 1994). Page and Goodman's (2001) analyses of the intron sequence of the serum albumin gene and intergenic and flanking regions of the γ^1- and γ^2- globin genes, supported this clade very strongly (93% bootstrap value). Interestingly, a study by Mohammadali et al. (1995) found that *Gorilla*, *Pan* and *Homo* also share an ORF (open-reading frame) sequence overlapping exon 1 in the MYC loci, not observed in *Pongo*. A recent karyological study showed that *Pan*, *Gorilla* and *Homo* share a pericentric inversion on human chromosome 11 (and its equivalent in African apes) also not shared with *Pongo* (Conte et al., 1998).

In summary, it is widely accepted that African apes and humans form a monophyletic group to the exclusion of *Pongo* and that *Hylobates* occupy a basal position within the hominoids. Much of the debate about hominoid phylogeny rests in the taxonomic arrangement within the (*Homo*, *Gorilla*, *Pan*) clade. In the next section I shall discuss some aspects of this debate and summarise the evidence in support of a chimpanzee and human clade.

3.3.3 Chimpanzee and human clade

The debate regarding hominoid phylogeny is now mainly focused on the evolutionary relationships of humans, chimpanzees and gorillas. Most molecular studies strongly support a (*Homo, Pan*) clade. The same taxonomic arrangement has also been

recently supported by soft-tissue evidence (Gibbs et al., 2000, 2002). Hard-tissue morphology, in contrast, seems to support a (*Gorilla, Pan*) clade.

a) Morphological evidence

Groves and Paterson (1991) used five different datasets containing craniodental and postcranial characters from *Homo*, *Pan*, *Gorilla* and *Pongo* to generate phylogenetic hypotheses for these taxa. The favoured solution supported a *Pan-Gorilla* clade although the authors acknowledged that their analysis produced contrasting topologies that seemed equally acceptable. In fact, the morphological approach to the study of hominoid phylogeny has long favoured a hypothesis in which the African apes share a common ancestor not shared with humans (Figure 3-2). Only recently an analysis based on non-skeletal (soft-tissue) morphological traits has found a strong support for the (*Homo, Pan*) clade (Gibbs et al., 2000, 2002).

Various morphological similarities can be cited in support of the (*Gorilla, Pan*) clade and in support of the (*Homo, Pan*) clade (Table 3-7). The main argument in favour of the former taxonomic arrangement centres on two character complexes shared by gorillas and chimpanzees: one related to knuckle-walking and the other to thin dental enamel. Given the complex nature of these two traits, which are composed of a number of functionally related characters, it has been argued that it is unlikely that they evolved independently in these two lineages, and since they are not shared with humans, they seem to strongly support an African ape clade. However, as pointed out by Mann and Weiss (1996), in view of new fossil discoveries, this line of evidence may need to be reconsidered, as explained below.

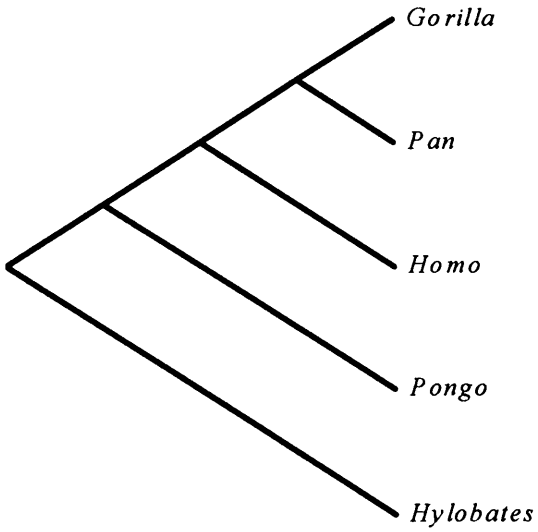

Figure 3-2. Phylogenetic relationships of hominoids from skeletal data.
This cladogram illustrates the phylogenetic relationships of apes and humans recovered from skeletal characters. The African apes are grouped in one clade to the exclusion of humans.

The discovery of the early hominin species *Ardipithecus ramidus* (White et al., 1994) showed that thin enamel is probably the primitive state for *Homo*, *Pan* and *Gorilla*, and therefore a symplesiomorphy of gorillas and chimps rather than a synapomorphy. Interestingly, the newly described *Sahelanthropus tchadensis* (Brunet et al., 2002), a species that lived close to the split of hominins from chimpanzees, possesses enamel thickness of the molar teeth intermediate between *Pan* and *Australopithecus*. Furthermore, a recent analysis of extant and fossil hominoids using skeletal features of the distal radius indicated that two of the earliest representatives of the human lineage, *Australopithecus anamensis* and *A. afarensis*, possessed anatomical specialisations of the wrist related to knuckle-walking (Richmond and Strait, 2000; see also Corruccini, 1978; Corruccini and McHenry, 2001; Richmond and Strait, 2001). This finding suggests that the common ancestor of humans, gorillas and

chimpanzees may have been a knuckle-walker and in this case this locomotory behaviour would be a primitive retention for the African apes (Mann and Weiss, 1996; Pilbeam, 1996; Collard and Aiello, 2000), a possibility that had been previously considered by some authors (Sarich, 1971; Lewis, 1989; Shea and Inouye, 1993) but rejected by others (e.g. Tuttle, 1969; Andrews, 1987; Andrews and Martin, 1987; Susman and Stern, 1991). It also refutes the hypothesis that knuckle walking evolved in parallel in the African apes (Dainton and Macho, 1999).

Table 3-7. Characters in support of different sister-group relationships for the African apes and humans.

Sister groups	**Shared similarities**	References
(*Homo,Pan*)	I^2 similar in size and shape to I^3	Andrews and Martin, 1987
	Basal keel of lower canine absent	Groves and Paterson, 1991
	Pendulous scrotum	Groves and Paterson, 1991
	Ankle epiphyses fuse at same time as hip and elbow	Groves and Paterson, 1991
(*Gorilla,Pan*)	Proportion Pattern 1 Enamel	Groves and Paterson, 1991
	Thumb short relative to body weight	Groves and Paterson, 1991
	Dorsal extension of articular surface of metacarpals	Groves and Paterson, 1991
	Flexor digitorum superficialis strongly developed	Groves and Paterson, 1991

The characters listed in this table are some of the traits commonly listed in the literature in support of the close relationship between humans and chimpanzees (*Homo, Pan*), and between gorillas and chimpanzees (*Gorilla, Pan*).

b) Molecular evidence

A growing amount of evidence suggests that, in some groups of primates (e.g. papionins and hominoids), molecular phylogenies are more reliable than phylogenies based on morphology. Morphology is the phenotypic expression of the information carried by DNA and therefore it can only ever be used as a proxy for molecular data (Collard and Wood, 2001). Many phylogenetic hypotheses produced using molecular techniques find strong support by multiple lines of independent evidence (Ruvolo, 1997), which is the best way of gaining support for a phylogenetic hypothesis. In addition, unlike most molecular traits, bone is a dynamic and multifunctional tissue and, as a result, is subject to changes throughout ontogeny due to environmental stimuli (Lieberman, 1995, 1996, 1997, 1999; Lieberman et al., 1996). These changes can potentially obscure the phylogenetic signal carried by this type of data and produce unreliable phylogenies.

Phylogenetic methodologies as applied to molecular data have also been tested successfully using organisms whose evolutionary histories are known, e.g. lab-generated mice strains (Fitch and Atchley, 1987) and bacteriophage T7 strains (Hillis et al., 1992). These studies concluded that, in phylogenetics, molecular data are superior to morphological and life-history data. Analogous tests for skeletal phylogenies have not yielded similarly successful results (Fitch and Atchley, 1987).

Most molecular studies strongly support a (*Homo*, *Pan*) clade with *Gorilla* as its sister-taxon (Figure 3-3). Only a few (e.g. Goodman, 1962, 1963; Sarich and Wilson, 1967; Benveniste and Todaro, 1976) were unable to confidently resolve the

relationships within the African apes and human clade. However, rather than supporting other taxonomic arrangements, they point to a 'trichotomy' as the best solution. Weak support for a (*Homo*, *Pan*) clade was provided by amino acid sequence analyses (Goodman et al., 1983, 1989); η-globin gene sequence analyses (Koop et al., 1986; although later work favoured a closer relationship between chimps and humans, Koop et al., 1989); immunoglobin ε pseudogene sequence analysis (Ueda et al., 1989); and Ruano et al.'s (1992) analysis of the HOX2 gene.

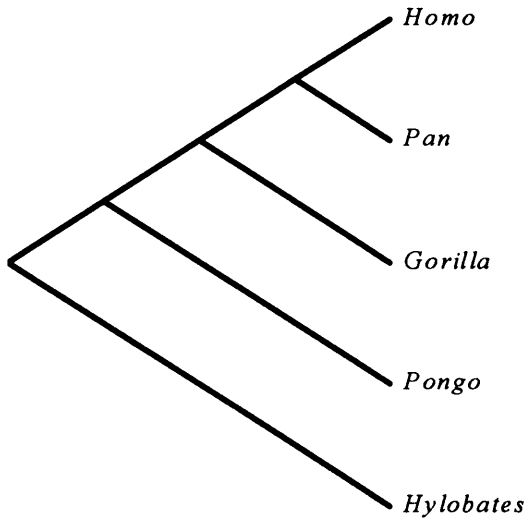

Figure 3-3. Phylogenetic relationships of hominoids from molecular data.
This cladogram illustrates the phylogenetic relationships of apes and humans recovered from molecular data. Humans and chimpanzees are more closely related to each other than to any other ape. The same topology was recently also recovered from soft-tissue data.

A trichotomy was indicated as the best solution in a study of terminal bands on metaphase chromosomes in great apes and humans (Deinard et al., 1998). These bands, composed of 32bp repeat sequences (minisatellites), are present on terminal sites of 21 of the 48 chromosome arms (plus 2 interstitial sites) of gorillas and both

species of chimps. However, they do not occur either in *Homo* or in *Pongo*. Cytogenetic evidence has been argued to provide strong evidence for a (*Gorilla*, *Pan*) clade, because it provides complex genetic traits unlikely to have evolved in parallel (Marks, 1993). However, it should be noted that the processes underlying chromosome evolution are not well understood (Andrews, 1987) and cytogenetic studies have provided support for each of the possible topological arrangements within the (*Homo*, *Pan*, *Gorilla*) clade (e.g. Miller, 1977; Yunis and Prakash, 1982; Stanyon and Chiarelli, 1982; Marks, 1983, 1993). Interestingly, in a paper from the classic book "Classification and Human Evolution" (Ed. Washburn, 1963), Klinger et al. concluded that "the chromosome set of *Pan troglodytes troglodytes* more closely resembles that of man" (1963:236). The trichotomy problem was also addressed recently by Satta et al. (2000). They compared 45 nuclear loci in humans, chimpanzees and gorillas and other primate species and found that 60% of them supported a *Pan-Gorilla* clade, while 40% supported the alternative arrangements. Overall, there is relatively little molecular evidence in support of a (*Gorilla*, *Pan*) clade (e.g. Brown et al., 1982; Templeton, 1983; Djian and Green, 1989; Conte et al., 1998).

As Ruvolo (1994) has pointed out, most DNA sequence analyses unequivocally support an African apes and human clade. For example, statistically significant support for this clade can be found in Perrinpecontal and colleagues' (1992) study of the δ-β-globin intergenic region, and Barriel and colleagues' (1993) analysis of the pseudo ε-globin gene. More recently, Barriel's (1997) parsimony analysis of the pseudo ε-globin gene from 13 species of primates (including *P. paniscus*, *P. troglodytes*, *Gorilla*, *Pongo*, *Homo* and *Hylobates*) also strongly supported a (*Homo*,

Pan) clade (93% bootstrap value). Particularly strong evidence is provided by mitochondrial DNA (e.g. Horai et al., 1992; Ruvolo, 1994). The analysis of the number of base substitutions on complete sequences of hominoid mt-DNA (Horai et al., 1995) showed that the sequences of *Pan* and *Homo* are the most similar. It is noteworthy that the only region of the mitochondrial genome that disagrees with this conclusion (the 12SrRNA sequence, which nests *Gorilla* and *Pan* together) is not considered valuable and reliable for phylogenetic inference. Horai and colleagues (1995) have suggested that the conflict may derive from chance alone. Evidence from MYC loci of African apes and humans (Mohammadali et al., 1995) and variations in ribosomal DNA spacers (Suzuki et al., 1994) also support an earlier departure of *Gorilla* from the chimpanzee-human lineage.

An interesting additional line of evidence comes from the CMT1A-REP sequence on human chromosome 17 (Keller et al., 1999). This sequence consists of two copies of a short stretch of DNA at the proximal and distal ends of a 1.5-Mb region containing a dosage-sensitive gene. A comparative analysis among primates showed that the primitive condition includes only the distal element of this sequence (as observed in gorillas, orangutans, gibbons, baboon and strepsirrhine taxa). However, only humans and both species of chimps share a proximal element that can be interpreted as a synapomorphy of a (*Homo*, *Pan*) clade. Similarly, a study of the Y-chromosome indicated that male humans and male chimpanzees also share a DNA fragment (λ-YH2D6) not shared with male gorillas and male orangutans (no homologous sequence was detected in the females of any of these taxa) (Rasheed et al., 1991).

Data from non-coding sequences of nuclear DNA also seems to point to a sister-group relationship between humans and chimps (e.g. Bailey et al., 1992; Goodman et al., 1994). Recently, maximum-parsimony and maximum-likelihood were applied to sequence data from two unlinked nuclear loci, the intron sequences of the serum albumin gene (on human chromosome 4) and the intergenic and flanking regions of the linked γ^1- and γ^2- globin genes (on human chromosome 11) (Page and Goodman, 2001). Both analyses gave statistically significant support to monophyly of the two chimpanzee species and to a (*Homo*, *Pan*) clade (96% bootstrap support). More evidence from non-coding nuclear DNA is found in a ~1.0 Kb intergenic HOXB6 sequence (Deinard and Kidd, 1999). Comparison of this region among humans and great apes highlighted two nucleotide substitutions shared by humans and the two species of chimps only. However, the authors were cautious in making any phylogenetic inference from this data and suggested a 'trichotomy' as the best representation for the speciation among African apes and humans, since the study showed that a high level of genetic polymorphism existed within the common ancestor of *Homo*, *Pan* and *Gorilla*.

More recently, various statistical approaches to the question of hominoid phylogeny have been undertaken in an attempt to evaluate the confidence that can be invested in current molecular phylogenies. Czelusniak and Goodman (1995) employed goodness-of-fit statistics to compare the multinomial distributions of nucleotide character patterns expected from 16 models of hominoid evolution, with the observed distribution of nucleotide patterns. They based their statistical evaluation on orthologous non-coding sequences from the γ haemoglobin genomic region. P-values (i.e. probabilities of obtaining goodness-of-fit values higher than the observed ones)

were estimated under the assumption that very low probabilities falsify the hypothesis of relationship. All the possible 16 unrooted topologies for the five extant hominoid genera (including an arrangement that represent an African ape and human trichotomy) had P-values smaller than 0.01, except the one in which humans and chimps were sister groups.

Lastly, in what is widely considered to be the definitive study on hominoid molecular relationships, Ruvolo (1997) applied a multiple-locus test to group all DNA sequences available for studying hominoid evolutionary history into independent datasets. She obtained 14 independent groups, 11 of which supported a (*Homo*, *Pan*) clade; one supported a (*Pan*, *Gorilla*) clade; and one supported a (*Homo*, *Gorilla*) clade. The multiple-locus test favoured a (*Homo*, *Pan*) clade and rejected the alternative hypotheses (at the 0.002 significance level). Ruvolo (1997: 248) concluded that the available DNA sequences are enough to consider the question of the hominoid trichotomy "confidently resolved".

3.3.4 Conclusion

Many authors now agree that the molecular data for the hominoids strongly support a human-chimpanzee clade with gorilla as their sister group. Morphological characters that were traditionally used to support a gorilla-chimpanzee clade can be classified as primitive for the African ape and human clade and therefore uninformative about the evolutionary relationships among these groups. A recent composite phylogeny of 203 primate species was produced in a meta-analysis of published phylogenetic studies (Purvis, 1995). The phylogenies used were recovered from various types of evidence

and using different phylogenetic techniques, e.g. maximum-likelihood trees, cladistic analyses of morphological, molecular, karyotipic and behavioural characters, phenograms based on morphological and behavioural data. The consensus tree featured 160 nodes. All the relationships among apes and humans were correctly resolved and a close relationship between *Homo* and *Pan* was supported. In other words, the amount of evidence and studies accumulated so far support a phylogeny for the apes and humans consistent with the consensus molecular tree.

The evidence discussed in this chapter illustrates that there is a conflict between hominoid molecular and some morphological phylogenies. This was emphasised in a study by Barriel (1997) in which 72 skeletal characters were used in a cladistic analysis of hominoids using Cercopithecoidea and Platyrrhini as outgroups. The most parsimonious cladogram supported *Homo* as the sister-group of the African apes but the genus *Pan* was paraphyletic, with *P. troglodytes* being more closely related to *Gorilla* than to *P. paniscus*. This topology was also weakly supported and changed completely when just one soft-tissue and two behavioural characters were added to the analysis. In contrast, the phylogeny generated using molecular data ($\psi\eta$-globin gene) produced a strongly supported tree in which *Pan* was monophyletic and more closely related to *Homo* than to *Gorilla*. The 'total evidence' (*sensu* Kluge, 1989), represented by a matrix that combined molecular, morphological and behavioural data, yielded one most parsimonious tree identical to the one obtained from the molecular dataset and this was 'retained as the best supported phylogenetic hypothesis' (Barriel, 1997: 55). In conclusion, a 'total evidence approach' to the problem of hominoid phylogeny indicates that a (*Homo*, *Pan*) clade is the current best hypothesis on the relationships among African apes and humans (Pilbeam, 1996).

3.4 Systematics of the outgroup taxa (*Cercopithecus, Colobus* and *Papio*)

Three groups of Old World monkeys (Superfamily Cercopithecoidea, Gray, 1821) were included in the cladistic analyses to root the cladograms: *Cercopithecus*, *Colobus* and *Papio*. These genera belong to the Family Cercopithecidae (Gray, 1821). This family is divided into two subfamilies, Cercopithecinae (Gray, 1821), which includes *Cercopithecus* and *Papio*, and Colobinae (Jerdon, 1867), which includes *Colobus*. Skeletal differences are present although they are usually subtle (Groves, 2000). The following sections briefly summarise the taxonomy, biogeography and phylogenetic relationships of these three outgroup taxa.

3.4.1 Genus *Papio* (Linnaeus, 1758): baboons

Baboons belong to a group of monkeys collectively known as the papionins (Tribe Papionini, Burnett, 1828) that also includes *Theropithecus*, *Mandrillus*, *Cercocebus*, *Lophocebus* and *Macaca*. Baboons are found primarily in Africa where they populate the savannah and the margins of the forest belt. A small population is also found in southern Arabia. Five phenotypically distinct species are commonly recognised for this genus (Table 3-8) mainly from pelage patterns. Species hybridisation is known to occur between some neighbouring populations (Groves, 2001).

Table 3-8. Taxonomy and biogeography of the genus *Papio*.

Species name	Common name
Papio hamadryas (Linnaeus, 1758)	Sacred (or Mantled/Hamadryas) baboon
Papio cynocephalus (Linnaeus, 1766)	Yellow baboon
Papio ursinus (Kerr, 1792)	Chacma baboon
Papio papio (Desmarest, 1820)	Guinea baboon
Papio anubis (Lesson, 1827)	Olive baboon

Data from Groves (2001).

3.4.2 Genus *Cercopithecus* (Linnaeus, 1758): guenons

Guenons are a large and diverse group of primates that live in sub-Saharan Africa. They occupy many different habitats from woodlands, to swamp forests, low-land, mid-land and highland forests, alpine moor-land and the dry edges of deserts (Butynski, 2002). There is no consensus over the taxonomy of the group. Recent taxonomic classifications for the guenons differ in the total number of species (ranging from 23 to 36) and in what species should be placed within *Cercopithecus*. The narrow definition of guenons includes only the members of the genus *Cercopithecus* (e.g. Groves, 2001). A broader definition of guenons, on the other hand, also includes *Miopithecus*, *Allenopithecus*, and *Erythrocebus*, that is, all the genera within the Tribe Cercopithecini (Gray, 1821). The latter is currently the most widely adopted scheme (Butynski, 2002). Here, I follow Grubb et al.'s (2002) taxonomic scheme for the genus *Cercopithecus* – reported in (Butynski, 2002) – which includes 19 species (Table 3-9).

Table 3-9. Taxonomy and biogeography of the genus *Cercopithecus*.

Species name	Common name
C. dryas (Schwarz, 1932)	Salongo monkey
C. diana (Linnaeus, 1758)	Diana and Roloway monkey
C. aethiops (Linnaeus, 1758)	Vervet, Grivet, Tantalus, Green and Malbrouck Monkeys
C. cephus (Linnaeus, 1758)	Mustached guenons
C. nictitans (Linnaeus, 1766)	Greater spot-nosed monkey
C. petaurista (Schreber, 1774)	Lesser spot-nosed monkey
C. mona (Schreber, 1775)	Mona monkey
C. ascanius (Audebert, 1799)	Red-tailed monkey
C. mitis (Wolf, 1822)	Blue monkey
C. pogonias (Bennett, 1833)	Crowned Monkeys
C. campbelli (Waterhouse, 1838)	Campbell's Mona Lowe's Mona
C. erythrotis (Waterhouse, 1838)	Red-eared guenon
C. erythrogaster (Gray, 1866)	White-throated guenon
C. neglectus (Schlegel, 1876)	De Brazza's monkey
C. preussi (Matschie, 1898)	Preuss's monkey
C. lhoesti (Sclater, 1899)	L'Hoest's monkey
C. sclateri (Pocock, 1904)	Sclater's guenon
C. hamlyni (Pocock, 1907)	Owl-faced monkey
C. solatus (Harrison, 1988)	Sun-tailed monkey

Data from Groves (2001)

3.4.3 Genus *Colobus* (Illinger, 1811): black-and-white Colobus monkeys

The genus *Colobus* is one of the African genera of the subfamily Colobinae. Colobines are anatomically, ecologically and socially diverse (Oates and Davies, 1994). They inhabit forest and woodland habitats in tropical Africa and South and East Asia. The genus includes monkeys with long black or black-and-white pelage. There are five species currently assigned to this genus (Oates et al., 1994; Groves, 2001) and these are listed in Table 3-10. Each species has a different coat pattern and can be distinguished craniodentally from the others (Verheyen, 1962; Oates et al., 1994).

Table 3-10. Taxonomy and biogeography of the genus *Colobus*

Species name	Common name
Colobus polykomos (Zimmermann, 1780)	King Colobus
Colobus vellerosus (I. Geoffroy, 1834)	Ursine Colobus
Colobus guereza (Rüppell, 1835)	Mantled Guereza
Colobus satanas (Waterhouse, 1838)	Black Colobus
Colobus angolensis (Sclater, 1860)	Angolan Colobus

Data from Groves (2001)

3.4.4 Phylogenetic relationships

The phylogenetic relationships within the outgroup are taken from Purvis' (1995) composite phylogeny and are illustrated in Figure 3-4. According to this cladogram, *Colobus*, *Papio* and *Cercopithecus* form a clade in which *Papio* and *Cercopithecus*

are more closely related to each other than either is to *Colobus*. This arrangement is also supported by Shoshani et al.'s (1996) cladistic analysis, which was based on 264 morphological characters, and which found a strong support for a cercopithecine clade (99%) to the exclusion of colobines. The same arrangement is supported by recent phylogenetic analyses of two serum albumin gene's intron sequences, and non-coding sequences of the γ^1-γ^2 globin genes (Page and Goodman, 2001) which found a very strong bootstrap support for a cercopithecine clade (100%) and for a cercopithecid clade (100%).

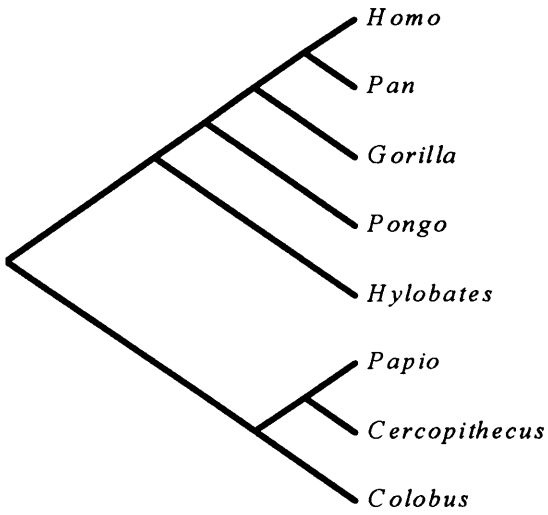

Figure 3-4. Molecular relationships of the ingroup and outgroup taxa.
This cladogram illustrates the molecular relationships of the hominoid ingroup and the cercopithecine outgroups. This cladogram is the one against which the cladograms generated from nerve- and vessel-related characters will be evaluated later in this project.

3.5 Summary

In this chapter I have presented an overview of the taxonomy and biogeography of the extant hominoids and discussed their phylogenetic relationships. I described the

morphological and molecular evidence in support of (or against) each of the clades present in their molecular relationships, with particular emphasis on the affinities among African apes and humans. The aim of this account was to provide support to the assumption that the relationships among apes and humans are well understood and strongly supported by the available evidence, particularly the vast amount of molecular studies published to date. As discussed at the beginning of the chapter, that the true phylogeny of the extant hominoids can be considered known for the purposes of further analysis, is one of the main assumptions of this study.

In sum, many authors now agree that the molecular data for the hominoids strongly support a human-chimpanzee clade with gorilla as their sister group. Orangutans are the sister-group of the African apes and humans, while gibbons occupy a basal position within the hominoid clade. I have also shown that morphological characters that were traditionally used to support a gorilla-chimpanzee clade are probably best classified as primitive for the African ape and human clade and therefore uninformative about the evolutionary relationships among these groups. Overall, the evidence presented and discussed in this chapter provides strong support for the assumption that the relationships among apes and humans are well understood and strongly supported by the available evidence.

Chapter 4. MATERIALS AND METHODS

4.1 Description of sample

The sample used in this study comprised representatives of the five extant hominoid genera – *Pan, Gorilla, Pongo, Hylobates* and *Homo* – plus three Old World monkey taxa – *Papio, Cercopithecus* and *Colobus*. The sample is described in details in Table 4-1. The specimens were examined at the Natural History Museum (London), the Duckworth Laboratory (Cambridge), the Royal Museum of Central Africa (Tervuren), the State Collection for Anthropology and Palaeoanatomy (Munich), the Anthropological Institute and Museum, University of Zurich-Irchel (Zurich), and the Swedish Natural History Museum (Stockholm).

In order to provide an accurate representation of the morphological variation present in these taxonomic groups, individuals from as many subspecies as possible were included. Unfortunately, some subspecies (e.g. *Gorilla gorilla beringei* and *Pan troglodytes verus*) are underrepresented in museum collections. The number of species present in each hominoid and cercopithecine genus varies from one (e.g. *Homo*) to 14 (e.g. *Hylobates*) (Groves, 2001). In the case of genera with more than two species (i.e. *Hylobates*, *Colobus*, *Cercopithecus*, *Papio*), I sampled only two of the best represented species in the museum collections. These limits were imposed by the need to study adults of known sex, and by the need to gather a reasonable amount of data for numerous variables, which is time-consuming.

Information on the sex of each specimen was gathered from museum catalogues and specimen labels. Individuals of both sexes were included in the analysis in equal numbers as far as possible. In the case of *Hylobates* (*Symphalangus*) *syndactylus* the museum collections were strongly biased towards males, so the females of this species are underrepresented in my sample. All specimens were adult individuals. This was ascertained from the information provided by the museum catalogues, the labels on the specimens and the pattern of tooth eruption. When these were incongruent, priority was given to the pattern of tooth eruption, as explained below.

Braga (1995) considered two age categories. The first, called Adult 1 (A_1), included individuals with a complete permanent dentition before the fusion of the spheno-occipital synchondrosis. This age group ranges between 12 and 14 years in the great apes, and between 18 and 21 years in humans. The second, referred to as Adult 2 (A_2), included specimens that showed a complete permanent dentition and a fused spheno-occipital synchondrosis. This age category corresponded to individuals older than 14 years in the great apes, and individuals older than 21 years in humans. However, Prat (2003) observed in her sample of great apes and humans five human specimens with a complete spheno-occipital synchondrosis but an incomplete permanent dentition. It follows that she could not assign a part of her sample to either A_1 or A_2. Hence she defined adults based solely on the presence of a complete permanent dentition. This corresponds to an age of at least 12 years in great apes, and at least 18 years in humans. For this reason and because I did not carry out any ontogenetic analysis of the characters I studied, I followed Prat's (2003) identification system of adult specimens.

Table 4-1. Sample size and composition.

Genus	Species	Subspecies	N	N_M	N_F
Pan	*P. paniscus*		30	14	16
	P. troglodytes	*P.t.troglodytes*	12	6	6
		P.t.verus	5	4	1
		P.t.schweinfurthii	13	7	6
			60	**31**	**29**
Gorilla	*G. gorilla*	*G.g.gorilla*	13	7	6
		G.g.graueri	14	7	7
		G.g.beringei	3	2	1
			30	**16**	**14**
Pongo	*P. pygmaeus*	*P.p.pygmaeus*	19	10	9
		P.p.abelii	12	4	8
			31	**14**	**17**
Hylobates	*H. moloch*		20	8	12
	H. lar		10	6	4
H. (Symphalangus)	*H. (S.) syndactylus*		29	21	8
			59	**35**	**24**
Colobus	*C. polykomos*		11	5	6
	C. angolensis		10	5	5
			21	**10**	**11**
Papio	*P. ursinus*		10	6	4
	P. anubis		10	4	6
			20	**10**	**10**
Cercopithecus	*C. aethiops*		11	5	6
	C. mona		10	5	5
			21	**10**	**11**
Homo	*H. sapiens*		**48**	**25**	**23**
		TOTAL	**290**	**151**	**139**

See Appendix I for full description of the samples. Numbers in bold represent totals by genus and by sex.

4.2 Character analysis

The characters examined and the way they were scored are described and illustrated in more details in Appendix II. The following variables were taken into account whenever possible: the number of occurrences on each side of the skull, the size of the main/largest feature, its shape and structure, and its location in relationship to other

anatomical features (Msuya and Harrison, 2001). The definitions in Appendix II are taken from Gray's Anatomy (1999) and Hauser and De Stefano (1989) unless otherwise stated.

The frequency and metric values of the characters examined are summarised in Appendix III. For multi-state non-metric characters ($ZTFP_1$, $ZTFP_2$, ZOFP, MaFP, PaF, ZFFP and PEFP) the frequencies of the character states were such that no single character state could be described as being taxon-specific in any of the species considered. In these cases, following Pleijel (1995), each character state was treated as a character on its own and scored as absent (0) or present (1). For example, the position of the zygomatico-temporal foramen ($ZTFP_1$), originally scored as sutural (0), zygomatic (1) or frontal (2), was split into three separate characters: zygomatico-temporal foramen on the frontal bone ($ZTFP_1a$): absent (0) and present (1); zygomatico-temporal foramen on the suture ($ZTFP_1b$): absent (0) and present (1); and zygomatico-temporal foramen on the zygomatic bone ($ZTFP_1c$): absent (0) and present (1). Thus, a total of 112 characters was reached (Table 4-2). Twenty-one of these were metric and 91 were non-metric, frequency characters.

These 112 characters were subjected to four preliminary analyses. The first of these evaluated the amount of intra-observer error in order to determine measurement reliability. The second looked for differences between the right and left sides of the skull. The third assessed the amount of sexual dimorphism in the data. The last preliminary analysis looked for non-phylogenetic correlations between pairs of characters within each species.

Table 4-2. Soft tissue-linked characters used in this study.

No	CODE	CHARACTER	TYPE
1	IOF	Accessory infraorbital foramina	Frequency
2	ZTF	Zygomatico-temporal foramina	Frequency
3	ZFF	Zygomatico-facial foramina	Frequency
4	PEF	Posterior ethmoid foramen	Frequency
5	MaF	Mastoid foramen	Frequency
6	IOB	Infraorbital bridge	Frequency
7	ION	Infraorbital notch	Frequency
8	ICIO	Infraorbital canal internal opening, anterior	Frequency
9	IOG	Infraorbital groove	Frequency
10	SLGB	Supralacrimal structures	Frequency
11	SON	Supraorbital notch	Frequency
12	SOF	Supraorbital foramen	Frequency
13	$ZTFP_1b$	Zygomatico-temporal foramen position, sutural	Frequency
14	$ZTFP_1c$	Zygomatico-temporal foramen position, zygomatic	Frequency
15	$ZTFP_1a$	Zygomatico-temporal foramen position, frontal	Frequency
16	$ZTFP_2b$	Zypomatico-temporal foramen position, plate	Frequency
17	$ZTFP_2a$	Zygomatico-temporal foramen position, bar	Frequency
18	ZOFPb	Zygomatico-orbital foramen position, sutural	Frequency
19	ZOFPa	Zygomatico-orbital foramen position, frontal	Frequency
20	ZOFPc	Zygomatico-orbital foramen position, zygomatic	Frequency
21	ZFN	Zygomatico-facial notch	Frequency
22	ZFFPc	Zygomatico-facial foramen position, zygomatic	Frequency
23	ZFFPa,b	Zygomatico-facial foramen position, corpus	Frequency
24	AEFP	Anterior ethmoid foramen position, sutural	Frequency
25	FRo	Foramen rotundum	Frequency
26	OcF	Occipital foramen	Frequency
27	PEFPb	Posterior ethmoid foramen position, sutural	Frequency
28	SOFi	Superior orbital fissure	Frequency
29	PEFPa	Posterior ethmoid foramen position, frontal	Frequency
30	MMAE	Middle meningeal artery emissaries	Frequency
31	MaFPb	Mastoid foramen position, sutural	Frequency
32	MaFPa	Mastoid foramen position, mastoid	Frequency
33	MaFPc	Mastoid foramen position, occipital	Frequency
34	SMB	Stylomastoid bridge	Frequency
35	SMFP	Stylomastoid foramen position, posterior to biporionic line	Frequency
36	PaF_1	Parietal foramen, parietal	Frequency
37	PaF_2	Parietal foramen, sutural	Frequency
38	PaF_3	Parietal foramen, occipital	Frequency
39	$CaCP_1$	Carotid canal position, posterior to biporionic line	Frequency
40	$CaCP_2$	Carotid canal position, at level with Basion	Frequency
41	IOFSz	Infraorbital foramen size	Metric
42	ZTFSz	Zygomatico-temporal foramen size	Metric
43	ZFFSz	Zygomatico-facial foramen size	Metric

Table 4-2, continued. Soft tissue-linked characters used in this study.

44	MaFSz	Mastoid foramen size	Metric
45	SMFSz	Stylomastoid foramen size	Metric
46	CaCSz	Carotid canal size	Metric
47	JuFL	Jugular foramen length	Metric
48	HyCSz	Hypoglossal canal size	Metric
49	FOvSz	Foramen ovale size	Metric
50	GPFSz	Greater palatine foramen size	Metric
51	LPFSz	Lesser palatine foramen size	Metric
52	MeFSz	Mental foramen size	Metric
53	MbFSz	Mandibular foramen size	Metric
54	$IOFP_1$	Infraorbital foramen position, minimum sutural distance	Metric
55	$IOFP_2$	Infraorbital foramen position, transverse sutural distance	Metric
56	$MbFP_1$	Mandibular foramen position, Gonion	Metric
57	FMaSz	Foramen Magnum size	Metric
58	InCL	Incisive canal diameter	Metric
59	$MeFP_1$	Mental foramen position	Metric
60	InCP	Incisive canal position	Metric
61	$IOFP_3$	Infraorbital foramen position	Metric
62	IJPE	Infrajugular process expression	Frequency
63	HyC	Hypoglossal canal divisions	Frequency
64	ICC	Intermediate condylar canal	Frequency
65	CoC	Condylar canal	Frequency
66	CoCO	Condylar canal internal opening, jugular	Frequency
67	CPC	Craniopharyngeal canal	Frequency
68	MgF	Marginal Foramen	Frequency
69	FOv	Foramen ovale, complete medial wall	Frequency
70	FOvP	Foramen ovale position, sutural	Frequency
71	MBC	Median basilar canal	Frequency
72	JuB	Jugular bridging	Frequency
73	FMaS	Foramen Magnum, round shape	Frequency
74	$FMaP_2$	Foramen Magnum position, posterior to stylomastoids	Frequency
75	$FMaP_1$	Foramen Magnum position, posterior to biporionic line	Frequency
76	InF	Innominate canal	Frequency
77	FSp	Foramen spinosum	Frequency
78	FVe	Foramen of Vesalius	Frequency
79	PSB	Pterygospinous bridge	Frequency
80	PAB	Pterygoalar bridge	Frequency
81	FSpP	Foramen spinosum position, sutural	Frequency
82	FLa	Foramen lacerum	Frequency
83	RaC_2	Squamosal foramen	Frequency
84	RaC_1	Postglenoid foramen	Frequency
85	GPFP	Greater palatine foramen position, sutural	Frequency

Table 4-2, continued. Soft tissue-linked characters used in this study.

86	PCr	Palatine crests	Frequency
87	LPF	Lesser palatine foramen	Frequency
88	LPFP	Lesser palatine foramina position, sutural	Frequency
89	MeF	Accessory mental foramen	Frequency
90	$MbFP_2$	Mandibular foramen position, above dental row	Frequency
91	SeC	Serres canal	Frequency
92	MoF	Molar foramen	Frequency
93	RMF	Retromolar foramen	Frequency
94	RoC	Robinson canal	Frequency
95	MyB	Mylohyoid Bridge	Frequency
96	CSF	Clinoidescaroticum foramen	Frequency
97	PCF	Posterior clinoid foramen	Frequency
98	IFF	Inferior orbital fissure foramen	Frequency
99	$MeFP_2$	Mental foramen position, under P3	Frequency
100	InC	Incisive canal, single or double	Frequency
101	PFn	Palatine fenestrae	Frequency
102	SMFS	Stylomastoid foramen shape, round	Frequency
103	IOFS	Infraorbital foramen shape, round	Frequency
104	CaCS	Carotid canal shape, round	Frequency
105	GPFS	Greater palatine foramen shape, round	Frequency
106	MeFS	Mental foramen shape, tear-shaped	Frequency
107	ZTFS	Zygomaticotemporal foramen shape, round	Frequency
108	MaFS	Mastoid foramen shape, round	Frequency
109	LPFS	Lesser palatine foramen shape, round	Frequency
110	MbFS	Mandibular foramen shape, round	Frequency
111	ZFFS	Zygomaticofacial foramen shape, round	Frequency
112	SGB	Supragenial bridge	Frequency

4.2.1 Intra-observer error

The intra-observer error was determined for both metric and non-metric variables. Six specimens (12 sides) were chosen from the sample and the characters were scored and measured twice: one *Colobus angolensis*, one *Papio ursinus*, one *Cercopithecus aethiops*, one *Pongo pygmaeus*, one *Pan troglodytes* and one *Pan paniscus*. The error was computed in each case as follows.

*a) Metric variables (*Er*)*

The intra-observer error *Er* for the ith variable was calculated as:

$$Er_i = \frac{|X - X'|}{\overline{X}} \times 100$$

where X is the original measurement, X' is the second measurement, $\overline{X}$ is their average. This method follows Chamberlain and Wood (1987). An overall value for the intra-observer error was computed as the mean of all the Er_i values. This was 8.66%, which is relatively high. In order to investigate which factors may be at the source of this relatively high error rate, I calculated the mean error for each specimen. These are reported in Table 4-3.

The average intra-observer error per specimen varied from 4.52% (*Pan troglodytes*) to 16.65% (*Colobus angolensis*). These values are also relatively high, indicating that the metric variables used in this study are subject to a high degree of intra-observer error. It is also clear that the specimens that are subject to the greatest errors are the three small-bodied cercopithecine specimens, *Colobus angolensis*, *Cercopithecus aethiops* and *Papio ursinus*. The large-bodied *Pan troglodytes*, *Pan paniscus* and *Pongo pygmaeus* show lower values. This suggests that the accuracy of these measurements is affected by the small size of these primates. Smaller primates will have relatively smaller foramina, and as features become smaller, it is more difficult to define their margins. If this is true then measurements based on clear landmarks (e.g. position measurements) will be the most precise and the size measurements for

the smaller foramina will be less precise than the measurements for the larger foramina.

Table 4-3. Average intra-observer errors for the remeasured specimens

Specimen		Sex	Side	%Er	%Ag
Colobus	*angolensis*	M	R	13.26	96.70
Colobus	*angolensis*	M	L	16.65	100.00
Papio	*ursinus*	M	R	10.20	94.51
Papio	*ursinus*	M	L	11.87	95.00
Cercopithecus	*aethiops*	F	R	12.95	97.80
Cercopithecus	*aethiops*	F	L	8.26	100.00
Pongo	*pygmaeus*	F	R	5.05	92.31
Pongo	*pygmaeus*	F	L	5.64	92.50
Pan	*troglodytes*	M	R	4.52	92.31
Pan	*troglodytes*	M	L	5.08	97.50
Pan	*paniscus*	F	R	4.82	96.70
Pan	*paniscus*	F	L	5.82	93.75
			OVERALL	8.66	96.00

The percentage error for metric variables (%Er) and % agreement for non-metric variables (%Ag) are listed for 12 specimens. The average values are highlighted at the bottom of the table.

In order to identify the measurements that were most affected by this phenomenon, the average error for each measurement was calculated over the 12 specimens (Table 4-4). These values range from 1.38 % ($InCP_1$) to 26.41% (LPFSz). The variables at the bottom of the table have the highest errors (LPFSz, MaFSz, HyCSz, IOFSz, etc.) and measure the size of the smaller foramina (lesser palatine foramina, infraorbital foramina, hypoglossal canal, etc.). The most precise measurements instead are those that quantify the position of foramina (e.g. $InCP_1$, $MeFP_1$, $IOFP_1$, $IOFP_2$, $MbFP_1$) and the size of the largest foramen, the foramen magnum (FMaSz). These measurements were taken using clear landmarks. Thus, these observations match the predictions

made in the previous paragraphs: as features become smaller, it is more difficult to define their margins and therefore to measure them precisely. Measurements of small foramina will then be affected by higher errors than position characters and measurements of large foramina.

Accordingly, measurements with an average error greater than 11.00% were later excluded from the analyses. These characters are highlighted in Table 4-4. They are all characters that describe the size of the smaller foramina of the skull.

Table 4-4. Intra-observer errors for each metric variables.

No	Code	%Er
60	InCP	1.38
57	FMaSz	1.65
58	InCL	2.35
56	$MbFP_1$	2.49
47	JuFL	2.70
59	$MeFP_1$	3.88
61	$IOFP_1$	4.93
43	ZFFSz	4.94
55	$IOFP_3$	7.17
52	MeFSz	7.36
46	CaCSz	10.17
54	$IOFP_2$	10.71
45	SMFSz	12.53
50	GPFSz	12.96
53	MbFSz	13.31
42	ZTFSz	15.17
44	MaFSz	18.93
49	FOvSz	19.62
41	IOFSz	22.00
48	HyCSz	25.80
51	LPFSz	26.41

The percentage errors are averages of the 12 remeasured specimens and they are listed in ascending order. Values highlighted were excluded from further analyses.

*b) Non-metric variables (*Ag*)*

For non-metric variables the average intra-observer error was computed as the percentage of agreement (*%Ag*) between the original observation and the second observation. There was an overall 96% agreement between the two observations (Table 4-3). Accordingly, all non-metric variables were retained in the subsequent analyses.

4.2.2 Side differences

Side differences in the expression of the characters were evaluated for separate taxa using Student's t-tests for metric data and chi-square tests for non-metric data. The results of these tests show that in the case of metric characters there was never a significant asymmetry between the two sides of the skull. In the case of non-metric characters, when comparisons were possible, a significant difference between right and left sides was observed in only one variable in one taxon, the position of the mental foramen relative to the lower third premolar (*Hylobates* $MeFP_2$, $p<0.05$).

The comparisons were not possible when the two frequency values were constant for right and left sides. In this case no significant difference was assumed between the two sides of the skull.

4.2.3 Sex differences

Differences between the sexes were also examined. Statistical tests were carried out to evaluate significant differences ($p<0.05$) between males and females at the generic level. Discrete characters were compared in males and females using 2x2 chi-square tests, whilst metric measurements were compared using Student's t-test (2-tailed). The assumption of normality of the metric variables was checked by carrying out a series of Kolmogorov-Smirnov tests for each metric variable, for each sex group, at the generic level. When the assumption of normality was not met by a variable, the non-parametric Mann-Whitney test was used instead. The results of these tests showed that the following variables were not normally distributed: ZFFSz in *Gorilla* ($p<0.01$, both sexes) and in *Homo* ($p<0.01$, both sexes), InCP in *Pan* ($p<0.05$, females) and *Homo* ($p<0.05$, males), Go in *Pongo* ($p<0.05$, males), MeFSz in *Papio* ($p<0.05$, females), and $IOFP_3$ in *Hylobates* ($p<0.01$, females).

Every taxon was sexually dimorphic for at least one character. However, no single character was dimorphic in all of the taxa. Most of the overlap occurred for metric characters (highlighted in Table 4-5). Among apes and humans, *Hylobates* was the taxon with the greatest number of dimorphic characters (18 characters) while *Pongo* was the least dimorphic (two characters). This is counter-intuitive because gibbons are generally considered to be the least dimorphic apes and orangutans the most dimorphic (see section 8.3).

Table 4-5. Sexual dimorphism of the soft tissue-linked characters in each genus.

#	Code	Go	Pan	Ho	Po	Hy	Pa	Ce	Co
1	IOF					<0.01			
3	ZFF					<0.00			
4	PEF					<0.00			
7	ION			<0.05					
10	SLGB	<0.05		<0.05					
13	$ZTFP_1b$		<0.05						
14	$ZTFP_1c$		<0.05						
15	$ZTFP_1a$	<0.05							
21	ZFN					<0.05			
22	ZFFPc					<0.01			
24	AEFP	<0.05				<0.01			
25	FRo		<0.05						
27	PEFPb					<0.01			
28	SOFi					<0.05			
29	PEFPa			<0.05					
32	MaFPa				<0.05				
43	ZFFSz						<0.05		
46	CaCSz	<0.00	<0.05			<0.00	<0.05	<0.00	
47	JuFL	<0.05				<0.05		<0.05	
52	MeFSz	<0.00				<0.05	<0.01		
54	$IOFP_2$	<0.00					<0.05		
55	$IOFP_3$		<0.05				<0.01		
56	$MbFP_1$	<0.00		<0.05		<0.00	<0.01	<0.05	
57	FMaSz					<0.05		<0.05	
58	InCL	<0.05				<0.05			<0.05
59	$MeFP_1$		<0.05						
60	InCP					<0.01			
66	CoCO	<0.05							
72	JuB		<0.01						
81	FSpP							<0.01	
82	FLa		<0.01						
86	PCr						<0.01		
89	MeF	<0.05							
92	MoF		<0.05						
95	MyB	<0.01							
96	CSF					<0.05		<0.05	
97	PCF				<0.05				
102	SMFS					<0.01			
110	MbFS		<0.05						
111	ZFFS					<0.05		<0.05	
	Total	12	10	3	2	18	7	7	1

Metric variables are highlighted in the table. Numbers represent p-values of comparisons between sexes (see text for explanation). Ce=*Cercopithecus*, Co=*Colobus*, Ho=*Homo*, Hy=*Hylobates*, Go=*Gorilla*, Pan=*Pan*, Pa=*Papio*, Po=*Pongo*.

4.2.4 Character correlations

One of the assumptions of cladistics is that characters should be independent. Characters may be correlated for two reasons. First they may be logically correlated due to the way they are defined (Sneath and Sokal, 1973). Careful choice of the characters can easily eliminate this type of correlation. Second, they may be morphologically integrated. That is, they may evolve as a unit (McCollum, 1999; Lovejoy et al., 1999, 2002; McCollum and Sharpe, 2001; Strait, 2001; Nadal-Roberts and Collard, 2005). This type of correlation is more difficult to identify. Strait (2001) and Strait and Grine (2004) recommended testing hypotheses of morphological integration before deeming any suite of traits to be non-independent. They suggested assuming independence if such tests cannot be performed, until otherwise shown (see also section 8.4). Non-phylogenetic character correlations were examined here using the procedure outlined by Nadal-Roberts and Collard (2005).

A series of bivariate correlations were undertaken among the characters for each separate genus. The number of significant correlations was then tabulated for each pair of characters. Because eight taxa are examined in this study, the maximum number of intraspecific significant correlations for any two characters is eight. If two traits were correlated in all of the eight taxa then it was assumed that the evolution of the two traits was not independent. Of the correlated pair, the character that correlated with the greatest number of other traits was excluded from the analysis. This technique finds support in Strait (2001) who, in a study of morphological integration in the primate basicranium, found a good agreement between the results of similar

intraspecific comparisons using bivariate correlations and the results of multivariate factor analysis.

In order to assess the significance of correlations between pairs of non-metric variables I carried out a series of 2x2 chi-square tests of independence ($p<0.05$). In some cases these tests were not meaningful because the characters were constant. Correlations among continuous variables were evaluated using Pearson's correlation coefficient. When at least one of the variables was not normally distributed then the correlations were investigated using the non-parametric Spearman's rank coefficient. Normality of the metric variables was assessed using a Kolmogorov-Smirnov for each variable at the generic level ($p<0.05$). The latter showed that three variables were not normally distributed: ZFFSz in *Gorilla* and *Homo* ($p<0.01$), FMaSz in *Pan* ($p<0.01$) and InCP in *Pan*, *Homo* and *Hylobates* ($p<0.01$).

The results showed that only one pair of metric variables was significantly correlated in all taxa: the minimum and transverse distances of the infraorbital foramen to the zygomaxillary suture ($IOFP_1$ and $IOFP_2$). When comparisons were possible among non-metric variables, no single correlation was found to be statistically significant in all of the eight taxa at the same time. In 14 comparisons the correlations were not meaningful in any of the taxa. Following Strait and Grine (2004) and Nadal-Roberts and Collard (2005), these traits were treated as independent.

The main problem with this approach was that the statistical techniques available for studying correlations of non-metric with metric characters are limited. Because of the nature of the discrete data (i.e. binary), it was not possible to examine correlations

between metric and non-metric variables since the techniques that mix these two types of information generally require non-metric values to be at least of an ordinal scale.

4.2.5 Body size

In phylogenetic analysis, size variables need to be corrected for the confounding effects of body size differences among taxa. The primates included in this study vary considerably in body mass. It is reasonable to expect that the larger apes (gorillas, orangutans, chimps and humans) have foramina of larger size than the smaller apes and cercopithecines (gibbons, colobus monkeys, guenons and baboons). In a phylogenetic analysis it is important to take this factor into account in order to evaluate to what extent the variation of the size of a foramen across the species studied can actually be explained by common ancestry and not just as a side effect of differences in body size. For this purpose, it is useful to work with the size of a foramen per unit of body mass.

Museum collections rarely have information on the body mass of the individuals of whom they carry the skeletal material. Therefore, it was necessary to employ here a proxy for body mass. I elected to use orbital height. Aiello and Wood (1994) found that estimates of body mass using the orbital height are the only ones, out of a series of cranial predictors, that agree with the postcranial predictors. They stated that "orbital height should be the preferred cranial predictor" (Aiello and Wood, 1994: 424). With this in mind, I measured the left orbital height of each specimen, and all metric traits were then scaled using this variable. The surface areas of four foramina (foramen magnum, mental foramen, zygomatico-facial foramen and carotid canal)

were approximated to the area of an ellipse (see Appendix II for a full description of the characters that describe foramen size). Before scaling these four characters to the orbital height, I took the square root of the area of each foramen. This is because orbital height is a linear measurement, whilst the area of an ellipse is a quadratic function.

The method used here to adjust metric data for the confounding effects of body size differences among taxa assumes the relationship between each variable and body size to be isometric. This assumption is unlikely to be met rigorously by all the variables. However, the main alternative method for correcting for body size differences, regression-based size adjustment, has equally serious drawbacks (Jungers et al., 1995; Lycett and Collard, 2005). In fact, regression-based methods are dependent on both the line-fitting technique and the dataset employed to generate the regression equation (Aiello, 1992; Falsetti et al., 1993; Martin, 1993; Jungers et al., 1995). Jungers et al. (1995) have also found that allometric methods of body size adjustment can be unsuccessful in correctly identifying specimens of the same shape. For these reasons, I chose not to use regression-based methods to adjust for body size differences.

Body size also influences the expression of non-metric, quasi-continuous characters (Berry, 1967; Berry and Berry, 1971; Thoma, 1981). The expression of these traits is thought to be the result of a number of alleles at different loci acting additively. These alleles control an underlying continuous variable that is expressed only if it reaches a threshold value. Below this critical value the trait is not expressed. This threshold value varies with age, sex and body size (Berry and Berry, 1971; Hauser and De

Stefano, 1989). Unfortunately, there is presently no way to correct for this effect of body size on the expression of non-metric traits.

4.3 Phylogenetic analysis

The phylogenetic relationships among the extant apes and humans were recontructed through cladistic analysis (Hennig, 1966). There is a large published literature on this subject (e.g. Smith, 1994; Kitching et al., 1998). What follows is a brief explanation of some of the principles of cladistic analysis and the description of the cladistic techniques used in this study.

In its purest theoretical form, cladistics is a method that organises objects (e.g. taxa) in a pattern of nested groups or clades. In the context of phylogenetics, the aim of cladistics is to discover sister-group relationships within a group of taxa through the identification of shared derived character states or synapomorphies (Forey, 1990). From a cladistic point of view these are the only characters that are informative about phylogeny because they define monophyletic groups (i.e. an ancestor and all of its descendants). Shared primitive characters (symplesiomorphies) define paraphyletic groups (i.e. an ancestor and some of its descendants) and cannot be relied upon to infer sister-group relationships (Forey, 1990; Smith, 1994; Kitching et al., 1998).

One of the first steps in Hennigian phylogenetics is the definition of the polarity of character states (i.e. the direction of transformation from plesiomorphic to apomorphic states). The importance of this process is that, by the identification of derived states, it allows recognition of monophyletic groups and differentiation from

paraphyletic and polyphyletic groups (Smith, 1994). It also allows the establishment of the evolutionary history of the characters under study (Clark and Curran, 1986). The method most frequently used to determine character polarity is comparison with an outgroup. The simplest definition of this method is the following: "For a given character with two or more states within a group, the state occurring in related groups is assumed to be the plesiomorphic state" (Maddison et al., 1984: 83). The logic, limits and implementations of this definition have been widely discussed in the literature (e.g. Watrous and Wheeler, 1981; Farris, 1982; Maddison et al., 1984; Donoghue and Cantino, 1984; Colless, 1985; Clark and Curran, 1986). Nixon and Carpenter (1993) provided a clear and helpful review of the development of this technique from a historical perspective and the reader is referred to this paper for a clear discussion of the basic concepts, and misunderstandings, about outgroup analysis.

The result of a cladistic analysis is a hierarchical structure of taxa that is usually represented in the form of a tree or cladogram. A cladogram is a hypothesis, 'the best explanation of the distribution of characters, be them morphological, behavioural, or any other, in the organism under study, using all of the facts available' (Ashlock, 1974: 82). There are different approaches to cladogram construction, based on two different principles: parsimony and compatibility (Ashlock, 1974). Parsimony methods, by which the number of assumptions made to explain the distribution of characters among a group of taxa is reduced to the minimum, assume that evolution occurs through the shortest path (Felsenstein, 1983; Sober, 1983). When using this principle, a cladistic analysis is frequently referred to as parsimony analysis. Compatibility, instead, looks for the collection of characters that finds the highest

level of compatibility as the criterion for choosing the best cladogram. Two characters are compatible when the groups that they support do not conflict with each other. Parsimony is by far the most commonly used principle and will also be the method adopted in this study.

It is possible to generate a tree in a parsimony analysis without a priori determination of the polarity of the characters. In this case, the result of parsimony analysis is an unrooted tree. The root can be placed on the tree by including one or more outgroups in the initial analysis and then use this outgroup to find the root (Colless, 1985; Clark and Curran, 1986). The only assumption here is that the root is basal to the ingroup (Clark and Curran, 1986). This technique is implemented in PAUP*4.0 (Swofford, 1998), the phylogenetic program used in this study to carry out the cladistic analyses, and it is the procedure adopted here.

4.3.1 Coding methods

The outcome of parsimony analysis is influenced by character coding (Archie, 1985; Goldman, 1988; Pleijel, 1995; Wiens, 1995, 2001; Kitching et al., 1998). When coding characters it is desirable to select a division of characters and character states accurate enough to reflect the taxonomic relationships among organisms (Kitching et al., 1998). There is no fixed rule on how to achieve this and different methods have been proposed by different workers. Although these are extensively reviewed and evaluated in the published literature (e.g. Archie, 1985; Pleijel, 1985; Wiens, 1995, 2001; Smith and Gutberlet, 2001), there is no clear argument on which of the methods

is the 'best'. In fact, analyses often produce different results according to the coding method used.

The metric and frequency characters were coded in this study using different methods depending on the type of variable. The methods used are described below.

a) Divergence Coding

This method was first described by Thorpe (1984). In its original protocol, it was used for coding metric variables. Pairwise comparisons of character means are carried out in a group of taxa using Student's t-tests. For each character, a significance table ($p<0.05$) is constructed in which each cell (ij) represents the comparison between taxon I and taxon J. If the character mean value for taxon I is significantly greater (or smaller) than that for taxon J then the cell (ij) will be assigned a significance value of +1 (or –1). As this is a symmetrical matrix, the value for cell (ji) will be –1. If there is no significant difference between the two taxa then the value of (ij) will be 0. Next, these significance values are summed for each column and a suitable constant integer is added to the calculated sums to make them positive. The results are a series of coding values that provide a measure of how much the taxa have significantly diverged from each other. These values are treated as ordered in the cladistic analysis. This means that a change from a hypothetical character state 1 to character state 5 is assumed to have occurred progressively through state 2, then to state 3 and finally to state four. I applied this method to the metric variables used in this study. When the variables were not normally distributed, in this case I used a Mann-Whitney non-parametric test instead of a t-test.

This technique can be applied to frequency characters as well as metric characters as long as the test statistics are changed. Since I have not yet encountered a study that has applied this method to frequency variables, I will describe the protocol used in some detail.

The procedure has three steps. The first is to assess if differences between frequency values between taxa I and J are statistically significant ($p<0.05$). This is done using 2x2 chi-square tests. The test statistic is estimated using the well-known formula,

$$\chi^2 = \sum \frac{\left(|Obs - Exp| - 0.5\right)^2}{Obs},$$

which is Yates' correction for continuity of the chi-square statistic formula (degrees of freedom equal to 1). Given a pair of taxa I and J with sample sizes N_i and N_j, the number of observed occurrences of a characters are Obs_i and Obs_j. The respective frequencies are:

$$f_i = \frac{Obs_i}{N_i} \qquad f_j = \frac{Obs_j}{N_j}.$$

Testing the null hypothesis of no difference between f_i and f_j is equivalent to assuming that the samples are drawn from a single taxonomic population in which the frequency of the trait is:

$$F = \frac{Obs_i + Obs_j}{N_i + N_j}.$$

This value can be used to compute the number of expected occurrences of the trait in the two samples under the null hypothesis of no difference, as follows:

$$Exp_i = \frac{F}{N_i} \qquad Exp_j = \frac{F}{N_j}.$$

The test statistics is then compared to a chi-square distribution. If χ^2 is greater than the critical value at the 95% level ($p<0.05$) then we conclude that the two frequencies are significantly different and therefore the null hypothesis can be rejected. If χ^2 is smaller than the critical value than the null hypothesis cannot be rejected.

The second step is to create a 'significance matrix' in which the results of the pairwise chi-square comparisons between taxa are summarised for each character. Cell (i,j) represents the comparison between taxa I and J. The results are coded as follows. If there is no significant difference between f_i and f_j then a 'significance value' of 0 is allocated to the (i,j) cell in the matrix. If f_i is significantly greater than f_j a value of +1 is allocated to (i,j); finally, if f_i is significantly lower than f_j then a value of –1 is assigned. The significance matrix is symmetrical and therefore (j,i)=-(i,j).

In the third and final step, the significance values are summed for each taxon and a constant positive integer is added to make all the taxon totals positive. In the case of eight taxa, the integer was set to +7. A coding value is thus obtained for each taxon that provides a measure of how much their values have significantly diverged from each other. These values are treated as ordered in the cladistic analyses.

These steps are repeated for each trait. In some cases the chi-square tests cannot be performed because the frequency values of a trait for the two taxa are equal to 0, i.e. the trait is absent in both taxa. When this happens the frequencies are treated as non-different and a divergence value of 0 is assigned to the two taxa. When the expected frequencies are less than five then Fisher's exact test is generally applied. However,

the sample sizes in these analyses were always greater than 40, so I followed Siegel and Castellan's (1988) recommendation to use the normal chi-square formula.

b) Binary Coding

The aim of this coding method is to obtain a binary representation of the variation observed, e.g. present/absent, yes/no. In the case of frequency data, each character can be thought of as having two possible states: absent (0) or present (1). This is applicable at different levels depending on the minimum frequency value we choose for a feature to be considered present in a population. In this analysis, first a summary frequency table was constructed with taxa arranged in rows and characters in columns. Then, for each taxon, a character was coded as 1 (present) if its frequency of occurrence was more than 5%. Otherwise, it was coded as 0 (absent).

For metric variables, this division was achieved using the gap-weighting method (see below) and setting the numbers of gaps to one. This can be thought of as being equivalent to coding the size of a foramen as large or small, and the position of a foramen as high or low on the bone where it is located. For index variables the critical value was set to 25%.

c) Baum's Coding

This method is based on Baum's (1988) system for coding continuous characters. For metric variables, taxa are ranked by their minimum values. If there are any ties, the

taxa involved are ranked by their mean values. If there are still ties, then taxa are ranked by their maximum values. A code is subsequently assigned to each taxon based on their rank order. The character states are then treated as ordered states in the cladistic analyses.

I also applied a modified version of this method to the frequency data. First a summary table of the frequencies values of each character was constructed. These were then ranked across each genus in ascending order and the rank was then used in the cladistic analyses as the characters state (treated as ordered).

d) Segment Coding

This method can be applied to both metric and frequency variables. The segment coding method for frequency traits used in this study is based on Wiens' (1993, 1995) 'frequency-bins' method for frequency data. The 100% scale is first divided into 25 intervals or 'bins' of equal size (0=0%-3%, 1=4%-7%, 2=8%-11% etc.). The length and maximum number of intervals used are dictated by the number of coding values the cladistic program allows: in the case of PAUP* 4.0b this is 25. Each frequency value is then assigned to one of the bins labelled '0' to '24' (Table 4-6). The character states thus obtained are then ordered assuming that a feature must go through a polymorphic stage between absence and fixation.

The segment coding method for metric characters is based on Thiele's (1993) gap-weighting method for continuous variables. The first step is to standardize the variables if the variances are not equal. Here I used the transformation

$$X_s = \log(X+1)$$

where X_s is the standardized measurement. The mean values for each taxon are then ranked in ascending order and range standardized using the formula:

$$X_s = n \times \frac{X - \min}{\max - \min}$$

where n is the number of 'gaps'. For consistency with the number of bins selected for non-metric traits, I set number of gaps to 24. The values obtained are then rounded to the nearest integer. These coding values are treated as multistate ordered characters.

Table 4-6. Coding values used in the segment coding method.

Interval range	Segment/Bin	Paup Code
0-3	0	0
4-7	1	1
8-11	2	2
12-15	3	3
16-19	4	4
20-23	5	5
24-27	6	6
28-31	7	7
32-35	8	8
36-39	9	9
40-43	10	A
44-47	11	B
48-51	12	C
52-55	13	D
56-59	14	E
60-63	15	F
64-67	16	G
68-71	17	H
72-75	18	J
76-79	19	K
80-83	20	L
84-87	21	M
88-91	22	N
92-95	23	P
96-100	24	Q

Each interval range corresponds to one of 25 segments, or bins. Each bin is then suitably coded for use in the phylogenetic software PAUP.

4.3.2 Parsimony analysis

Parsimony analyses were performed with the aid of two computer programs, PAUP* 4.0b, Phylogenetic Analysis Using Parsimony (Swofford, 1998) and MacClade (Maddison and Maddison, 2001). These programs are specifically designed for cladistic analysis and allow the user to choose among various options such as the character type (ordered/unordered), the type of character-optimisation criterion and the type of algorithm used to recover the most parsimonious clades. They also allow alteration of datasets, the definition of character subsets, the deletion of taxa from the analyses and bootstrap analysis. Together PAUP and MacClade enable one to estimate goodness-of-fit statistics associated with the most parsimonious solutions and to evaluate the number of parsimony informative characters.

For each dataset, a 'branch-and-bound' search was employed to recover the most parsimonious solutions using the default ACCTRAN (accelerated transformation) character-optimisation criterion. The goodness-of-fit statistics associated with these topologies (tree-length, consistency index, homoplasy index, retention index and rescaled consistency index) were recorded together with the number of parsimony informative characters and the number of synapomorphies that support each clade. Cladograms were rooted using the outgroup method in an 'unconstrained simultaneous analysis' (cf. Clark and Curran, 1986). The chosen outgroups were *Papio*, *Cercopithecus* and *Colobus*.

4.3.3 Bootstrap analysis

Bootstrap analyses (Felsenstein, 1985b) were performed to assign a level of statistical confidence to the most parsimonious clades. This method is widely used in phylogenetic analyses in biological anthropology (e.g. Collard and Wood, 2000; Gibbs et al., 2000, 2002; Strait and Grine, 2004). The original data matrix is randomly sampled with replacement to produce pseudo-matrices of equal size (replicates). The number of pseudo-matrices generated can be set using the appropriate option in PAUP. Here, 10,000 replicates were used, following Collard and Wood (2000) and Gibbs et al. (2000, 2002). Cladograms are generated for each pseudo-matrix and then the majority-rule consensus cladogram of all the bootstrap trees is computed. This tree features all the clades that find the majority of support in the bootstrap analysis. For each clade, a bootstrap proportion is computed – i.e. the number of times a particular clade is recovered from the pseudo-matrices – and it is expressed in percentage. This is taken as the support for a clade. The bootstrap value represents the strength with which a phylogenetic technique supports a particular clade (Hillis and Bull, 1993).

"Bootstrapping provides us with a confidence interval within which is contained not the true phylogeny but the phylogeny that would be estimated on repeated sampling of many characters from the underlying pool of characters. As such it may be misleading if the method used to infer phylogenies is inconsistent" (Felsenstein, 1985: 786). However, many researchers treat bootstrap values as the probability of a particular clade being true (Hillis and Bull, 1993) and a clade with a high level of support is generally considered to be accurate.

A confidence level can be set for the bootstrap consensus cladogram and, following Hillis and Bull (1993), Collard and Wood (2000) and Gibbs et al. (2000, 2002), in this analysis this was set to 70%. This means that only clades with bootstrap values greater than or equal to 70% were considered statistically significant and appeared in the bootstrap consensus cladogram. Clades with bootstrap values of between 70% and 80% were considered weakly supported; clades with values of between 80% and 90% were considered moderately supported; and clades with bootstrap greater than 90% were considered strongly supported.

4.3.4 Tree congruence

The rationale of this study was to generate phylogenetic hypotheses for the extant hominoids using characters related to nerves and vessels, and then compare the morphological trees with the strongly supported consensus molecular cladogram for this group of primates. Congruence between the morphology-based trees and the molecular tree would indicate that the osseous characters used in these analyses are reliable for recovering the correct phylogeny of the hominoids.

Tree-congruence is a methodology that is widely used in systematics to test methods of phylogenetic reconstruction (e.g. Mickevich, 1978; Miyamoto and Fitch, 1995; Wiens, 1998; McCracken et al., 1999; Collard and Wood, 2000; Gibbs et al., 2000, 2002; Masters and Brothers, 2002). Although its analytical value is often subjected to criticism (e.g. Kluge, 1998; Strait and Grine, 2004), most criticisms are generally directed to the comparison of trees generated from subset of characters to assess the phylogenetic usefulness of traits. As I explained in Chapter 3, in this study it can be

confidently assumed that the phylogeny of the hominoids is well understood from molecular data and therefore congruence of the morphology-based cladograms with the consensus molecular tree can safely be considered informative about the usefulness of morphological datasets for phylogenetic inference.

4.4 Hypothesis testing

In this section the hypotheses tested in this project and the methodologies used to test them are outlined. Details of the criteria of acceptance or rejection of the hypotheses are also provided.

4.4.1 Hypothesis 1a: Osteological characters associated with nerves and vessels are reliable for recovering the phylogenetic relationships of hominoid primates at the generic level.

Four datasets were prepared to test this hypothesis. The first dataset included all three cercopithecine taxa in the outgroup (Analysis 1a.1). The second included only *Papio* (Analysis 1a.2), the third only *Cercopithecus* (Analysis 1a.3) and the fourth only *Colobus* (Analysis 1a.4). Each dataset comprised 11 continuous variables and 90 discrete variables. The variables were coded using the coding methods described in section 4.4.1. Dataset A (Divergence coding) coded both discrete and continuous variables using the divergence method. Dataset B (Binary coding) coded discrete variables using the binary method and the continuous variables using the gap-

weighting method (setting the number of gaps to one). Dataset C (Baum's coding) coded both discrete and continuous variables using Baum's method. Dataset D (segment coding) coded the discrete variables using the segment method and the continuous variables using gap-weighting (setting the number of gaps to 24).

Parsimony analyses were performed on each dataset to obtain an estimate of the phylogenetic relationships of the taxa under study. The branch-and-bound algorithm in PAUP* 4.0b was used to recover the most parsimonious solutions. The tree statistics associated with the most parsimonious solutions (tree-length, consistency index, homoplasy index, retention index and rescaled consistency index) were also recorded, together with the number of parsimony informative characters. The hypothesis was considered to be supported if the shortest tree was identical to the hominoid molecular phylogeny. If more than one MPT was recovered, the hypothesis was considered to be supported if the strict consensus of the shortest solutions was consistent with the molecular cladogram. For each topology the number of molecular clades recovered was also noted. Also the topology of the next most parsimonious solution was recovered and compared to the molecular cladogram.

The bootstrap tests were performed on the same datasets, using the bootstrap command in PAUP* 4.0b and the branch-and-bound search option. The number of bootstrap replicates was set to 10,000 in each analysis. Only clades present in more than 70% of the pseudo-trees were retained. The consensus trees were also compared to the molecular phylogeny to evaluate if the clades that found statistical support were 'true' molecular clades, or 'false' clades.

The performance of each test was evaluated by computing two indices: the outgroup success index (S_O), which measures the average rate of success in recovering molecular clades for each outgroup but varying the coding method; and the coding method success index (S_C), which measures the average rate of success in the recovery of molecular clades for the same coding method but using different outgroups. These indices were calculated using the following formulas:

$$So = \sum_{i} \frac{Oci}{4 \times Eci} \qquad Sc = \sum_{j} \frac{Ocj}{4 \times Ecj}$$

where for each outgroup (S_O) and for each coding method (S_C), Ec is the total number of expected molecular clades (six when all outgroups are included in the analyses, and four when only one outgroup is used to root the trees), O_C is the observed number of molecular clades, 'i' varies among coding methods and 'j' varies among outgroup composition respectively. A value of 0 indicates that no molecular clade was recovered, whilst a value of 1 indicates that all the molecular clades were recovered. Therefore, the higher the number, the more successful the test.

The results of these analyses were also compared to cladograms generated from 'standard' cranial datasets. In other words from those datasets based on cranial characters recurrently used in the literature to make inferences about primate, and in particular hominid, phylogeny. Two cladograms were chosen. One is based on a dataset of qualitative characters and was taken from a paper published by Collard and Wood (2000). The other is based on a dataset of standard cranial measurement taken from Serdoz (2001).

The qualitative dataset used by Collard and Wood (2000) consisted of 96 craniodental characters recorded on a sample of the five hominoid genera plus an outgroup

(*Colobus*). The data matrix was compiled from various sources and the reader is referred to the literature cited in Collard and Wood (2000) for a detailed list of the original sources.

The metric dataset was prepared using data collected for my M.Sci. dissertation (Serdoz, 2001). Thirty standard craniometric measurements were originally recorded on a mixed-sex sample that comprised 20 *Gorilla gorilla*, 20 *Homo sapiens*, 19 *Pan troglodytes*, one *Pan paniscus*, 20 *Pongo pygmaeus*, and 20 specimens of an outgroup, *Colobus*. This sample was supplemented with 20 specimens from the genus *Hylobates* in order to make it comparable with the vessel and nerve linked dataset. The 30 morphometric traits (Table 4-7) comprised measurements of the palate (1-8), the mandible (9,10), the face (11-23) and the cranial vault (24-30). These were taken with Vernier callipers (± 0.05 mm) and spreading callipers (± 0.5 mm). The confounding effect of body size differences was corrected for by scaling the data with the geometric mean (Jungers et al., 1995). This adjustment produces skulls of equal volume but leaves their shape unchanged. For each individual, the geometric mean of the 30 measurements employed in this analysis was taken as a proxy for the size of the individual. Each measurement was then scaled by its geometric mean.

The dataset underwent the same coding procedures employed for the discrete variables: Divergence coding (a), Binary coding (b), Baum's coding (c) and Segment coding (d). The four data matrices were then subjected to parsimony analyses to generate phylogenetic hypotheses and bootstrap analyses to assign a level of statistical support to the clades recovered.

4.4.2 Hypothesis 1b: Osteological characters associated with nerves and vessels are reliable for recovering the phylogenetic relationships of hominoid primates at the specific level.

The methodologies and criteria used to test this hypothesis are identical to the ones employed to test Hypothesis 1a. Except in this case the operational taxonomic units adopted were species for the ingroup. The genus *Pan* was split into the species *Pan paniscus* and *Pan troglodytes,* while the genus *Hylobates* was split into two taxa: *Hylobates syndactylus* and *Hylobates spp.* The latter group is formed by two species: *H. lar* and *H. moloch.* Therefore, the datasets now included 10 taxa.

Four sets of parsimony and bootstrap analyses were carried out on these dataset. These differed in the composition of the outgroup, which was formed by the three cercopithecine taxa in the first set (Analysis 1b.1), only *Papio* in the second set (Analysis 1b.2), only *Cercopithecus* in the third (Analysis 1b.3) and only *Colobus* in the fourth (Analysis 1b.4). In each set of tests, four data matrices were analysed. These varied in the coding procedures adopted: (a) divergence coding, (b) binary coding, (c) Baum's coding and (d) segment coding. Parsimony analyses (branch-and-bound algorithm) were performed on each dataset using PAUP* 4.0b to recover the most parsimonious solutions. The hypothesis was considered to be supported if the shortest tree was identical to the hominoid molecular phylogeny, or if more than one MPT was recovered, if the strict consensus of the shortest solutions was consistent with the molecular cladogram. Also the topology of the next, slightly less parsimonious solution was recovered and compared to the molecular cladogram. The bootstrap tests (branch-and-bound search and 10,000 replicates) were performed on

the same datasets. Only clades present in more than 70% of the pseudo-trees were retained. The consensus trees were also compared to the molecular phylogeny to evaluate if the clades that found statistical support were 'true' molecular clades, or 'false' clades.

The success indices, S_O and S_C, were computed to evaluate the success of the tests in the recovery of molecular clades and the effects of methodological choices such as outgroup composition and coding method. These indices were described in more detail in section 4.5.1. In this case the number of expected molecular clades was eight when all three outgroups were used to root the trees, and six when only one outgroup was used to root the cladograms. The results of these analyses were also compared to the results of the analyses at the generic level.

4.4.3 Hypothesis 2: Sexual dimorphism plays an important role in the reconstruction of hominoid phylogenetic relationships from skeletal data.

As discussed previously all taxa are sexually dimorphic in at least one character (cf. section 4.3.3). It seems reasonable to suppose that these differences between the sexes may affect the outcome of phylogenetic analysis (cf. Collard, 1998). Hence, this hypothesis investigates the effects of sexual dimorphism in the phylogenetic analysis. It predicts that if differences between the sexes do not affect the outcome of phylogenetic studies, the cladograms generated from sex-specific datasets will be consistent with each other and with the cladograms generated from the mixed-sex dataset. This hypothesis was divided into two sub-hypotheses.

(a) Hypothesis 2a: Male-specific datasets produce phylogenies consistent with the mixed-sex dataset.

(b) Hypothesis 2b: Female-specific datasets produce phylogenies consistent with the mixed-sex phylogenies.

Two datasets were prepared, one for males and one for females. These datasets were then used to produce phylogenetic hypotheses from the hominoids using the same protocol as the one described for hypothesis 1a and 1b. The first series of analyses (Analyses 2a.1 to Analysis 2a.4) tested Hypothesis 2a by rooting the cladograms derived from the male dataset first using all three cercopithecine taxa and then only one outgroup at a time. The same was done for the female dataset (Analysis 2b.1 to 2b.4). In each analysis the characters were coded using four different coding methods as described previously: (a) divergence coding, (b) binary coding, (c) Baum's coding and (d) segment coding.

The results of these analyses were then compared with each other and with the results of the equivalent mixed-sex analysis. The hypothesis was deemed supported if the results from the sex-specific datasets produced phylogenetic hypotheses that were not compatible with each other and with the mixed-sex results. They were also compared to the consensus molecular cladogram to investigate which if any of the datasets performed better in recovering the hominoid molecular phylogeny.

Table 4-7. Craniometric measurements used in this study.

#	Measurement	Description	Reference
1	Maxillo-alveolar breadth	Minimum distance between the outer surface of the alveolar process at the midpoint of the second upper molar (ekm-ekm).	Wood (1991) #88
2	Incisive canal-palatomaxillary suture	Chord distance between the posterior edge of the incisive canal and the palatomaxillary suture.	Wood (1991) #92
3	I^1-I^2 alveolar length	Chord distance between Prosthion and the midpoint of the interalveolar septum between I^2 and C^1.	Wood (1991) #94
4	P^3-P^4 alveolar length	Minimum chord distance between the midpoints of the interalveolar septa between C/P^3 and P^4/M^1.	Wood (1991) #96
5	M^1-M^3 alveolar length	Minimum chord distance between the midpoint of the interalveolar septum between P^4/M^1 and the most posterior of the walls of the M^3 alveoli.	Wood (1991) #97
6	Intercanine distance	Minimum distance between the upper canine alveoli.	Wood (1991) #98
7	P^4 interalveolar distance	Minimum chord distance between the palatal walls of the P^4 alveoli.	Wood (1991) #100
8	M^2 interalveolar distance	Minimum chord distance between the palatal walls of the M^2 alveoli.	Wood (1991) #101
9	Symphyseal height	Minimum distance between the base of the symphysis and Infradentale.	Wood (1991) #141
10	Maximum symphyseal depth	Maximum depth of the mandibular symphysis at right angles to symphyseal height.	Wood (1991) #142
11	Superior facial height	Chord distance between Nasion and Prosthion (nas-pros).	Wood (1991) #43
12	Alveolar height	Chord distance between Nasospinale and Prosthion (ns-pros).	Wood (1991) #45
13	Bizygomatic breadth	Chord distance between zygion (zyg-zyg).	Wood (1991) #52

Table 4-7, continued. Craniometric measurements used in this study.

14	Bimaxillary breadth	Chord distance between Zygomaxillare (zm-zm).	Wood (1991) #53
15	Anterior interorbital breadth	Chord distance between Maxillofrontale (mf-mf).	Wood (1991 #55
16	Orbital height	Maximum distance between the superior and inferior orbital margins in a direction perpendicular to the orbital breadth.	Wood (1991) #57
17	Minimum malar height	Minimum chord distance between the inferior orbital margin and the inferior border of the zygomatic process of the maxilla.	Wood (1991) #59
18	Maximum nasal width	Maximum width of nasal aperture at whatever height it occurs at the anterior nasal aperture.	Wood (1991) #68
19	Nasal height	Chord distance between Nasion and Nasospinale (nas-ns).	Wood (1991) #69
20	Sagittal length of nasal bones	Chord distance from Nasion to Rhinion (nas-rhi).	Wood (1991) #71
21	Zygomaxillare-Porion	Chord distance between Zygomaxillare and Porion (zm-po).	Wood (1991) #127
22	Upper facial prognathism	Chord distance between Porion and Glabella (po-g).	Chamberlain (1987) #F15
23	Lower facial prognathism	Chord distance between Porion and Alveolare (po-ids).	Chamberlain (1987) #F16
24	Glabella-Opisthocranion	Chord distance between Glabella and Opisthocranion (g-op).	Wood (1991) #1
25	Parietal sagittal length	Chord distance between Bregma and Lambda (br-lam).	Wood (1991) #25
26	Biporionic breadth	Chord distance between Porion (po-po).	Wood (1991) #11
27	Glabella-Bregma	Chord distance between Glabella and Bregma (g-br).	Wood (1991) #17

Table 4-7, continued. Craniometric measurements used in this study.

28	Postglabellar sulcus-Bregma	Chord distance between the deepest point of the postglabellar sulcus and Bregma.	Wood (1991) #19
29	Occipital sagittal length	Chord distance between Lambda and Opisthion (lam-opn).	Wood (1991) #39
30	Foramen magnum maximum width	Maximum distance in the coronal plane between the inner margins of the foramen magnum.	Wood (1991) #77

Chapter 5. RESULTS I: MAIN HYPOTHESIS (1a)

In this chapter I report the results of parsimony and bootstrap analyses undertaken to test the hypothesis that cranial characters related to nerves and vessels are reliable for recovering the phylogenetic relationships of the extant hominoids. This hypothesis predicts that if soft tissue-linked traits are suitable for phylogenetic reconstruction they will produce phylogenies consistent with the strongly supported consensus molecular cladogram for this group of primates.

Four sets of cladistic analyses were carried out to generate hypotheses of relationships for the hominoids: one set included all three cercopithecine taxa in the outgroup, one included only *Papio,* one only *Cercopithecus* and one only *Colobus*. Each set of analyses was run on four different data-matrices, which differed from each other in the way the characters were coded to make the data suitable for phylogenetic analysis (Divergence Coding, Binary Coding, Baum's Coding and Segment Coding). Parsimony analysis was used to generate phylogenetic hypotheses. The topologies of the next most parsimonious cladograms were also examined. Following Collard and Wood (2000, 2001) and Gibbs et al. (2000, 2002), bootstrap tests were run to recover statistically significant clades at the 70% confidence limit (Hillis and Bull, 1993).

The results of the tests were compared to the consensus molecular phylogeny for the hominoids, which is widely considered to be accurate (Ruvolo, 1997). The hypothesis was considered to be supported if the topology of the most parsimonious cladogram derived from the nerve- and vessel-related osteological characters was consistent with the molecular cladogram. The latter condition was deemed to exist when a single most

parsimonious tree was found and it was identical to the hominoid molecular cladogram, or when more than one tree was recovered and their strict consensus was compatible with the molecular phylogeny. If the best solutions disagreed with the molecular cladogram then the hypothesis was rejected. To facilitate the assessment of the value of this group of characters in phylogenetic studies, their utility was measured in terms of number of molecular clades present in the most parsimonious trees and in comparison to results from parsimony and bootstrap analyses based on standard craniometric characters.

5.1 Hypothesis 1a: Cranial characters associated with nerves and vessels produce reliable phylogenies for the hominoids at the generic level

5.1.1 Analysis 1a.1

In this set of analyses, all three cercopithecine taxa (*Papio, Cercopithecus* and *Colobus*) were included as outgroups. The shortest cladograms produced in the parsimony analyses are illustrated in Figure 5-1, and the tree statistics (tree length, consistency index, homoplasy index, retention index and number of parsimony-informative characters) associated with these solutions are reported in Table 5-1. The results of the bootstrap analyses are shown in Figure 5-2.

a) Divergence Coding

This dataset produced one most parsimonious tree (MPT). This tree (Figure 5-1a) placed *Hylobates* at the base of the hominoid clade, and *Pongo* as the sister taxon of African apes and humans. *Gorilla* and *Pan* were more closely related to each other than either was to *Homo*. The tree also placed the outgroup taxa in a single clade. Within this group *Colobus* was the sister taxon of a clade formed by *Papio* and *Cercopithecus*, which was consistent with the consensus molecular cladogram. Therefore, all but one molecular clades were recovered in this analysis.

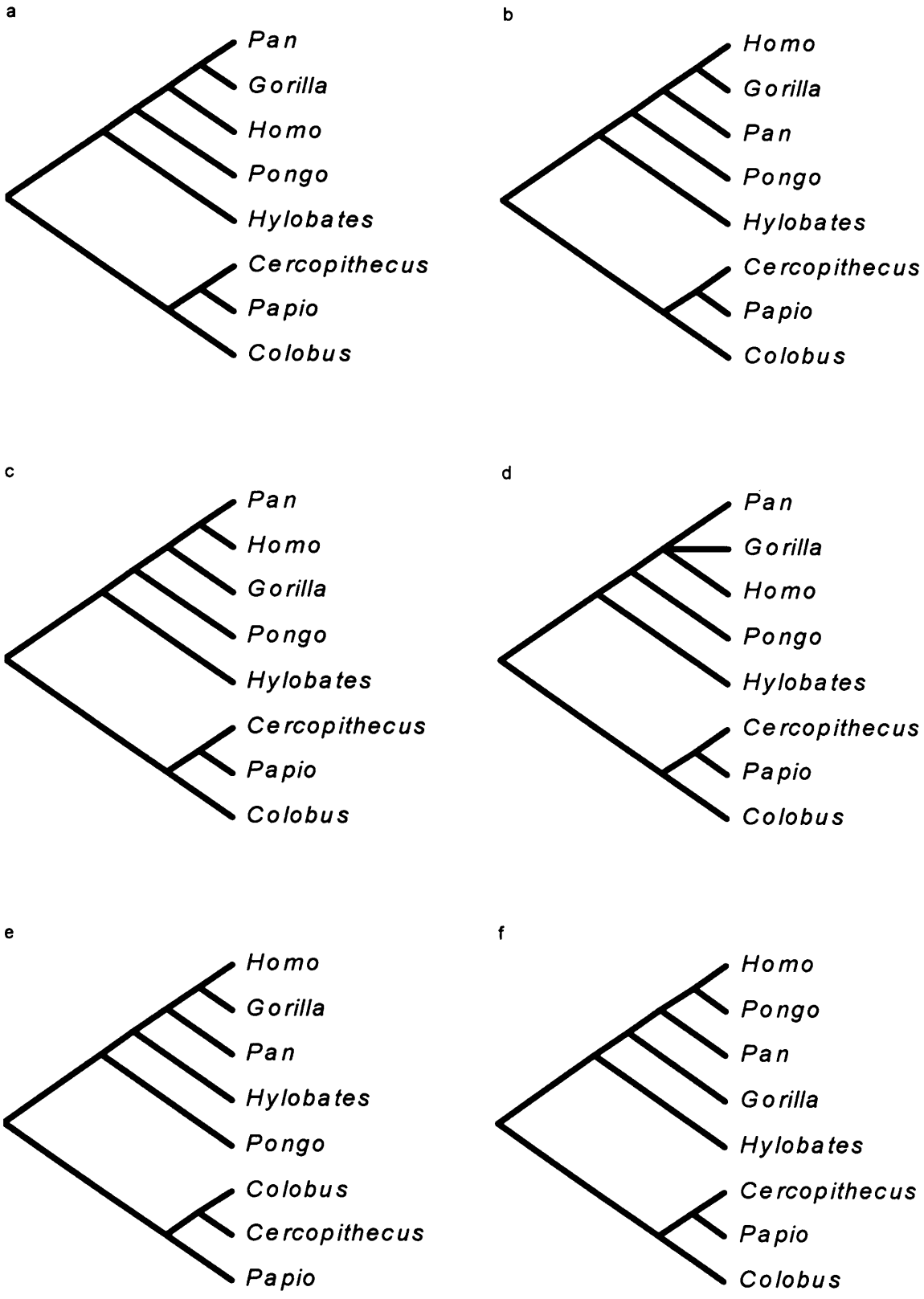

Figure 5-1. Analysis 1a.1: MPTs recovered in the parsimony analyses.
(a) Divergence Coding; (b, c, d) Binary Coding; (e) Baum's Coding; (f) Segment Coding.

Table 5-1. Analysis 1a.1: Tree Statistics associated with MPTs.

Coding Methods	TL	CI	HI	RI	PI
Divergence	1649	0.58	0.42	0.44	92
Binary	149	0.50	0.50	0.45	63
Baum	1303	0.53	0.47	0.38	101
Segment	2460	0.59	0.41	0.44	96

TL= Tree Length; CI= Consistency Index; HI= Homoplasy Index; RI= Retention Index; PI= Number of Parsimony Informative Characters.

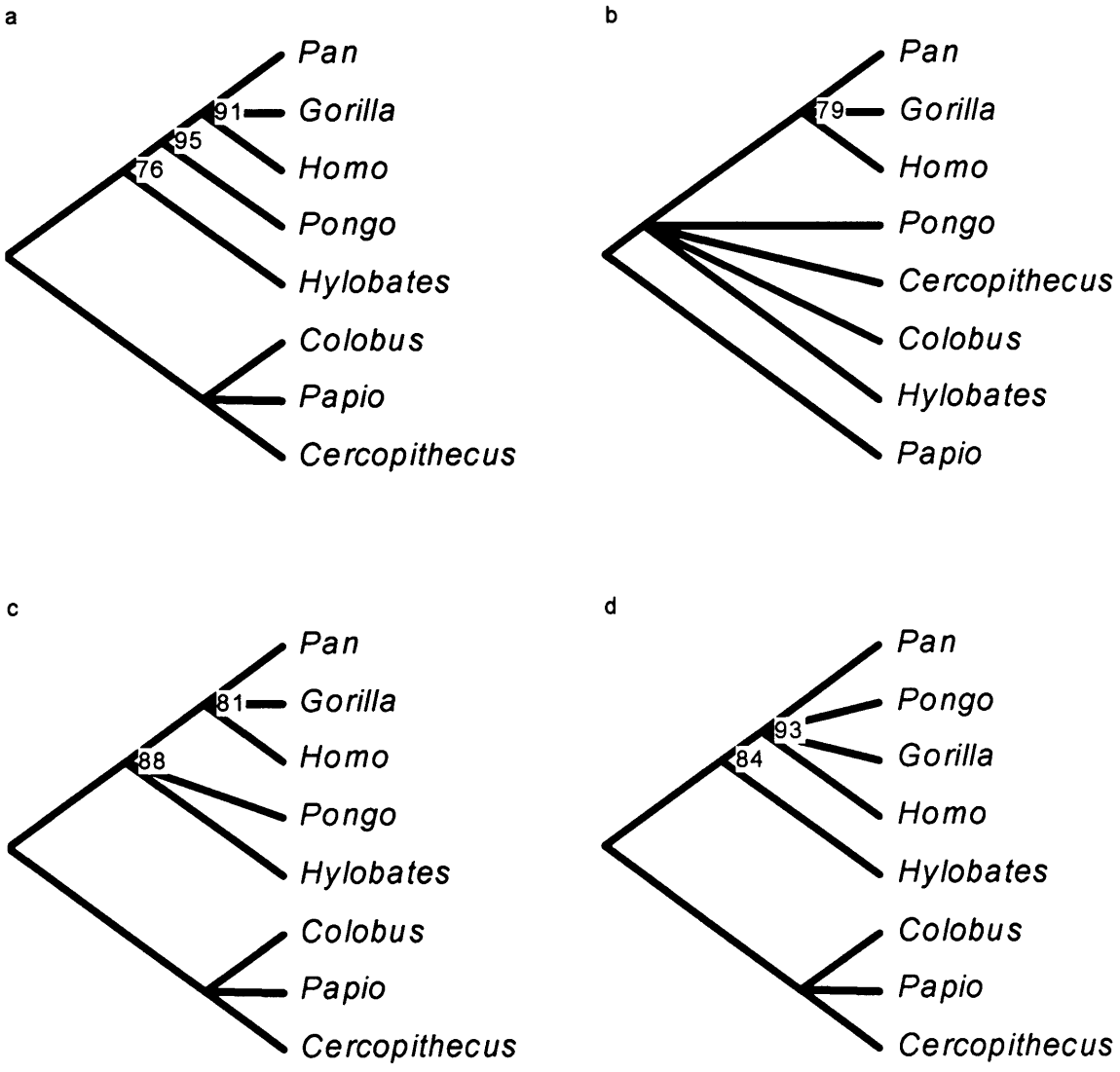

Figure 5-2. Analysis 1a.1: Results of the bootstrap analyses.
(a) Divergence Coding; (b) Binary Coding; (c) Baum's Coding; (d) Segment Coding.

The next most parsimonious tree was eight steps longer and it also disagreed with the molecular phylogeny. This solution differed from the previous one in placing *Pan* next to a clade that comprised *Gorilla* and *Homo*. The rest of the tree was identical to the one described above.

The bootstrap analysis yielded a 70% consensus tree that was only partially resolved (Figure 5-2a). Three clades were recovered and these were consistent with the molecular relationships. The great ape and human clade (95%), and the African ape and human clade (91%) were strongly supported, whilst the hominoid clade found a relatively weak level of support (76%).

b) Binary Coding

This dataset yielded two MPTs. The first (Figure 5-1b) placed *Pan* next to a clade formed by *Gorilla* and *Homo*. *Pongo* was the sister taxon of the African apes and humans, and *Hylobates* was placed at the base of the hominoid clade. The three cercopithecine outgroups formed a monophyletic group and their molecular relationships were correctly recovered. The second tree (Figure 5-1c) was identical to the consensus molecular cladogram. The strict consensus of these two solutions (Figure 5-1d) was consistent with the molecular phylogeny although it failed to resolve the African ape and human trichotomy.

Seven solutions were only one step longer than the shortest ones and did not agree with the hominoid molecular cladogram. Their strict consensus did not support the monophyletic relationships within the hominoids, and placed *Colobus* and

Cercopithecus in this group. None of the hominoid molecular relationships were recovered apart from an African ape and human trichotomy.

The bootstrap analysis generated a consensus tree that was largely unresolved (Figure 5-2b). It contained only one molecular clade: the African ape and human clade. This was relatively weakly supported (79%).

c) Baum's Coding

A single MPT was recovered in this analysis. It was not consistent with the hominoid molecular phylogeny (Figure 5-1e). Instead, it contained a clade in which *Gorilla* and *Homo* were more closely related to each other than either was to *Pan*, and another in which *Hylobates* was positioned as the sister taxon of the African apes and humans. *Pongo* occupied a basal position within the hominoid clade. The three outgroup taxa were recognised as a monophyletic group but their relationships disagreed with the molecular cladogram: *Papio* was placed as the sister group of a clade that comprised *Colobus* and *Cercopithecus*. Hence, three molecular clades were recovered in this analysis: the hominoid clade, the African ape and human clade and the cercopithecine clade.

The next most parsimonious tree was one step longer than the most parsimonious solution. It did not agree with the molecular cladogram and supported a phylogeny in which *Pongo* was the basal taxon within the hominoid clade. *Hylobates* was the sister taxon of the African apes and humans, and *Homo* was placed closer to *Gorilla* than to

Pan. Within the outgroup clade, *Cercopithecus* and *Papio* formed a clade next to *Colobus*, which is consistent with the molecular relationships.

When this dataset was bootstrapped, the 70% consensus tree was only partially resolved but it was consistent with the molecular hypothesis (Figure 5-2c). It contained two clades. The first was a moderately supported hominoid clade (88%). The second was a moderately supported trichotomy comprising African apes and humans (81%).

d) Segment Coding

The MPT recovered in this analysis did not agree with the consensus molecular phylogeny (Figure 5-1f). It supported the hominoids as a monophyletic group and all the molecular relationships among the cercopithecine taxa were correctly recovered. In addition, *Hylobates* occupied a basal position within the hominoids. However, *Gorilla* was placed next to a clade that comprised *Pan*, *Homo* and *Pongo*. Within the latter *Homo* and *Pongo* shared a common ancestor not shared with *Pan*.

The next most parsimonious tree was three steps longer. It featured a hominoid clade, a great ape and human clade, and an African ape and human clade. Inconsistent with the molecular tree, *Pan* was placed next to a clade formed by *Gorilla* and *Homo*. As in the previous solution, the molecular relationships within the outgroup were correctly recovered.

The bootstrap analysis yielded a consensus tree (Figure 5-2d) that was largely unresolved and recovered only two molecular clades. These were a strongly supported great ape and human clade (93%) and a moderately supported hominoid clade (84%).

5.1.2 Analysis 1a.2

Below are reported the results of the cladistic analyses run excluding *Colobus* and *Cercopithecus* from the study and using *Papio* as the only outgroup. The most parsimonious solutions are illustrated in Figure 5-3 and the associated tree statistics are listed in Table 5-2. The 70% consensus cladograms generated when the datasets were bootstrapped are illustrated in Figure 5-4.

a) Divergence Coding

The branch-and-bound search returned one single MPT that was identical to the hominoid molecular cladogram (Figure 5-3a).

The next best solution was three steps longer than the previous one. The topology of this tree differed from that of the molecular cladogram in that it posited a sister-group relationship between *Gorilla* and *Pan* to the exclusion of *Homo*. *Pongo* was placed next to the African apes and humans, while *Hylobates* occupied a basal position within the hominoid clade. Therefore, three molecular clades were recovered.

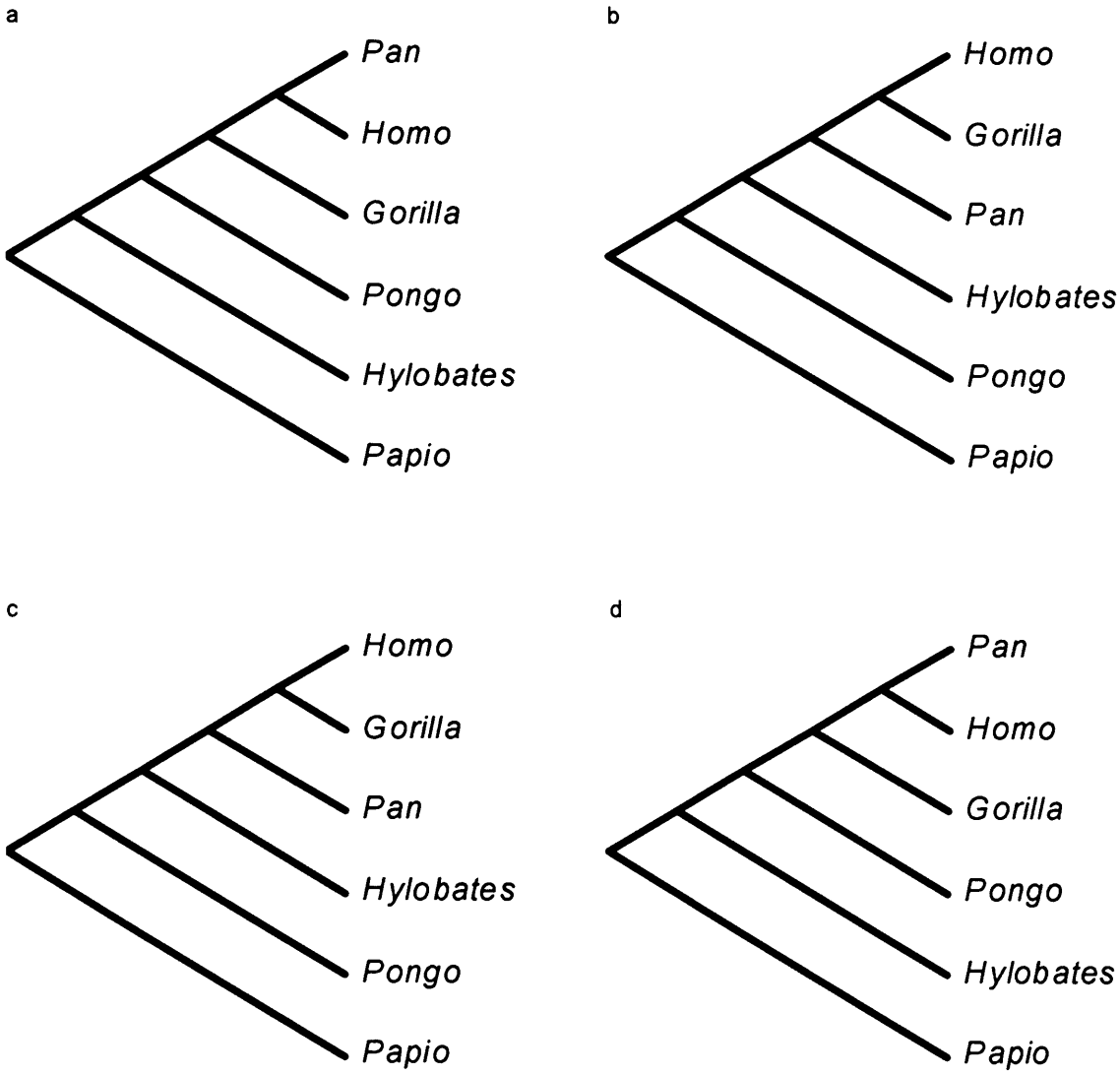

Figure 5-3. Analysis 1a.2: MPTs recovered in the parsimony analyses.
(a) Divergence Coding; (b) Binary Coding; (c) Baum's Coding; (d) Segment Coding.

Table 5-2. Analysis 1a.2: Tree Statistics associated with MPTs.

Coding Methods	TL	CI	HI	RI	PI
Divergence	1055	0.66	0.34	0.39	87
Binary	125	0.55	0.45	0.39	52
Baum	778	0.64	0.36	0.36	101
Segment	2075	0.68	0.32	0.35	94

TL= Tree Length; CI= Consistency Index; HI= Homoplasy Index; RI= Retention Index; PI= Number of Parsimony Informative Characters.

The bootstrap analysis generated two molecular clades, a moderately supported African ape and human clade (83%), and a weakly supported great ape and human clade (74%). The rest of the cladogram was unresolved (Figure 5-4a).

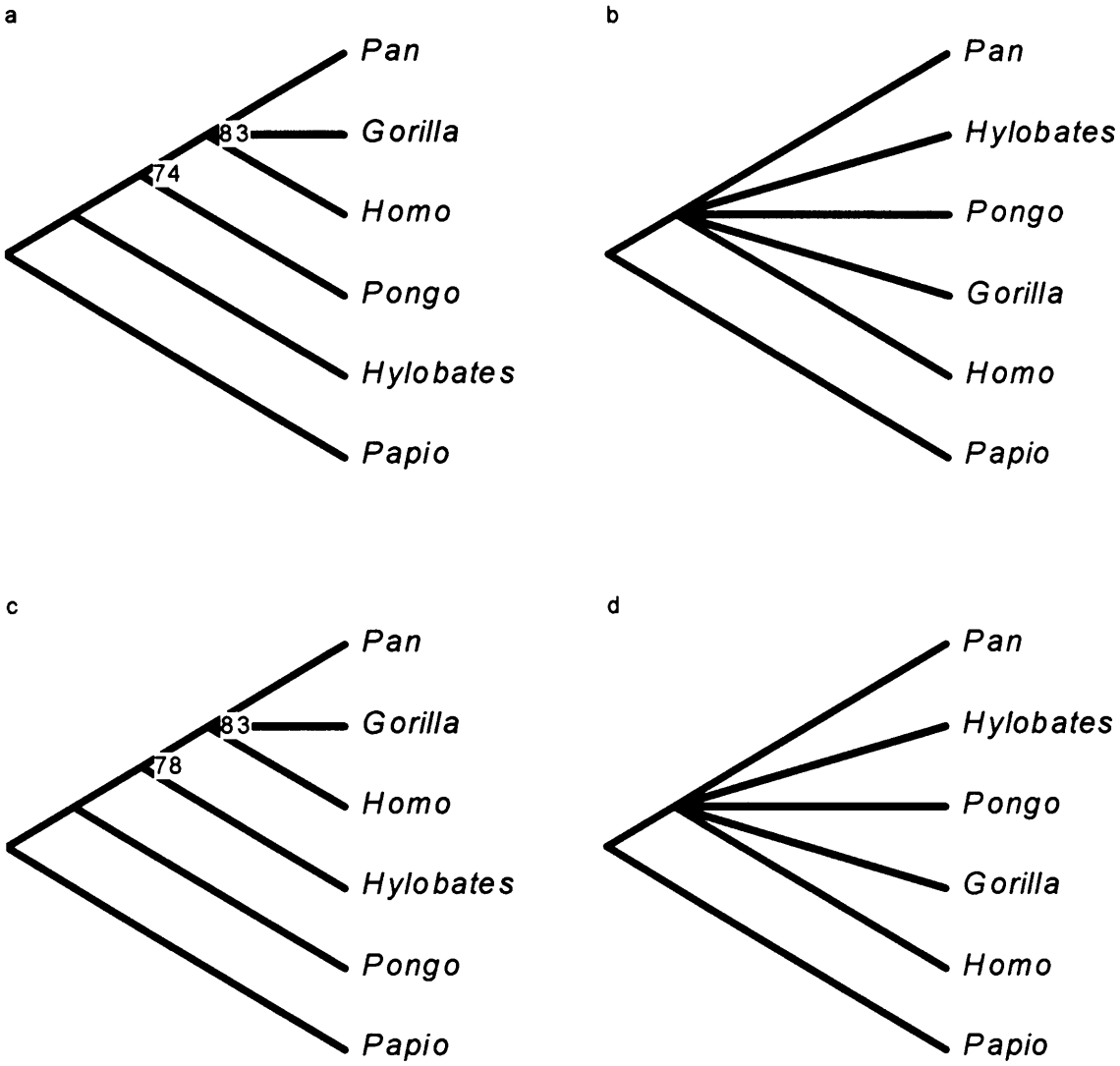

Figure 5-4. Analysis 1a.2: Results of the bootstrap analyses.
(a) Divergence Coding; (b) Binary Coding; (c) Baum's Coding; (d) Segment Coding.

b) Binary Coding

The MPT recovered in the parsimony analysis was inconsistent with the molecular phylogeny (Figure 5-3b). It supported a sister-group relationship between *Gorilla* and *Homo* to the exclusion of *Pan*. It also placed *Hylobates* next to the African apes and humans, while *Pongo* occupied a basal position within the hominoid clade. Therefore, only two molecular clades were found: the hominoid clade, and the African ape and human clade.

The next three trees were one step longer than the previous one and one of them was consistent with the molecular cladogram. Their strict consensus was characterised by two trichotomies. The first comprised the African apes and *H. sapiens*. The second consisted of *Pongo*, *Hylobates* and the (*Gorilla, Homo, Pan*) clade. This topology was consistent with the molecular results although it only supported two clades.

The bootstrap analysis yielded a consensus tree that was unresolved (Figure 5-4b). No clade was supported by 70% or more of the bootstrap replications.

c) Baum's Coding

The phylogenetic hypothesis produced in this analysis did not agree with the consensus molecular phylogeny (Figure 5-3c). It supported *Gorilla* and *Homo* as sister taxa to the exclusion of *Pan*, and placed *Hylobates* – rather than *Pongo* – as the sister group of the African apes and humans. Therefore, only two molecular clades were recovered: the hominoid clade and the African ape and human clade.

The next shortest tree was seven steps longer than the most parsimonious tree, and it too was inconsistent with the molecular cladogram. It recovered the sister-group relationship between chimpanzees and humans, but failed to recognise the great apes and humans as a monophyletic group. Instead, this tree placed *Hylobates* as the sister taxon of the African apes and humans.

The bootstrap consensus tree generated in this analysis featured two weakly supported clades (Figure 5-4c). The first one, an African ape and human trichotomy, was consistent with the hominoid molecular phylogeny and was moderately supported (83%). The second clade was weakly supported and incongruent with the molecular results. It comprised *Hylobates* and the African apes and humans (78%).

d) Segment Coding

The MPT recovered in this analysis (Figure 5-3d) agreed with the hominoid consensus molecular cladogram.

The next most parsimonious tree was three steps longer. It differed from the shortest solution in placing *Pongo* and *Homo* in a single clade to the exclusion of *Pan*. *Gorilla* was the sister group of the clade formed by *Homo*, *Pan* and *Pongo*, while *Hylobates* occupied a basal position within the hominoids.

The bootstrap cladogram produced from this dataset did not yield any clades at the 70% confidence level (Figure 5-4d).

5.1.3 Analysis 1a.3

In the next set of analyses, *Colobus* and *Papio* were excluded from the study and *Cercopithecus* was the only outgroup used. The shortest cladograms found in the parsimony analyses are presented in Figure 5-5 and the associated tree statistics are reported in Table 5-3. The consensus cladograms generated in the bootstrap tests are illustrated in Figure 5-6.

a) Divergence Coding

A single MPT was found in this part of the analysis (Figure 5-5a). Its topology did not agree with the molecular tree. It failed to support the sister-group relationship between humans and chimpanzees. Instead, it placed *Homo* and *Gorilla* in a clade to the exclusion of *Pan*. The rest of the tree was identical to the molecular cladogram. Hence, it successfully recovered three molecular clades: the African ape and human clade, the great ape and human clade and the hominoid clade.

The next solution was two steps less parsimonious than the shortest one. It differed from the most parsimonious tree in placing *Pan* – rather than *Homo* – closer to *Gorilla*.

When this dataset was bootstrapped, the 70% consensus tree featured two clades consistent with the molecular phylogeny (Figure 5-6a): a strongly supported (92%) great ape and human clade; and a weakly supported African ape and human clade (78%) in which *Homo*, *Pan* and *Gorilla* formed a trichotomy.

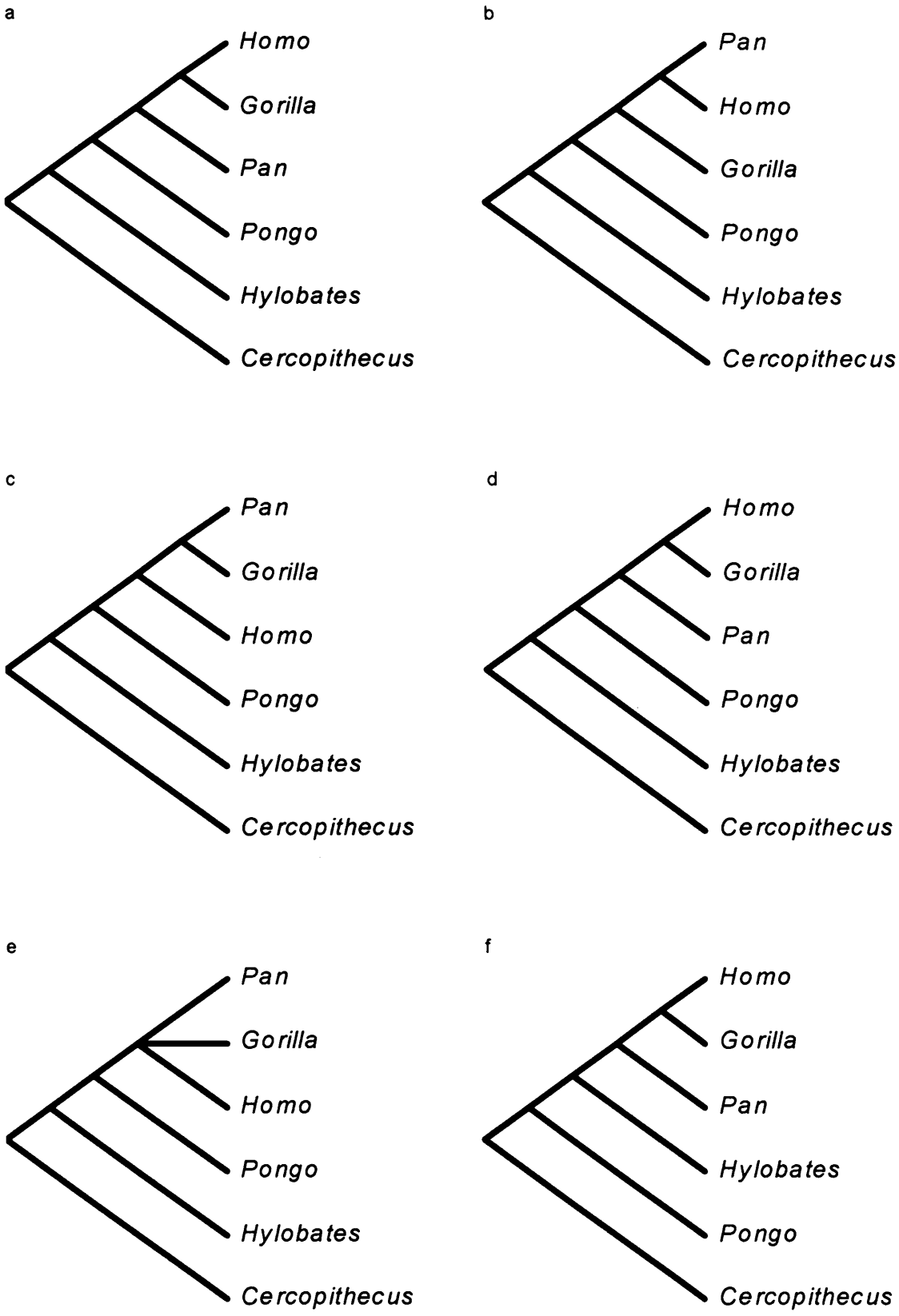

Figure 5-5. Analysis 1a.3: MPTs recovered in the parsimony analyses.
(a) Divergence Coding; (b,c,d,e) Binary Coding; (f) Baum's Coding, (g) Segment Coding.

g

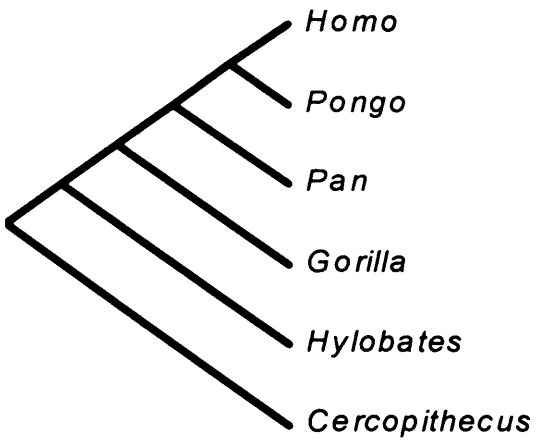

Figure 5-5, continued. Analysis 1a.3: MPTs recovered in the parsimony analyses.

Table 5-3. Analysis 1a.3: Tree Statistics associated with MPTs.

Coding Methods	TL	CI	HI	RI	PI
Divergence	1034	0.67	0.33	0.39	88
Binary	124	0.58	0.32	0.39	48
Baum	846	0.63	0.37	0.33	99
Segment	2234	0.69	0.31	0.39	92

TL= Tree Length; CI= Consistency Index; HI= Homoplasy Index; RI= Retention Index; PI= Number of Parsimony Informative Characters.

b) Binary Coding

The branch-and-bound search found three MPTs. One of these was congruent with the consensus molecular cladogram for the hominoids (Figure 5-5b). The second (Figure 5-5c) featured a hominoid clade, a great ape and human clade and an African ape and human clade. However, it did not support a monophyletic relationship between *Pan* and *Homo*. Instead, it placed *Homo* as the sister taxon of a clade that comprised *Pan* and *Gorilla*. The third tree (Figure 5-5d) differed from the previous two in placing *Pan* next to a clade formed by *Homo* and *Gorilla*. The strict consensus of the three

trees (Figure 5-5e) was consistent with the molecular phylogeny. It featured a hominoid clade, a great ape and human clade, and an African ape and human trichotomy.

The next five solutions were only two steps less parsimonious than the three MPTs. Their strict consensus featured a polytomy composed of the five hominoid genera.

One molecular clade was recovered at the 70% significance level when this dataset was bootstrapped (Figure 5-6b): a weakly supported African ape and human clade (75%). The relationships among the other taxa were unresolved.

c) Baum's Coding

This analysis recovered one MPT that differed from the consensus molecular cladogram. This tree (Figure 5-5f) supported a monophyletic relationship between *Gorilla* and *Homo* to the exclusion of *Pan*. It also placed *Hylobates* next to the African apes and humans, and *Pongo* in a basal position within the hominoid clade. Thus, two molecular clades were supported by this solution: the hominoid clade and the African ape and human clade.

The next two MPTs were only two steps longer. One of them had the same topology as the molecular tree. Their strict consensus was consistent with the molecular phylogeny although it did not resolve the relationships among the African apes and humans. Instead, *Gorilla*, *Homo* and *Pan* formed a trichotomy.

The bootstrap consensus tree was largely unresolved (Figure 5-6c). Only one clade was moderately supported and consistent with the molecular relationships, the African ape and human clade (83%).

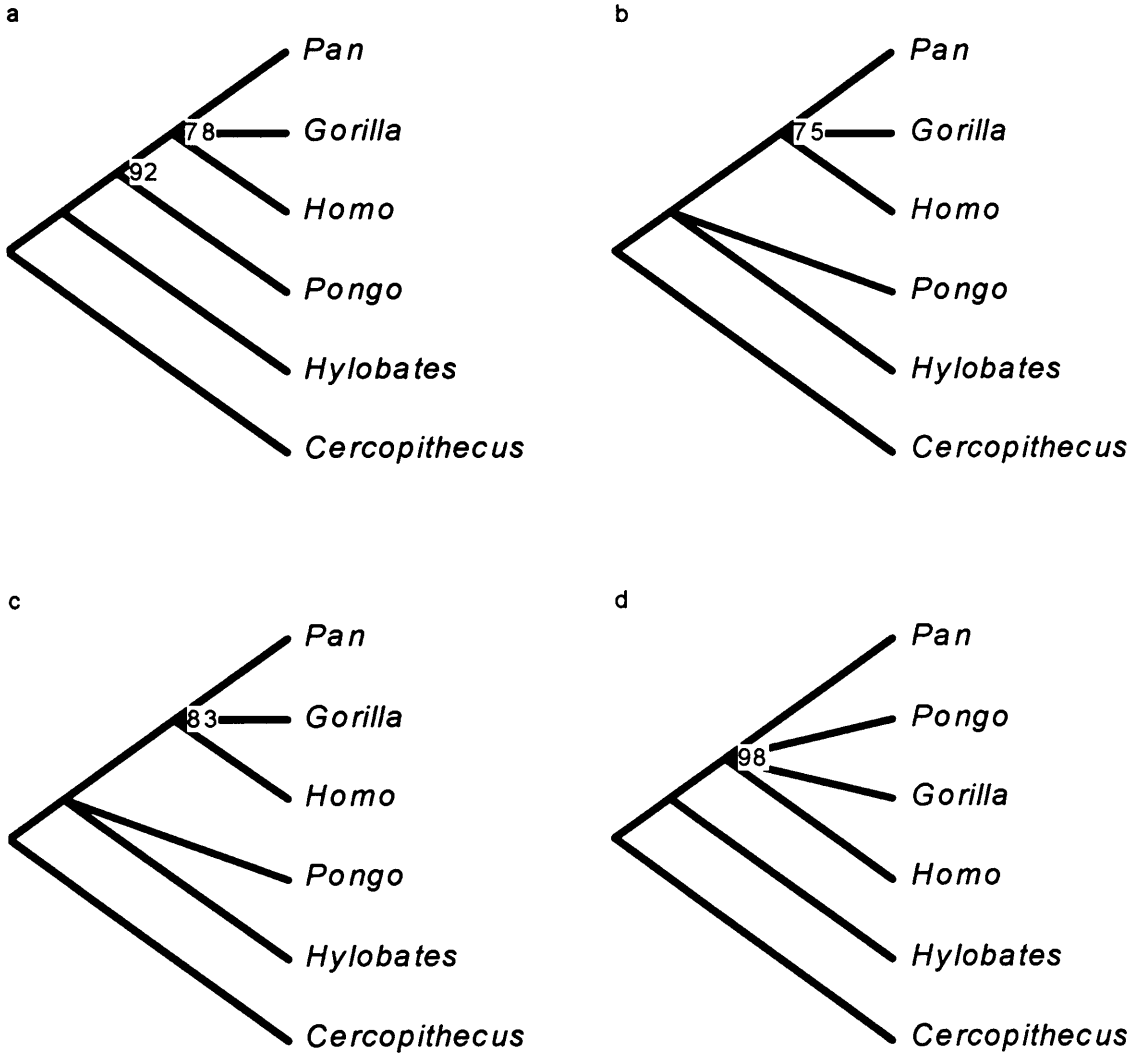

Figure 5-6. Analysis 1a.3: Results of the bootstrap analyses.
(a) Divergence Coding; (b) Binary Coding; (c) Baum's Coding; (d) Segment Coding.

d) Segment Coding

This analysis produced a MPT that differed from the hominoid molecular cladogram (Figure 5-5g). It supported two molecular clades: the hominoid clade, and the great ape and human clade. However, it failed to recover the African apes and human as a monophyletic group. Instead, it placed *Homo* and *Pongo* in a clade next to *Pan*.

The next solution was 10 steps longer. It featured a hominoid clade, a great ape and human clade, and an African ape and human clade. Within the latter clade, *Pan* was the sister taxon of a clade comprising *Homo* and *Gorilla*.

This dataset yielded a bootstrap consensus tree that contained one molecular clade, the great ape and human clade (Figure 5-6d). This was highly significant (98%). No other clade was recovered at the 70% confidence level.

5.1.4 Analysis 1a.4

The next set of analyses was run using *Colobus* as the outgroup and excluding *Papio* and *Cercopithecus* from the study. The most parsimonious solutions are illustrated in Figure 5-7 and their tree statistics are reported in Table 5-4. The 70% consensus cladograms generated in the bootstrap analyses are presented in Figure 5-8.

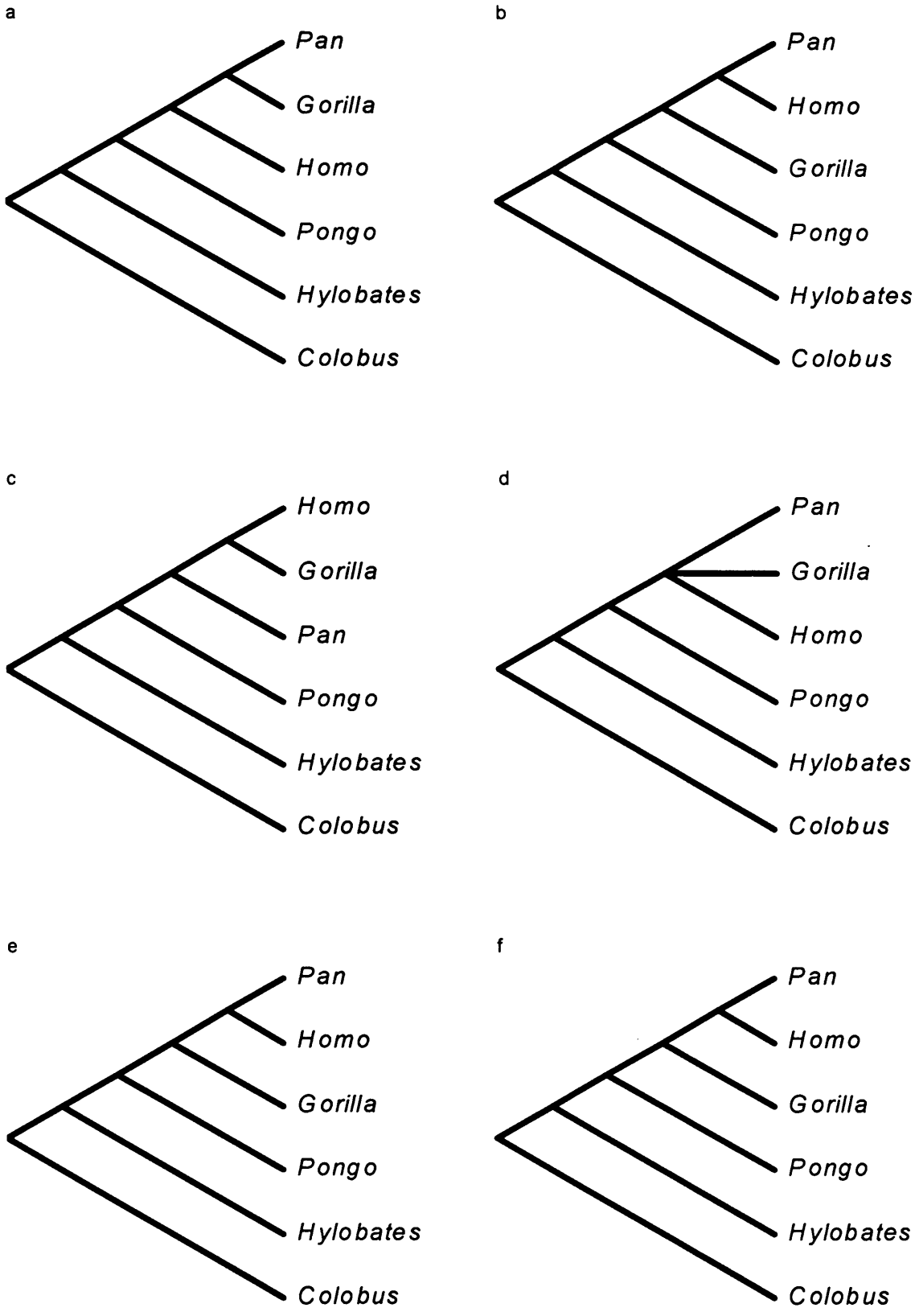

Figure 5-7. Analysis 1a.4: MPTs recovered in the parsimony analyses.
(a) Divergence Coding; (b,c,d) Binary Coding; (e) Baum's Coding; (f) Segment Coding.

Table 5-4. Analysis 1a.4: Tree Statistics associated with MPTs.

Coding Methods	TL	CI	HI	RI	PI
Divergence	1018	0.67	0.33	0.42	86
Binary	114	0.57	0.43	0.41	51
Baum	778	0.64	0.36	0.36	99
Segment	1927	0.69	0.31	0.40	93

TL= Tree Length; CI= Consistency Index; HI= Homoplasy Index; RI= Retention Index; PI= Number of Parsimony Informative Characters.

a) Divergence Coding

The branch-and-bound search returned one minimum length solution that disagreed with the molecular cladogram (Figure 5-7a). This tree supported a phylogeny in which *Pan* and *Gorilla* formed a clade, and *Homo* was their sister taxon. *Pongo* shared an ancestor with the African apes and humans not shared with *Hylobates.* The latter was placed at the base of the hominoid group. Hence, three molecular clades were recovered.

The next most parsimonious tree was two steps longer than the shortest tree. It differed from the hominoid molecular cladogram in supporting a close relationship between *Homo* and *Gorilla* to the exclusion of *Homo.*

The bootstrap consensus tree generated from this dataset (Figure 5-8a) was congruent with the molecular cladogram for the hominoids. The relationships among African apes and humans were not resolved and this trichotomy was moderately supported (86%). The great ape and human clade was strongly supported (99%).

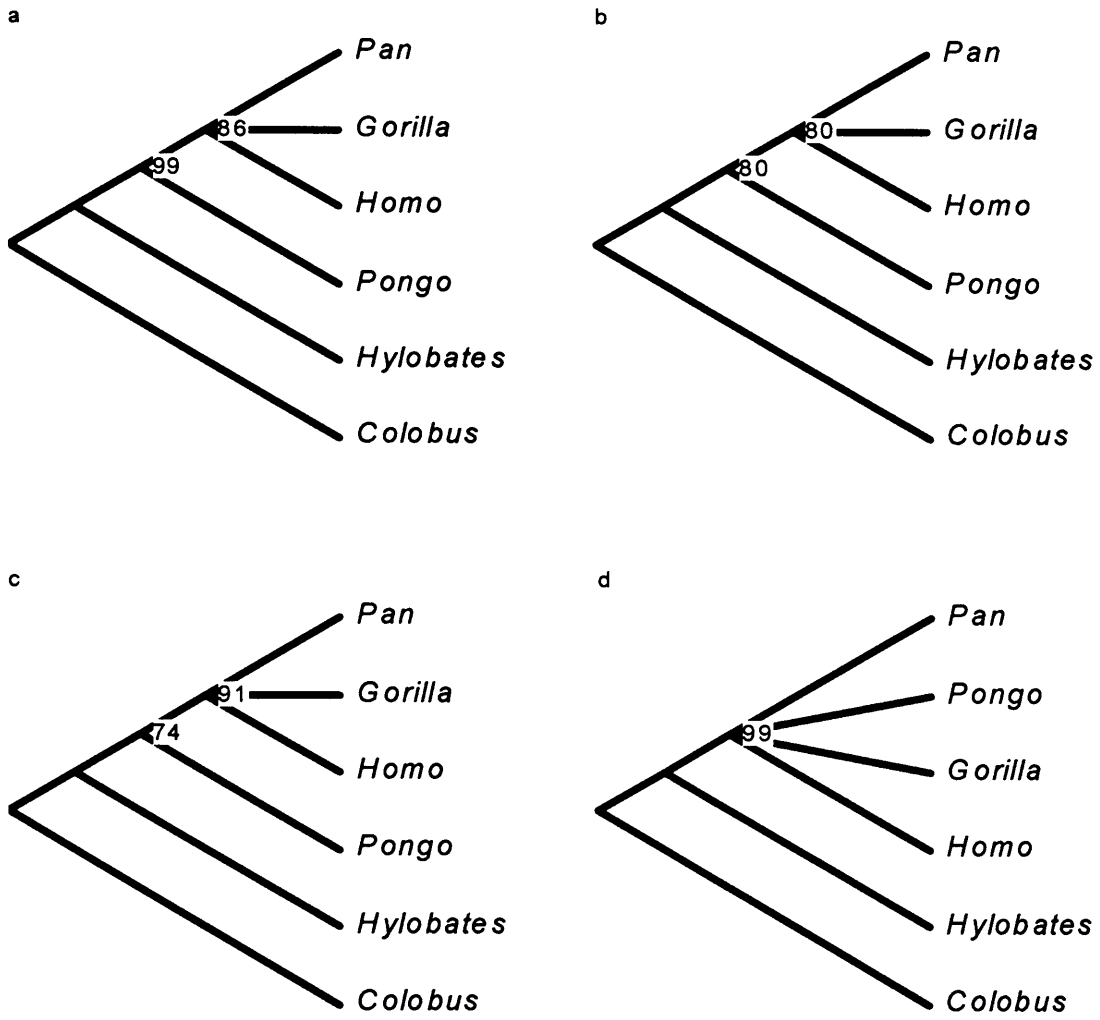

Figure 5-8. Analysis 1a.4: Results of the bootstrap analyses.
(a) Divergence Coding; (b) Binary Coding; (c) Baum's Coding; (d) Segment Coding.

b) Binary Coding

Two most parsimonious trees were produced in this analysis. One tree supported all four hominoid molecular clades (Figure 5-7b). The other differed from the molecular cladogram in placing *Homo* and *Gorilla* in a clade to the exclusion of *Pan* (Figure 5-7c). The strict consensus of these solutions was consistent with the molecular phylogeny and featured an African ape and human trichotomy (Figure 5-7d).

The next most parsimonious solution was two steps longer and differed from the previous ones in placing *Homo* next to a clade that comprised *Gorilla* and *Pan*.

The bootstrap consensus cladogram was only partially resolved at the 70% confidence level (Figure 5-8b). The African ape and human clade was moderately supported (80%), as was the great ape and human clade (80%). These clades were consistent with the molecular results.

c) Baum's Coding

A single most parsimonious tree was recovered from this dataset. It supported all four hominoid molecular clades (Figure 5-7e).

The next most parsimonious solution was two steps longer and disagreed with the molecular tree in placing *Gorilla* and *Homo* in a single clade to the exclusion of *Pan*.

The bootstrap tree generated from this dataset was compatible with the molecular cladogram (Figure 5-8c). Two clades were supported: the great ape and human clade (75%), and the African ape and human clade (91%). The relationships within the latter clade were not resolved at the 70% significance level.

d) Segment Coding

This dataset also yielded one most parsimonious tree that was identical to the molecular cladogram (Figure 5-7f).

The next shortest tree was one step longer and differed from the previous one in placing *Pan* as the sister taxon of a clade formed by *Gorilla* and *Homo*.

The consensus tree generated in the bootstrap analysis was mostly unresolved (Figure 5-8d). The only clade present comprised *Gorilla*, *Homo*, *Pan* and *Pongo*. This was consistent with the molecular results and statistically highly significant (99%).

5.1.5 Summary of Results

The results of the tests described above partially support the hypothesis that cranial characters related to nerves and vessels are useful for recovering the phylogenetic relationships of the extant hominoids. They can be summarised as follows:

a) Parsimony analyses

The level of success of a parsimony analysis was measured in terms of number of molecular clades found in the shortest tree or, when more than one most parsimonious tree was found, in terms of number of molecular clades present in the strict consensus of all the MPTs. These are listed in Table 5-5 according to coding method and outgroup used. The number of molecular clades expected if the hypothesis is correct (E_C) is equal to the total number of clades present in the molecular tree. This is six when all three cercopithecine genera are included in the outgroup (eight taxa), and four when only one genus is included in the outgroup (six taxa).

Table 5-5. Number of molecular clades recovered in the parsimony analyses.

Outgroup	All	*Papio*	*Cercopithecus*	*Colobus*
Ec	6	4	4	4
Divergence	5	4	3	3
Binary	5*	2**	3*	3*
Baum	3	2	2**	4
Segment	4	4	2	4

Ec, number of molecular clades expected if H_0 was true; *, consensus of multiple MPTs consistent with molecular cladogram; **, all molecular clades present in the next MPT.

Four of the 16 analyses found a single MPT that correctly recovered all the molecular relationships among these primate taxa. In two of them, *Colobus* was the only cercopithecine taxon included in the outgroup, and the datasets were coded using Baum's and the segment methods. In the other two cases, *Papio* was the outgroup used to root the trees, and the data were coded using the divergence and segment methods. In three tests (marked with a single asterisk in Table 5-5), more than one MPT was found and their strict consensus was consistent with the molecular phylogeny. In these cases, the relationships within the African ape and human clade were not resolved. All three tests were carried out using the binary method to code the characters. The first included all three cercopithecine taxa in the outgroup, the second only *Cercopithecus*, and the third only *Colobus*.

As explained earlier, the hypothesis was considered supported if the morphology-based cladograms were consistent with the molecular phylogeny. This condition was deemed to exist when a single most parsimonious tree was found and it was identical to the hominoid molecular cladogram, or when more than one tree was recovered and their strict consensus was compatible with the molecular phylogeny. If the best solutions disagreed with the molecular cladogram then the hypothesis was rejected.

Under these strict criteria we can conclude that the hypothesis was only supported by the results of seven tests out of 16. In two further analyses (marked with two asterisks in Table 5-5) all the molecular relationships were found in the second-best most parsimonious tree or one of the second-best most parsimonious trees.

These results suggest that outgroup choice and coding procedures have an important effect on the outcome of phylogenetic reconstruction. If for example the parsimony analysis was run including only *Colobus* in the outgroup and using Baum's method to code the characters, the MPT recovered would fully agree with the molecular phylogeny. However, if *Papio* was the only cercopithecine taxon included in the outgroup, the minimum length cladogram recovered would differ considerably from the consensus molecular tree. This also has an impact on the conclusions drawn on whether the hypothesis tested in this project was supported by the results or not. In fact, if we relied only on the result of the first test (*Colobus*/Baum's coding) we would conclude that the hypothesis was supported and that cranial characters related to nerves and vessels carry a reliable phylogenetic signal. However, from the results of the second test (*Papio*/Baum's) we would conclude that the hypothesis was not supported and therefore we would reject it.

Table 5-6. Success index based on outgroups (S_O) and on coding methods (S_C).

Outgroup	All	*Papio*	*Cercopithecus*	*Colobus*
S_O	0.71	0.75	0.63	0.88
Method	Divergence	Binary	Baum	Segment
S_C	0.83	0.71	0.63	0.79

In order to evaluate the impact of methodological choices on the results of the analyses, two 'success' indices were calculated in order to identify the conditions under which more molecular clades were successfully recovered: the mean success rate for each outgroup (S_O), and the mean success rate for each coding method (S_C). Their computation was described in the 'Materials and Methods' chapter and the results are presented in Table 5-6.

When *Colobus* was the only cercopithecine taxon included in the analyses the success rate was highest (S_O=0.88). In this case, the full molecular cladogram was recovered three times out of four tests (Table 5-5). The next most successful outgroup was *Papio* (S_O=0.75), followed by the tests where all three outgroup taxa were used to root the trees (S_O=0.71). The index was lowest when only *Cercopithecus* was used to root the trees (S_O=0.63).

The coding method that on average produced the greatest number of molecular clades, independent of the outgroup used, was the divergence method (S_C=0.83), followed by segment coding (S_C=0.79) and binary coding (S_O=0.71). Baum's method scored the lowest success rate (S_C=0.63).

b) Bootstrap analyses

The results of the bootstrap tests are summarised in Table 5-7. Every clade that was resolved at the 70% confidence level in the bootstrap consensus trees is represented in the table by a 'plus' or a 'minus' sign. A 'plus' sign represents a 'true' (i.e. molecular)

clade, whereas a 'minus' sign represents a 'false' clade. Each sign is associated with a subscripted letter that indicates the level of statistical support (i.e. bootstrap value) for that clade: 's' stands for a support value greater than 90% (strong support), 'm' for a value of between 80% and 90% (moderate support), 'w' for a value of between 70% and 80% (weak support).

This table shows that the number of clades recovered at the 70% confidence level ranged between zero and three, with a mode of two. All the resolved clades were 'true' molecular clades except in one case. When *Papio* was the only cercopithecine taxon included in the tests and Baum's coding procedures was adopted, one false clade that comprised *Gorilla*, *Homo*, *Hylobates* and *Pan* was resolved at the 70% confidence level, but this found only a weak statistical support (78%).

Table 5-7. Number of clades supported by the bootstrap analyses.

Outgroup	*All*	*Papio*	*Cercopithecus*	*Colobus*
Divergence	$+_w+_s+_s$	$+_w+_m$	$+_w+_s$	$+_m+_s$
Binary	$+_w$		$+_w$	$+_m+_m$
Baum	$+_m+_m$	$-_w+_m$	$+_m$	$+_w+_s$
Segment	$+_m+_s$		$+_s$	$+_s$

+, 'true' clades; -, 'false' clades; 's', strongly supported (>90%); 'm', moderately supported (>80%); 'w', weakly supported (>70%).

A closer examination of the bootstrap results shows that the African ape and human trichotomy was the clade most often recovered in the analyses (Figure 5-9) but the relationships among its component taxa (*Gorilla*, *Pan* and *Homo*) were never resolved. The great ape and human clade also appeared frequently in the bootstrap consensus cladograms. The most resolved consensus cladograms were produced when the divergence method was used to code the data (between two and three clades). This

also yielded the greatest number of statistically significant clades (four). In terms of outgroup choice, using all three taxa or just *Colobus* to root the cladograms produced the highest number of strongly supported clades. In contrast, including just *Papio* in the analyses produced no highly significant clade. Indeed, using this outgroup, few clades were resolved overall (no clade in two cases, and two clades in the other two cases).

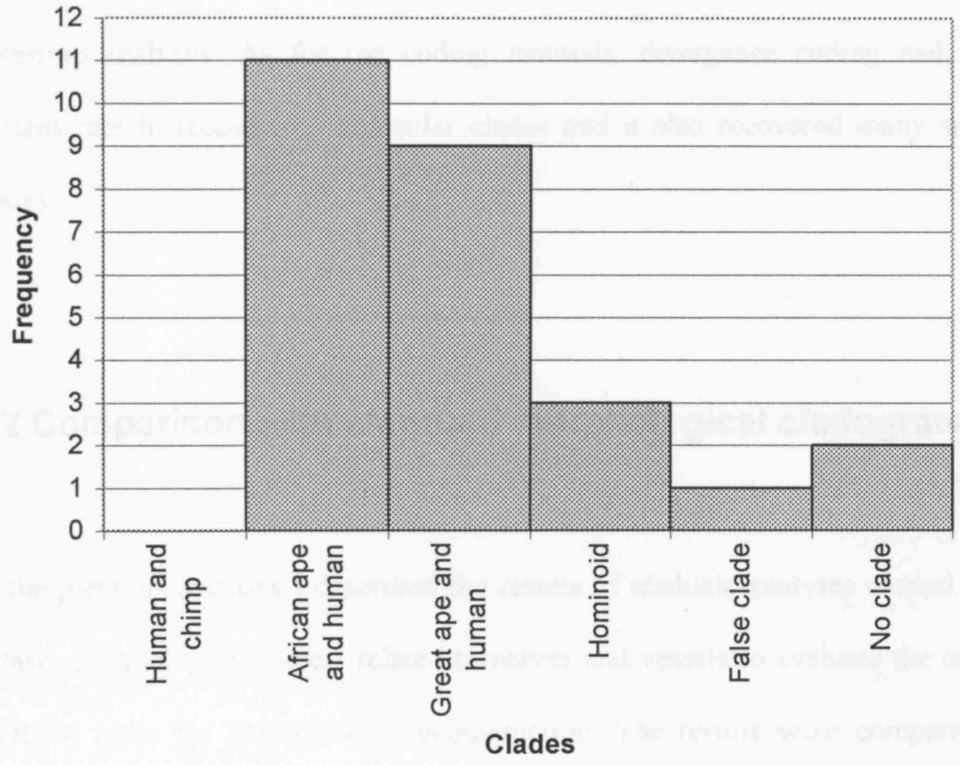

Figure 5-9. Frequency of recovery of each molecular clade in the bootstrap analyses.

c) Summary

The results of the parsimony and bootstrap tests described in this section only partially supported the hypothesis that cranial traits associated with nerves and vessels produce reliable phylogenies for the hominoids (at the generic level). It emerged that the

results of the phylogenetic analyses were strongly influenced by methodological choices such as the outgroup composition and the coding procedure adopted.

It was possible to identify the conditions under which the hypothesis was more strongly satisfied. This particular set of tests indicated that a single-taxon outgroup was most effective. When *Colobus* was the preferred cercopithecine taxon, the highest success rates in recovering the molecular phylogeny of the hominoids were achieved; and higher level of statistical support were recovered for molecular clades in the bootstrap analyses. As for the coding methods, divergence coding had a higher success rate in recovering molecular clades and it also recovered many significant clades.

5.2 Comparison with standard morphological cladograms

In the previous sections I described the results of cladistic analyses carried out on a dataset containing characters related to nerves and vessels to evaluate the usefulness of these traits for phylogenetic reconstruction. The results were compared to the consensus molecular cladograms for the hominoid, which is assumed to be correct, in order to assess whether or not the hypothesis was supported by the data. In this section the results of these analyses are compared to cladograms generated from 'standard' cranial datasets. In other words from those datasets based on cranial characters recurrently used in the literature to make inferences about primate, and in particular hominid, phylogeny.

Two cladograms were chosen. One is based on a dataset of qualitative characters and was taken from a paper published by Collard and Wood (2000). The other is based on a dataset of standard cranial measurements taken from Serdoz (2001).

5.2.1 Qualitative dataset

The qualitative dataset used by Collard and Wood (2000) consisted of 96 craniodental characters recorded on a sample of the five hominoid genera plus an outgroup (*Colobus*). The data matrix was compiled from various sources and the reader is referred to the literature cited in the paper for a detailed list of the original sources. When this dataset was subjected to parsimony analysis the cladogram produced placed *Hylobates* at the base of the hominoid clade (Figure 5-10a). It also placed *Homo* and *Pongo* in one clade, and next to another clade that comprised *Pan* and *Gorilla*. In other words, two out of four molecular groups were recovered, the hominoid clade and the great ape and human clade. The bootstrap analysis only recovered one clade that was inconsistent with the consensus molecular cladogram (Figure 5-10b). It supported *Gorilla* and *Pan* as sister taxa, and was statistically strongly supported (92%).

When these results are compared with the results of the soft tissue-linked datasets it is clear that the latter yield stronger and more reliable phylogenetic hypotheses. It is noteworthy that a cladogram compatible with the molecular phylogeny was recovered three times out of the four parsimony analyses that included only *Colobus* in the outgroup (Analysis 1a.4 and Table 5-5). In the fourth analysis, three (out of four) molecular clades were recovered. Furthermore, the bootstrap tests recovered in most

cases two clades that were moderately and strongly supported (Table 5-7). Only in one case (segment coding) was a single molecular clade found and this was strongly supported. These clades were always 'true' clades.

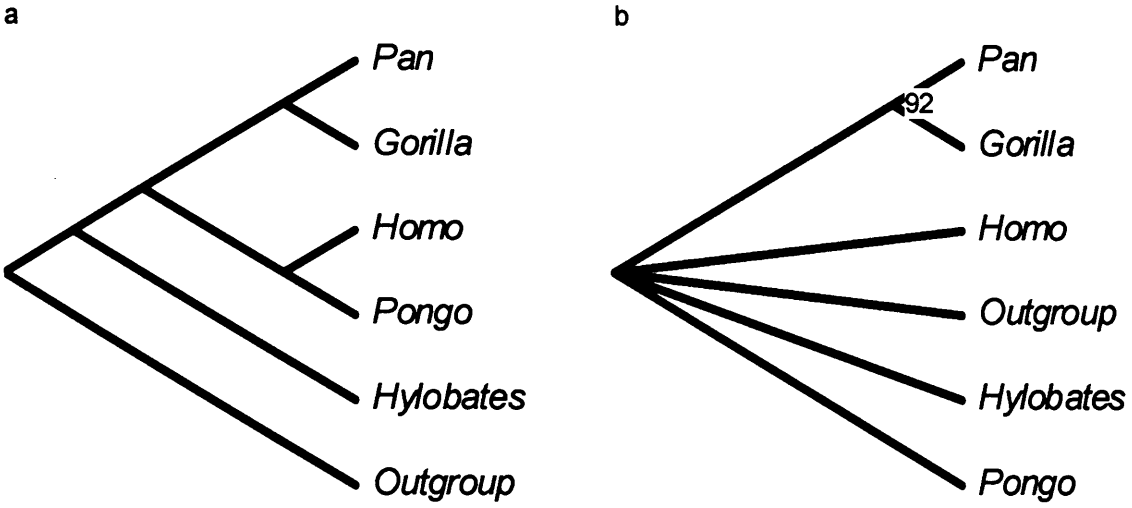

Figure 5-10. Hominoid cladograms generated from a qualitative dataset from Collard and Wood (2000).
a) Most parsimonious tree; b) Consensus bootstrap tree (70% confidence level).

Hence, the datasets based on soft-tissue linked characters produced stronger and more reliable phylogenetic hypotheses than the datasets based on standard qualitative traits.

5.2.2 Quantitative dataset

The metric dataset was prepared using unpublished data collected for my M.Sci. dissertation (Serdoz, 2001). Thirty standard craniometric measurements were originally recorded on a mixed-sex sample that comprised 20 *Gorilla gorilla*, 20 *Homo sapiens*, 19 *Pan troglodytes*, one *Pan paniscus*, 20 *Pongo pygmaeus*, and 20 specimens of an outgroup, *Colobus*. This sample was supplemented with 20

specimens from the genus *Hylobates* in order to make it comparable with the vessel- and nerve-related datasets. The 30 morphometric traits comprised measurements of the palate (1-8), the mandible (9,10), the face (11-23) and the cranial vault (24-30) (Table 4-7). These were taken with Vernier callipers (± 0.005 mm) and spreading callipers (± 0.5 mm). The confounding effect of body size differences was corrected for by scaling the data with the geometric mean.

The dataset underwent the same coding procedures employed in the previous analyses. Coding metric measurements using the binary method is not meaningful in terms of presence/absent. However – as explained in section 4.4.2b – it is still possible to apply the gap-weighting procedure to the dataset setting the number of gaps to one. The four data matrices thus obtained where then subjected to parsimony analyses to generate phylogenetic hypotheses. Bootstrap analyses were carried out to assign a level of statistical support to these hypotheses. The most parsimonious cladograms are illustrated in Figure 5-11 while the consensus bootstrap trees are presented in Figure 5-12.

a) Divergence Coding

The first dataset was coded using the divergence method. The parsimony analysis returned one single most parsimonious cladogram that did not agree with the molecular phylogeny for the hominoids (Figure 5-11a). It supported a phylogenetic hypothesis in which the hominoids were split into two main clades. In the first clade *Pongo* was the sister taxon of a group formed by *Homo* and *Hylobates*. In the second clade *Gorilla* and *Pan* shared a common ancestor not shared with the other taxa.

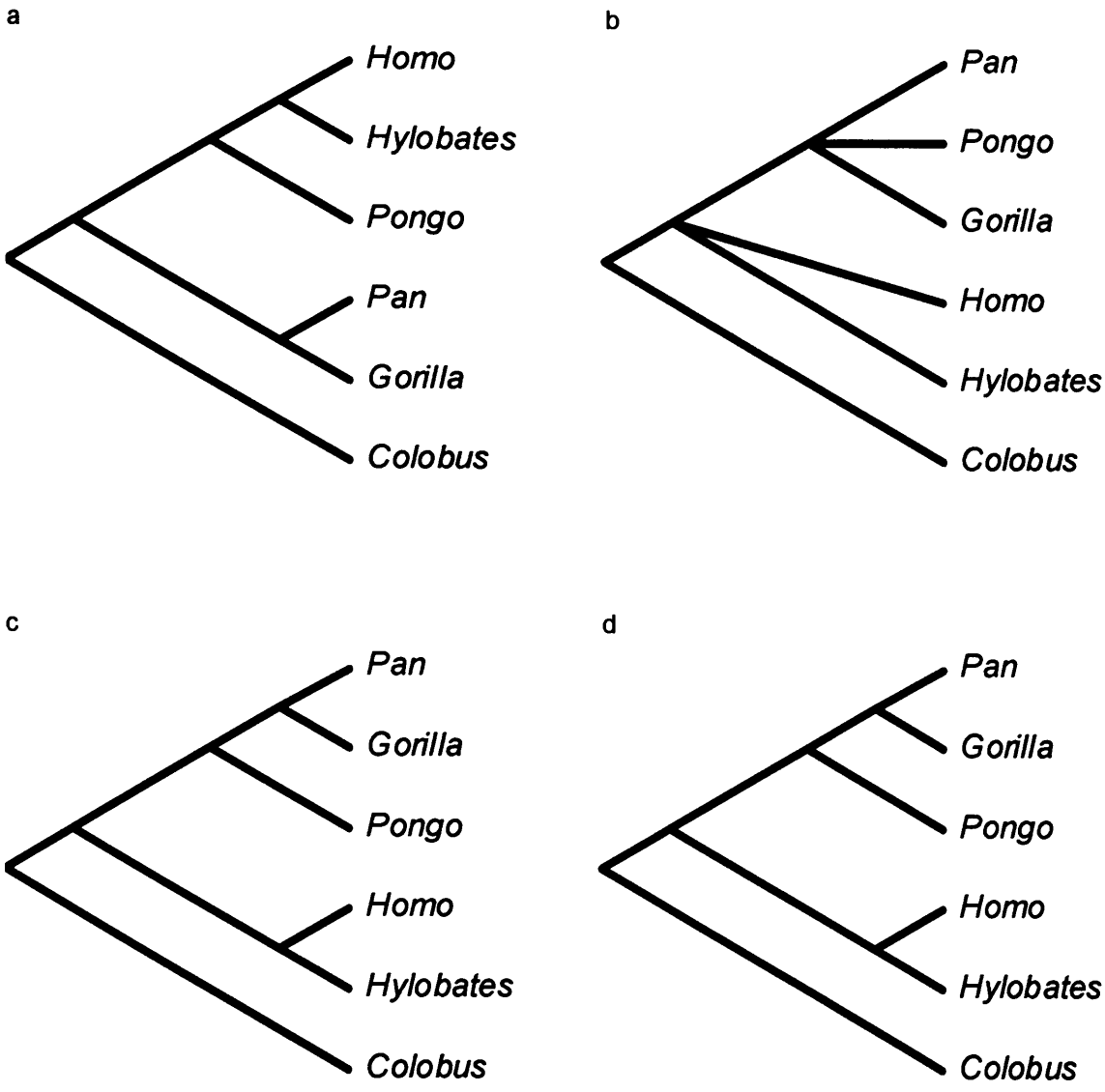

Figure 5-11. MPTs recovered from the craniometric dataset.
a) Divergence Coding; b) Binary Coding (strict consensus of 3 trees); c) Baum's Coding; d) Segment Coding.

Therefore, only one molecular clade was found in this analysis. The bootstrap test (Figure 5-12a) recovered two significant clades at the 70% confidence level: the African ape clade (72%) and a clade formed by *Homo* and *Hylobates* (100%). Neither of these agreed with the molecular results.

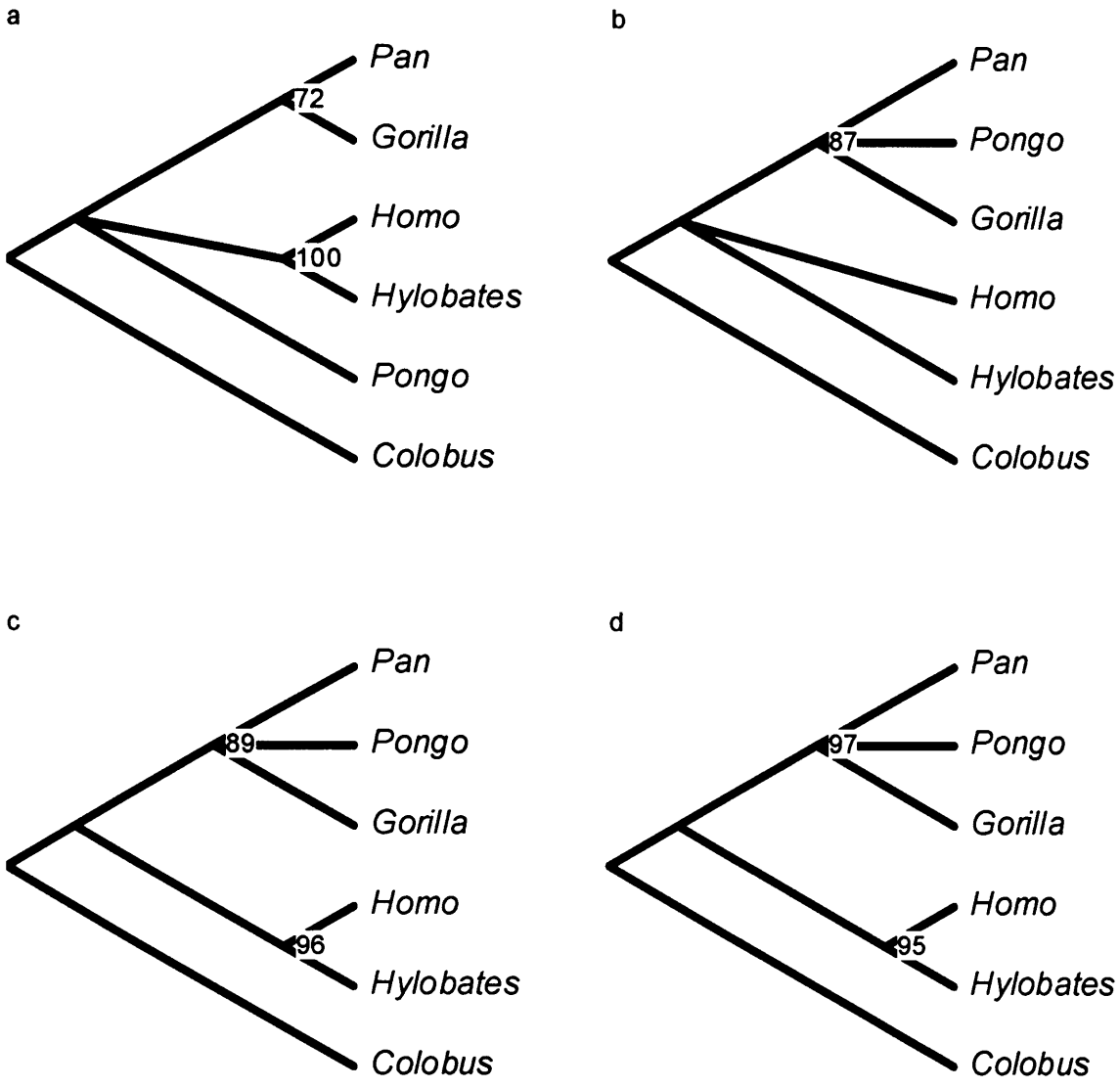

Figure 5-12. Bootstrap cladograms generated from the craniometric dataset.
a) Divergence Coding; b) Binary Coding; c) Baum's Coding; d) Segment Coding.

b) Binary Coding

Three minimum-length trees were found in the parsimony analysis and none of them agreed with the molecular tree. Their strict consensus featured a trichotomy formed by *Homo*, *Hylobates* and a clade that included *Pan*, *Gorilla* and *Pongo* (Figure 5-11b). The relationships within the latter group were not resolved. Therefore, only one molecular clade was recovered. The bootstrap analysis (Figure 5-12b) supported only

one clade that comprised *Pan*, *Gorilla* and *Pongo* (87%) and was therefore inconsistent with the molecular phylogeny of the hominoids.

c) Baum's Coding

The parsimony analysis returned one most parsimonious solution that was not consistent with the molecular cladogram (Figure 5-11c). It recovered a clade formed by *Homo* and *Hylobates*, next to another clade formed by *Gorilla*, *Pan* and *Pongo*. Within the latter, *Gorilla* and *Pan* were more closely related to each other than either was to *Pongo*. Hence, only one molecular clade was present in this solution. The bootstrap test returned two clades (Figure 5-12c): one comprised *Homo* and *Hylobates* (96%) and another one comprised *Gorilla*, *Pan* and *Pongo* (89%). Neither agreed with the molecular results.

d) Segment Coding

The last dataset was coded using the segment method. One most parsimonious tree was found in the parsimony analysis (Figure 5-11d), and again it did not agree with the molecular phylogeny. As in the previous analysis, it supported a clade formed by *Homo* and *Hylobates* next to a clade formed by the great apes. Also, *Gorilla* and *Pan* were more closely related to each other than either was to *Pongo*. Therefore just one molecular clade was supported. The bootstrap test recovered two clades that were very strongly supported although inconsistent with the molecular phylogeny (Figure 5-12d). One was formed by *Homo* and *Hylobates* (95%), and one was formed by *Gorilla*, *Pan* and *Pongo* (97%).

e) Summary of Results

None of the parsimony analyses described in this section recovered the hominoid molecular phylogeny. In fact, they never presented more than one molecular clade, the hominoid clade, and the average rate of success (S_O) was thus 0.25. This is low compared to the equivalent value for the analysis of the soft tissue-related traits, which for *Colobus* was 0.88.

Overall, these phylogenetic hypotheses supported a close relationship between *Homo* and *Hylobates*, and between *Pan* and *Gorilla*. Notably, the clades that found statistical support at the 70% confidence level were all false clades. Some of these found a very high statistical support. This was not the case for the datasets based on soft tissue-linked characters from which moderately and strongly supported 'true' clades were recovered.

These results suggest that cranial characters related to nerves and vessels produce phylogenies more reliable than those obtained from standard craniometric measurements, at the generic level.

5.3 Summary

In this chapter I have reported the analyses that investigated the hypothesis that characters of the primate cranium related to nerves and vessels may be reliable for

reconstructing the phylogenetic history of the hominoids at the generic level. Using this type of information, I constructed a series of datasets that were subjected to cladistic analysis in order to obtain estimates of the phylogenetic relationships of apes and humans. The resulting trees were then compared to the consensus hominoid molecular phylogeny, which is strongly supported and hence assumed to be correct. They were also compared to morphological cladograms based on standard craniodental datasets.

The hypothesis was partially supported by the results of these tests. Seven out of the 16 phylogenetic hypotheses generated from the morphology-based data-matrices agreed in all parts with the molecular cladogram. When the nerve- and vessel-related datasets were bootstrapped, the consensus cladograms were consistent with the molecular phylogeny in all cases but one, independent of the coding method used or the outgroup chosen to root the trees.

It emerged that the topologies of the minimum-length solutions varied depending on the composition of the outgroup and on the coding procedure adopted to make the data suitable for cladistic analysis. The conditions under which the hypothesis was satisfied were summarised in Table 5-5 and Table 5-6. Incorporating only *Colobus* in the tests produced more successful results in terms of number of molecular clades recovered. It also helped recover true clades with statistically significant bootstrap values. In terms of coding methods, the two procedures that performed better were the divergence method and the segment method.

Chapter 6. RESULTS II: HYPOTHESIS 1b

In the next set of analyses I investigated the effect of using species instead of genera as the operational taxonomic unit in the cladistic analyses. In order to do this, the *Hylobates* sample was split into a taxon comprising specimens of *Hylobates syndactylus* and a taxon comprising specimens belonging to *H. lar* and *H. agilis* (named *Hylobates spp*). The *Pan* sample was also split into two species: *Pan troglodytes* and *Pan paniscus*. The other hominoid taxa were left unchanged, except throughout this chapter they will be referred to with the name of their component species, i.e. *Gorilla gorilla*, *Homo sapiens* and *Pongo pygmaeus*.

The datasets were subjected to the same analytical procedures adopted to test Hypothesis 1a and described in the Materials and Methods chapter. The resulting trees were compared to the consensus molecular cladogram for the extant hominoids shown below (Figure 6-1).

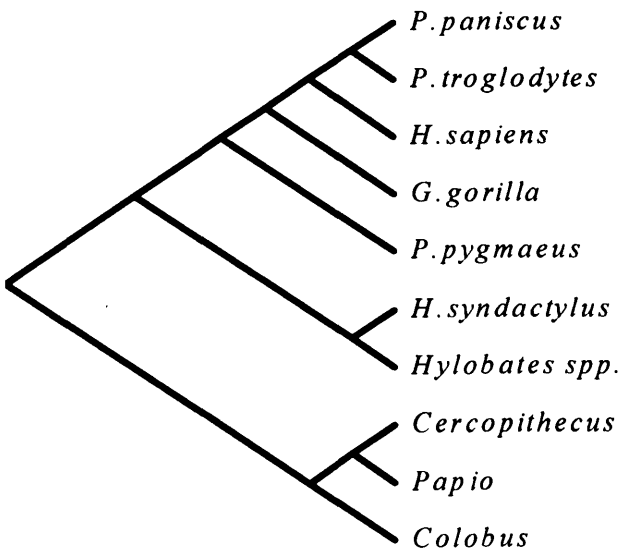

Figure 6-1. Hominoid molecular cladogram showing species-level relationships.

6.1 Hypothesis 1b: Cranial characters associated with nerves and vessels produce reliable phylogenies for the hominoids at the specific level.

6.1.1 Analysis 1b.1

In this set of analyses, all three cercopithecine taxa (*Cercopithecus*, *Colobus* and *Papio*) were used to root the trees. The most parsimonious cladograms discussed in this section are illustrated in Figure 6-2, and the associated tree statistics are reported in Table 6-1. The results of the bootstrap tests are presented in Figure 6-3.

a) Divergence coding

This parsimony analysis returned a single most parsimonious tree (Figure 6-2a) that did not agree with the molecular cladogram. It recognised the hominoids as monophyletic and correctly recovered the molecular relationships among the outgroup taxa. It also supported an African ape and human clade. However, it placed *H. syndactylus* at the base of the hominoid clade, and *Hylobates spp* next to a great ape and human clade. It also placed the two chimpanzee species in a clade next to a clade formed by *H. sapiens* and *G. gorilla*. Therefore, six molecular clades were recovered in this analysis.

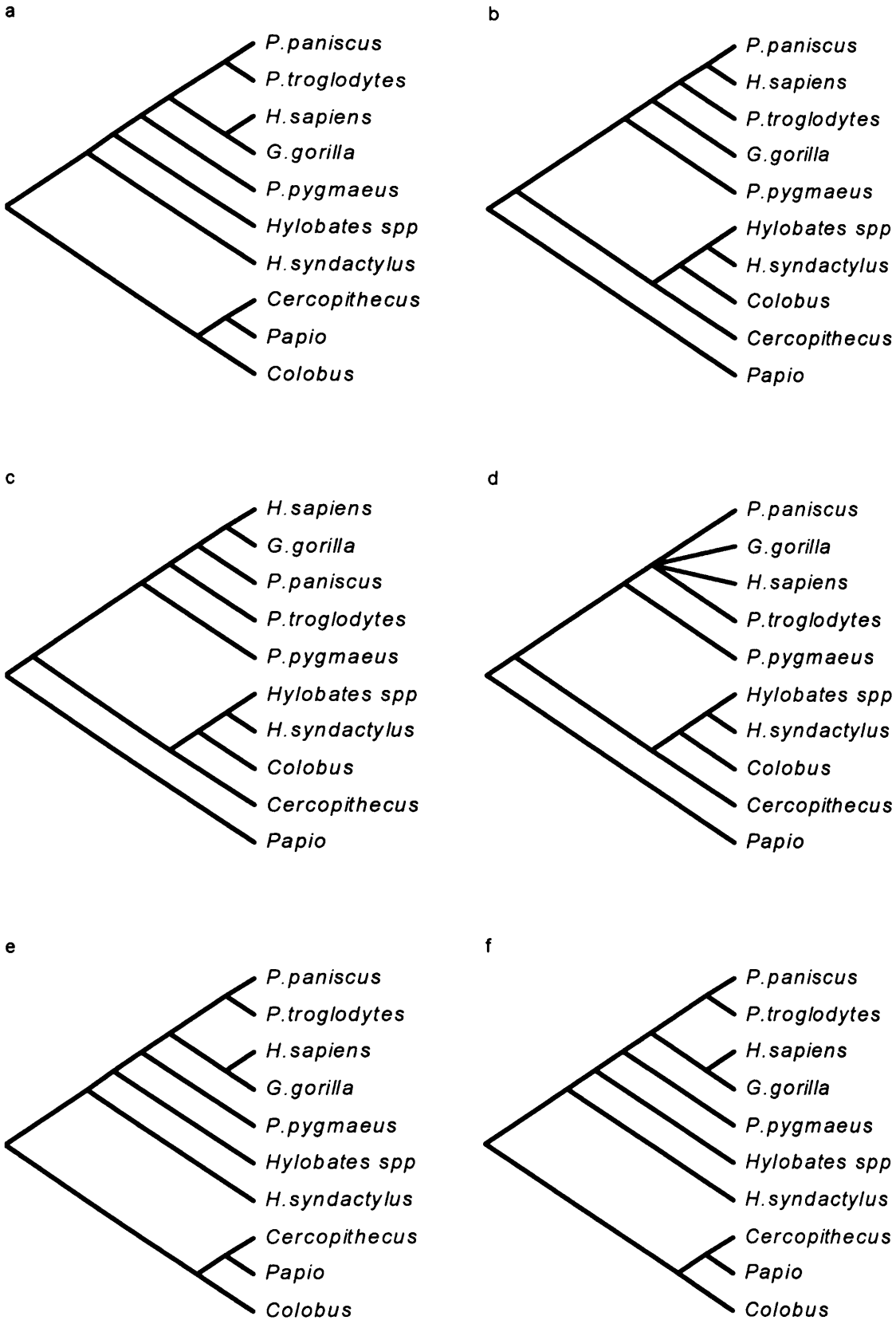

Figure 6-2. Most parsimonious trees produced in Analysis 1b.1.
(a) Divergence coding; (b, c, d) Binary coding; (e) Baum's coding; (f) Segment coding.

Table 6-1. Tree statistics associated with Analysis 1b.1.

Coding Method	TL	CI	HI	RI	PI
Divergence	2359	0.51	0.49	0.45	92
Binary	166	0.46	0.54	0.50	67
Baum	1942	0.45	0.55	0.38	101
Segment	3020	0.52	0.48	0.44	97

TL= tree length; CI= consistency index; HI= homoplasy index; RI= retention index PI= number of parsimony informative characters.

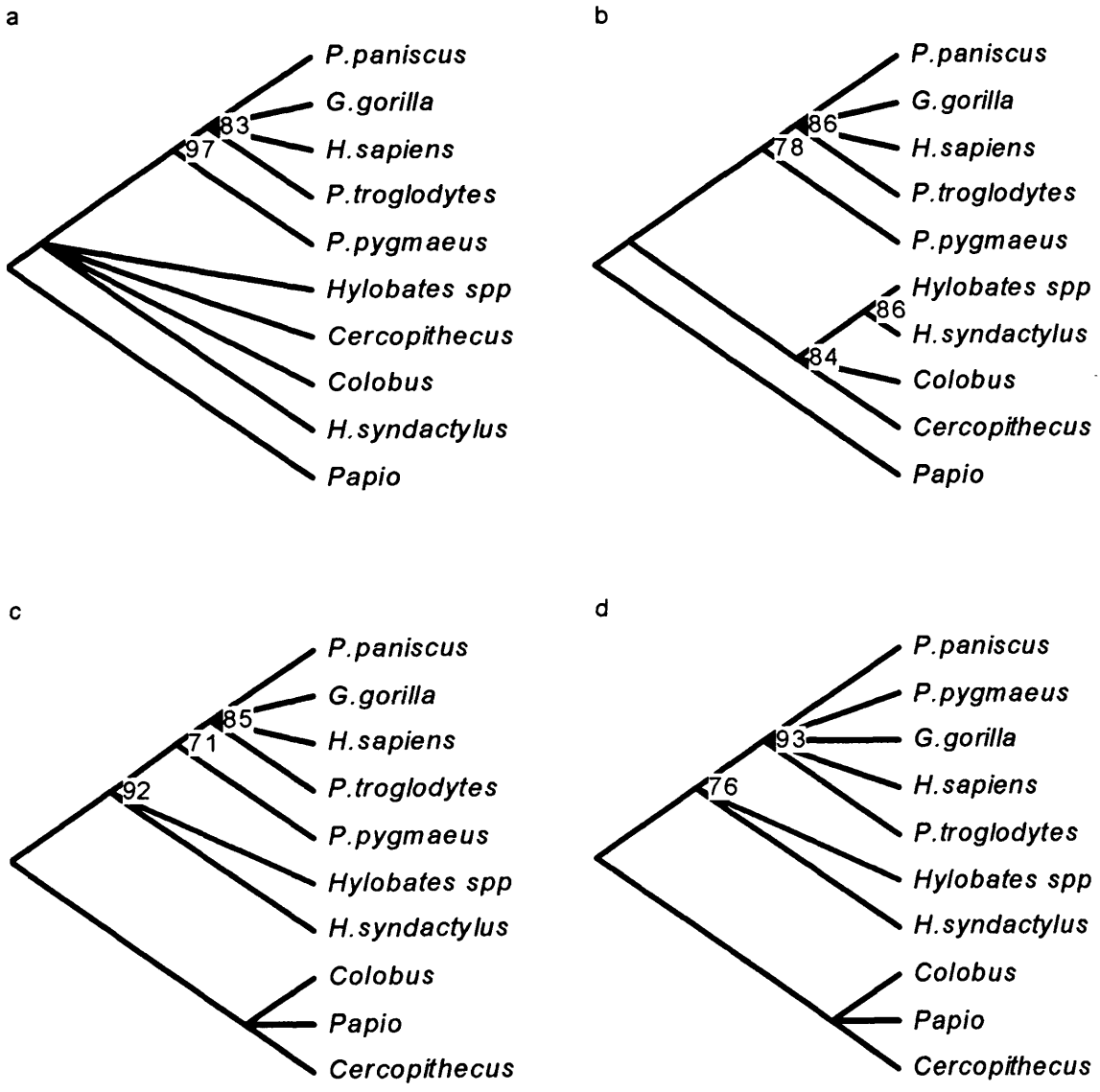

Figure 6-3. Bootstrap consensus cladograms generated in Analysis 1b.1.
(a) Divergence coding; (b) Binary coding; (c) Baum's coding; (d) Segment coding.

The next tree was nine steps longer. It contained the great ape and human clade, and the African ape and human clade. Within the latter clade, the two chimpanzee species formed a monophyletic group next to a clade that comprised *H. sapiens* and *G. gorilla*. This cladogram failed to recognise the hominoids as a monophyletic group and, instead, placed *Colobus* and *Cercopithecus* in a clade with gibbons and siamangs. Within this group, *Colobus* was incorrectly linked with the hylobatids to the exclusion of *Cercopithecus*. *Papio* appeared at the base of the cladogram.

The bootstrap analysis generated a consensus tree that featured two clades (Figure 6-3a) that were consistent with the molecular phylogeny. The African ape and human clade was moderately supported (83%). The great ape and human clade was highly significant (97%). The rest of the tree was unresolved.

b) Binary coding

Two most parsimonious trees were recovered from this dataset. None of them was consistent with the hominoid molecular cladogram, and none of them supported the hominoids as a monophyletic group. The first tree (Figure 6-2b) presented a phylogenetic hypothesis in which *P. troglodytes* was the sister-group of a clade that comprised *H. sapiens* and *P. paniscus*. This branch was then joined by *Gorilla gorilla* to form an African ape and human clade, and then by *Pongo pygmaeus* to form a great ape and human clade. At the base of the tree, another branch comprised the hylobatids and two cercopithecine taxa, *Colobus* and *Cercopithecus*. Within this clade, *Hylobates* and *H. syndactylus* formed a single clade that was joined, first, by *Colobus* and then by *Cercopithecus*. *Papio* was at the base of the tree. The second tree (Figure 6-2c)

featured a clade in which *G. gorilla* and *H. sapiens* formed a monophyletic group to the exclusion of *P. paniscus*. This clade was then joined by *P. troglodytes* to form the African ape and human clade, and next by *P. pygmaeus* to form the great ape and human clade. The rest of the tree was identical to the first one. The strict consensus of these two solutions was not consistent with the molecular phylogeny; it is shown in Figure 6-2d. Four molecular clades were present in this cladogram: the hylobatid clade, the great ape clade and the African ape and human clade. The tree could not be rooted in a way such that the hominoids were monophyletic. Instead *Colobus* and *Cercopithecus* were placed in a clade with hylobatids.

The next six most parsimonious solutions were only one step longer than the previous ones and none of them agreed with the molecular phylogeny. Their strict consensus featured three molecular clades: the African ape and human clade, the great ape and human clade and the hylobatid clade. The rest of the tree was unresolved.

The bootstrap consensus tree (Figure 6-3b) produced three clades that agreed with the molecular results. The first was the moderately supported African ape and human clade (86%). The relationships within this group were not resolved at the 70% significance level. The second was the weakly supported great ape and human clade (78%). The third molecular clade included *Hylobates* and *S. syndactylus* and was also moderately supported (86%). The rest of the cladogram was not resolved.

c) Baum's coding

This dataset produced a single minimum length tree that did not agree with the hominoid molecular cladogram (Figure 6-2e). It supported an African ape and human clade in which *H. sapiens* was the closest relative of *G. gorilla* next to a clade formed by the two chimpanzee species. This branch was joined, first, by *P. pygmaeus* and then by *Hylobates spp*. The other gibbon species, *H. syndactylus*, was positioned at the base of the hominoid clade. The cercopithecine outgroups formed a separate branch in which, consistent with the molecular results, *Cercopithecus* and *Papio* were more closely related to each other than either was to *Colobus*. Therefore, six of the eight molecular clades were recovered in this analysis.

The next two most parsimonious solutions were two steps longer than the shortest tree. Their strict consensus did not agree with the hominoid molecular phylogeny. It recovered an African ape and human clade, a great ape and human clade, a hylobatid clade and a hominoid clade. It also supported a sister group relationship between *H. sapiens* and *G. gorilla*, and one between the two chimpanzee species. The relationships among the three outgroups were not resolved.

This dataset generated a partially resolved bootstrap tree (Figure 6-3c). All the clades recovered in this analysis were consistent with the molecular phylogeny. The first clade was a moderately supported African ape and human polytomy (85%). The second one was a weakly supported great ape and human clade (71%). The third clade was a strongly supported hominoid clade (92%).

d) Segment coding

The single most parsimonious tree recovered in this analysis did not agree with the molecular cladogram (Figure 6-2f). It supported a hominoid clade, a great ape and human clade, an African ape and human clade, and a chimpanzee clade. It also recovered the correct relationships among the outgroup taxa. Inconsistent with the molecular tree, it placed *Hylobates spp* next to the great ape and human clade and *H. syndactylus* at the base of the hominoid clade. It also placed *H. sapiens* and *G. gorilla* in a single clade next to chimpanzees. Therefore, six molecular clades were correctly recovered.

The next most parsimonious solution was one step longer. It also differed from the molecular cladogram and its topology was similar to that of the best tree. It recovered a hominoid clade, a great ape and human clade, an African ape and human clade, and a chimpanzee clade. Humans and gorillas were placed, again, in a single clade. However, in this case, *Hylobates spp* and *H. syndactylus* were organised in a monophyletic clade at the base of the hominoid clade.

When this dataset was bootstrapped, two clades were recovered at the 70% confidence level (Figure 6-3d). The first one was a great ape and human clade, which was well supported (93%). The second was a weakly supported hominoid clade (76%). Both groups were consistent with the molecular relationships. The rest of the tree was unresolved.

6.1.2 Analysis 1b.2

In the next set of tests, the parsimony analyses were run excluding *Colobus* and *Cercopithecus* from the study and using *Papio* to root the trees. The most parsimonious cladograms are shown in Figure 6-4 and the associated tree statistics are reported in Table 6-2. The bootstrap trees are illustrated in Figure 6-5.

a) Divergence coding

This analysis returned a single most parsimonious tree (Figure 6-4a). The topology of this tree was not congruent with the hominoid molecular cladogram. It supported five molecular clades: the hominoid clade, a hylobatid clade, a great ape and human clade, an African ape and human clade, and a chimpanzee clade. However, it failed to recover the sister group relationship between humans and chimps. Instead, it placed *H. sapiens* and *G. gorilla* in a clade next to the two chimpanzee species.

The next most parsimonious solution was three steps longer than the best tree. It was identical to the consensus molecular cladogram.

The bootstrap analysis produced a partially resolved consensus tree containing two molecular clades (Figure 6-5a). The first clade comprised the African apes and humans and was moderately supported (85%). The second comprised *Hylobates spp* and *H. syndactylus* and was strongly supported (91%). No other clade was supported at the 70% confidence level.

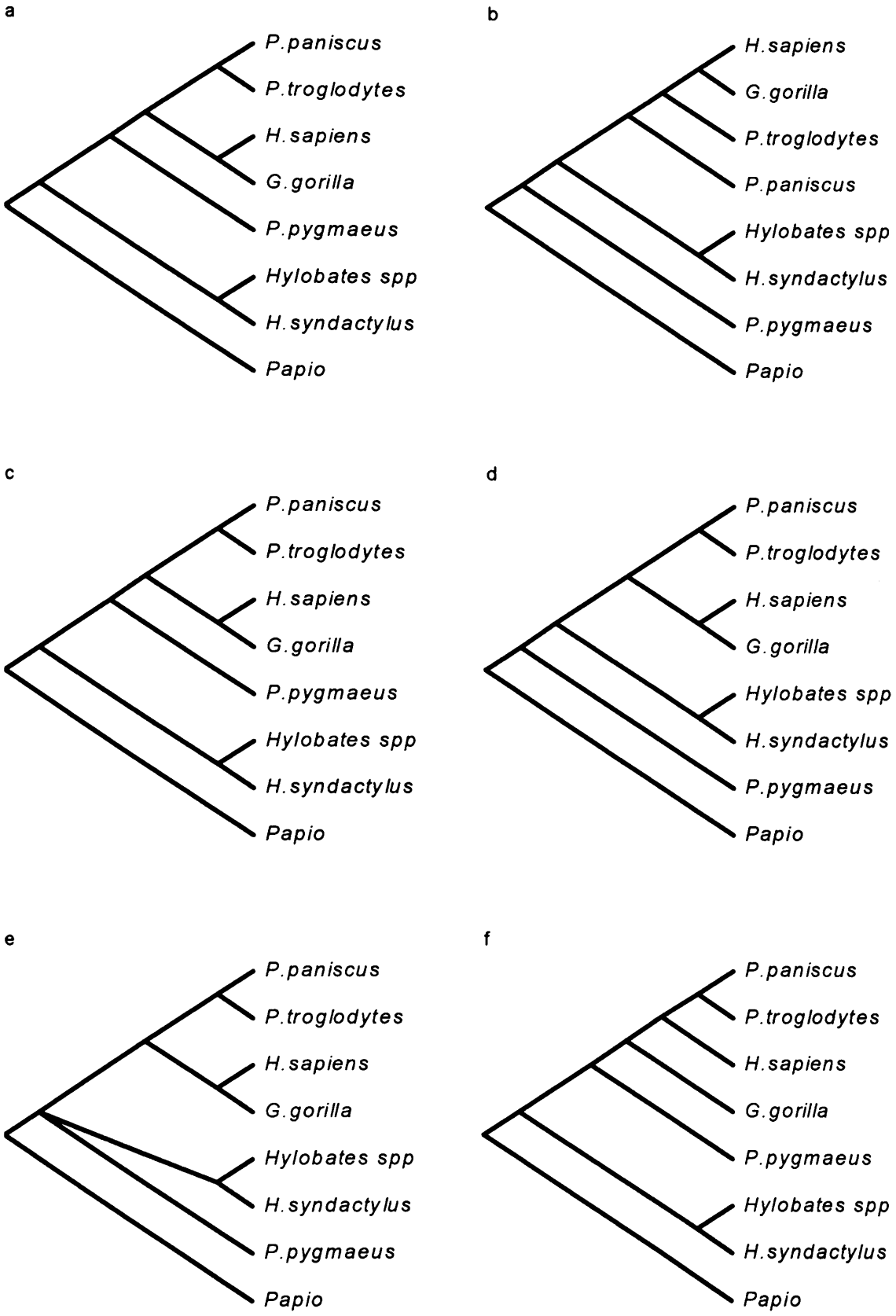

Figure 6-4. Most parsimonious trees produced in Analysis 1b.2.
(a) Divergence coding; (b) Binary coding; (c, d, e) Baum's coding; (f) Segment coding.

Table 6-2. Tree statistics associated with Analysis 1b.2.

Coding Method	TL	CI	HI	RI	PI
Divergence	1649	0.57	0.43	0.41	91
Binary	144	0.51	0.49	0.45	61
Baum	1297	0.53	0.47	0.35	101
Segment	2605	0.60	0.40	0.40	95

TL= tree length; CI= consistency index; HI= homoplasy index; RI= retention index; PI= number of parsimony informative characters.

b) Binary coding

The single most parsimonious tree found in this analysis was not consistent with the molecular results (Figure 6-4b). According to this tree, *H. sapiens* and *G. gorilla* were more closely related to each other than either was to *P. troglodytes*. This clade was joined next by *P. paniscus* to form an African ape and human clade. This solution did not support a great ape and human clade. Instead, it placed the two hylobatid species in a clade next to the African apes and humans, while *P. pygmaeus* occupied a basal position within the hominoids. Hence, only three molecular clades were recovered.

The next two most parsimonious solutions were only one step longer and neither of them agreed with the molecular phylogeny. Their strict consensus was largely unresolved. It featured only one clade, the hylobatid clade. The rest of the topology was unresolved.

This dataset generated a bootstrap consensus tree that featured one molecular clade (Figure 6-5b). This clade was a moderately supported *Hylobates spp.* and *H. syndactylus* clade (89%). The rest of the tree was not resolved.

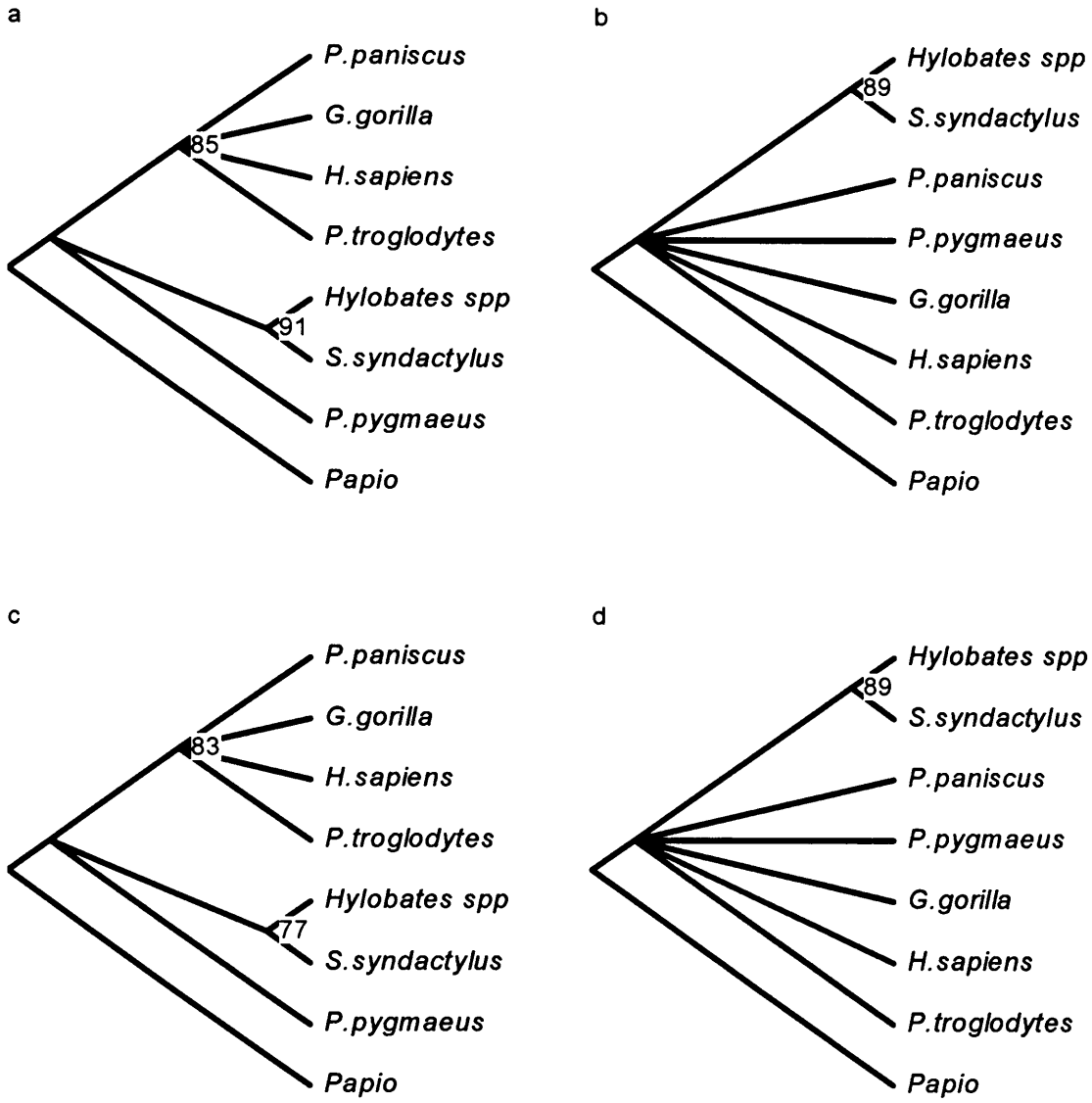

Figure 6-5. Bootstrap consensus cladograms generated in Analysis 1b.2.
(a) Divergence coding; (b) Binary coding; (c) Baum's coding; (d) Segment coding.

c) Baum's coding

The two most parsimonious trees recovered from this dataset did not agree with the molecular phylogeny for the hominoids. The first tree (Figure 6-4c) supported a phylogenetic hypothesis in which *Hylobates spp.* and *H. syndactylus* formed a single clade and occupied a basal position within the hominoids. A great ape and human

clade and an African ape and human clade were also recovered. Within the latter, *P. paniscus* was positioned as the sister-taxon of *P. troglodytes*. However, the sister group relationship between humans and chimpanzees was not supported. Instead, *H. sapiens* was positioned as the sister group of *G. gorilla*. The second minimum length tree (Figure 6-4d) was similar to the previous one but in this solution the hylobatids were place next to African apes and humans, whilst *P. pygmaeus* sat at the base of the hominoid clade. The strict consensus tree did not agree with the molecular phylogeny (Figure 6-4e). It featured a trichotomy formed by the hylobatid clade, *P. pygmaeus* and the African ape and human clade. Within the latter group, *P. paniscus* and *P. troglodytes* formed a monophyletic group, placed next to a clade that comprised *H. sapiens* and *G. gorilla*. Hence, four molecular clades were supported in this analysis.

The next most parsimonious tree was three steps longer than the shortest tree. It also disagreed with the molecular cladogram. It contained a hominoid clade, a hylobatid clade, a great ape and human clade, and an African ape and human clade. However, within the latter it placed *H. sapiens* as the sister taxon of *G. gorilla*. This group was joined, first, by *P. paniscus* and then by *P. troglodytes*.

The bootstrap analysis recovered only two molecular clades (Figure 6-5c). One was the African ape and human clade. This was moderately supported (83%) but the relationships among its component taxa were not resolved. The second was the clade formed by *Hylobates* and *H. syndactylus*. This was weakly supported (77%).

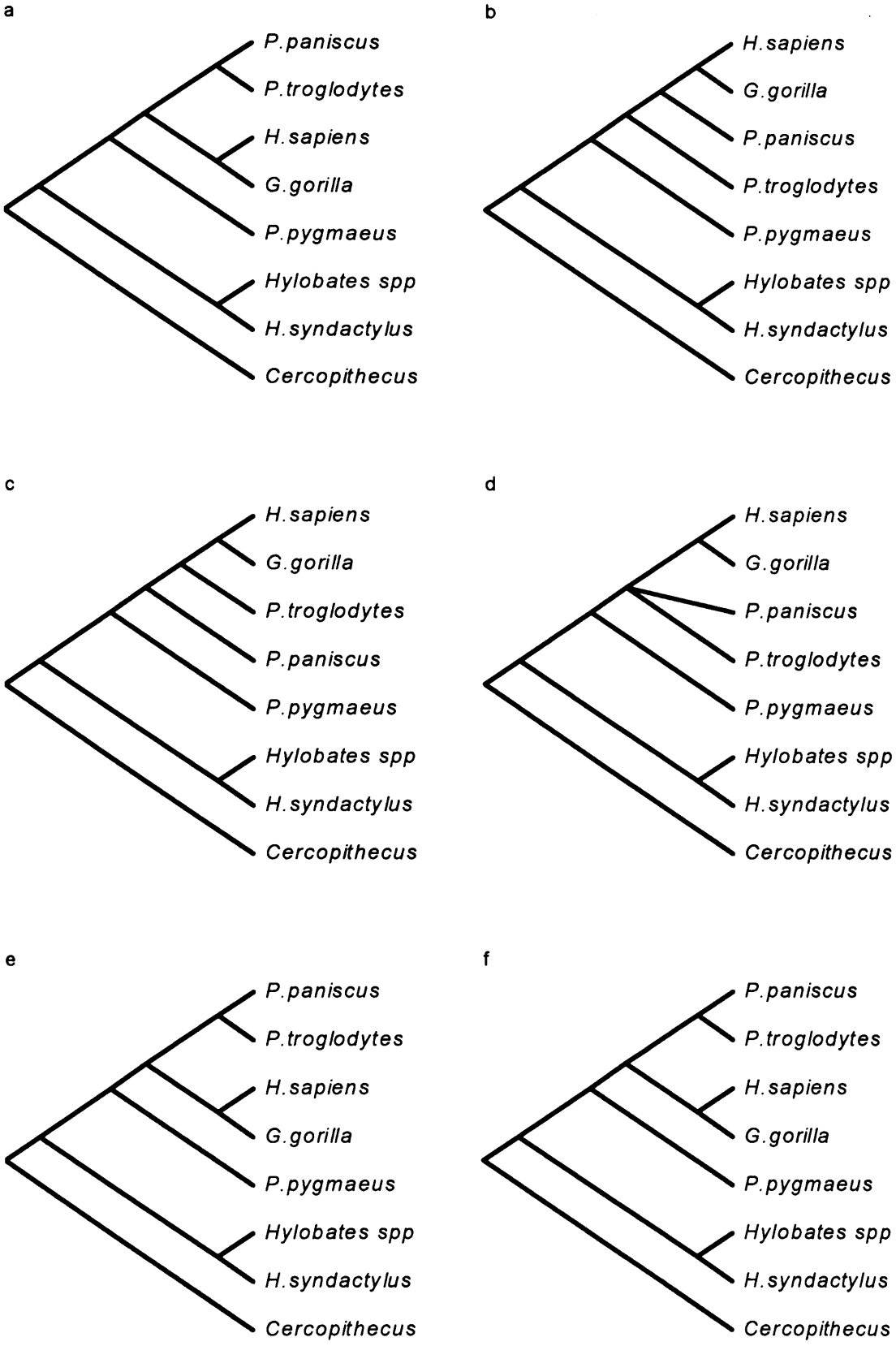

Figure 6-6. Most parsimonious trees produced in Analysis 1b.3.
(a) Divergence coding; (b, c, d) Binary coding; (e) Baum's coding; (f) Segment coding.

Table 6-3. Tree statistics associated with Analysis 1b.3.

Coding Method	TL	CI	HI	RI	PI
Divergence	1619	0.57	0.43	0.42	87
Binary	150	0.53	0.47	0.49	67
Baum	1310	0.52	0.48	0.34	99
Segment	2514	0.59	0.41	0.40	93

TL= tree length; CI= consistency index; HI= homoplasy index; RI= retention index; PI= number of parsimony informative characters.

d) Segment coding

The best solution recovered in this analysis was a tree that had the same topology as the hominoid molecular cladogram (Figure 6-4f).

The next best tree was four steps longer and disagreed with the molecular relationships in placing *H. sapiens* as the sister-group of *G. gorilla*, next to the chimpanzee clade. The rest of the tree was consistent with the molecular results.

The bootstrap cladogram generated from this dataset was mostly unresolved (Figure 6-5d). The only clade that found statistical support at the 70% confidence level was the *Hylobates spp* and *H. syndactylus* clade (89%).

6.1.3 Analysis 1b.3

The following section reports the results of the parsimony and bootstrap analyses in which *Cercopithecus* was the only outgroup used. The most parsimonious trees are

illustrated in Figure 6-6 and the associated tree statistics are reported in Table 6-3. The consensus cladograms generated in the bootstrap analyses are presented in Figure 6-7.

a) Divergence coding

This parsimony analysis found a most parsimonious tree that for the most part agreed with the molecular phylogeny (Figure 6-6a). It recovered the great ape and human clade, recognised the sister-group relationship between *Hylobates* and *H. syndactylus*, and suggested that the Hylobatids were the first hominoids to diverge. However, it also suggested that *G. gorilla* and *H. sapiens* formed a clade next to a clade comprising the two species of chimpanzee. Hence, all but one of the molecular clades was recovered.

The next most parsimonious tree was eight steps longer and its topology also differed from that of the hominoid molecular cladogram. It placed *H. sapiens* and *G. gorilla* in a single clade, and positioned *P. paniscus* as their sister taxon. This group was then joined by *P. troglodytes*. The rest of the tree was consistent with the molecular phylogeny.

The bootstrap cladogram contained three clades (Figure 6-7a) consistent with the consensus molecular phylogeny. The first one, the African ape and human clade, was moderately supported (81%). The taxonomic relationships within this clade were unresolved. The second one, the great ape and human clade, was statistically

significant (94%). The third clade included *Hylobates spp* and *H. syndactylus* and was weakly supported (70%).

b) Binary coding

This analysis returned two most parsimonious trees. Neither of them agreed with the molecular phylogeny for the hominoids. The first tree (Figure 6-6b) placed gorillas and humans in a single clade. This was then joined first by *P. paniscus* and then by *P. troglodytes* to form the African ape and human clade. The rest of the tree was identical to the molecular cladogram. The second tree (Figure 6-6c) was similar to the previous one. The only difference was in the positions of the two chimpanzee species. In this solution, *P. troglodytes* was the sister-taxon of the human and gorilla clade. This branch was then joined by *P. paniscus*. The strict consensus of these two solutions (Figure 6-6d) featured a trichotomy formed by *P. paniscus*, *P. troglodytes* and a clade that comprised *G. gorilla* and *H. sapiens*. The rest of the tree supported all other molecular relationships. Therefore, four molecular clades were recovered in this analysis.

None of the three next most parsimonious solutions was compatible with the molecular phylogeny. These trees were only one step longer than the best solutions and differed from each other in the taxonomic arrangements within the African ape and human clade. Their strict consensus featured a polytomy formed by the African apes and humans. The rest of the tree was identical to the molecular cladogram.

When this dataset was bootstrapped two clades were recovered, both of which were consistent with the hominoid molecular phylogeny (Figure 6-7b). The first was the African ape and human clade (90%); the second was the great ape and human clade (91%). The rest of the relationships were not resolved at the 70% significance level.

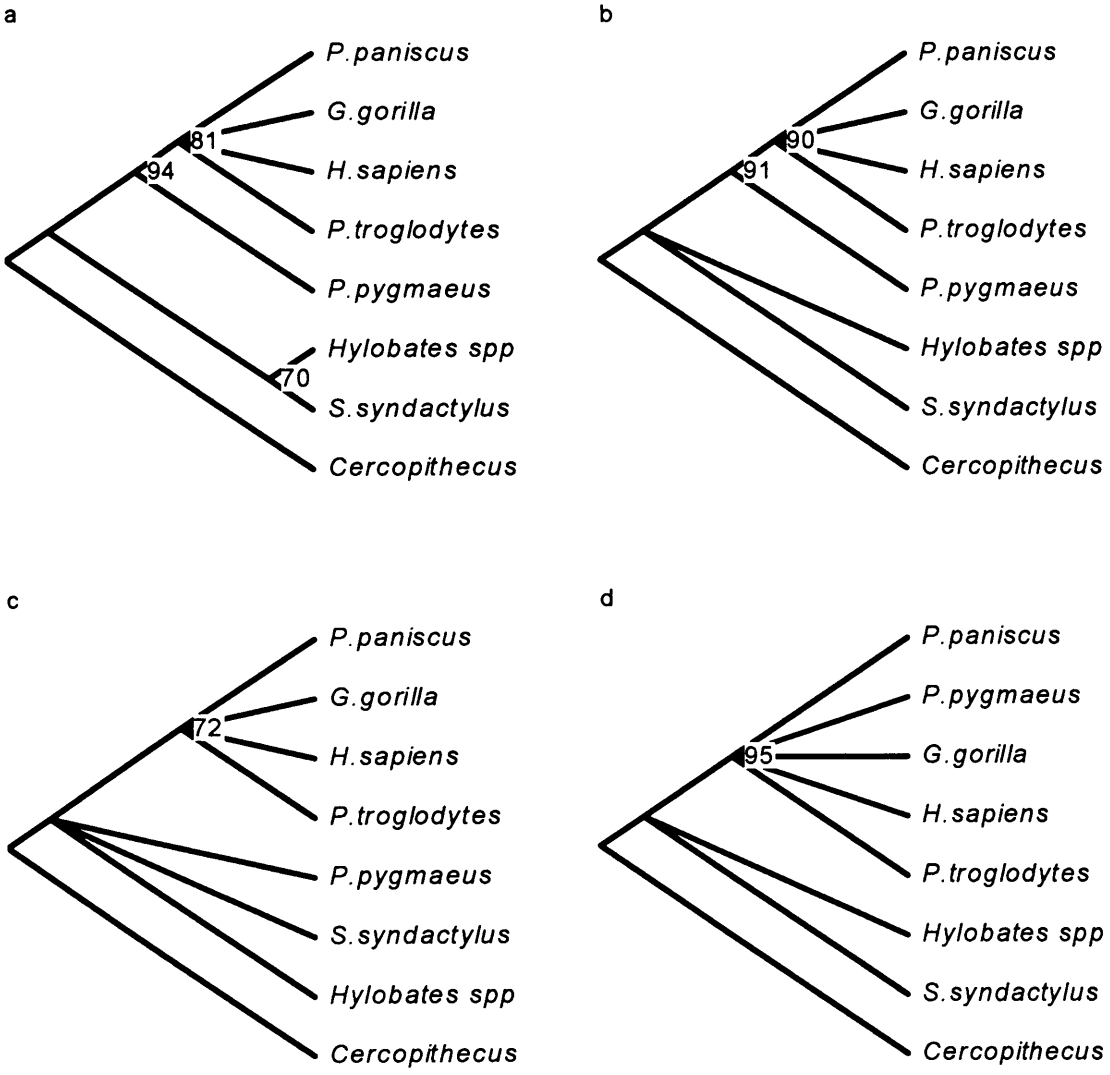

Figure 6-7. Bootstrap consensus cladograms generated in Analysis 1b.3.
(a) Divergence coding; (b) Binary coding; (c) Baum's coding; (d) Segment coding.

c) Baum's coding

The shortest solution found in this analysis (Figure 6-6e) supported a phylogenetic hypothesis in which the African apes and humans were split into two clades. One comprised gorillas and humans; the other consisted of the two chimpanzee species. The African ape and human clade was joined by *P. pygmaeus* to form a great ape and human clade. The two hylobatid taxa, *Hylobates spp* and *H. syndactylus*, formed a monophyletic group at the base of the hominoid clade. Hence, five of the six molecular clades were recovered in this analysis.

The next most parsimonious tree was five steps longer and it also disagreed with the molecular cladogram. It differed from the shortest solution with regards to the relationships within the African ape and human clade. In this tree, the genus *Pan* was not monophyletic. Instead, *P. paniscus* was placed closer to the clade that comprised gorillas and humans than to *P. troglodytes*.

The bootstrap analysis produced one clade consistent with the molecular phylogeny (Figure 6-7c). This was the African ape and human clade and it was weakly supported (72%). The rest of the tree was unresolved.

d) Segment coding

This dataset produced a most parsimonious tree (Figure 6-6f) that supported a sister-group relationship between gorillas and humans. The rest of its topology was identical

to the hominoid molecular tree. Therefore five of the six molecular clades were recovered in this analysis.

The next most parsimonious solution was nine steps longer than the previous one. It also disagreed with the molecular phylogeny. Its topology was similar to that of the shortest tree except it did not support the monophyletic relationships of the two hylobatid species. Instead, it placed *Hylobates spp* as the sister taxon of the great ape and human clade, and *H. syndactylus* at the base of the hominoid clade.

The consensus tree generated in the bootstrap analysis was mostly unresolved (Figure 6-7d). One clade, consistent with the molecular phylogeny, found a statistical support above the 70% confidence limit: a very strongly supported great ape and human clade (95%).

6.1.4 Analysis 1b.4

In the next set of analyses, *Colobus* was the only outgroup used to root the trees. The results of the parsimony analyses are shown in Figure 6-8, and the associated cladogram statistics are listed in Table 6-4. The cladograms produced in the bootstrap analyses are illustrated in Figure 6-9.

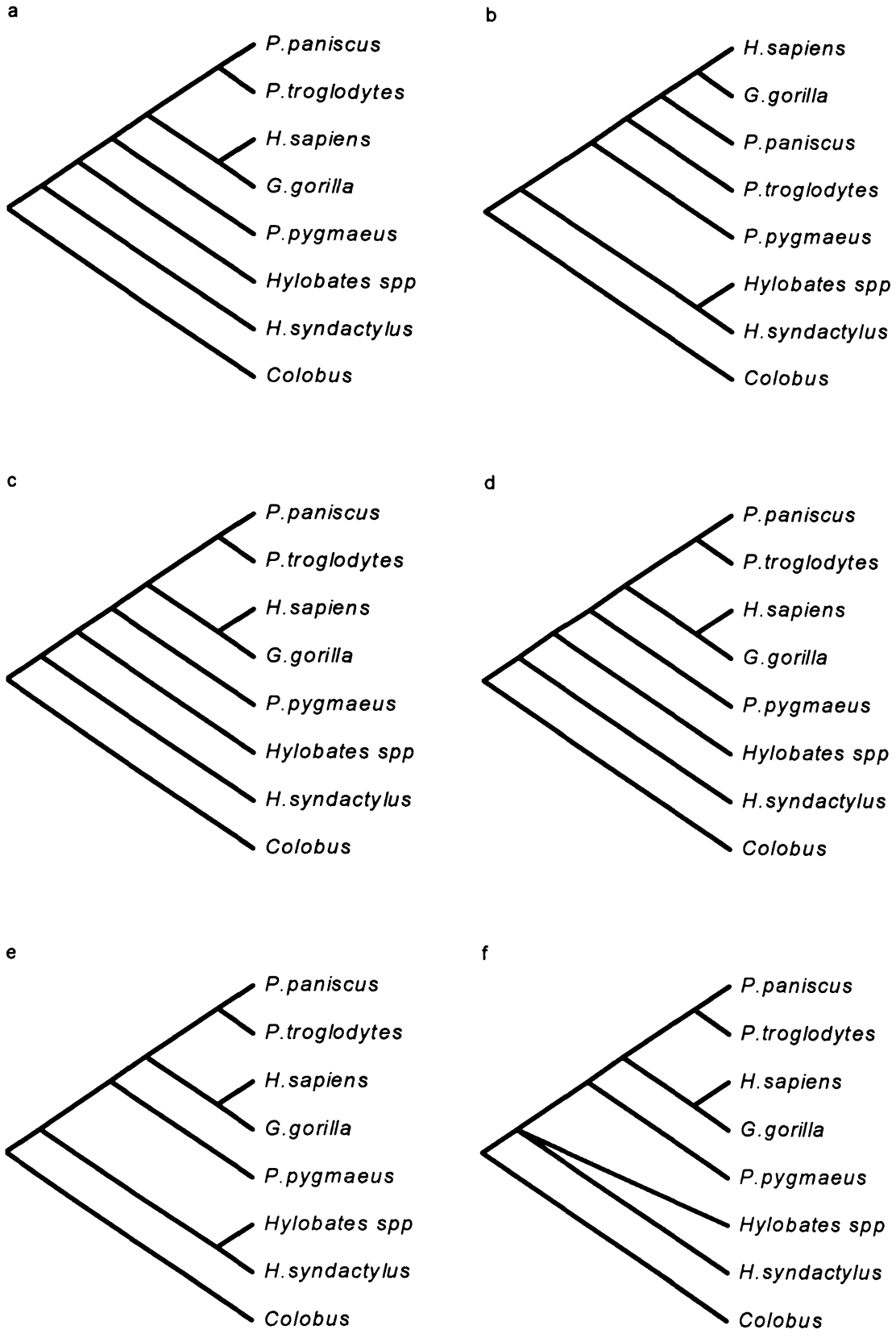

Figure 6-8. Most parsimonious trees produced in Analysis 1b.4.
(a) Divergence coding; (b) Binary coding; (c) Baum's coding; (d, e, f) Segment coding.

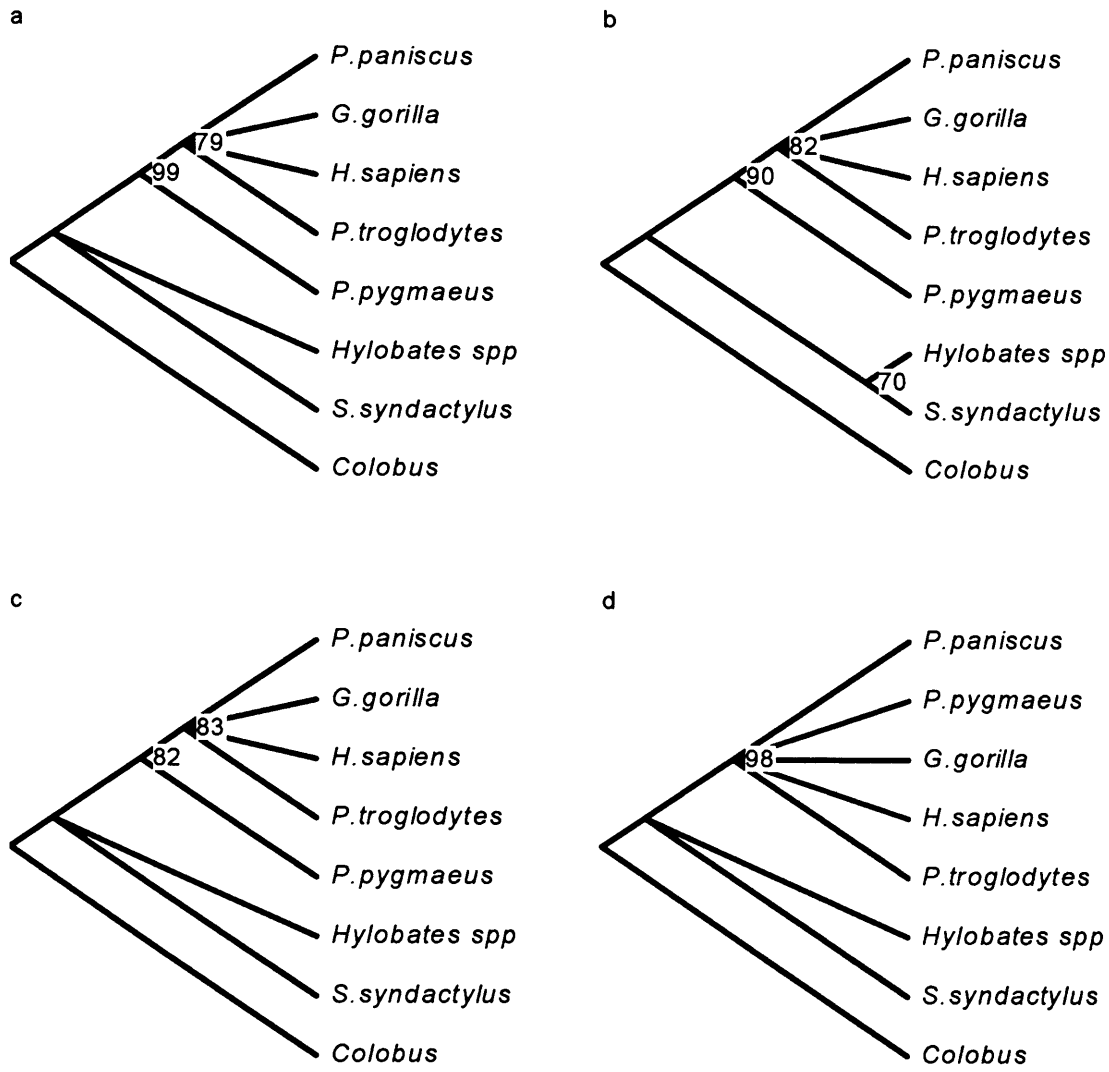

Figure 6-9. Bootstrap consensus cladograms generated in Analysis 1b.4.
(a) Divergence coding; (b) Binary coding; (c) Baum's coding; (d) Segment coding

Table 6-4. Tree statistics associated with Analysis 1b.4.

Coding Method	TL	CI	HI	RI	PI
Divergence	1642	0.57	0.43	0.43	87
Binary	132	0.53	0.47	0.50	59
Baum	1296	0.52	0.48	0.35	99
Segment	2486	0.59	0.41	0.41	94

TL= tree length; CI= consistency index; HI= homoplasy index; RI= retention index; PI= number of parsimony informative characters.

a) Divergence coding

A single most parsimonious tree was found (Figure 6-8a). This tree contained four molecular clades: the hominoid clade, the great ape and human clade, the African ape and human clade, and the common chimpanzee and bonobo clade. It failed to recognise the monophyletic relationship of *Hylobates spp* and *H. syndactylus*, and the sister-group relationship between humans and chimps. Instead, it placed *Hylobates spp* closer to the great apes and humans, and humans closer to gorillas.

The next most parsimonious tree was three steps longer than the most parsimonious solution. It differed from the latter in recovering the monophyletic relationship between *Hylobates spp.* and *H. syndactylus*, basally within the hominoids.

The bootstrap cladogram derived from this dataset was only partially resolved (Figure 6-9a). The great ape and human clade was statistically highly significant (99%), whilst the African ape and human clade was weakly supported (79%). Therefore, this analysis only supported two molecular clades.

b) Binary coding

The single most parsimonious tree found in this analysis (Figure 6-8b) did not agree with the molecular phylogeny. It supported a sister-group relationship between *H. sapiens* and *G. gorilla*. The two species of the genus *Pan* formed a paraphyletic group, with *P. paniscus* placed closer to the human and gorilla clade than *P.*

troglodytes. The African apes and humans were then joined by *P. pygmaeus*, and the two hylobatid groups were located at the base of the hominoid clade. Hence, four molecular clades were present in this solution.

The next four trees were only two steps longer than the previous one. None of them was consistent with the molecular tree, and they differed from each other in the relative arrangements of the African apes and humans. Their strict consensus was consistent with the molecular phylogeny. It featured a polytomy that comprised *G. gorilla*, *H. sapiens*, *P. paniscus* and *P. troglodytes*. This group was then joined by *P. pygmaeus* to form the great ape and human clade. The hylobatids occupied a basal position within the hominoid clade.

The bootstrap tree was partially resolved (Figure 6-9b). Three molecular clades were recovered: a moderately supported African ape and human clade (82%), a strongly supported great ape and human clade (90%), and a weakly supported hylobatid clade (70%).

c) Baum's coding

This parsimony analysis returned a single best solution (Figure 6-8c) that was incompatible with the molecular phylogeny. This tree supported a phylogenetic hypothesis in which *G. gorilla* and *H. sapiens* were sister taxa and closely related to the two species of chimpanzee, which formed a monophyletic group. It also supported a great ape and human clade. However, it did not position the two hylobatid groups in

a single clade at the base of the hominoid clade. Instead it placed *Hylobates spp* closer to the great apes than *H. syndactylus*. Hence four molecular clades were recovered.

The next most parsimonious tree was only one step longer than the best solution. It differed from the previous solution in placing the two hylobatid species in a single clade at the base of the hominoid clade, consistent with the molecular results.

The bootstrap tree generated in this analysis was only partially resolved (Figure 6-9c). Two molecular clades received a moderate level of statistical support, the African ape and human clade (83%), and the great ape and human clade (82%). The rest of the relationships were not resolved.

d) Segment coding

The two most parsimonious trees recovered in this analysis did not agree with the hominoid molecular phylogeny. The first tree (Figure 6-8d) featured four molecular clades: the hominoid clade, the great ape and human clade, the African ape and human clade, and the chimpanzee clades. It failed to recover the monophyletic relationship between gibbons and siamangs, and the sister group relationship between humans and chimpanzees. Instead, it placed *Hylobates spp.* closer to the great apes than to *H. syndactylus*, and *H. sapiens* next to *G. gorilla*. The second tree (Figure 6-8e) differed from the previous one in placing the two hylobatid species in a single clade at the base of the hominoid clade. Their strict consensus is shown in Figure 6-8f. It supported a monophyletic relationship between *H. sapiens* and *G. gorilla*, and also

between *P. paniscus* and *P. troglodytes*. It placed *P. pygmaeus* next to the African ape and human clade but was ambiguous about the position of the two hylobatid species.

The next most parsimonious tree was two steps longer and had the same topology as the consensus molecular phylogeny.

The bootstrap analysis generated a single highly significant molecular clade (Figure 6-9d), the great ape and human clade (98%). The rest of the relationships were unresolved.

6.1.5 Summary of results

The hypothesis that cranial characters related to nerves and vessels produce reliable phylogenies for the hominoids at the species level is only partially supported by the results of the tests described in this section.

a) Parsimony analysis

Hypothesis 1b was not supported by the parsimony analyses described above. The number of molecular clades successfully recovered in these tests is summarised in Table 6-5, according to coding method and outgroup employed. All of the hominoid molecular clades were recovered in only one case out of 16. In this test *Papio* was the only cercopithecine taxon included in the outgroup, and the data were coded using the

segment method. In one other test (marked with a single asterisk in Table 6-5) all the molecular relationships were found in the next most parsimonious tree.

Table 6-5. Number of molecular clades recovered in the parsimony cladograms.

Outgroup	All	*Papio*	*Cercopithecus*	*Colobus*
Ec	8	6	6	6
Divergence	6	5*	5	4
Binary	3	3	4	4
Baum	6	4	5	4
Segment	6	6	5	4

Ec, number of molecular clades expected if H_0 was true; *, all molecular clades present in the next MPT.

Table 6-6. Success index based on outgroups (S_O) and on coding method (S_C).

Outgroup S_O	All 0.66	*Papio* 0.75	*Cercopithecus* 0.79	*Colobus* 0.67
Method S_C	Divergence 0.77	Binary 0.55	Baum 0.73	Segment 0.81

The mean success rate in the recovery of the molecular clades for each outgroup (S_O) and for each coding method (S_C) is summarised in Table 6-6. The number of expected molecular clades is eight when all cercopithecine taxa are included in the analyses (10 taxa), and six when only one outgroup is used (eight taxa). On average the highest rate of success was scored when *Cercopithecus* was the outgroup taxon included in the analyses (S_O= 0.75). This is followed by *Papio* (S_O= 0.75) and *Colobus* (S_O= 0.67). The worst results were produced when all three cercopithecine taxa were included in the outgroup (S_O=0.66). In terms of coding methods, the best performance occurred

with the segment (S_O= 0.81) and the divergence coding (S_O= 0.77), followed by Baum's (S_O= 0.73). The binary method scored the worst success index (S_O= 0.55).

b) Bootstrap analyses

The results of the bootstrap tests support Hypothesis 1b and are summarised in Table 6-7. As in the case of the analyses at the generic level, the bootstrap consensus cladograms were never fully resolved but they were always consistent with the consensus molecular phylogeny. The number of clades recovered ranged from one to three. A closer look at the consensus cladograms reveals that the African ape and human clade, and the great ape and human clade, were the two most frequently recovered clades (11 analyses, Figure 6-10). The other two clades that found some support were the clade formed by the hylobatid species, and the hominoid clade (when all three outgroups were included in the analyses). None of the other relationships was supported at the 70% confidence level.

Table 6-7. Number of clades supported by the bootstrap analyses.

Outgroup	All	*Papio*	*Cercopithecus*	*Colobus*
Divergence	$+_m+_s$	$+_m+_s$	$+_w+_m+_s$	$+_w+_s$
Binary	$+_w+_m+_m$	$+_m$	$+_s+_s$	$+_w+_m+_s$
Baum	$+_w+_m+_s$	$+_w+_m$	$+_w$	$+_m+_m$
Segment	$+_w+_s$	$+_m$	$+_s$	$+_s$

+, 'true' clades; -, 'false' clades; 's', strongly supported (>90%); 'm', moderately supported (>80%); 'm', weakly supported (>70%).

Overall, the highest number of clades was yielded when all three outgroups were used to root the trees (10), whilst the lowest number were produced when only *Papio* was included in the outgroup. Furthermore, in accordance with the analyses carried out at the generic level, the divergence coding method generated more strongly supported clades (four) than any other method.

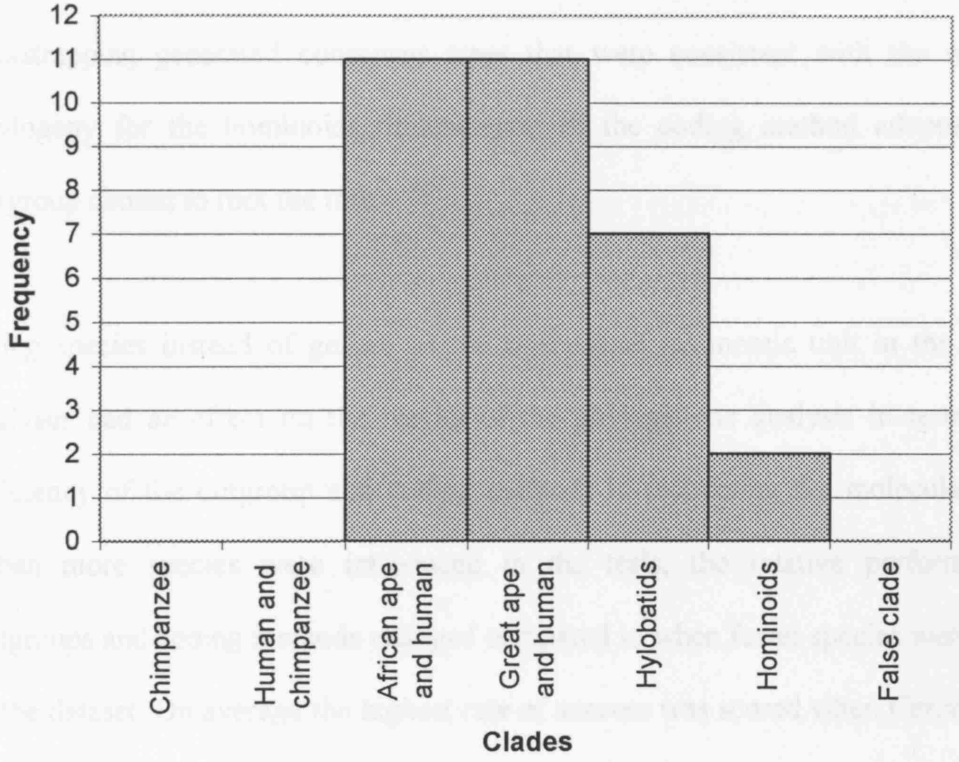

Figure 6-10. Frequency of recovery of each molecular clade in the bootstrap analyses.

6.2 Summary

The results of the analyses described in this section only partially supported the hypothesis that cranial traits associated with nerves and vessels are useful for

recovering the phylogenetic relationships of the hominoids at the specific level. The hypothesis was not supported by the parsimony analyses. However, the bootstrap consensus cladograms were always consistent with the hominoid molecular phylogeny. Hence, the bootstrap tests supported the hypothesis that nerve- and vessel-related traits are phylogenetically informative. Like in the analyses carried out at the generic level, methodological choices like outgroup composition and coding procedures influenced the outcome of the parsimony analyses. Furthermore, bootstrapping generated consensus trees that were consistent with the molecular phylogeny for the hominoids, independent of the coding method adopted or the outgroup chosen to root the tree.

Using species instead of genera as the operational taxonomic unit in the cladistic analyses had an effect on the results of the phylogenetic analysis in terms of the efficiency of the outgroup and coding methods in recovering the molecular clades. When more species were introduced in the tests, the relative performance of outgroups and coding methods changed compared to when fewer species were present in the dataset. On average the highest rate of success was scored when *Cercopithecus* was the outgroup taxon included in the analyses (S_O= 0.75). In terms of coding methods, the best performance occurred with the segment (S_O= 0.81) and the divergence coding (S_O= 0.77).

Chapter 7. RESULTS III: SEXUAL SELECTION-DRIVEN HOMOPLASY

In this chapter I describe the results of analyses run to investigate the possibility that sexual dimorphism has an important impact on phylogenetic analyses of primate morphology ('Sexual selection-driven homoplasy' hypothesis). The null hypothesis was that sexual dimorphism does not have any significant effect on the outcome of phylogenetic reconstruction. In other words, male and female hominoids are equally prone to homoplasy. The prediction was that if sexual dimorphism is not a confounding factor in phylogenetic inference, then the results of cladistic analyses based on sex-specific datasets will not differ significantly from each other and from the equivalent results of the mixed-sex dataset.

To test this hypothesis, two sets of data matrices were prepared, one for males and one for females. The tests were performed at the genus level only. In each set, one matrix included all three cercopithecine taxa in the outgroup, one included only *Papio*, one only *Cercopithecus* and one only *Colobus*. Each matrix comprised the same characters studied in the mixed-sex analyses and was constructed using four different coding methods: Divergence coding, Binary coding, Baum's coding and Segment coding. The implementation of these was explained in the Materials and Methods chapter. Next, these datasets were subjected to parsimony analyses to generate phylogenetic hypotheses, and bootstrap analyses were run to evaluate the statistical support for these hypotheses. The results of the sex-specific analyses were then compared to each other and to the results of the relevant mixed-sex analyses.

Agreement between the trees generated from male- and female-specific datasets was deemed to support the null hypothesis (i.e. sexual dimorphism does not affect the outcome of phylogenetic analysis). In contrast, disagreement was taken to indicate that sexual dimorphism affects the outcome of phylogenetic analysis. Agreement was established on the basis of congruence between the sex-specific MPT (or, in case of multiple MPTs, their strict consensus).

The results of the sex-specific analyses were also compared to the consensus molecular tree for the hominoids in order to determine whether males or females were better at recovering the phylogenetic relationships of the hominoids. In primates, sexual selection acts mainly on males to produce secondary sexual characters that may be a source of homoplasy. Therefore, if the 'sexual selection-driven homoplasy' hypothesis is supported, it can be predicted that, unlike male-specific datasets, female-specific datasets should produce phylogenies consistent with the hominoid consensus molecular cladogram.

The description of the results of each set of analyses is followed by a short summary of the results in which the level of support for each hypothesis is assessed.

7.1 Hypothesis 2a: Male-specific datasets generate phylogenies that are consistent with the mixed-sex phylogenies

7.1.1 Analysis 2a.1

In this section I report on the results of the parsimony and bootstrap tests in which all three cercopithecine taxa were included in the outgroup. The minimum length trees found are illustrated in Figure 7-1, and the associated tree statistics are listed in Table 7-1. The 70% consensus bootstrap cladograms are presented in Figure 7-2.

a) Divergence coding

The parsimony analysis found two best solutions neither of which agreed with the consensus molecular phylogeny. One tree (Figure 7-1a) failed to group the hominoids in a monophyletic clade. It featured two main branches. One comprised *Hylobates* and two cercopithecine taxa, *Colobus* and *Cercopithecus*. Within this group, *Cercopithecus* was placed next to a clade that consisted of *Hylobates* and *Colobus*. The second branch comprised the great apes and humans. The molecular relationships within this clade were correctly recovered. *Pongo* was the first taxon to branch off from this lineage, and within the African apes and humans, *Gorilla* was the sister group of a clade that comprised *Homo* and *Pan*. The other shortest tree (Figure 7-1b) differed from the previous one in the arrangement within the African ape and human clade. In this solution the molecular relationships were not recovered and *Homo*

appeared as the sister group of *Gorilla* and *Pan*. This solution also differed from the shortest tree in placing the three outgroups in a single clade. The molecular relationships within the latter group were correctly recovered. This topology was identical to the one generated from the mixed-sex dataset (Figure 5-1a). The strict consensus of the two most parsimonious cladograms (Figure 7-1c) derived from the male dataset featured a great ape and human clade in which *Homo*, *Pan* and *Gorilla* formed a trichotomy. The rest of the tree was unresolved.

The bootstrap analysis recovered two clades (Figure 7-2a). The African ape and human trichotomy was weakly supported (78%), while the great ape and human clade received strong statistical support (94%). These groups were consistent with the molecular results. The rest of the tree was not resolved at the 70% confidence level.

b) Binary coding

This analysis returned two most parsimonious solutions. Neither of them agreed with the hominoid molecular phylogeny. The first tree (Figure 7-1d) presented all the molecular relationships within the great ape and human clade, but it did not recognise the cercopithecine taxa as a monophyletic group. Instead it placed *Cercopithecus* next to a clade that comprised *Colobus* and *Hylobates*. *Papio* was at the base of the tree. The second solution (Figure 7-1e) differed from the first one in placing *Pan* and *Gorilla* in a single clade to the exclusion of *Homo*. It also recognised the three outgroups as a monophyletic group and correctly recovered their molecular relationships. The strict consensus of these trees (Figure 7-1f) featured an African ape and human trichotomy, as well as a great ape and human clade. The rest of the

cladogram was not resolved. These solutions differed from those of the mixed-sex dataset (Figure 5-1b,c).

The bootstrap analysis recovered one clade that was consistent with the molecular phylogeny (Figure 7-2b): the African ape and human clade (89%). The rest of the phylogeny was not resolved at the 70% confidence level.

c) Baum's coding

This dataset returned a single MPT that did not agree with the molecular phylogeny (Figure 7-1g). Its topology supported a phylogenetic hypothesis in which gorillas and humans shared a common ancestor not shared with chimpanzees. Orangutans were the sister taxon of the African apes and humans, and the gibbon genus was at the base of the hominoid clade. The three cercopithecine outgroups were recognised as a monophyletic group and their molecular relationships were correctly recovered. This tree did not agree with the solution generated from the mixed dataset (Figure 5-1e).

The bootstrap analysis produced a consensus tree that contained three molecular clades (Figure 7-2c). The branch that comprised humans, chimpanzees and gorillas was moderately supported (89%). The hominoid clade was also moderately supported (83%) and, within the outgroup clade, the clade formed by *Papio* and *Cercopithecus* was only weakly supported (78%). Therefore, all of the recovered clades were consistent with the molecular data.

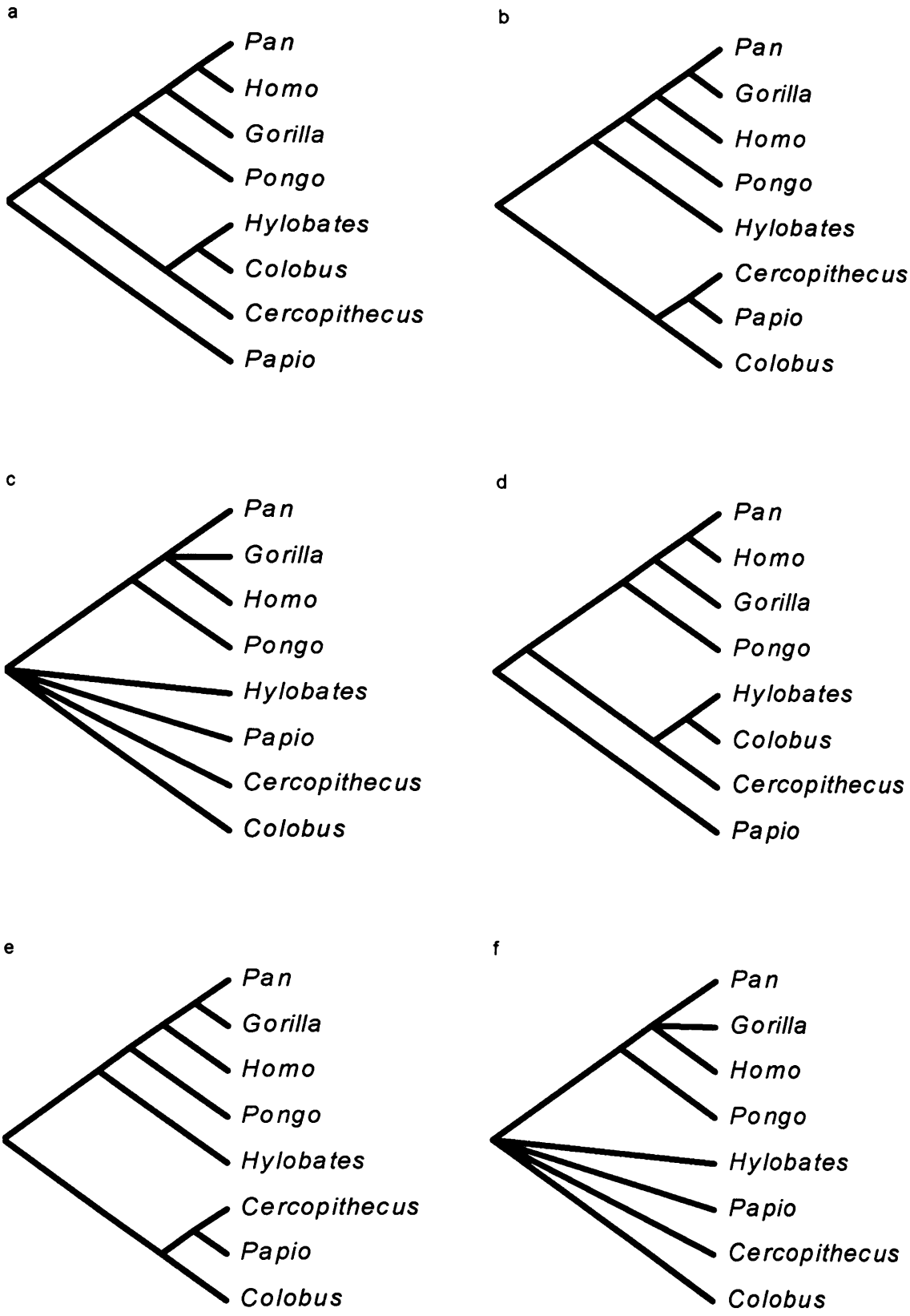

Figure 7-1. Cladograms produced in parsimony analysis 2a.1.
(a, b, c) Divergence Coding, (d, e, f) Binary Coding, (g) Baum's, (h) Segment

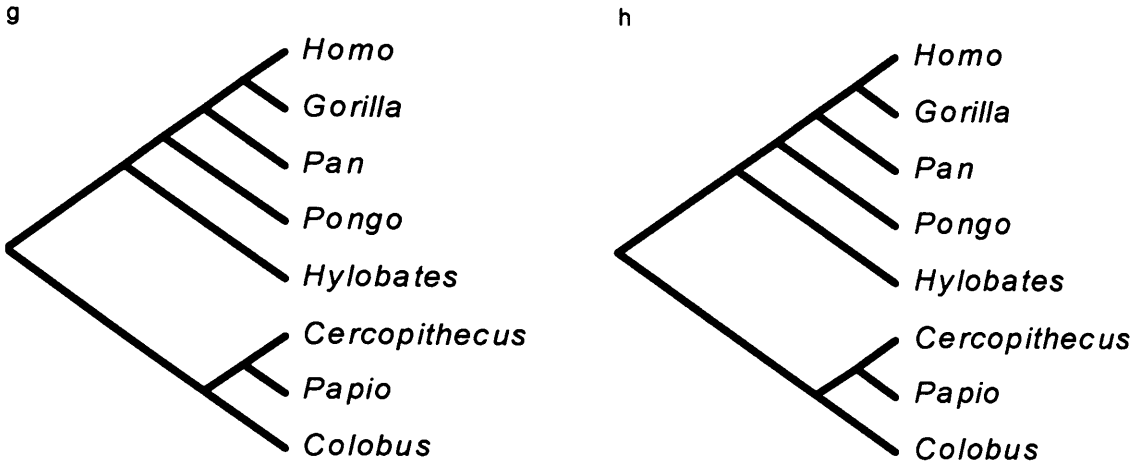

Figure 7-1, continued. Cladograms produced in parsimony analysis 2a.1.

Table 7-1. Tree statistics associated with Analysis 2a.1.

Coding Method	TL	CI	HI	RI	PI
Divergence	1368	0.59	0.41	0.45	85
Binary	140	0.50	0.50	0.47	58
Baum	1254	0.53	0.47	0.39	98
Segment	2663	0.59	0.41	0.42	97

TL= tree length, CI= consistency index, HI= homoplasy index, RI= retention index, PI= number of parsimony informative characters

d) Segment coding

In this analysis a single solution was found that did not agree with the molecular phylogeny (Figure 7-1h). It supported a single clade for *Homo* and *Gorilla* to the exclusion of *Pan*; *Pongo* was the sister group of the African apes and humans; the hominoids formed a monophyletic group. Within the outgroup clade, the molecular relationships were recovered correctly. This tree also differed from the one recovered from the mixed-sex dataset (Figure 5-1f).

The bootstrap analysis generated a consensus tree that contained one molecular clade (Figure 7-2d): the great ape and human clade. This was moderately supported (87%). The rest of the relationships were not resolved at the 70% confidence level.

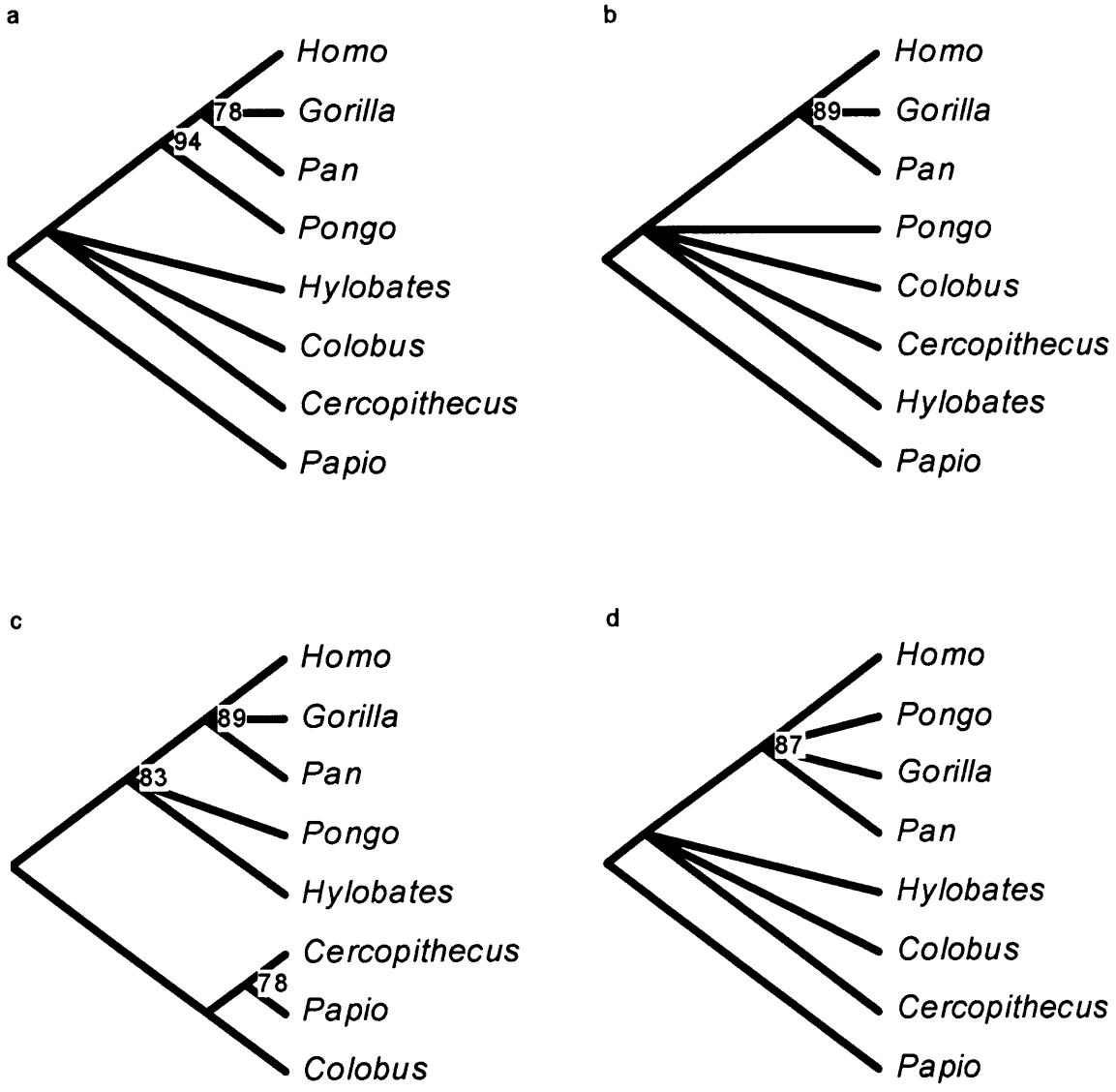

Figure 7-2. Bootstrap consensus cladograms generated in Analysis 2a.1.
(a) Divergence Coding, (b) Binary Coding, (c) Baum's Coding, (d) Segment Coding

7.1.2 Analysis 2a.2

In the next set of analyses, *Papio* was the only outgroup taxon used to root the trees. The minimum length trees found in the parsimony analyses are shown in Figure 7-3, and their associated tree statistics are listed in Table 7-2. Figure 7-4 illustrates the consensus cladograms generated in the bootstrap analyses.

a) Divergence coding

The MPT found in this part of the analysis (Figure 7-3a) was not consistent with the molecular tree. It supported a phylogenetic hypothesis in which *Homo* and *Pongo* were sister taxa and they were joined, first, by *Pan* and, then, *Gorilla* to form a great ape and human clade. *Hylobates* was placed at the base of the hominoid clade. This tree differed from the tree recovered in the mixed-sex analysis (Figure 5-3a).

The bootstrap analysis did not recover any clades at the 70% confidence level (Figure 7-4a).

b) Binary coding

This dataset produced two most parsimonious cladograms that were inconsistent with the molecular phylogeny of the hominoids. The first tree (Figure 7-3b) disagreed with the molecular cladogram in placing humans as the sister taxon of a clade that comprised *Gorilla* and *Pan*. The second tree (Figure 7-3c) placed *Hylobates* as the sister group of *Homo*. This clade was joined, first, by *Pan* and, then, by *Gorilla*, while

Pongo was placed at the base of the hominoid clade. These solutions differed from the MPT found in the mixed-sex analysis (Figure 5-3b). Their strict consensus is shown in Figure 7-3d. It featured a polytomy formed by African apes and *Hylobates*. This clade was then joined by *Pongo*.

The bootstrap test (Figure 7-4b) did not recover any clade at the 70% support level.

c) Baum's coding

In this case, one MPT was recovered (Figure 7-3e). It was compatible with the molecular phylogeny. However, its topology was different from the one found in the mixed-sex analysis (Figure 5-3c).

The bootstrap analysis generated two molecular clades (Figure 7-4c): a very strongly supported African ape and human clade (97%), and a weakly supported great ape and human clade (74%). No other clade was recovered at the 70% confidence level.

d) Segment coding

The best tree found in this analysis (Figure 7-3f) was different from the molecular cladogram and also from the best tree found in the mixed-sex analysis (Figure 5-3d). It supported a clade in which *Pongo* and *Homo* shared a common ancestor to the exclusion of *Pan*. This group was then joined by *Gorilla* to form the great ape and human clade, and *Hylobates* was placed at the base of the hominoid clade.

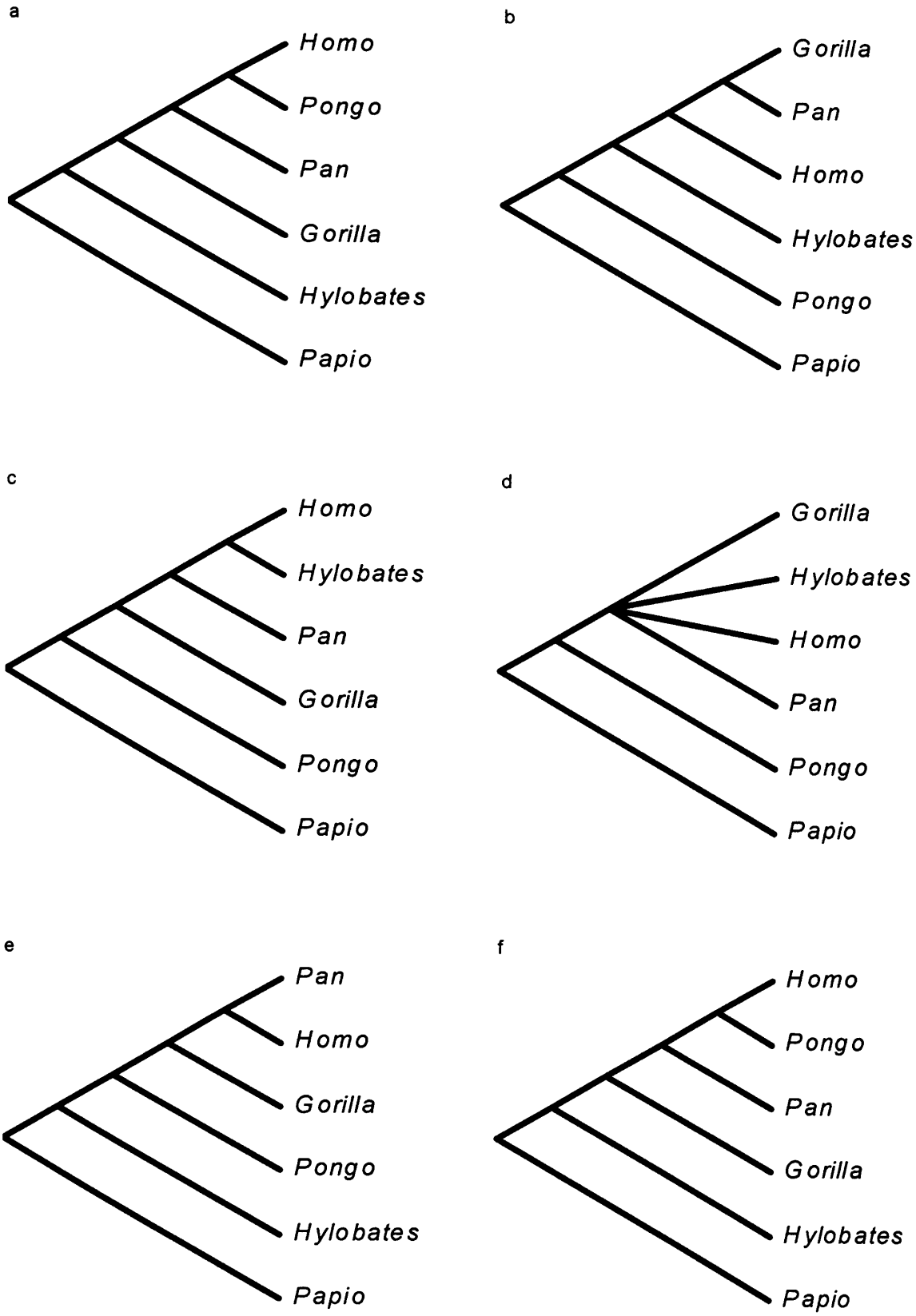

Figure 7-3. MPTs produced in Analysis 2a.2.
(a) Divergence Coding, (b, c, d) Binary Coding, (e) Baum's Coding, (f) Segment Coding

Table 7-2. Tree statistics associated with Analysis 2a.2.

Coding Method	TL	CI	HI	RI	PI
Divergence	912	0.66	0.34	0.40	81
Binary	115	0.56	0.44	0.42	45
Baum	587	0.67	0.33	0.42	97
Segment	2225	0.69	0.31	0.38	94

TL= tree length, CI= consistency index, HI= homoplasy index, RI= retention index, PI= number of parsimony informative characters

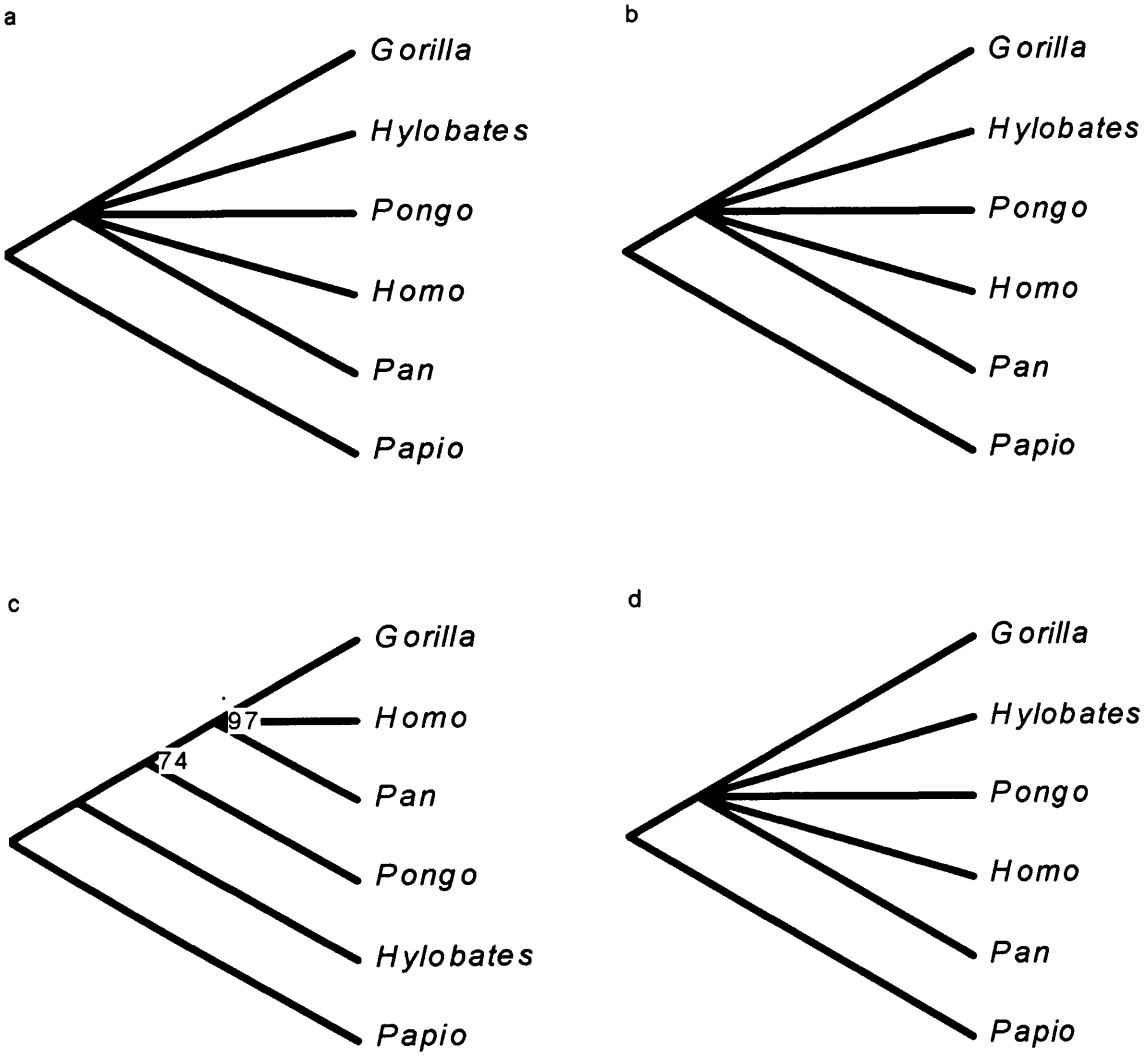

Figure 7-4. Bootstrap consensus cladograms generated in Analysis 2a.2.
(a) Divergence Coding, (b) Binary Coding, (c) Baum's Coding, (d) Segment Coding

The bootstrap analysis did not recover any clades at the 70% confidence level (Figure 7-4d).

7.1.3 Analysis 2a.3

This section describes the results of the parsimony and bootstrap tests run when *Cercopithecus* was the only taxon used to root the cladograms. The most parsimonious solutions are illustrated in Figure 7-5, and their associated statistics are reported in Table 7-3. The bootstrap cladograms are shown in Figure 7-6.

a) Divergence coding

A single MPT was recovered in this analysis (Figure 7-5a). Contrary to the molecular results, this tree supported a sister-group relationship between *Gorilla* and *Homo* to the exclusion of *Pan*. The African ape and human clade, the great ape and human clade and the hominoid clade were correctly recovered. This topology coincided with the tree obtained from the mixed-sex dataset (Figure 5-5a).

The bootstrap analysis generated two clades (Figure 7-6a). The great ape and human clade found a weak level of statistical support (76%), while the African ape and human clade found a moderate level of support (85%). Both clades were consistent with the molecular results.

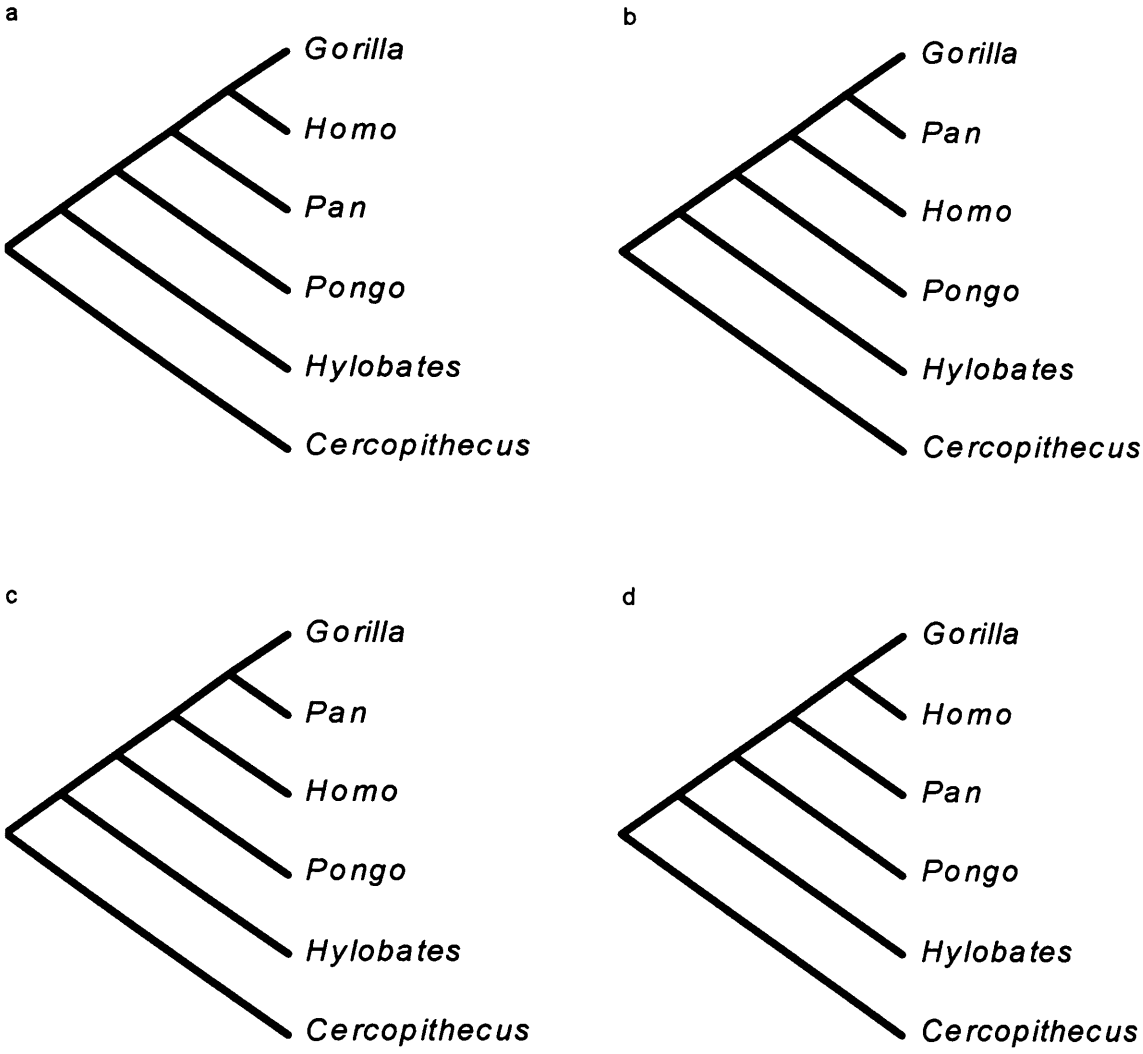

Figure 7-5. MPTs produced in Analysis 2a.3.
(a) Divergence Coding, (b) Binary Coding, (c) Baum's Coding, (d) Segment Coding

Table 7-3. Tree statistics associated with Analysis 2a.3.

Coding Method	TL	CI	HI	RI	PI
Divergence	863	0.67	0.33	0.43	78
Binary	103	0.60	0.40	0.49	44
Baum	422	0.76	0.24	0.63	94
Segment	2098	0.70	0.30	0.41	92

TL= tree length, CI= consistency index, HI= homoplasy index, RI= retention index, PI= number of parsimony informative characters

b) Binary coding

The shortest tree found in this analysis (Figure 7-5b) differed from the molecular cladogram in placing *Pan* and *Gorilla* in a single clade to the exclusion of *Homo*. The rest of the topology was consistent with the molecular phylogeny. This tree was also identical to one of the MPTs found in the mixed-sex analysis (Figure 5-5c). It is perhaps worth noting that one of the two next most parsimonious solutions supported all the molecular relationships and it was only two steps less parsimonious than the shortest tree.

When this dataset was bootstrapped, the consensus tree featured two molecular clades (Figure 7-6b): the strongly supported great ape and human clade (90%), and the weakly supported African ape and human clade (79%).

c) Baum's coding

As with the previous analysis, this dataset recovered a single MPT that differed from the molecular cladogram in placing *Pan* and *Gorilla* in a single clade to the exclusion of *Homo* (Figure 7-5c). This arrangement was also dissimilar to the one found in the mixed-sex analyses (Figure 5-5f).

The bootstrap consensus tree resolved three clades (Figure 7-6c). Two of these, the great ape and human clade and the African ape and human clade, were consistent with the molecular phylogeny and highly significant (both 100%). The third, which comprised *Gorilla* and *Pan*, was inconsistent with the molecular data. This false-positive clade was also strongly supported (96%).

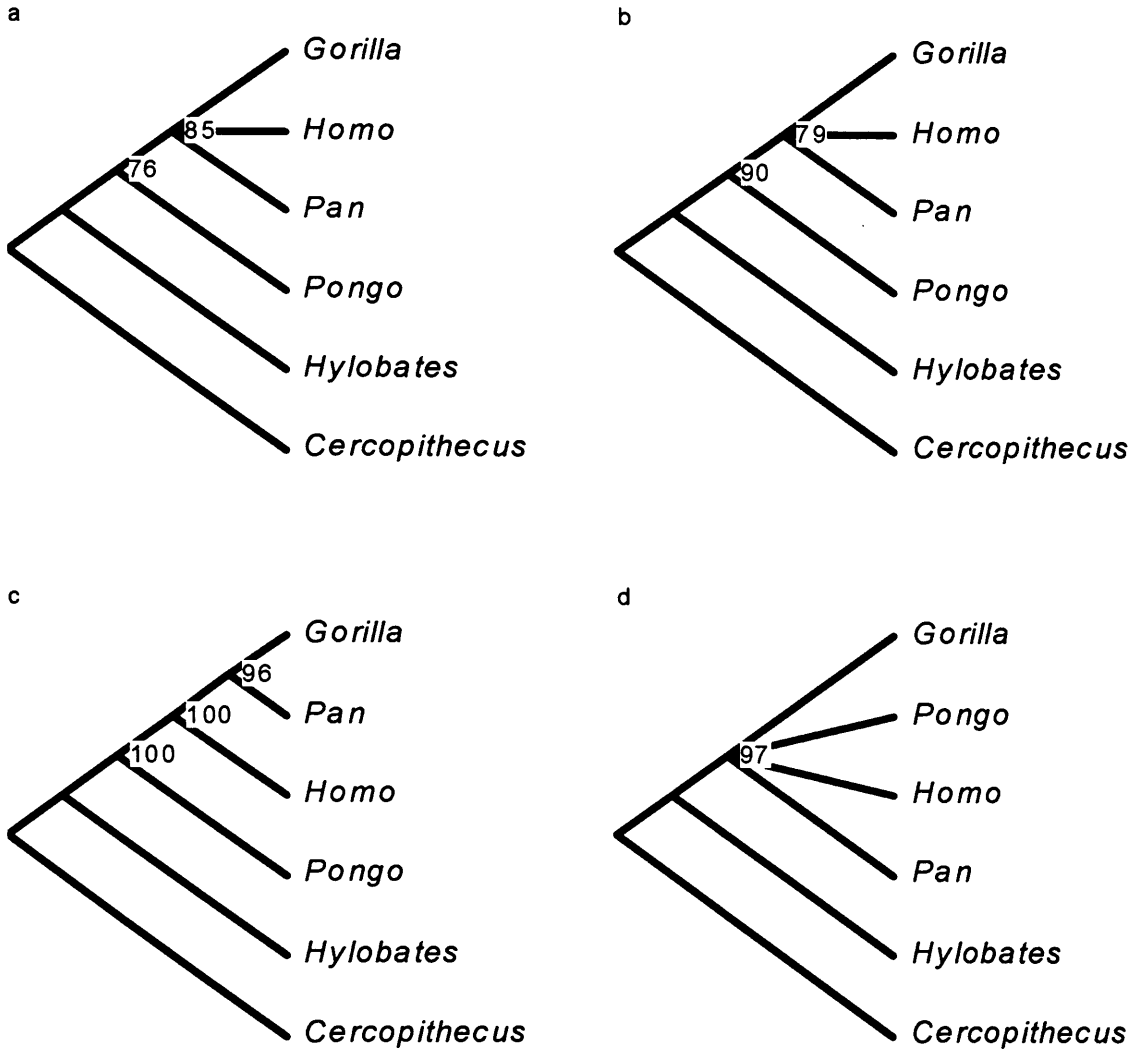

Figure 7-6. Bootstrap consensus cladograms generated in Analysis 2a.3.
(a) Divergence Coding, (b) Binary Coding, (c) Baum's Coding, (d) Segment Coding

d) Segment coding

The parsimony analysis produced one MPT (Figure 7-5d) that was incongruent with the molecular results. The topology of this tree suggested that *Gorilla* and *Homo* were more closely related to each other than either was to *Pan*. The orangutans were positioned as the sister group of the African apes and humans, and the gibbons occupied a basal position within the hominoid clade. This tree was also different from the mixed-sex solution (Figure 5-5g).

The bootstrap analysis recovered only one molecular clade (Figure 7-6d), the great ape and human clade. This group was strongly supported (97%).

7.1.4 Analysis 2a.4

In this section, *Papio* and *Cercopithecus* were excluded from the analysis and *Colobus* was the only outgroup taxon employed. Figure 7-7 presents the best solutions found in the parsimony analyses and Table 7-4 reports the associated tree statistics. The bootstrap trees discussed in the section below are illustrated in Figure 7-8.

a) Divergence coding

The parsimony analysis recovered one most parsimonious solution (Figure 7-7a) that was different from the hominoid molecular cladogram. It contained three molecular clades (the hominoid clade, the great ape and human clade and the African ape and human clade) but it did not support the sister-group relationship between humans and chimps. Instead, it placed *Homo* and *Gorilla* in a single clade to the exclusion of *Pan*. This topology was also different from the topology of the best tree found in the mixed-sex analysis (Figure 5-7a).

The bootstrap analysis produced two molecular clades (Figure 7-8a). The African ape and human clade was moderately well supported (85%), while the great ape and human clade received strong statistical support (99%).

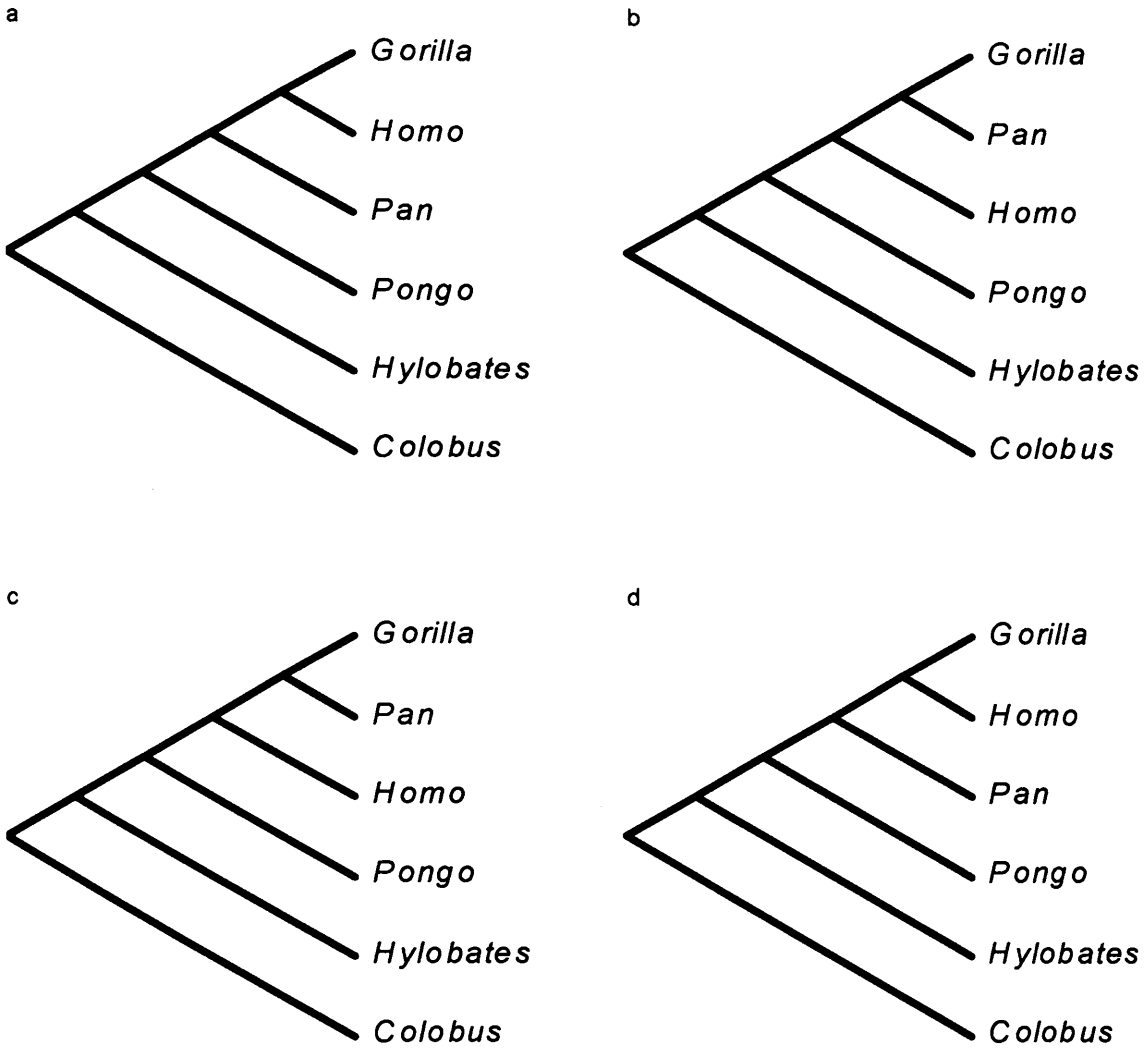

Figure 7-7. MPTs produced in Analysis 2a.4.
(a) Divergence Coding, (b) Binary Coding, (c) Baum's Coding (d) Segment Coding

Table 7-4. Tree statistics associated with Analysis 2a.4.

Coding Method	TL	CI	HI	RI	PI
Divergence	864	0.68	0.32	0.47	78
Binary	106	0.58	0.42	0.49	45
Baum	423	0.76	0.24	0.62	93
Segment	2068	0.70	0.30	0.43	94

TL= tree length, CI= consistency index, HI= homoplasy index, RI= retention index, PI= number of parsimony informative characters

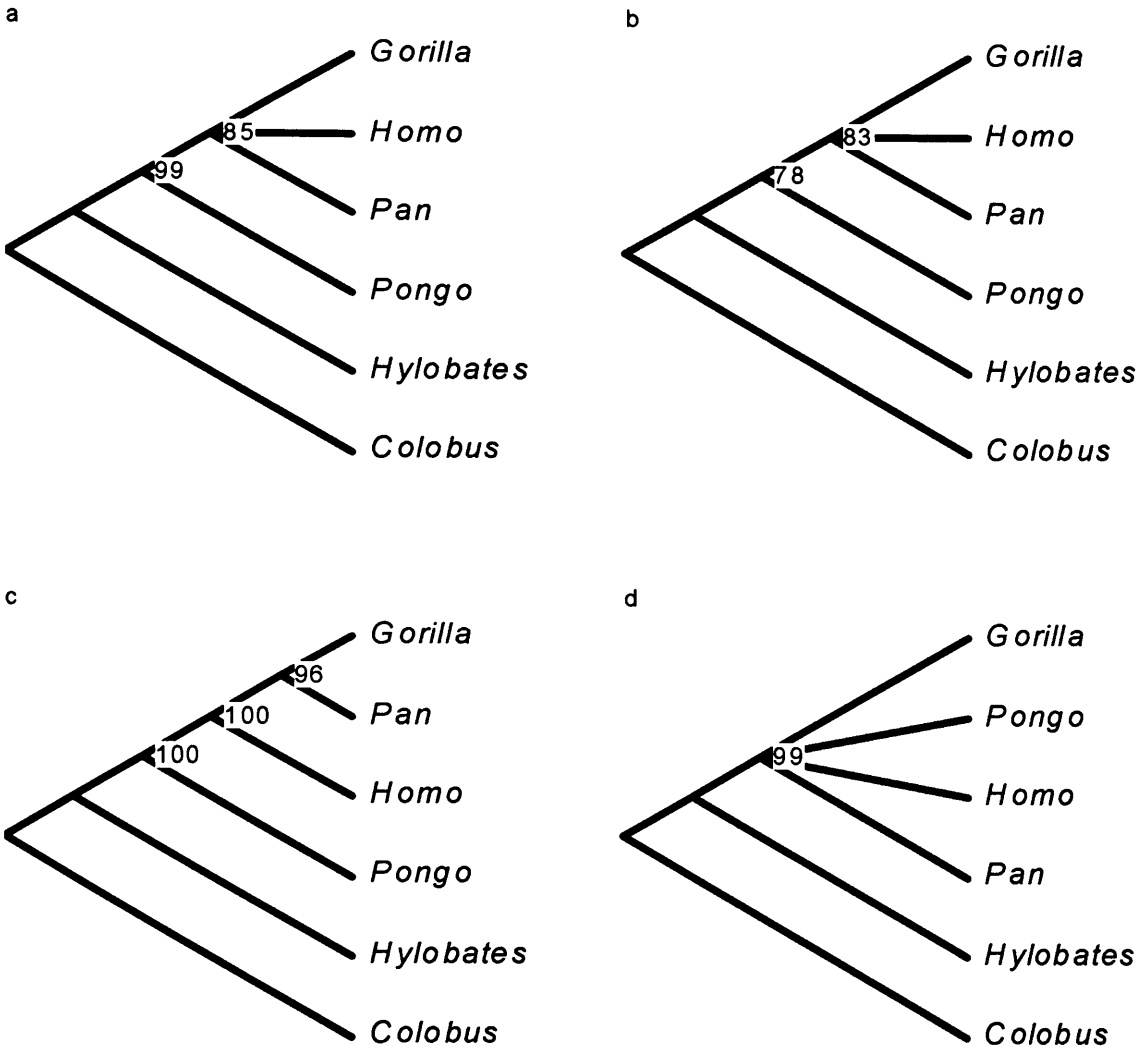

Figure 7-8. Bootstrap consensus cladograms generated in Analysis 2a.4.
(a) Divergence Coding, (b) Binary Coding, (c) Baum's Coding, (d) Segment Coding

b) Binary coding

The MPT found in this analysis was inconsistent with the hominoid molecular phylogeny (Figure 7-7b). It supported *Homo* as the sister group of a clade that comprised *Pan* and *Gorilla*. All the other molecular clades were correctly recovered. This topology did not agree with either of the two MPTs recovered in the mixed-sex analysis (Figure 5-7b,c). Notably, one of the two next most parsimonious solutions recovered all four molecular clades and was two steps longer than the shortest tree.

The bootstrap tree generated from this dataset (Figure 7-8b) recovered two molecular clades. The great ape and human clade was weakly supported (78%), whilst the African ape and human clade was moderately supported (83%).

c) Baum's coding

The MPT found in this part of the analysis differed from the molecular cladogram in supporting an African ape clade to the exclusion of *Homo* (Figure 7-7c). All the other molecular clades were correctly recovered. This topology also disagreed with the MPT found in the mixed-sex analysis (Figure 5-7e). The next shortest solution coincided with the molecular tree but was 20 steps less parsimonious than the MPT.

The bootstrap test generated three clades (Figure 7-8c): the great ape and human clade, the African ape and human clade and the African ape clade. The first two were consistent with the molecular results, while the third one was not. All of them were statistically highly significant, with bootstrap values of 100%, 100% and 96% respectively.

d) Segment coding

This dataset produced a single MPT that disagreed with both the mixed-sex dataset results and the molecular results (Figure 7-7d). It supported a common ancestor for *Gorilla* and *Homo* not shared with *Pan*. The rest of the cladogram was identical to the

molecular tree. The next solution was 10 steps longer than the shortest one and it supported all the molecular clades.

The bootstrap tree recovered one clade (Figure 7-8d), a great ape and human clade (99%). This was consistent with the molecular phylogeny.

7.1.5 Summary of results

The hypothesis that male hominoids generate phylogenies that are consistent with the mixed-sex phylogenies is not fully supported by the results described above. Of the 16 tests described above, six produced results that agreed with the results of the equivalent mixed-sex analyses. These are illustrated in Table 7-5. Agreement between the results from male-specific datasets and from mixed-sex datasets is indicated in the table by a 'plus' sign, whilst a 'minus' sign indicates disagreement. It should be noted that in three cases (highlighted with an asterisk in the Table 7-5) the comparisons were positive even when the MPTs produced by the two datasets differed from each other. This was because one or both of the datasets yielded multiple MPTs and agreement was reached between their strict consensus trees. So effectively identical results were obtained only in three analyses.

Only three tests produced minimum length trees that were compatible with the hominoid molecular cladogram. This is shown in Table 7-6, where a 'plus' sign stands for agreement between the morphological cladograms and the hominoid molecular cladogram, and a 'minus' sign represents disagreement between the two. These results suggest that male-specific datasets are not better at recovering phylogenetic

relationships than mixed-sex datasets, since the latter produced positive results in seven analyses (Table 5-5). It is noteworthy that in two of the three positive results (highlighted with a single asterisk in Table 7-6), agreement was reached by the strict consensus of two MPTs, neither of which was compatible with the molecular phylogeny. In five other analyses, indicated with two asterisks, all the molecular clades were recovered in the next best solution(s).

Table 7-5. Agreement between the results of the male-specific parsimony analyses and the mixed-sex analyses.

Coding Method	All outgroups	*Papio*	*Cercopithecus*	*Colobus*
Divergence	+	-	+	-
Binary	+*	+*	+	+*
Baum	-	-	-	-
Segment	-	-	-	-

+ denotes agreement, – denotes disagreement, * consensus tree of multiple MPTs agrees with mixed-sex results

Table 7-6. Agreement between the results of the male-specific analyses and the hominoid consensus molecular phylogeny.

Coding Method	All outgroups	*Papio*	*Cercopithecus*	*Colobus*
Divergence	+*	-**	-	-
Binary	+*	-	-**	-**
Baum	-	+	-	-**
Segment	-	-	-	-**

+ denotes agreement, – denotes disagreement , * consensus of multiple MPTs, ** all molecular clades supported in the next MPT

Lastly, the bootstrap tests (Table 7-7) produced two false positive clades. In both cases, a clade that comprised *Gorilla* and *Pan* was recovered and it was very strongly supported. In three analyses, all run using *Papio* as the only outgroup, no clade with a

statistical support of 70% or more was found. The clade that was most commonly recovered (Figure 7-9) was the great ape and human clade (11 times), followed by the African ape and human clade (10 times).

Table 7-7. Number of clades supported by the bootstrap analyses.

Coding Method	All outgroups	*Papio*	*Cercopithecus*	*Colobus*
Divergence	$+_w+_s$		$+_w +_m$	$+_m+_s$
Binary	$+_m$		$+_w+_s$	$+_w+_m$
Baum	$+_w+_m+_m$	$+_w+_s$	$-_s+_s+_s$	$-_s+_s+_s$
Segment	$+_m$		$+_s$	$+_s$

+, 'true' clades; -, 'false' clades; 's', strongly supported (>90%); 'm', moderately supported (>80%); 'w', weakly supported (>70%).

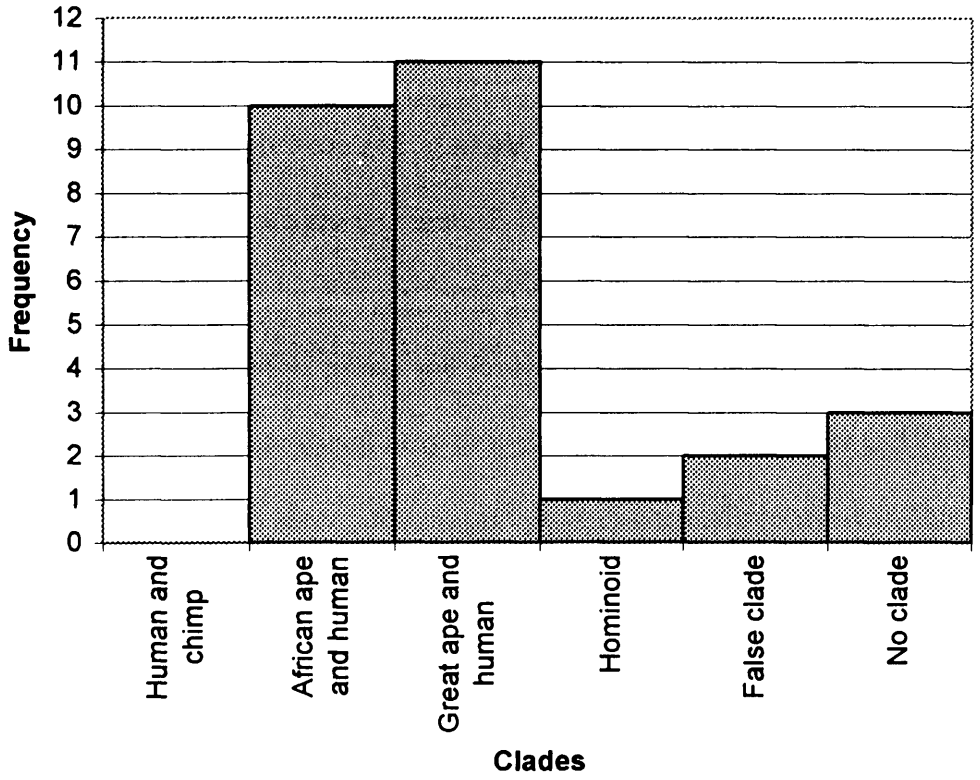

Figure 7-9. Frequency of recovery of each molecular clade in the bootstrap analyses.

7.2 Hypothesis 2b: Female hominoids generate phylogenies that are consistent with the mixed-sex phylogenies

7.2.1 Analysis 2b.1

The parsimony and bootstrap analyses described in this section were run including three cercopithecine taxa in the outgroup. The shortest trees are illustrated in Figure 7-10, and their associated tree statistics are reported in Table 7-8. The bootstrap consensus cladograms are presented in Figure 7-11.

a) Divergence coding

The parsimony analysis returned a single MPT that disagreed with the consensus hominoid molecular cladogram (Figure 7-10a). Its topology supported a phylogenetic hypothesis in which the hominoids formed a monophyletic group. *Hylobates* occupied a basal position within this group and *Pongo* was the sister taxon of the African apes and humans. *Homo* was placed next to a clade that comprised *Pan* and *Gorilla*. The molecular relationships among the outgroups were correctly recovered. This topology was consistent with the results of the mixed-sex analysis (Figure 5-1a). The next-best tree was identical to the consensus molecular cladogram but was seven steps longer than the MPT.

The bootstrap analysis recovered two clades consistent with the molecular results (Figure 7-11a). The first one was the great ape and human clade and it was strongly

supported (90%). The other clade was the hominoid clade and this was moderately supported (82%). The relationships within the rest of the tree were not resolved at the 70% confidence level.

b) Binary coding

The MPT found in this analysis supported all the molecular relationships both within the ingroup and the outgroup taxa (Figure 7-10b). It was also compatible with the consensus of the two MPTs found in the mixed-sex analyses (Figure 5-1d).

The bootstrap consensus cladogram was largely unresolved (Figure 7-11b). It recovered only one molecular clade, the hominoid clade, which was moderately supported (81%).

c) Baum's coding

This dataset produced a single most parsimonious solution (Figure 7-10c) that was identical to the consensus molecular tree. However, it differed from the solution of the equivalent mixed-sex analysis (Figure 5-1e).

The bootstrap analysis generated two clades that were consistent with the molecular phylogeny (Figure 7-11c). The first clade was the African ape and human clade, which was weakly supported (79%). The second clade, the hominoid clade, was strongly supported (96%).

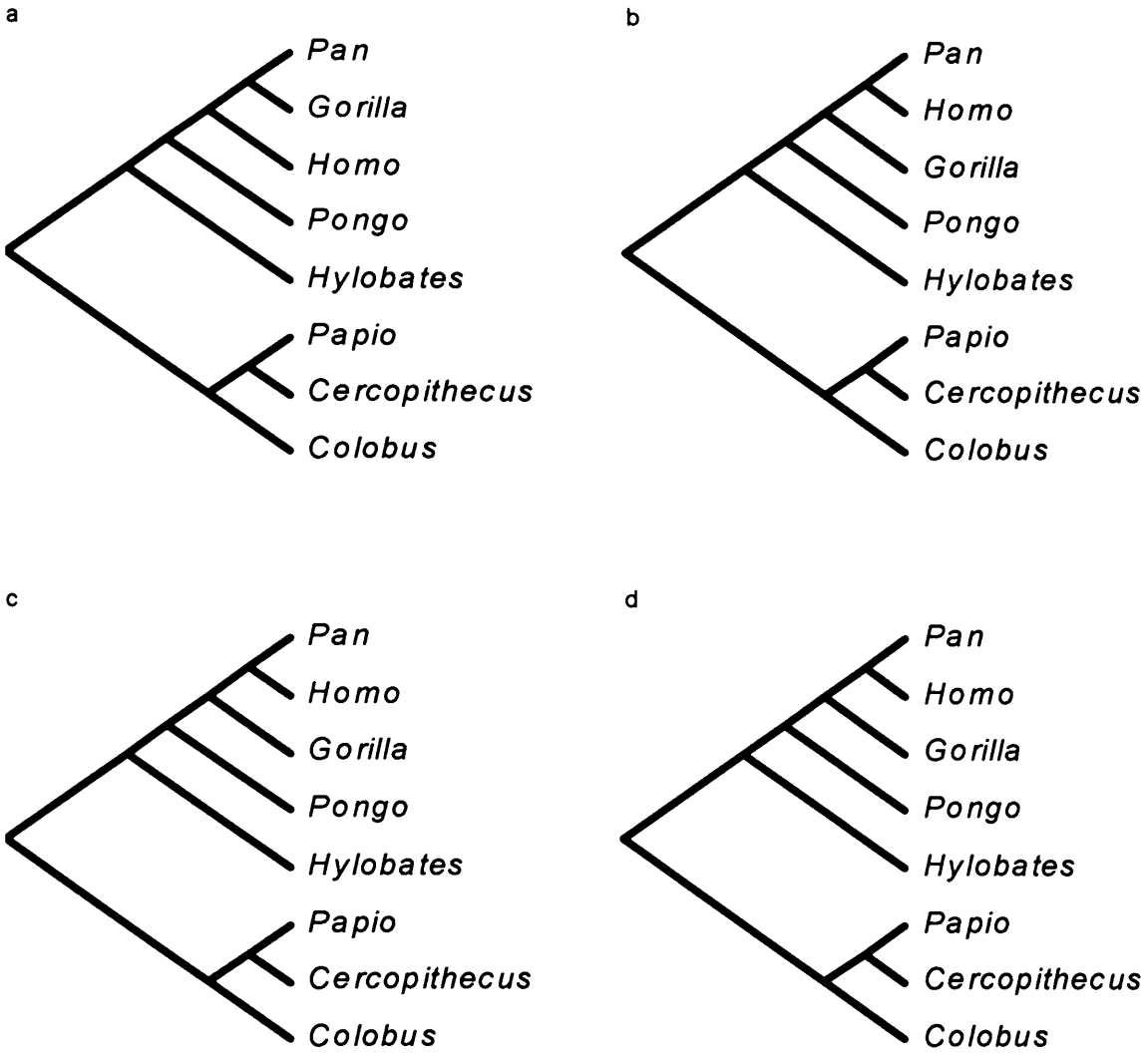

Figure 7-10. MPTs produced in Analysis 2b.1.
(a) Divergence Coding, (b) Binary Coding, (c) Baum's Coding, (d) Segment Coding

Table 7-8. Tree statistics associated with Analysis 2b.1.

Coding Method	TL	CI	HI	RI	PI
Divergence	1395	0.58	0.42	0.44	84
Binary	157	0.49	0.51	0.44	65
Baum	1283	0.53	0.47	0.38	99
Segment	2703	0.59	0.41	0.44	97

TL= tree length, CI= consistency index, HI= homoplasy index, RI= retention index, PI= number of parsimony informative characters

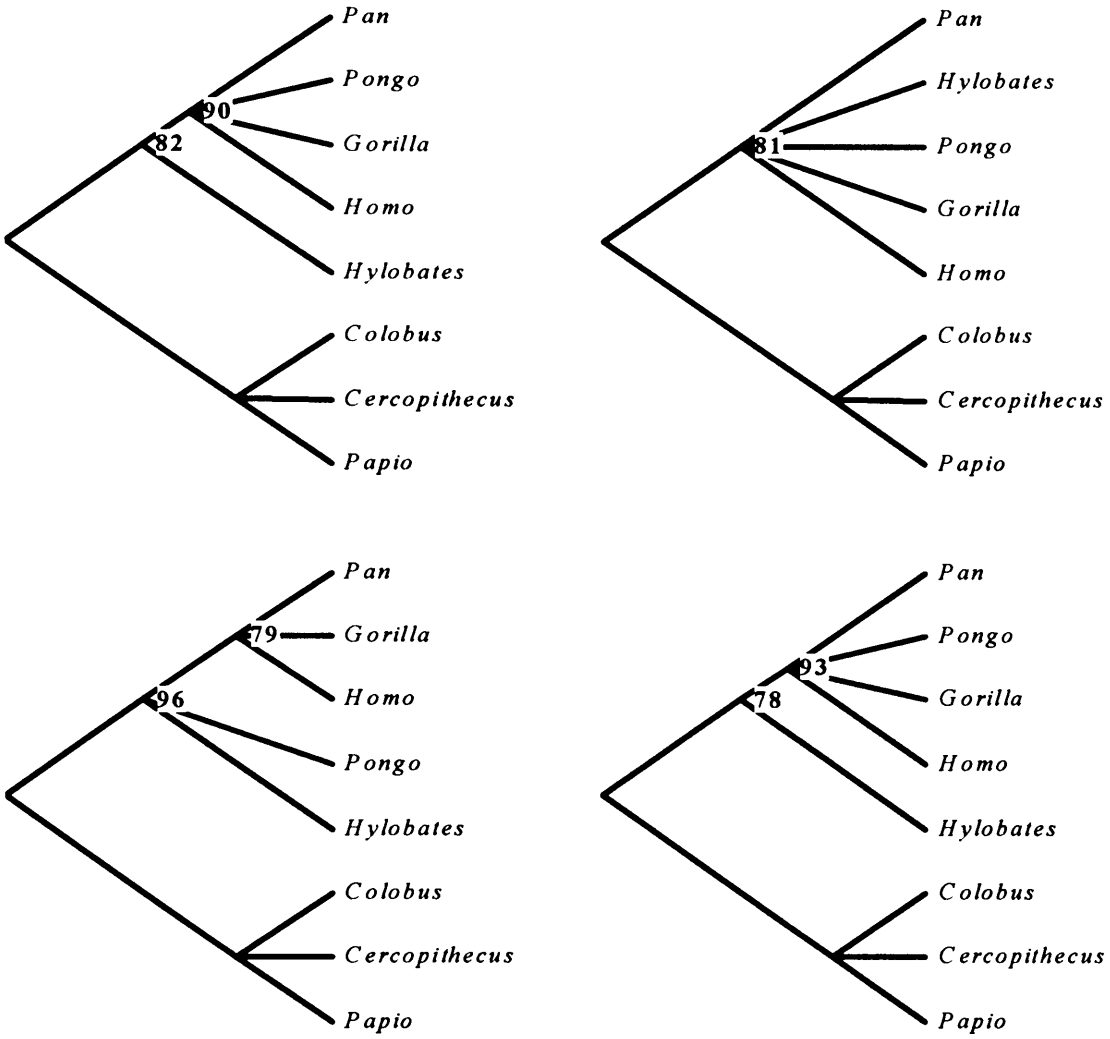

Figure 7-11. Bootstrap consensus cladograms generated in Analysis 2b.2.
(a) Divergence Coding, (b) Binary Coding, (c) Baum's Coding, (d) Segment Coding

d) Segment coding

This analysis returned a single MPT that agreed with the molecular cladogram and recovered all the molecular relationships within both the ingroup and the outgroup (Figure 7-10d). However, it did not agree with the MPT found in the mixed-sex analysis (Figure 5-1f).

The bootstrap analysis produced two clades (Figure 7-11d): the strongly supported great ape and human clade (93%), and the weakly supported hominoid clade (78%). Both these groups were consistent with the hominoid molecular phylogeny. The rest of the relationships were unresolved.

7.2.2 Analysis 2b.2

In the next set of analyses *Papio* was the only outgroup taxon included. The results of the parsimony analyses are shown in Figure 7-12, and the associated tree statistics are listed in Table 7-9. The consensus bootstrap trees are illustrated in Figure 7-13.

a) Divergence coding

The parsimony analysis yielded a single MPT that was identical to the molecular phylogeny (Figure 7-12a). This tree was also identical to the one found in the mixed-sex analysis (Figure 5-3a).

The bootstrap test did not recover any significant clade at the 70% confidence level (Figure 7-13a).

b) Binary coding

A single most parsimonious solution was recovered in this analysis (Figure 7-12b). It did not agree with the molecular cladogram. It placed *Pongo* at the base of the hominoid clade and *Gorilla* next to a clade that comprised *Pan*, *Homo* and *Hylobates*.

Within the latter clade, *Hylobates* was the sister group of a clade formed by humans and chimpanzees. This solution differed from the one yielded by the mixed-sex dataset (Figure 5-3b). One of the three next trees was identical to the hominoid molecular phylogeny and it was only two steps longer than MPT.

The bootstrap analysis recovered only one weakly supported clade (Figure 7-13b), the human and chimpanzee clade. This was consistent with the molecular results.

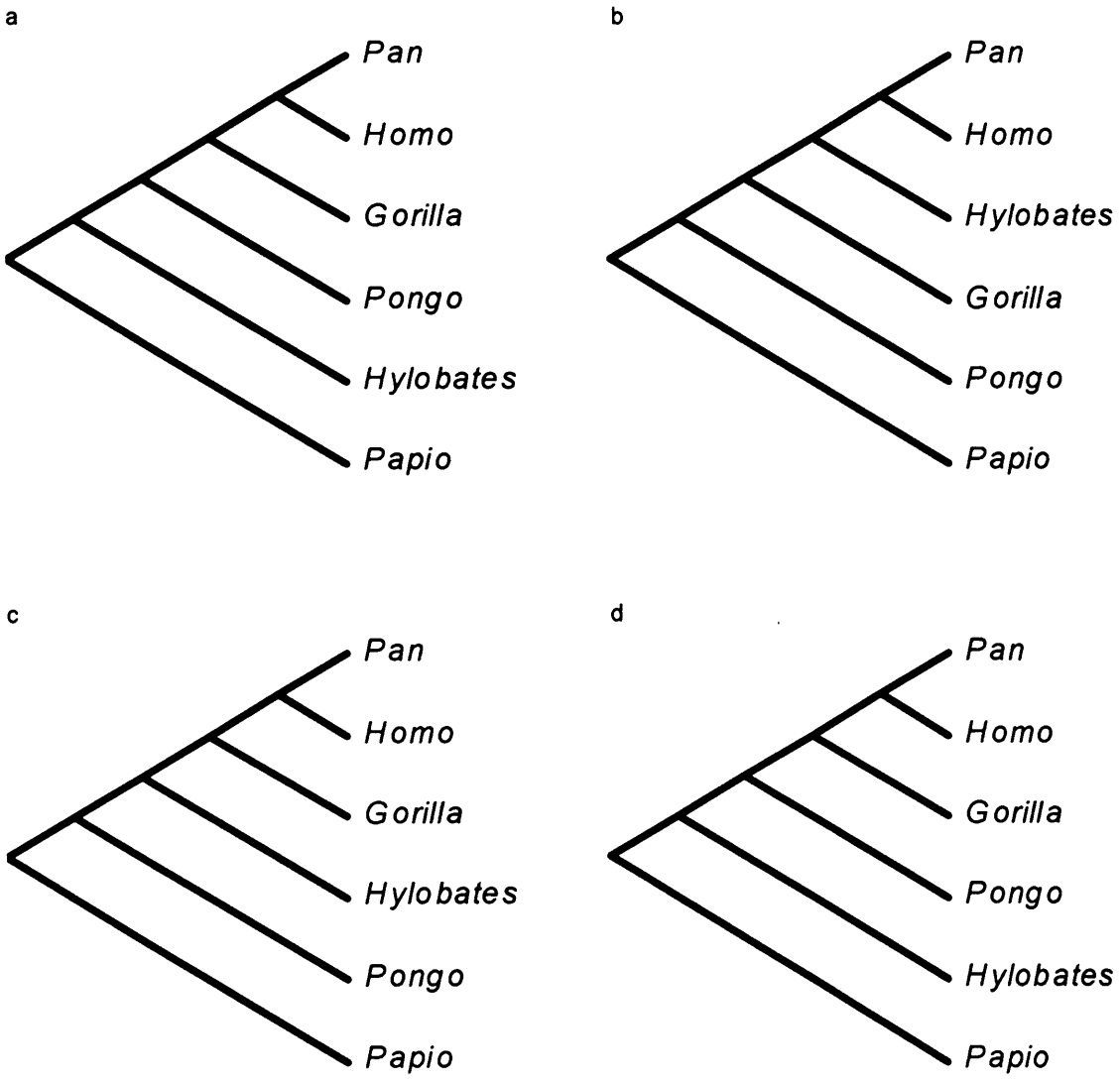

Figure 7-12. MPTs produced in Analysis 2b.2.
(a) Divergence Coding, (b) Binary Coding, (c) Baum's Coding, (d) Segment Coding

Table 7-9. Tree statistics associated with Analysis 2b.2.

Coding Method	TL	CI	HI	RI	PI
Divergence	898	0.65	0.35	0.37	79
Binary	121	0.56	0.44	0.38	48
Baum	777	0.63	0.37	0.35	98
Segment	2242	0.69	0.31	0.37	96

TL= tree length, CI= consistency index, HI= homoplasy index, RI= retention index, PI= number of parsimony informative characters

c) Baum's coding

This analysis produced a single MPT that did not agree with the molecular phylogeny (Figure 7-12c). The molecular relationships among *Gorilla*, *Pan* and *Homo* were correctly recovered. However, *Hylobates* appeared as the sister group of the African apes and humans, which was inconsistent with the molecular phylogeny. *Pongo* was left at the base of the hominoid clade. This topology also disagreed with the result from the mixed-sex dataset (Figure 5-3c).

The bootstrap consensus tree presented only one moderately supported molecular clade, the African ape and human clade (80%) (Figure 7-13c).

d) Segment coding

The shortest tree found in this analysis fully supported the hominoid molecular phylogeny (Figure 7-12d). It was also consistent with the MPT recovered in the mixed-sex analysis (Figure 5-3d).

The bootstrap test produced one weakly supported molecular clade (Figure 7-13d), the chimpanzee and human clade (73%). The rest of the tree was not resolved at the 70% confidence level.

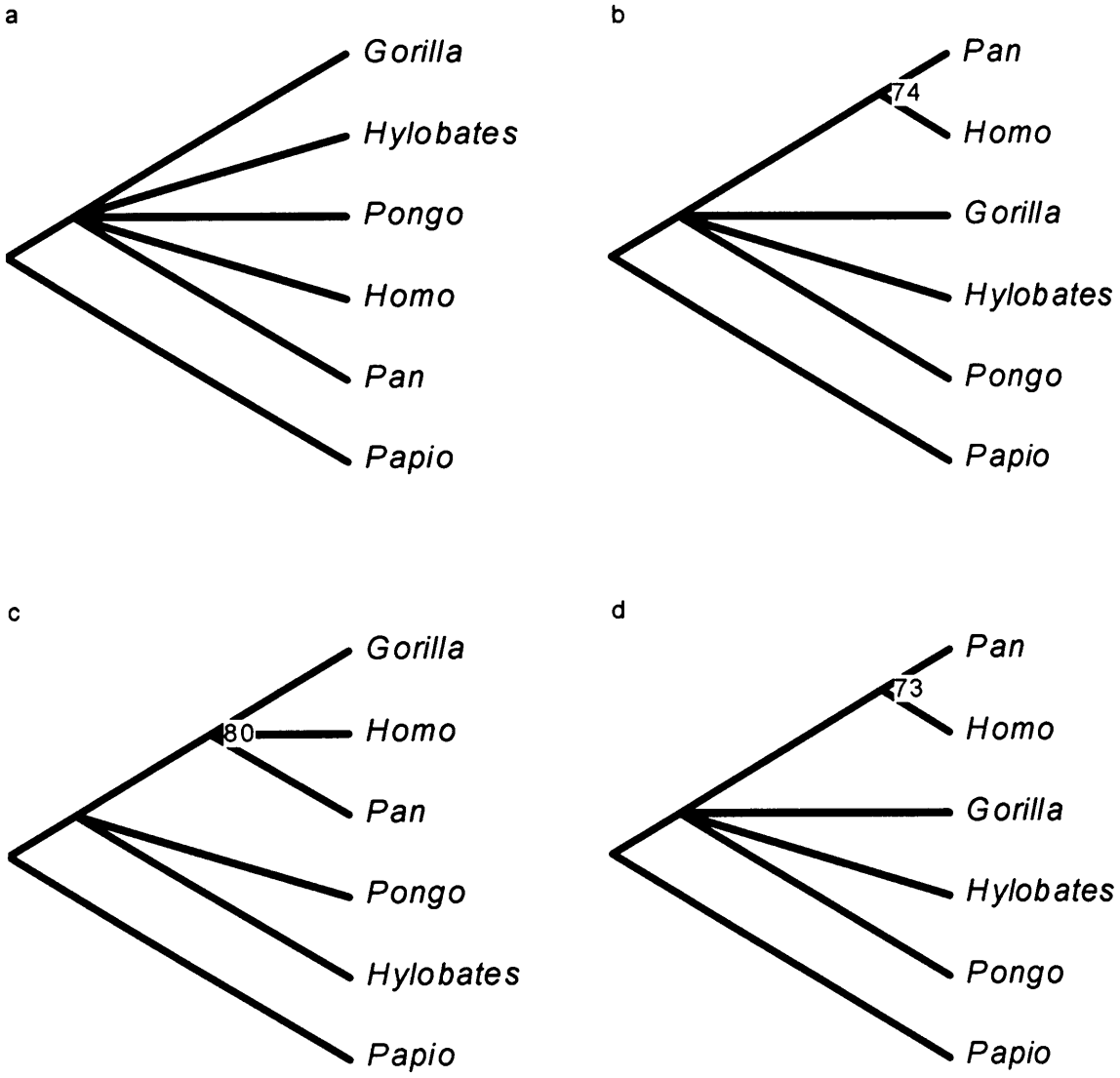

Figure 7-13. Bootstrap consensus cladograms generated in Analysis 2b.2.
(a) Divergence Coding, (b) Binary Coding, (c) Baum's Coding, (d) Segment Coding

7.2.3 Analysis 2b.3

In the next analyses, *Papio* and *Colobus* were excluded from the analyses and *Cercopithecus* was the only outgroup used. Figure 7-14 presents the results of the parsimony analyses; Table 7-10 reports their associated tree statistics. The bootstrap cladograms are shown in Figure 7-15.

a) Divergence coding

The single MPT found in this part of the analysis (Figure 7-14a) differed from the consensus molecular tree in placing *Pan* and *Gorilla* in a clade next to *Homo*. Consistent with the molecular phylogeny, the rest of the tree support the African ape and human clade, the great ape and human clade, and the hominoid clade. This solution differed from the MPT recovered in the mixed-sex analysis (Figure 5-5a). The next most parsimonious tree was six steps longer. It supported all the molecular relationships.

The consensus bootstrap cladogram (Figure 7-15a) contained only one clade consistent with the molecular phylogeny, the great ape and human clade, which was statistically highly significant (97%).

b) Binary coding

One MPT found in this analysis was identical to the hominoid molecular cladogram (Figure 7-14b). The other (Figure 7-14c) featured a great ape and human clade in

which *Gorilla* and *Pongo* formed a clade next to another clade formed by *Pan* and *Homo*. *Hylobates* appeared at the base of the hominoid clade. Their strict consensus is shown in Figure 7-14d. It featured a trichotomy formed by *Pongo, Gorilla* and a clade that comprised *Pan* and *Homo*. *Hylobates* occupied a basal position within the hominoids. This tree is consistent with both the molecular phylogeny and the consensus cladogram of the three MPTs found in the mixed-sex analysis (Figure 5-5e).

The bootstrap test did not generate any significant clade at the 70% confidence level (Figure 7-15b).

c) Baum's coding

The MPT supported all the molecular relationships of the hominoids (Figure 7-14e). However, it differed from the most parsimonious solution found in the mixed-sex analysis (Figure 5-5f).

The bootstrap tree featured one molecular clade (Figure 7-15c), the African ape and human clade. This group was weakly supported with a bootstrap values of 79%.

d) Segment coding

One MPT (Figure 7-14f) was recovered from this dataset and it supported all the branches of the molecular phylogeny. However, it did not agree with the shortest tree produced in the mixed-sex analysis (Figure 5-3g).

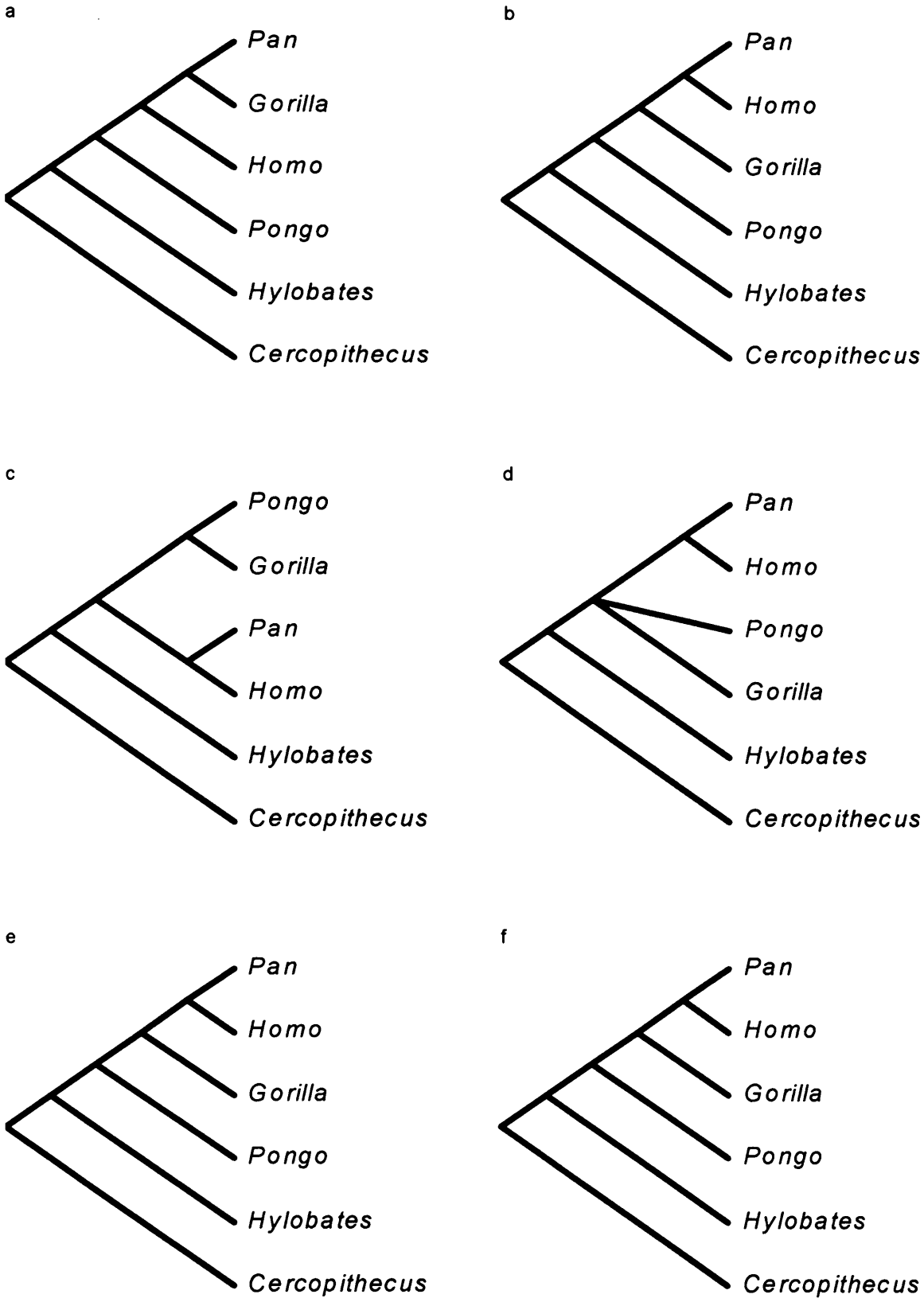

Figure 7-14. MPTs produced in Analysis 2b.3
(a) Divergence Coding, (b, c, d) Binary Coding, (e) Baum's Coding, (f) Segment Coding

Table 7-10. Tree statistics associated with Analysis 2b.3.

Coding Method	TL	CI	HI	RI	PI
Divergence	875	0.65	0.35	0.38	78
Binary	121	0.55	0.45	0.36	47
Baum	765	0.63	0.37	0.33	97
Segment	2159	0.69	0.31	0.39	94

TL= tree length, CI= consistency index, HI= homoplasy index, RI= retention index, PI= number of parsimony informative characters

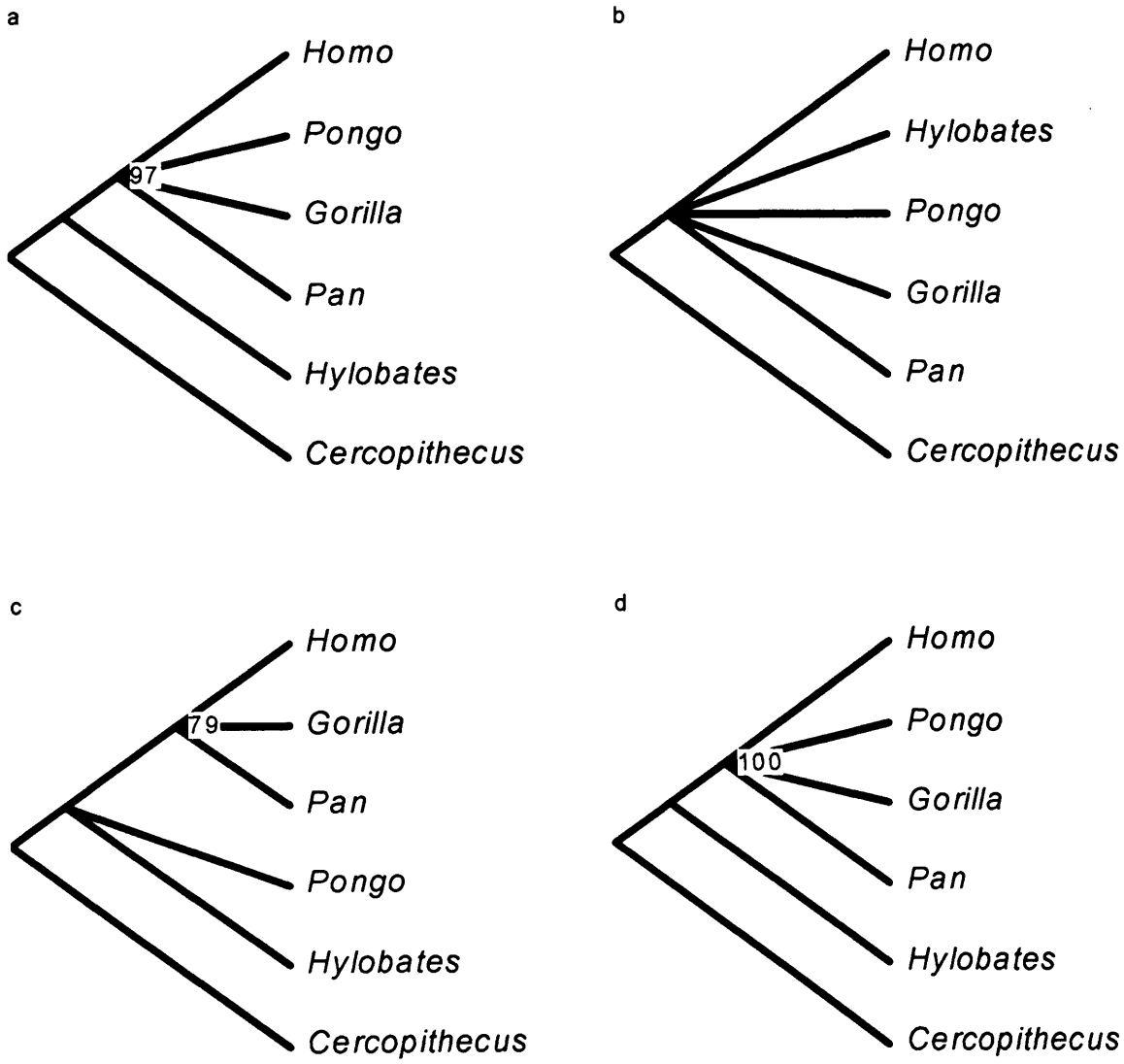

Figure 7-15. Bootstrap consensus cladograms generated in Analysis 2b.3.
(a) Divergence Coding, (b) Binary Coding, (c) Baum's Coding, (d) Segment Coding.

The bootstrap consensus cladogram (Figure 7-15d) generated only one highly significant clade, the great ape and human clade (100%). This was consistent with the molecular results.

7.2.4 Analysis 2b.4

In this last set of tests, *Cercopithecus* and *Papio* were excluded from the analyses, and *Colobus* was the only outgroup taxon used to root the cladograms. The MPTs recovered in the analyses are illustrated in Figure 7-16. The associated tree statistics are listed in Table 7-11. The bootstrap cladograms are shown in Figure 7-17.

a) Divergence coding

The parsimony analysis recovered two most parsimonious solutions. The first tree (Figure 7-16a) agreed with the hominoid molecular phylogeny. The other tree (Figure 7-16b) supported an African ape and human clade in which *Homo* was the sister group of a clade that comprised *Gorilla* and *Pan*. The great ape and human clade and the hominoid clade were also supported. Their strict consensus (Figure 7-16c) featured a hominoid clade, a great ape and human clade, and an African ape and human trichotomy. It was therefore consistent with both the hominoid molecular cladogram and the mixed-sex solution (Figure 5-7a).

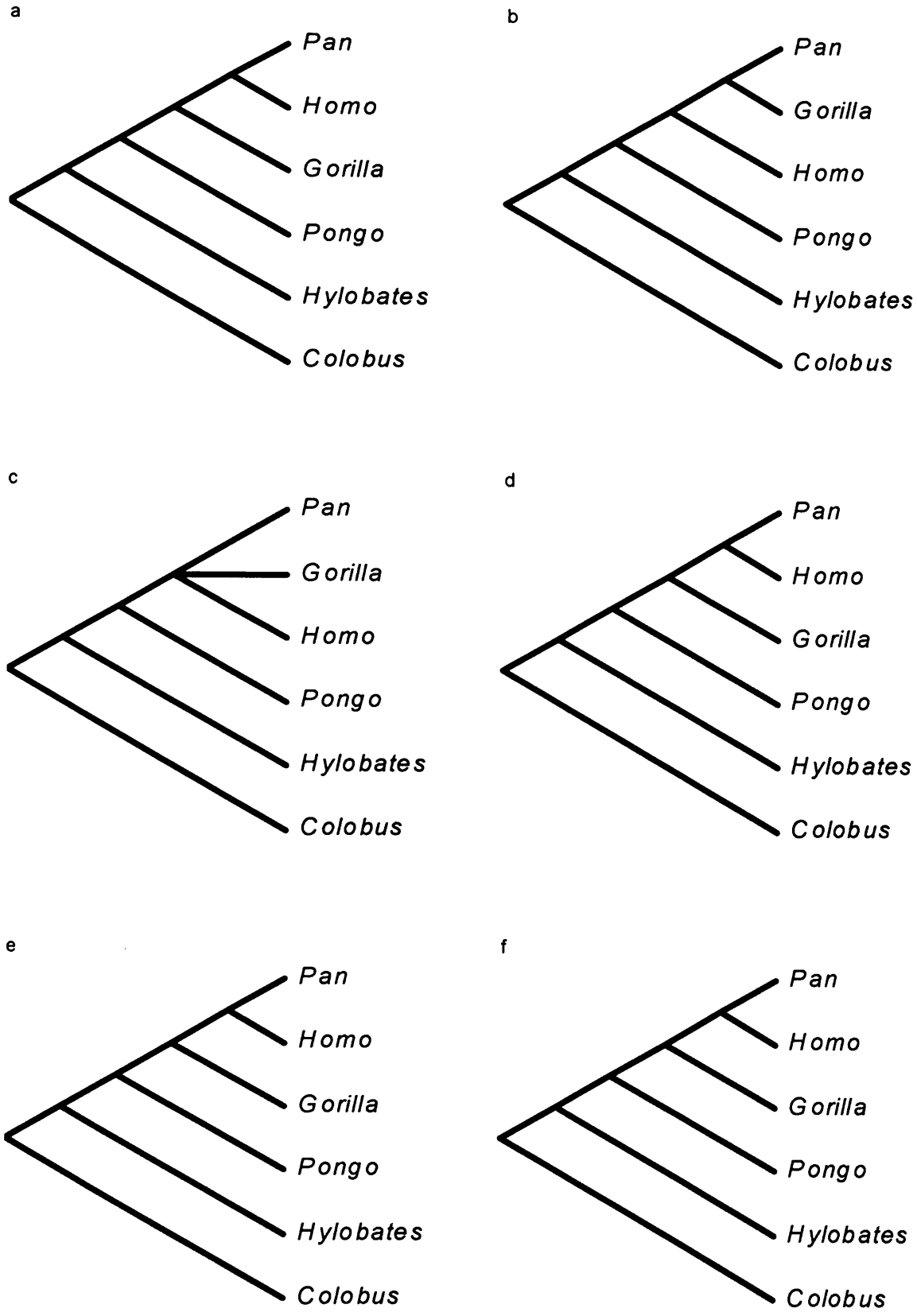

Figure 7-16. MPTs produced in Analysis 2b.4.
(a, b, c) Divergence Coding, (d) Binary Coding, (e) Baum's Coding, (f) Segment Coding

Table 7-11. Tree statistics associated with Analysis 2b.4.

Coding Method	TL	CI	HI	RI	PI
Divergence	863	0.67	0.33	0.40	79
Binary	114	0.58	0.42	0.44	49
Baum	761	0.64	0.36	0.36	98
Segment	2092	0.70	0.30	0.42	95

TL= tree length, CI= consistency index, HI= homoplasy index, RI= retention index, PI= number of parsimony informative characters

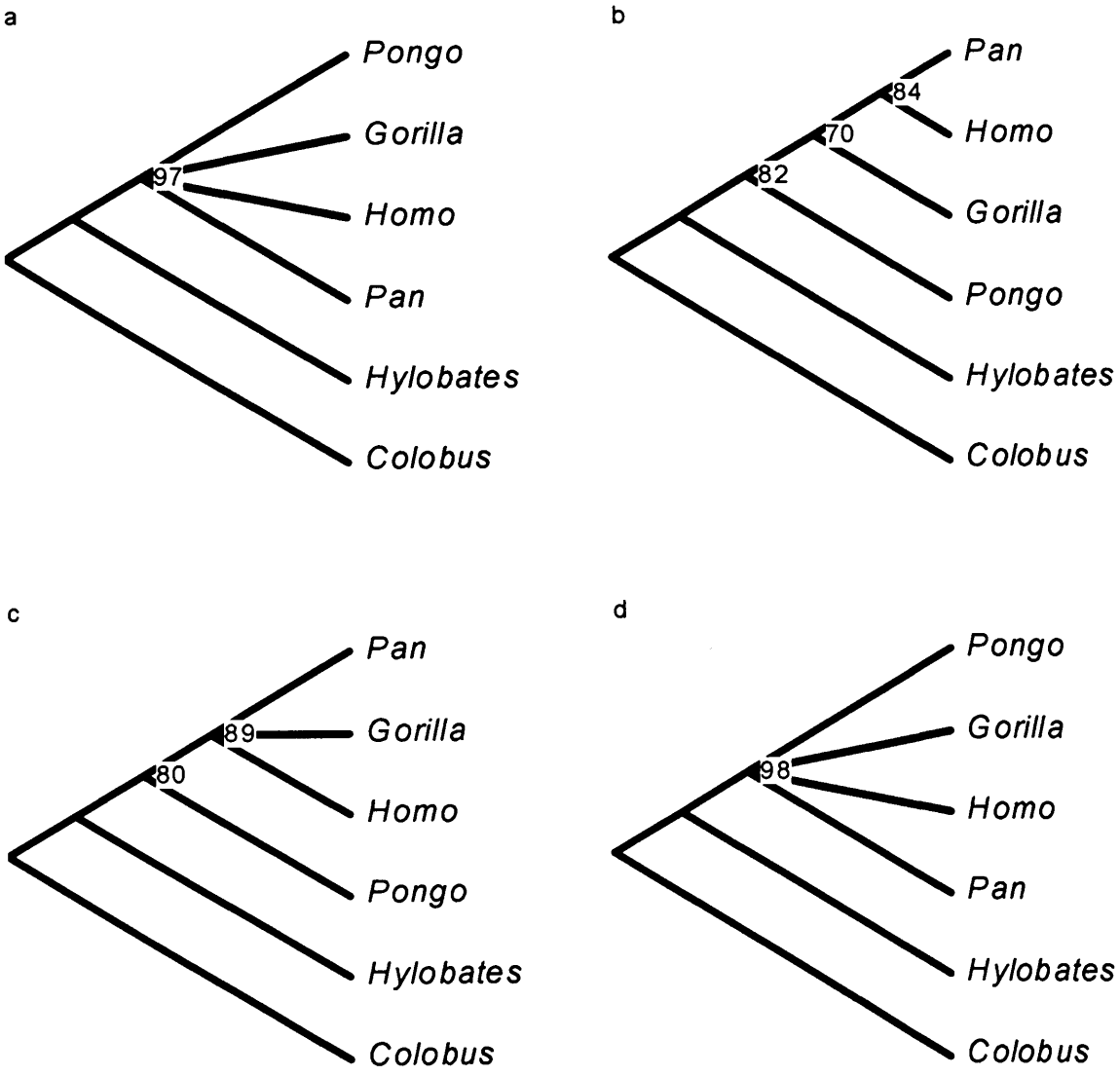

Figure 7-17. Bootstrap consensus cladograms generated in Analysis 2b.4.
(a) Divergence Coding, (b) Binary Coding, (c) Baum's Coding, (d) Segment Coding

Only one clade received statistical support in the bootstrap analysis (Figure 7-17a): the great ape and human clade, which was strongly supported (97%). This clade was consistent with the molecular results.

b) Binary coding

The MPT found in this analysis supported a phylogenetic hypothesis fully compatible with the molecular results (Figure 7-16d). It was also congruent with the consensus topology of the two MPTs obtained from the mixed-sex dataset (Figure 5-7d).

All the molecular clades were also supported by the bootstrap test (Figure 7-17b). The great ape and human clade was moderately supported (82%). The African ape and human clade was weakly supported (70%), while the human and chimpanzee clade was moderately supported (84%).

c) Baum's coding

This dataset returned a single MPT (Figure 7-16e) that was also identical to the hominoid molecular cladogram and to the MPT recovered in the mixed-sex analysis (Figure 5-7e).

The bootstrap consensus tree resolved two clades consistent with the molecular phylogeny: the great ape and human clade, and the African ape and human clade (Figure 7-17c). These clades were supported with bootstrap values of 80% and 89% respectively.

d) Segment coding

All molecular clades were also present in the MPT recovered in this analysis (Figure 7-16f). This topology was the same as the one found in the equivalent mixed-sex analysis (Figure 5-7f).

The bootstrap cladogram (Figure 7-17d) presented only one clade, the highly significant great ape and human clade (98%). This was congruent with the hominoid molecular tree.

7.2.5 Summary of results

The hypothesis that female-specific datasets generate phylogenies that are consistent with the mixed-sex phylogenies is, again, only partially supported by the tests described in this section. Nine out the 16 phylogenetic hypotheses generated from the female-specific datasets agreed with the phylogenies generated from the mixed-sex datasets (Table 7-12). In three analyses (marked with an asterisk in the table) one or both datasets generated multiple MPTs and therefore the comparisons were carried out between their strict consensus trees. Hence, effectively, six tests produced identical solutions between the mixed-sex and female-only datasets. This value is higher than the one for the male-only dataset (three, Table 7-5).

Interestingly, 12 out of the 16 analyses produced MPTs that were compatible with the hominoid molecular cladogram (Table 7-13). This suggests that female specimens are

more reliable than both the mixed-sex and male-only datasets for recovering the molecular phylogeny of the hominoids. To reiterate, the mixed-sex analyses recovered the molecular phylogeny seven times, while the male-specific analyses recovered it just three times. Only in four cases were the molecular relationships not fully recovered. In three of these (marked with two asterisks in Table 7-13) the next MPT, or the consensus of multiple trees, was consistent with the molecular phylogeny.

Table 7-12. Agreement between the results of the female-specific parsimony analyses and the mixed-sex analyses.

Coding Method	All outgroups	*Papio*	*Cercopithecus*	*Colobus*
Divergence	+	+	-	+*
Binary	+	-	+*	+*
Baum	-	-	-	+
Segment	-	+	-	+

+ denotes agreement, – denotes disagreement, * comparison between consensus of multiple MPTs

Table 7-13. Agreement between the results of the female-specific analyses and the hominoid consensus molecular phylogeny.

Coding Method	All outgroups	*Papio*	*Cercopithecus*	*Colobus*
Divergence	-**	+	-**	+*
Binary	+	-**	+*	+
Baum	+	-	+	+
Segment	+	+	+	+

+ denotes agreement, – denotes disagreement, * consensus of multiple MPTs , ** all molecular clades supported in the next MPT

Lastly, the bootstrap tests (Table 7-14) produced clades that were always consistent with the molecular phylogeny. The most frequently recovered molecular clade (Figure 7-18) was the great ape and human clade (eight times), followed by the African ape and human clade (five times) and the hominoid clade (four times). In three analyses a

clade formed by human and chimps was recovered although in two cases it was only weakly supported and in the third one it was moderately supported. In two further tests no clade with a statistical support of at least 70% was recovered.

Table 7-14. Number of clades supported by the bootstrap analyses.

Coding Method	All Outgroups	*Papio*	*Cercopithecus*	*Colobus*
Divergence	$+_m+_s$		$+_s$	$+_s$
Binary	$+_m$	$+_w$		$+_w+_m+_m$
Baum	$+_w+_s$	$+_m$	$+_w$	$+_m+_m$
Segment	$+_w+_s$	$+_w$	$+_s$	$+_s$

+, 'true' clades; -, 'false' clades; 's', strongly supported (>90%); 'm', moderately supported (>80%); 'w', weakly supported (>70%).

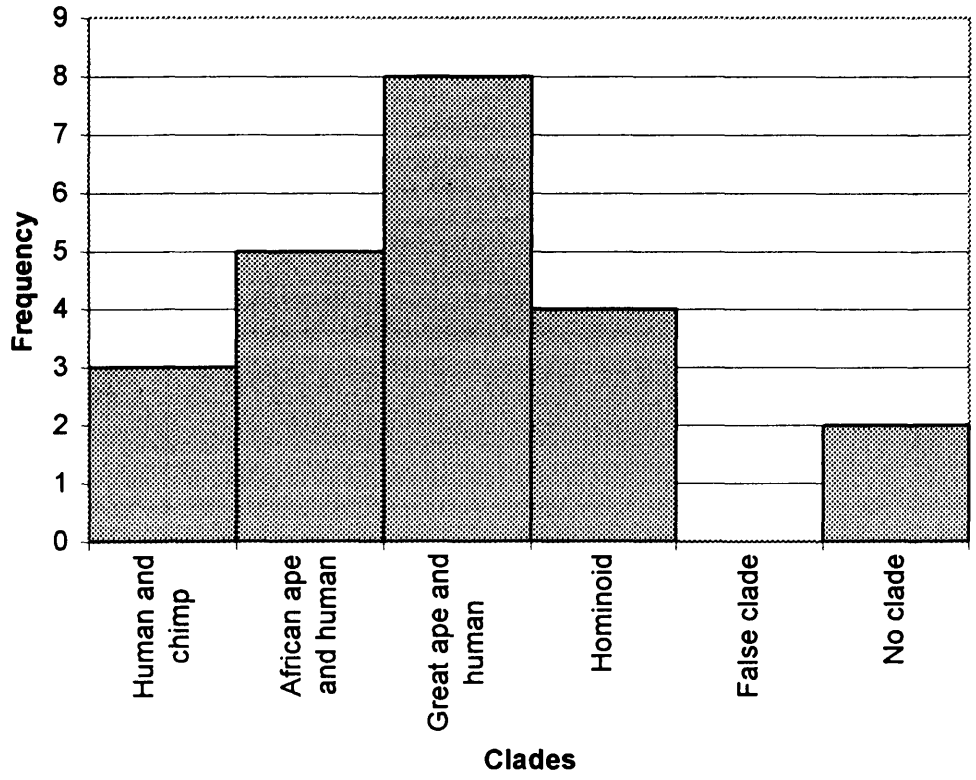

Figure 7-18. Frequency of recovery of each molecular clade in the bootstrap analyses.

7.3 Summary

The null hypothesis that sexual selection does not have any significant impact on the outcome of phylogenetic reconstruction is not supported by these results. In general, female-specific analyses and male-specific analyses produced results that differed (Table 7-15). In 12 of the 16 pairwise comparisons of equivalent analyses, the solutions derived from the male- and female-only datasets did not agree. In four tests (marked with an asterisk in the table) one or both of the datasets produced multiple MPTs that differed from each other but their strict consensus were compatible. Therefore, effectively the two datasets never produced the same solutions. Female-specific datasets produced six trees that were consistent with the mixed-sex results whereas the male-specific datasets produced only three such trees.

Table 7-15. Agreement between the results of the female-specific and the male-specific parsimony analyses.

Coding Method	All outgroups	*Papio*	*Cercopithecus*	*Colobus*
Divergence	+*	-	-	+*
Binary	+*	+*	-	-
Baum	-	-	-	-
Segment	-	-	-	-

+ denotes agreement, – denotes disagreement, * consensus of multiple MPTs

An interesting finding was that female-specific datasets recovered the full topology of the molecular cladogram 12 times out of 16, while male-specific datasets recovered the molecular topology only three times out of 16. The 'success indices' for outgroup and coding methods, calculated for the sex-specific analyses (Table 7-16), show that

the success rates in recovering molecular clades are consistently higher for female-only datasets (S_O=0.81-0.96, S_C=0.81-1.00) than for male-only datasets (S_O=0.56-0.75, S_C=0.52-0.83). Furthermore, all the statistically significant clades at the 70% confidence level recovered in female-specific bootstrap analyses were true clades, whilst male-specific analyses recovered two false clades. Notably, the clade formed by *Homo* and *Pan* was never supported in the male-specific analyses but it was recovered three times in the female-specific analyses. These results suggest that phylogenetic analyses of female-specific datasets based on vessel- and nerve-related characters generate phylogenies for the hominoids more reliable than male specific and mixed-sex datasets.

Table 7-16. Comparison of success indices (S_O and S_C) for male- and female-specific datasets.

		All outgroups	*Papio*	*Cercopithecus*	*Colobus*
S_O	M	0.58	0.56	0.75	0.75
	F	0.96	0.81	0.88	0.94
		Divergence	Binary	Baum	Segment
S_C	M	0.58	0.52	0.83	0.71
	F	0.83	0.81	0.94	1.00

M= male, F= female

In sum, the results of the tests described in this chapter support the hypothesis that sexual selection has an impact on phylogenetic inference and they also indicate that phylogenetic hypotheses generated from female-specific datasets are more reliable than male-specific datasets for recovering the molecular relationships of the hominoids at the generic level.

Chapter 8. DISCUSSION AND CONCLUSIONS

8.1 Phylogenetic utility of nerve- and vessel-related characters

This project set out to test the hypothesis that osseous characters related to nerves and vessels produce reliable phylogenies for the extant hominoids, and to compare the performance of these characters to the performance of standard craniodental characters. It also assessed the effects of methodological choices – namely coding procedure, outgroup choice and taxonomic level – on phylogenetic reconstruction. In addition, it evaluated the impact of sexual dimorphism on the outcome of hominoid cladistic analyses.

Two types of analyses were used to test this hypothesis, parsimony and bootstrapping. The hypothesis that nerve- and vessel-related osteological characters carry a reliable phylogenetic signal for the hominoids was partially supported by the results of the main analysis (Chapter 5). Seven of the 16 parsimony tests carried out to evaluate this hypothesis produced cladograms compatible with the consensus molecular phylogeny for this group of primates. In the other nine cases, the most parsimonious trees recovered were inconsistent with the molecular tree. Thus, the parsimony tests only partially supported this hypothesis. In contrast, the bootstrap tests produced clades consistent with the molecular cladogram in all but one case. Hence, the bootstrap tests strongly supported the hypothesis. The clades that received the strongest support were the African ape and human clade, and the great ape and human clade. The relationships among humans and African apes could not be resolved unambiguously.

These findings contrast with the results of the analyses based on standard craniodental characters. Trees generated from a craniometric dataset supported phylogenetic hypotheses for the hominoids that were inconsistent with the molecular results and that recovered only one molecular clade, the hominoid clade. The bootstrap trees generated from the same dataset placed a high level of support for the great ape clade and a clade formed by *Homo* and *Hylobates*. Both arrangements disagree with the molecular phylogeny. As Collard and Wood (2000) pointed out, the fact that false-clades receive a high level of support in the analyses of craniodental data is problematic, because clades that find a strong statistical support in bootstrap analyses are generally assumed to be correct. It follows that generating bootstrap cladograms from standard craniometric datasets can potentially be extremely misleading in the formulation of phylogenetic hypotheses for fossil primate taxa.

Overall, these results indicate that cranial characters related to nerves and vessels may be a better focus for hominoid phylogenetic analysis than standard craniodental characters. Why are characters related to nerves and vessels more reliable for phylogenetic inference than standard craniometric characters? Lieberman (1999) outlined seven criteria for selecting phylogenetically informative characters. Characters should be: 1) natural units; 2) discrete and/or quantifiable; 3) more variable between species than within species; 4) derived with respect to a common ancestor; 5) uncorrelated; 6) highly heritable; 7) and homologous. Nerve- and vessel-related traits meet most of these criteria. They are natural units of the primate skull (criterion 1). They are relatively easy to describe, and they can be characterised both qualitatively and quantitatively (criterion 2). There is some evidence that discrete

characters are not strongly correlated (criterion 5). This is also supported by analyses presented here (section 4.3.4). Furthermore, nerve- and vessel-related traits do not seem to be strongly influenced by environmental factors (criterion 6). Plus, homology can be readily established in closely related taxa such as the hominoids (criterion 7). Lastly, some studies (e.g. Msuya and Harrison, 1997; Braga, 2001) have shown trends from ancestral to more derived conditions in primates (criterion 4). The data concerning within- versus between-species variation (criterion 3) is still poor for many of these variants although high levels of overlapping intra-specific variation is to be expected for closely related species such as the hominoids (Hawks, 2004). A final notable characteristic is that a number of these traits do not seem to be under strong selective pressures but, rather, their population genetics seems to be controlled by random drift (Hanihara and Ishida, 2001d). In this context it is interesting to note that enlarged parietal foramina have been associated with a number of skeletal anomalies (Luker et al., 1998) as well as mental disorders such as the Potocki-Shaffer syndrome (Hall et al., 2001). Although this is unlikely to be a causal association, it is possible that a change in the number, size, shape or position of some nerve- and vessel-related traits may have, or may be correlated with, extremely deleterious effects, on individual fitness.

In summary, unlike standard craniodental characters, nerve- and vessel-related traits generate strongly supported clades that are consistent with the hominoid molecular phylogeny. These results suggest that cranial characters related to nerves and vessels may be a better focus for hominoid phylogenetic analysis than standard craniodental characters.

Three important findings also emerged from this study. First, cladistic analyses are strongly influenced by methodological choices such as coding method, outgroup choice and taxonomic level. Second, sexual dimorphism may be a source of homoplasy in phylogenetic analyses. Third, non-phylogenetic character correlation only seems to be a minor source of error in the recovery of phylogenetic hypotheses with nerve- and vessel-related traits. These findings and their implications for hominin evolutionary studies are discussed in the next sections.

8.2 Methodological choices in cladistics

The results of the analyses carried out in this study showed that the topologies of the minimum-length solutions varied depending on the coding procedure adopted, on the composition of the outgroup, and on the taxonomic level at which I operated (i.e. species vs genera). Interestingly, bootstrap tests seemed to be less affected by these factors and produced consensus cladograms that were consistent with each other.

These results have important implications for the formulation of hominin phylogenetic hypotheses and also for any study that relies on a clear and reliable phylogeny for making judgements about the reliability of character sets for phylogenetic analysis. For example, in this study, a dataset coded with Baum's method and that included only *Colobus* in the outgroup produced a most parsimonious cladogram that agreed with the hominoid molecular cladogram. Therefore, based on this test, the main hypothesis of this project would not be rejected. However, when the outgroup was changed to include only *Papio*, the minimum length cladogram

recovered differed considerably from the consensus molecular tree. In this case, following the rationale of this study, the hypothesis would be rejected.

8.2.1 Coding methods

The outcome of parsimony analysis was heavily influenced by character coding. This finding is consistent with previous work by Wiens (1995). He noted that, when little polymorphism is present in a dataset, no major differences are found in the topologies of the most parsimonious trees (MPTs) generated by different method. However, when a large number of discrete and intraspecifically variable characters are used in a parsimony analysis, considerable differences in the topologies of the MPTs can occur as a result of employing different coding techniques (Wiens, 1995). The datasets used in this project are largely composed of discrete polymorphic characters. Therefore, the results support Wien's prediction.

When genera were the Operational Taxonomic Unit, the coding method that, on average, produced the greatest number of molecular clades, as shown by the success indices calculated in Table 5-6, was the divergence method (S_C=0.83). This was followed by segment coding (S_C=0.79) and binary coding (S_O=0.71). Baum's method scored the lowest success rate (S_C=0.63). Similarly, in the bootstrap analyses the most resolved consensus cladograms were produced when the divergence method was used. This also yielded the greatest number of statistically significant clades. Baum's method was the only coding method that yielded a clade not consistent with the consensus molecular phylogeny, although this false-positive clade was weakly supported (Table 5-7).

The performance of the four coding methods can be assessed by looking at the tree statistics associated with the MPTs produced in the parsimony analyses (Wiens, 1995): the consistency index (CI), the retention index (RI) and the number of parsimony informative characters (PIC).

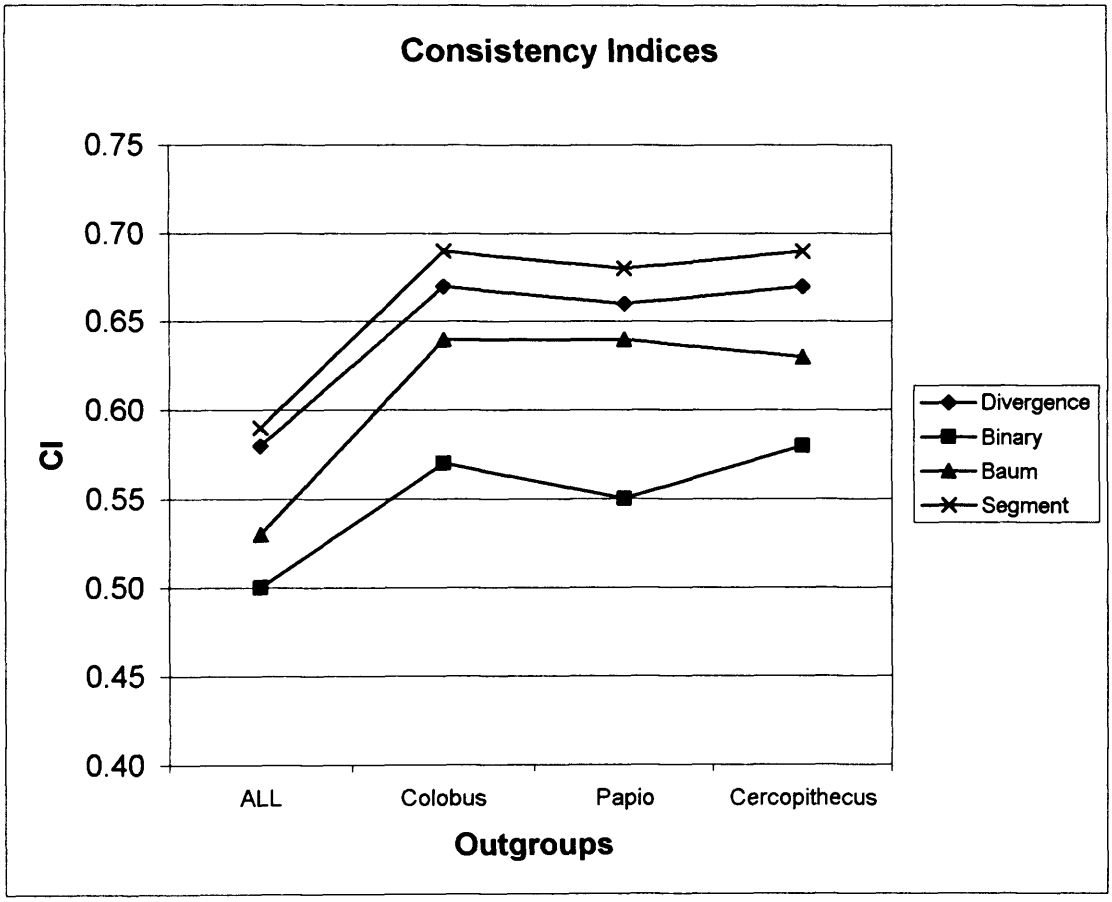

Figure 8-1. Consistency indices associated with the most parsimonious trees (excluding uninformative characters).

The consistency index measures the fit of characters to a cladogram and thus provides a measure of the amount of homoplasy present in the dataset (Farris, 1989). The CIs associated with the most parsimonious cladograms follow a similar trend for each coding method, the lines being more or less parallel (Figure 8-1). The segment

method for coding characters produced the highest values, followed by the divergence method and Baum's method. The binary method produced the lowest CI values. This index, however, is affected by the number of parsimony uninformative characters present in a dataset (Farris, 1989; Kitching et al., 1998), which varies depending on the coding method used. For this reason, in order to compare this statistic for different coding methods, the consistency index was computed here excluding uninformative characters from the calculations. The number of taxa also affects the value of this index (Kitching et al., 1998): internal consistency decreases if the number of taxa increases. This is evident in Figure 8-1, which shows that the indices are lowest when all three outgroups are used simultaneously.

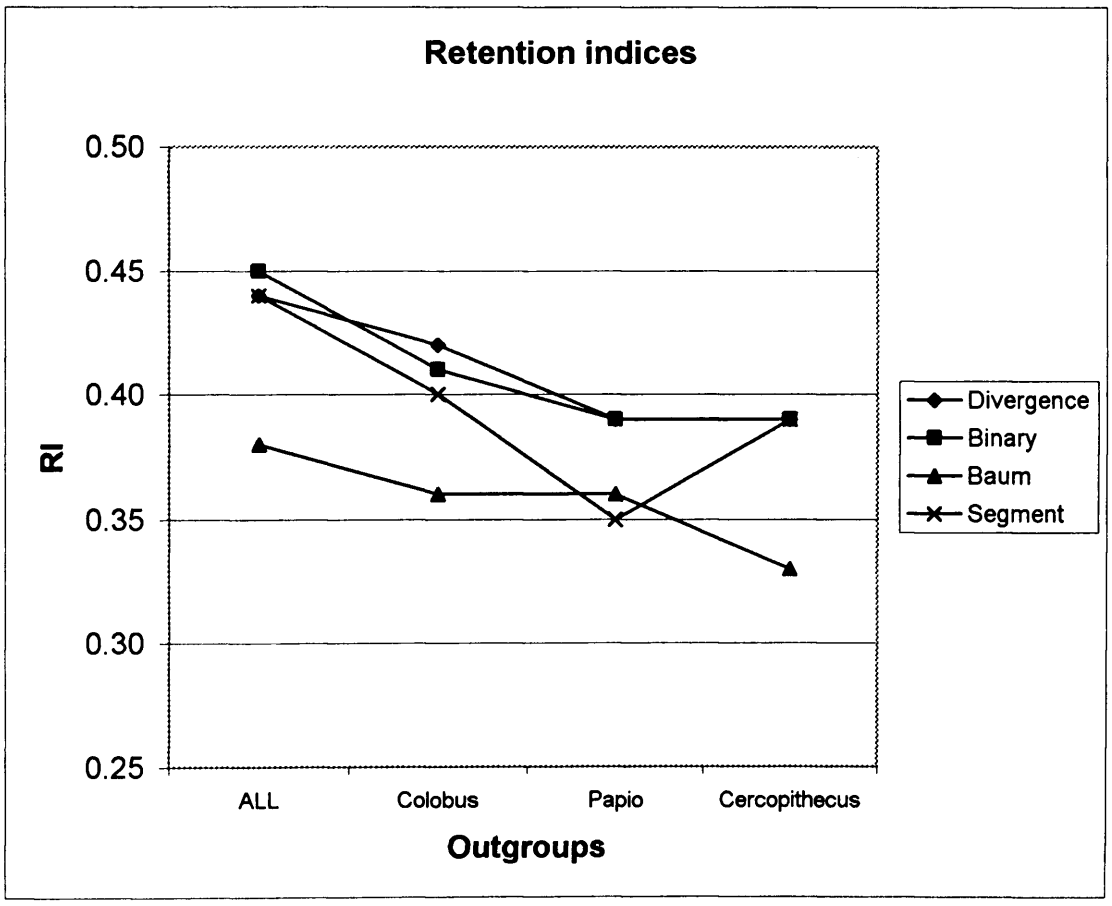

Figure 8-2. Retention indices (RIs) associated with the most parsimonious solutions.

Like the consistency index, the retention index (Figure 8-2) also measures the amount of homoplasy in a dataset, but in this case in terms of the amount of similarities that are retained as synapomorphies (Farris, 1989). The RIs returned by the datasets coded using the divergence and binary methods are the most similar to each other and they are also the highest in value. This suggests that more synapomorphies are identified by these coding procedures. The segment method also produces values similar to the ones yielded by the divergence and binary methods except in one case, i.e. when *Papio* is the only outgroup used. The indices produced using Baum's procedure are the lowest.

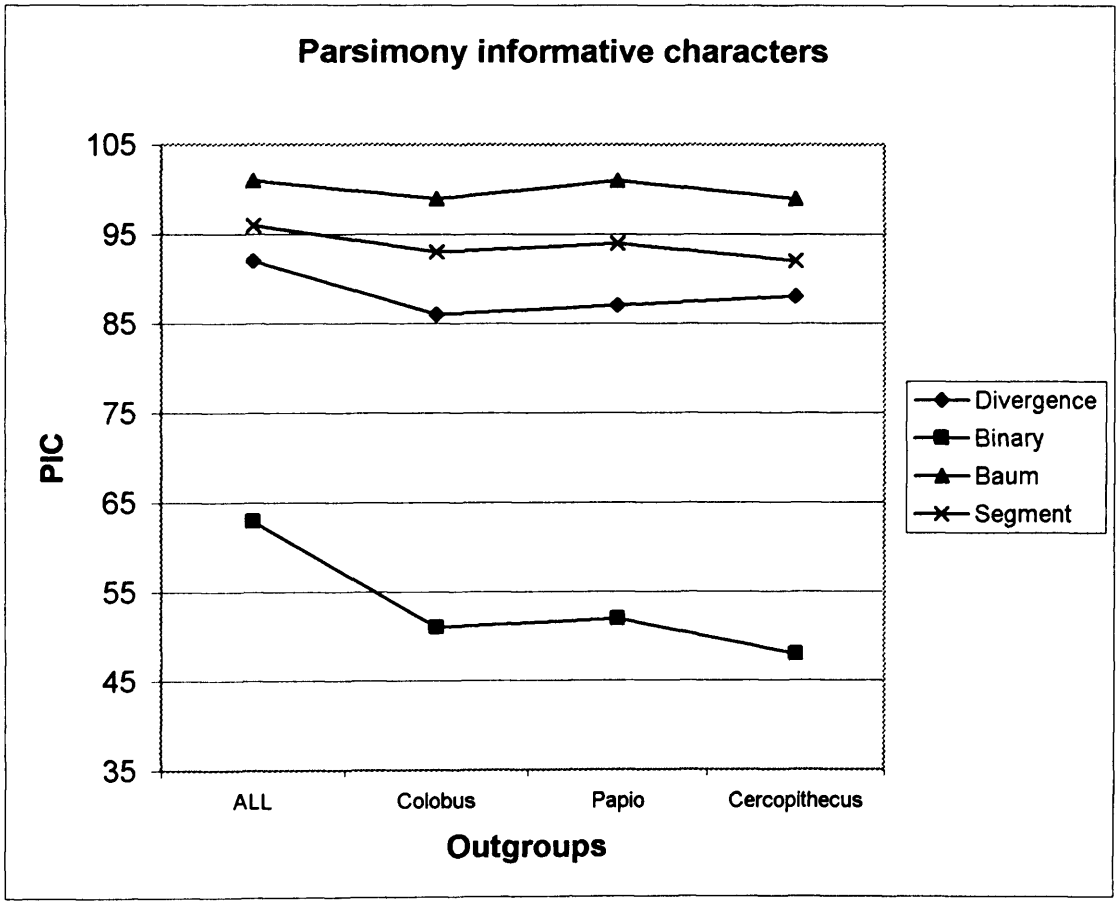

Figure 8-3. Number of parsimony informative characters (PIC) present in the analyses.

The number of parsimony informative characters also varies depending on the coding method used. In this case too, the lines generally follow a similar trend (Figure 8-3). Baum's method consistently produces the highest number of parsimony informative characters, followed by the segment method and the divergence method. The binary method instead always produces the lowest number of informative characters. As shown in the diagram in figure 8-3, the gap between the divergence method and the binary method is very large, highlighting the substantial loss of phylogenetic information in the datasets coded with the latter procedure. These findings are not surprising and they can be explained by the underlying principles of these coding methods.

These comparisons show that each method has points of strength and points of weakness. The binary method performs very poorly in terms of number of parsimony informative characters present in the datasets and in terms of internal consistency, as shown by the consistency indices. This suggests higher level of homoplasy in these datasets. However, it is the coding method that yields the highest retention indices, indicating that a large number of the similarities in the datasets can be interpreted as synapomorphies. Baum's coding method performs poorly both in terms of consistency indices and retention indices, suggesting relatively high homoplasy in the datasets. However, it is the procedure that yields that greatest number of parsimony informative characters. The segment method produces datasets with relatively low levels of homoplasy and relatively large proportions of synapomorphies, although the latter is dependent on the outgroup chosen. The number of parsimony informative characters is also relatively high. Lastly, the divergence method yields high retention indices

indicating a relatively large proportion of synapomorphies in the datasets. In this case, the relatively high consistency indices also indicate a low level of homoplasy compared to the other coding procedures.

In summary, from an examination of the CI, RI and PIC, it emerges that the segment and the divergence methods outperform the binary and Baum's methods. This is not surprising because both the divergence method and the segment method are conceptually more rigorous and sound than the binary method and Baum's method. Wiens (1995) showed that the 'frequency-bins' method, analogous to the segment method, generally performs better than other coding procedures in terms of number of parsimony informative characters, number of most parsimonious trees generated, phylogenetic signal and bootstrapping. The reason for this is that frequency bins maximise the amount of phylogenetic information in the data and reduce noise and sampling error by giving minimal weight to variants occurring at low frequencies (Wiens, 1995). The divergence method is also rigorous in that it is based on the evaluation of significant differences between scores (means of distributions or frequency values) using robust statistical tests (Student's t-test and Chi-square test). Therefore differences between taxa are weighted in terms of whether they are statistically significant or not. In contrast, the binary method and Baum's method do not maximise the amount of phylogenetic information present in the dataset and do not weight finely the differences between taxa. Both methods discard most of the variation present in the dataset, the former shrinking it into two classes, the latter ranking it by taxon (10 classes).

8.2.2 Outgroup choice

The use of different outgroups also affected the outcome of phylogenetic analyses. The results show that incorporating only *Colobus* in the parsimony tests produced more successful results in terms of number of molecular clades recovered as shown from the success indices computed in Table 5-6 (S_O=0.88). The next-best results were obtained using *Papio* (S_O=0.75) and then all three outgroups together (S_O=0.71). *Cercopithecus* produced the lowest number of molecular clades (S_O=0.63). The African ape and human trichotomy was the clade most often recovered in the bootstrap analyses (Figure 5-9) but the relationships among its component taxa (*Gorilla*, *Pan* and *Homo*) were never resolved. The great ape and human clade also appeared frequently in the bootstrap consensus cladograms.

That outgroup choice affects the result of cladistic analysis has been noted before by some authors (Colless, 1985; Kitching et al., 1998; Masters and Brothers, 2002). Masters and Brothers (2002) reported that the topology found in a cladistic analysis of 21 galagonid species using 36 parsimony informative craniodental characters varied with outgroup composition. The trees produced when lorises were adopted as outgroups differed from those produced using cheirogaleids; these two solutions also differed from the cladogram obtained when both outgroups were included in the analyses at the same time.

More recently, Nadal-Roberts and Collard (2005) investigated whether outgroup choice may have affected the analyses carried out by Collard and Wood (2000) and,

8.2.2 Outgroup choice

The use of different outgroups also affected the outcome of phylogenetic analyses. The results show that incorporating only *Colobus* in the parsimony tests produced more successful results in terms of number of molecular clades recovered as shown from the success indices computed in Table 5-6 (S_O=0.88). The next-best results were obtained using *Papio* (S_O=0.75) and then all three outgroups together (S_O=0.71). *Cercopithecus* produced the lowest number of molecular clades (S_O=0.63). The African ape and human trichotomy was the clade most often recovered in the bootstrap analyses (Figure 5-9) but the relationships among its component taxa (*Gorilla*, *Pan* and *Homo*) were never resolved. The great ape and human clade also appeared frequently in the bootstrap consensus cladograms.

That outgroup choice affects the result of cladistic analysis has been noted before by some authors (Colless, 1985; Kitching et al., 1998; Masters and Brothers, 2002). Masters and Brothers (2002) reported that the topology found in a cladistic analysis of 21 galagonid species using 36 parsimony informative craniodental characters varied with outgroup composition. The trees produced when lorises were adopted as outgroups differed from those produced using cheirogaleids; these two solutions also differed from the cladogram obtained when both outgroups were included in the analyses at the same time.

More recently, Nadal-Roberts and Collard (2005) investigated whether outgroup choice may have affected the analyses carried out by Collard and Wood (2000) and,

consequently, their conclusion that hominoid craniodental characters are not reliable for phylogenetic inference. Collard and Wood only employed one outgroup in their analyses, *Colobus*. Nadal-Roberts and Collard used two different outgroups, *Papio* and *Colobus*, in a cladistic analysis of 76 craniometric traits recorded on *Gorilla*, *Homo*, *Pan* and *Pongo*. Initially, they carried out parsimony and bootstrap tests including only *Colobus* in their analyses. The most parsimonious tree recovered in this case placed *Gorilla*, *Pan* and *Pongo* in a monophyletic group to the exclusion of *Homo*. *Pan* appeared as the sister taxon of a clade that included *Gorilla* and *Pongo*. Subsequently, they removed *Colobus* from the dataset and added *Papio*. The most parsimonious tree recovered in this case was identical to the one produced using *Colobus*. The bootstrap consensus cladograms produced in the two experiments were also identical. A clade formed by *Gorilla*, *Pan* and *Pongo* received some statistical support when using both *Colobus* and *Papio* (70% and 74% respectively). Nadal-Roberts and Collard concluded that using different outgroups did not affect the results of their phylogenetic analyses. Therefore, the results of Collard and Wood (2000), were also unlikely to have been affected by the choice of the outgroup.

Nadal-Roberts and Collard then carried out an additional analysis in which both *Colobus* and *Papio* were included simultaneously in the parsimony and bootstrap tests. The MPT recovered in this case differed from the one found in the previous two analyses. *Gorilla* appeared next to a clade that included *Homo*, *Pan* and *Pongo*, while *Pongo* was the sister taxon of a clade formed by *Homo* and *Pan*. The bootstrap analysis did not find any significant clade. These results are consistent with the results of the analyses based on nerve- and vessel-related characters and demonstrate that

outgroup composition can effectively alter the topology of the most parsimonious solutions and the bootstrap support for a particular clade.

Colless (1985) pointed out that differences in results in parsimony analyses using different outgroups are due to character incompatibility. In other words, different outgroups will contain a number of character states that define clades inconsistent with each other, resulting in different most parsimonious topologies. He recommended that a number of taxa, or groups of taxa, should be used as outgroups and then a consensus of the results should be drawn. With this suggestion in mind, I constructed a strict consensus tree from the cladograms produced by each outgroup, organised by coding method. These are illustrated in Figure 8-4.

The strict consensus tree generated from the datasets coded using the divergence method, features a trichotomy formed by *Gorilla, Homo* and *Pan*. This clade is then joined by *Pongo*, while *Hylobates* is placed at the base of the tree (Figure 8-4a). The strict consensus tree built from the datasets coded using the binary method also contains an African ape and human trichotomy. However, this tree cannot resolve the position of *Pongo* and *Hylobates* (Figure 8-4b). The same topology is obtained when Baum's coding procedure is adopted (Figure 8-4c). Lastly, the MPTs generated using the segment method produced a strict consensus tree that presented a great ape and human clade but the relationships within the latter were unresolved. *Hylobates* was the basal taxon (Figure 8-4d).

These consensus trees are consistent with the hominoid molecular phylogeny although, as discussed in the previous section, the level of resolution of the tree

depends on the coding method. Once again, the best result is obtained from the datasets coded using the divergence method.

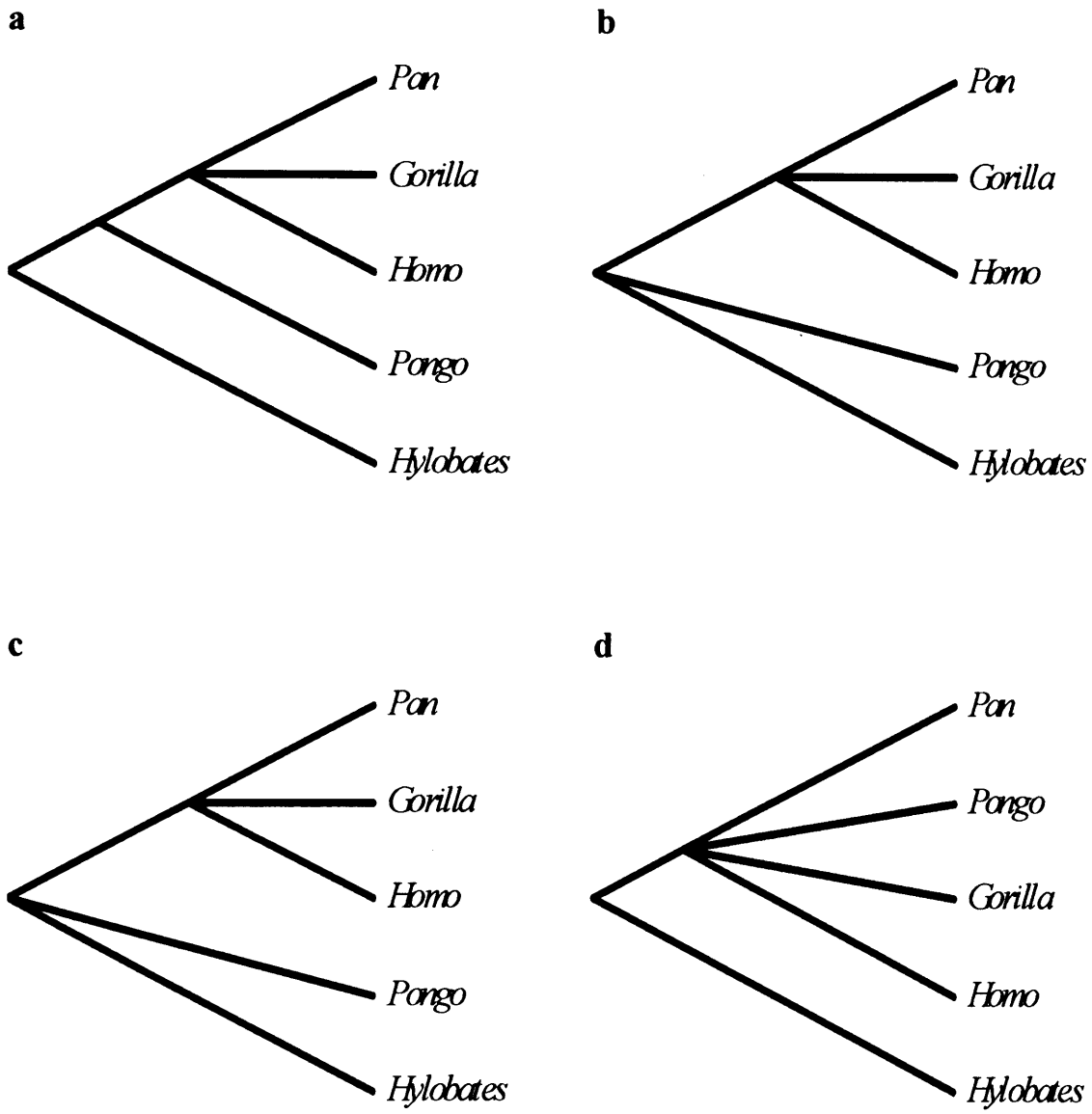

Figure 8-4. Strict consensus trees from analyses that used different outgroups. Strict consensus trees were generated from datasets coded using different outgroups and different coding methods: (a) divergence, (b) binary, (c) Baum and (d) segment methods.

8.2.3 Taxonomic level

When the genus *Pan* and the genus *Hylobates* were replaced by their component species, all of the hominoid molecular clades were recovered in only one case out of 16. In this test *Papio* was the only cercopithecine taxon included in the outgroup and the data were coded using the segment method. Therefore the hypothesis that cranial characters related to nerves and vessels are reliable for phylogenetic analysis at the specific level was not supported by the parsimony analyses. The bootstrap consensus cladograms were never fully resolved but they were always consistent with the consensus molecular phylogeny. As in the analyses carried out at the generic level, the most stable clades were the African ape and human clade, and the great ape and human clade. Hence, the bootstrap tests supported the hypothesis that nerve- and vessel-related traits are phylogenetically informative.

Overall, in this case too, the results seem to indicate that although nerve- and vessel-related osseous characters are not a panacea, they may be a better focus for phylogenetic studies of hominoid relationships than standard craniometric characters.

The adoption of a different taxonomic level had an effect on the results of the phylogenetic analysis in terms of the efficiency of the outgroup and coding methods in recovering the molecular clades. When species were introduced in the tests, the relative performance of outgroups and coding methods changed compared to when genera were analysed. On average the highest rate of success was scored when *Cercopithecus* was the outgroup taxon included in the analyses (S_O= 0.79), followed by *Papio* (S_O= 0.75) and *Colobus* (S_O= 0.67). The worst results were produced when

all three cercopithecine taxa were included in the outgroup (S_O=0.66). In terms of coding methods, the best performance occurred with the segment (S_O= 0.81) and the divergence coding (S_O= 0.77), followed by Baum's (S_O= 0.73). The binary method scored the worst success index (S_O= 0.55).

Working on a different taxonomic level also changed the conditions under which the analyses were more successful at recovering the molecular relationships. For example, at the generic level, *Colobus* was the outgroup that performed better in the tests, whereas here it is *Cercopithecus.* Interestingly, *Colobus* has the second-lowest success index in the analyses at the species level, a position occupied by *Cercopithecus* in the analyses at the generic level. Therefore, no clear guideline emerges from these results, on which should be the favourite outgroup used. In terms of coding methods, like in the analyses at the generic level, the segment and divergence methods outperform the binary and Baum's methods, although in this case the best results are produced by segment coding. As explained previously, the segment method and the divergence method stand out as superior to the other two coding methods, which is to be expected considering they are the two most rigorous methods.

Interestingly, in these sets of analyses too, bootstrapping always generated consensus trees that are consistent with the molecular phylogeny for the hominoids, reconciling the disparate results obtained from the parsimony tests.

8.3 Sexual dimorphism and homoplasy

Another important finding of this study is that sexual dimorphism plays an important role in the outcome of the phylogenetic analyses. When cladistic analyses were carried out on sex-specific datasets, the cladograms generated from the male-specific datasets were never identical to the cladograms generated from the female-specific datasets (Table 7-15). Female-specific datasets consistently outperformed male-specific datasets in the parsimony analyses in terms of both the number of times the whole consensus molecular cladogram was recovered, and the success rate in the recovery of molecular clades (S_O and S_C indices, Table 7-16). These results suggest that female-specific datasets are better at recovering the phylogenetic relationships of the hominoids than male-specific datasets, and that male specimens introduce a higher level of homoplasy in the data.

These findings are partly consistent with another recent study. Lycett and Collard (2005) investigated whether sexual dimorphism was a confounding factor in a series of analyses aimed at testing the homoiology hypothesis using papionins as the study group. In order to do this, they compared the results of analyses from a mixed-sex sample with the results of analyses from sex-specific samples. They found that sexual dimorphism did not confound their conclusions and their sex-specific results, like the mixed-sex results, contradicted the homoiology hypothesis. However, a close inspection of the most parsimonious cladograms recovered in their analyses reveals that the topologies of the shortest solutions were affected by this exercise to various degrees. A number of notable differences are present in the results of the male-specific, the female-specific and mixed-sex analyses. For example, the mixed-sex

low-to-moderate strain tree of Lycett and Collard (2005, Figure 3) places *Mandrillus* next to a clade that comprises *Papio* and *Theropithecus*. This group is then joined, in order, by *Cercocebus*, *Colobus* and *Macaca*. *Cercopithecus* and *Lophocebus* are equally distant from the other taxa and their relative position is not resolved. The female low-to-moderate-strain tree differs from the previous one in placing *Lophocebus* as the sister taxon of a clade formed by *Colobus*, *Cercocebus*, *Mandrillus*, *Papio* and *Theropithecus* instead of *Macaca*. The male low-to-moderate-strain tree differs from the mixed-sex equivalent in placing *Mandrillus* and *Papio* in a clade next to *Theropithecus*. These differences also indicate that male and female datasets can yield different phylogenetic hypotheses for the papionins. However, none of the trees generated in Lycett and Collard's tests was consistent with the consensus molecular phylogeny for the papionins, not even the female-specific cladograms. This is important because it suggests that, although sexual dimorphism may affect the results of phylogenetic reconstructions, it is not the only source of homoplasy and, in this case, not a major cause of error.

Table 8-1. Body size dimorphism in hominoid primates.

Species	Females	Males	Δ
Homo sapiens	46.5	53.5	7.0
Pongo pygmaeus	36.8	69.8	33.0
Gorilla gorilla	84.4	163.6	79.2
Pan troglodytes	35.7	44.0	8.3
Pan paniscus	33.0	41.5	8.5
Hylobates syndactylus	10.6	10.9	0.3
Hylobates lar	5.3	5.7	0.4

Mean body weights (kg) are reported for female and male samples of hominoid species (data from Creel, 1986). Δ=absolute difference between female and male weight.

Dimorphism is not a simple phenomenon. Sexual dimorphism is evident in many primate groups mainly in the form of body size dimorphism. Body size dimorphism is very strong in gorillas and orangutans, relatively weak in chimpanzees and humans, and minimal in *Hylobates* (Table 8-1). Recently, Plavcan (2002) reported a quantitative study of primate sexual dimorphism. He made several important observations. First, skull and jaw dimorphism increases with increasing body mass dimorphism, although this correlation is not a simple one. For example, while some species with low body mass dimorphism show a low number of significant differences between the sexes in craniofacial dimensions, others show numerous significant differences. Second, the most dimorphic regions of the primates skull are the face and the areas of muscle attachments, while the least dimorphic regions are the orbits, the cranial vault and the neurocranium. Third, the amount of craniofacial dimorphism is variable within species and this variation increases with increasing body size dimorphism. Plavcan also found that patterns of sexual dimorphism can vary considerably between species although closely related species tend to possess similar patterns of dimorphism.

Body size controls the expression of non-metric, quasi-continuous characters (Berry, 1967; Berry and Berry, 1971; Thoma, 1981). As discussed in Chapter 2, the expression of these traits is thought to be the result of a number of alleles at different loci acting additively. These alleles control an underlying continuous variable that is expressed only if it reaches a threshold value; below this critical value the trait is not expressed. This threshold value varies with age, sex and body size (Berry and Berry, 1971; Hauser and De Stefano, 1989). Therefore body size dimorphism may be related to the differential expression of nerve- and vessel-related characters in males and

females in strongly dimorphic species. From these considerations, it can be predicted that the groups with the highest degree of body size dimorphism (i.e. *Pongo* and *Gorilla*) will exhibit the highest level of skeletal dimorphism in nerve- and vessel-related traits. A comparison between males and females (Chapter 4, Table 4-6) showed that the group with the highest number of dimorphic traits is *Hylobates* (17 characters), the taxon with the least amount of body size dimorphism, followed by *Gorilla* (13 characters) and *Pan* (11 characters). *Pongo* has the lowest number of sexually dimorphic traits (3 characters). Orangutans display a high level of body size dimorphism among the hominoids and, for this reason, they would be expected to show a high level of dimorphism in these traits. Therefore, consistent with Plavcan's (2002) findings, the dimorphic expression of discrete variables does not necessarily correlate with body size dimorphism. The implications of these results for hominin phylogenetic studies are discussed below.

8.4 Non-phylogenetic character correlation

Morphological characters may be correlated for two reasons: logical and biological (Sneath and Sokal, 1973). Logical reasons are the ones arising from the way we define the characters themselves and can be avoided with a cautious selection of characters. Biological reasons include phylogeny, function, development and structure. Cladistic analysis relies on the presence of character correlations due to phylogenetic relationships (Nadal-Roberts and Collard, 2005). However, when character evolution is correlated for reasons other than phylogeny, changes in one character depend on conditions of another character (O'Keefe and Wagner, 2001). This is problematic because if two characters are not independent they may be the

expression of a single, underlying biological process, which then becomes the unit to account for in the phylogenetic analysis. Including both traits in a cladistic analysis would bias the analysis by over-representing the phylogenetically informative process. A recent simulation study has shown that when correlated characters are present in a dataset the tree topologies are less accurate and bootstrap values are inflated (O'Keefe and Wagner, 2001). Characters in cladistic analyses and other phylogenetic methods are assumed to be independent units of phylogenetic information (Kluge, 1989) – i.e. cladistic characters evolve independently of each other and are acquired independently of each other – despite the fact that theories in developmental, functional, architectural and molecular biology predict that correlated evolution should be a common phenomenon (Lovejoy et al., 1999, 2002; McCollum, 1999; McCollum and Sharpe, 2001; O'Keefe and Wagner, 2001).

Morphological integration is the principle that anatomical features can be so functionally, structurally, or developmentally related to each other that they essentially evolve as a unit (McCollum, 1999; Lovejoy et al., 1999, 2002; McCollum and Sharpe, 2001; Strait, 2001; Nadal-Roberts and Collard, 2005). Strait (2001) studied morphological integration in features of the catarrhine basicranium using multivariate statistical analyses. He found that the level of morphological integration was much lower then expected based only on functional interpretations of the hominid basicranium. Even so, when he generated phylogenetic hypotheses for the hominids correcting for morphological integration the trees produced differed from the ones generated when integration was not accounted for. This shows that non-phylogenetic character correlation affects the outcome of phylogenetic analysis and it is therefore a source of homoplasy in phylogenetic reconstruction. However, Strait (2001: 294) also

pointed out that "the concept of integration should be used in phylogenetic analysis only if hypotheses of integration can be adequately tested". Independence should be assumed if such tests cannot be performed, until shown otherwise.

Patterns of integration within one or a few taxa are not necessarily observed within a whole clade. Integration is relevant to phylogenetic analysis only if patterns of integrations are expressed across taxa (Strait, 2001). In other words if a group of traits evolves as a complex within species but independently among species then the characters should be considered phylogenetically independent.

McCollum (1999) has recently argued that most of the 20 traits commonly identified as synapomorphies of the paranthropines are in fact developmental by-products of possessing a large postcanine dentition and a small anterior dentition. She used facial growth models to demonstrate that this suite of characters are morphologically integrated and on this basis she concluded that despite the morphological similarities among the robust australopithecines, their phylogenetic relationships cannot be considered resolved. This concept was also employed by Lovejoy et al. (1999; 2002) who argued that current cladistic methods are unable to resolve the phylogeny of the hominins because the traits used to recover phylogenies do not include information on the morphogenesis of skeletal forms. Instead, hominid datasets rely on large lists of traits that are incorrectly assumed to be separately heritable simply because they can be separately observed and analysed. This process results in the atomisation of morphologies into suites of developmentally and functionally correlated characters (Lovejoy et al., 1999; 2002).

In this study, non-phylogenetic correlations were analysed using the procedure outlined by Nadal-Roberts and Collard (2005). If two traits were statistically correlated in all of the eight taxa then it was assumed that the evolution of the two traits was not independent and the character that correlated with the greatest number of other traits was excluded from the analysis. This technique finds support in Strait (2001) who, in a study of morphological integration in the primate basicranium, found a good agreement between the results of similar intraspecific comparisons using bivariate correlations and the results of multivariate factor analysis. Nadal-Roberts and Collard carried out a series of pairwise correlations on a dataset of metric variables calculating Pearson's correlation coefficient and estimating its statistical significance. If a correlation between any two traits was significant ($p<0.05$) in each taxon then they assumed that the traits were not independent and excluded the one that was correlated with the greatest number of characters. They found that 30 characters needed to be removed out of the 72 included in their study. Removing these traits did not affect the results of phylogenetic analysis and the tree produced in the correlation-corrected analyses was the same as the one produced in the analysis not corrected for correlations. The only effect was in the bootstrap analysis, in which no clade was recovered from the correlation adjusted dataset at the 70% confidence level. They concluded that ignoring non-phylogenetic character correlations has little impact on the assessment of utility of craniodental character in phylogenetic analysis.

Statistical correlations among characters were assessed in the first part of this study (section 4.3.4) using Pearson's correlation coefficient for metric variables and index variables that followed a normal distribution (11 variables), the non-parametric Spearman's rank correlation coefficient for index variables that did not follow a

normal distribution (one variable) and 2x2 chi-square tests for non-metric variables (91 variables). Due to the nature of the non-metric traits (nominal/binary), it was not possible to evaluate correlations between metric and non-metric variables. In fact, the techniques that mix these types of data require the non-metric variables to be of at least an ordinal scale. The results of this analysis showed that the amount of non-phylogenetic correlation in the dataset was relatively low (Table 4-7). Among the metric variables, only one correlation was significant in all taxa simultaneously. This was between the minimum and transverse distances of the infraorbital foramen to the zygomaxillary suture ($IOFP_2$, $IOFP_3$). Among the non-metric variables, the bivariate correlations were never significant in all taxa at the same time. However, in 14 cases correlations could not be computed because the variables were constant in all taxa and therefore correlations were not meaningful.

In order to investigate how character correlation affected the phylogenetic results, I carried out two analyses excluding 15 characters. Of the two metric characters that showed a significant correlation, $IOFP_2$ was correlated to other variables 37 times, while $IOFP_3$ was correlated to other variables 33 times. Therefore, following Nadal-Roberts and Collard (2005), I excluded $IOFP_2$ from the analysis. I also excluded the 14 non-metric characters for which correlations could not be computed (15-$ZTFP_1$a, 19-ZOFPa, 25-FRo, 35-SMFP, 38-PaF_3, 40-$CaCP_2$, 66-CoCO, 71-MBC, 75-$FMaP_1$, 83-RAC_2, 94-RoC, 95-MyB, 101-PFn, 112-SGB). I selected one dataset that had yielded the complete molecular topology in the previous round of analyses, and one dataset that returned the least number of molecular clades. The first featured *Papio* as the only outgroup in the dataset and the divergence method as the coding procedure

used. The second analysis featured *Papio* as the only outgroup taxon and Baum's as the coding method.

The first cladogram obtained when the 15 characters were excluded from the analyses was the same as the one produced when all the characters were included in the analyses. The branch-and-bound search returned one single MPT that was identical to the hominoid molecular cladogram (Figure 8-5a). The topologies of the consensus bootstrap cladograms were also comparable although the bootstrap values differed slightly, being overall lower when the correlated characters were excluded (Figure 8-5b). This is not surprising considering that bootstrap values increase with the number of characters included in the analysis. The second analysis produced a MPT that was not identical to the one obtained when all the characters were included in the analysis (Figure 8-5c). The phylogenetic hypothesis produced in the original analysis did not agree with the consensus molecular phylogeny (Figure 5-3c). Rather, it supported *Gorilla* and *Homo* as sister taxa to the exclusion of *Pan*, and placed *Hylobates* – rather than *Pongo* – as the sister group of the African apes and humans. When the correlated characters were excluded, the MPT featured a (*Pan*, *Homo*) clade next to *Gorilla*. The African apes and humans were joined by *Hylobates* and then *Pongo*. The bootstrap tree in the original analysis featured one molecular clade: the African ape and human clade. It also featured a weakly supported (71%) clade that disagreed with the molecular phylogeny and comprised the African ape and humans and *Hylobates*. When the correlated characters were excluded the false-clade did not find any support in the bootstrap analysis. Only the African ape and human clade was recovered (Figure 8-3d). This result can be explained by taking into consideration the reduction in the number of characters included in the analysis which affects the bootstrap value

of every clade. The false-clade was weakly supported in the original analysis. Excluding 15 characters lowered the bootstrap support to 69% which is just below the 70% confidence level.

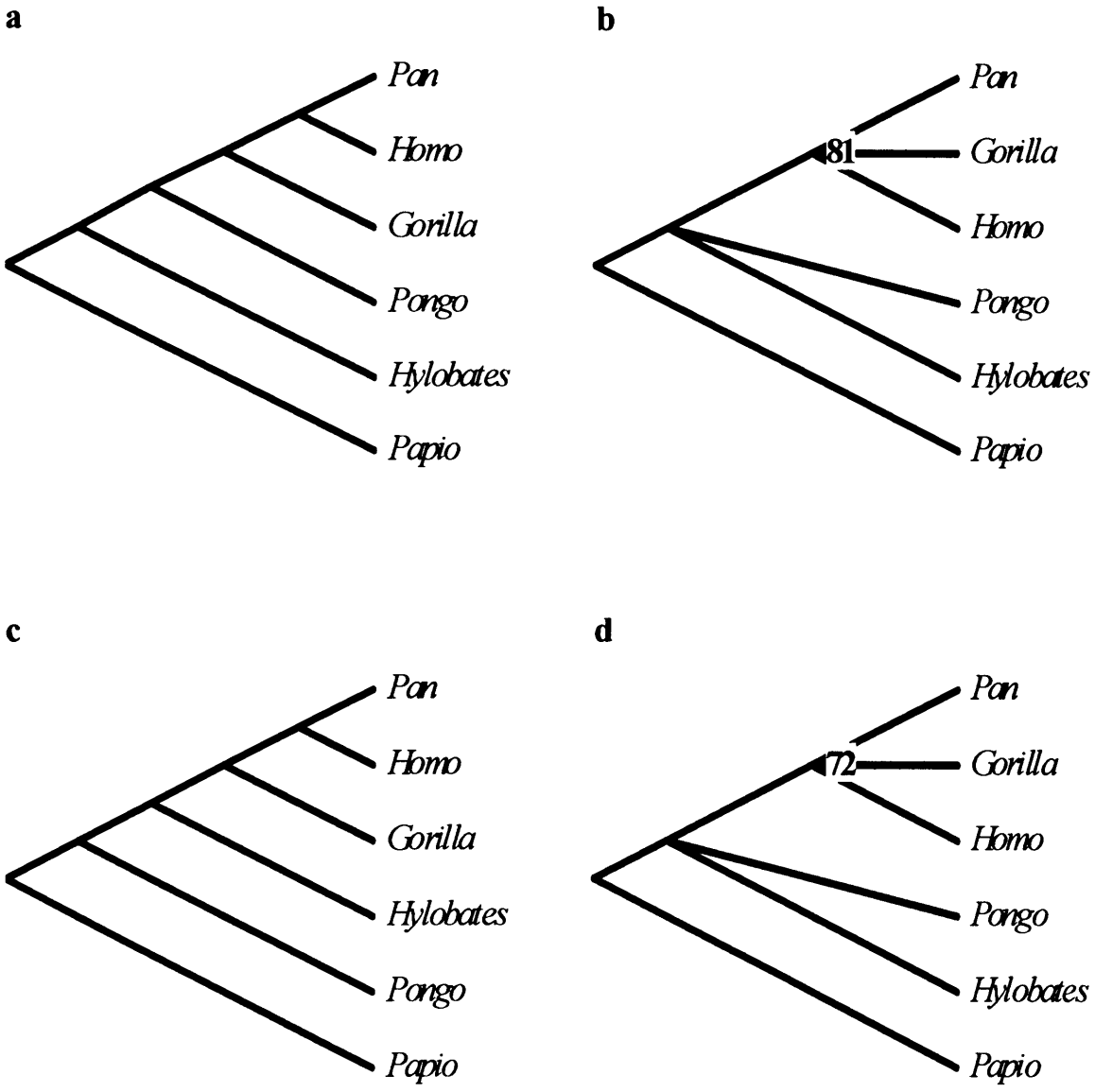

Figure 8-5. Non-phylogenetic character correlations.
Most parsimonious cladograms and bootstrap consensus cladograms generated when 15 characters, presumably correlated, were excluded from the analysis. Divergence coding (a,b) and Baum's coding (c,d).

In summary, the exclusion of the 15 non-independent characters moderately affected the cladistic analyses considered in this part of the study. The correlation-corrected datasets produced in one case the same most parsimonious tree as the non correlation-corrected dataset. In another case the correlation-corrected dataset yielded a MPT that supported a different phylogenetic hypothesis. Bootstrap analyses were affected in both tests. However, the results of the bootstrap analyses can be explained by simply taking into account the properties of the non-parametric bootstrap which is influenced by the number of characters included in the analysis. Hence, these findings indicate that non-phylogenetic character correlations may affect the results of phylogenetic studies based on nerve- and vessel-related characters.

8.5 Implications for hominin phylogenetic studies

The findings of this project have important implications for hominin evolutionary studies. Curnoe (2003) and Hawks (2004) have recently criticised hominin cladistic analyses on various grounds. They highlighted several problems that hamper the estimation of accurate phylogenetic relationships for the fossil hominins. Curnoe (2003) argued that the largest source of error in hominin cladistic analyses is the uncertainty over the number and composition of hominin species. This problem is superimposed on a number of methodological issues such as the choice of characters that are informative about phylogeny and independent of each other, the choice of 'suitable' outgroups and coding methods that do not rely on a priori assumptions of relationships, the use of parsimony as the criterion for choosing the best tree, and the treatment of within species variation. Similarly, Hawks (2004) stressed a number of problems in phylogenetic reconstruction that relate to the type of data and samples

commonly used in these analyses. He listed six obstacles to the estimation of reliable cladograms including 1) the small number of specimens in fossil hominin hypodigms, 2) the fragmentary nature of these specimens, 3) the close genetic affinities of the fossil taxa, 4) the poor definition of character states, 5) non-phylogenetic character correlations and 6) the poor understanding of the selective pressures that drive character evolution.

This study has emphasised a number of similar issues, especially the dependence of the results of phylogenetic reconstructions on the coding procedure adopted and on the outgroup chosen. The composition of the ingroup is also particularly problematic for fossil taxa because there is still a lot of controversy about the taxonomy of the hominins. This study also showed that sexual dimorphism may introduce a level of homoplasy in the data. The extent of the effects of non-phylogenetic correlations among characters in hominin cladistic analyses needs further evaluation. The results of this study are in line with the results of previous studies (Strait, 2001; Nadal-Roberts and Collard, 2005) that found character correlation to be a minor source of error in hominin phylogenetic estimates.

Cranial characters related to nerves and vessels seem to be more reliable for estimating hominoid phylogeny than standard craniodental data and therefore they may be a better focus for hominin phylogenetic reconstructions. However, these traits are very variable within the hominoid species and genera considered in the present study (Appendix III). This is problematic for the process of character coding because it makes it difficult to assign a taxon-specific character state to any of the taxa. In fact, the whole exercise of assigning a unique, present or absent state to a taxonomic unit is

dubious in the face of the observed polymorphisms. Unfortunately, however, this is the way recent cladistic studies treat within-species variation (Curnoe, 2003). For the fossil hominins, there is the additional problem of the inadequacy of the fossil record to thoroughly represent the morphological variation within each fossil taxon.

Related to this issue is the fact that discrete traits are likely to vary among closely related species only in relative frequency rather than in total presence or absence (Hawks, 2004). This is clearly reflected in the relative frequencies of occurrence of discrete traits among the extant hominoids. Closely related species like the fossil hominins are also likely to show similar patterns of polymorphisms and similar differences in the frequency values. The question of how to code for this variation in cladistic analysis becomes, then, of paramount importance. To account for it, a good sample size is necessary. The lack of adequate numbers of specimens in fossil hominin hypodigms does not allow a thorough appreciation of the morphological variation within each species.

The repercussions of these shortcomings of the fossil record on the techniques available are also clear. The divergence method used in this study outperformed all other coding methods in terms of number of molecular clades recovered and also in terms of bootstrap support for molecular clades. This coding method, however, is based on statistical techniques that require relatively large sample sizes and an accurate representation of the morphological variation in each taxon. The application of this method to hominin phylogenetic analyses is therefore implausible considering the poor qualities of these samples. Hawks (2004) showed that a majority-rule method (0 if <50%, 1 if >50%) for coding polymorphic characters performed better than other

coding methods in simulations of hominin cladistic analyses. This is because in a small sample a character that occurs in low frequency in a population is likely to be either present in low numbers or absent. A majority-rule method scores these as the same, reducing the potential introduction of homoplasy in the dataset. Although a majority method was not employed in this study, a modified version was created by lowering the presence/absent frequency threshold from 50% to 5%. The resulting binary coding method performed poorly in terms of internal consistency of the most parsimonious cladograms and in terms of the number of parsimony informative characters present in the datasets. However, as Hawks (2004) suggests, this may be the best option available in the case of small samples like those for the hominins. The results illustrated in Figure 8-4 show that the consensus cladograms generated for the results of the binary coded matrices using different outgroups is a cladogram consistent with the molecular phylogeny but with a poor resolution: only one clade was resolved, the African ape and human clade.

Another important point is that the differences between the trees generated from different outgroups, coding methods and ingroup composition were reconciled by the use of the bootstrap. Many studies of hominid phylogenetics have employed bootstrapping as a way of finding statistical support for clades (e.g. Lieberman et al., 1996; Collard and Wood, 1999, 2000, 2001; Gibbs et al., 2000, 2002; Cameron and Groves, 2004; Strait and Grine 2004). The results presented here indicate that this technique seems to be less affected by outgroup choice and coding procedure than parsimony analysis. The 70% consensus cladograms generated for the hominoids using characters related to nerves and vessels recovered clades consistent with each other and with the molecular cladogram. This is important because it suggests that

bootstrapping can be used as a way of 'correcting' for the noises introduced by methodological choices such as those described in this study. With this in mind, bootstrapping should become standard procedure in hominin phylogenetic analyses in order to assign a level of support of a dataset for a particular clade.

That is not to say that the results of bootstrap analyses necessarily produce accurate phylogenies. The results of the analyses carried out on the craniometric datasets show that bootstrap tests can still produce false-positive clades that are strongly supported (Figure 5-12). As discussed in Chapter 2, standard craniometric datasets contain large numbers of homoplastic characters (Collard and Wood, 2000; Masters and Brothers, 2002; Viguier, 2002) and this fact is a major source of inaccuracies in estimating tree branches.

Recent hominin cladistic studies yielded bootstrap consensus trees that were mostly unresolved. Cameron and Groves (2004) published the most extensive hominid cladistic study to date in terms of number of fossil groups included in the analysis. This analysis was based on 92 craniodental characters taken from the recent literature distributed through 16 fossil and four extant hominid taxa. The fossil groups included Miocene hominoid taxa (*Kenyapithecus*, *Dryopithecus*, *Graecopithecus* and *Sahelanthropus*) and Plio-Pleistocene hominin species belonging to the genera *Praeanthropus*, *Ardipithecus*, *Australopithecus*, *Kenyanthropus* and *Paranthropus*. The extant genera comprised *Homo*, *Pan*, *Gorilla* and *Pongo*. When this dataset was bootstrapped, only three clades were recovered at the 70% confidence level: the clade formed by *H. ergaster* and *H. sapiens* (88%), the clade formed by the three paranthropines species (91%) and, within the latter, the clade formed by *P. robustus*

and *P. boisei* (83%). Similarly, Strait and Grine (2004) produced a phylogeny based on 198 craniodental characters (including both traditional morphological traits and craniometric traits) recorded on a sample of 13 fossil – *Ar. ramidus*, *A. anamensis*, *A. africanus*, *A. garhi*, *Pr. afarensis*, *H. habilis*, *H. rudolfensis*, *H. ergaster*, *K. platyops*, *P. aethiopicus*, *P. robustus*, *P. boisei* and *S. tchadensis* – and 5 extant hominoid groups – *Homo*, *Pan*, *Gorilla*, *Pongo* and *Hylobates*. When only extant apes and humans were included in the tests, bootstrap analyses did not recover any significant clade at the 70% confidence level when all 198 characters were used. Two clades were recovered when craniometric characters were excluded from the analysis: a weakly supported clade formed by *G. gorilla* and *P. pygmaeus* (70%), and a strongly supported great ape and human clade (96%). When the fossil hominin taxa were incorporated in the analyses, only four clades were statistically significant at the 70% confidence level: a clade that comprised *H. ergaster* and *H. sapiens* (86%); the paranthropine clade (100%); a clade formed by *A. africanus*, *K. platyops*, the paranthropines and the *Homo* clade (85%); and finally the clade formed by the great apes and hominins (94%). The relationships among the other hominid taxa did not find any statistical support. Lastly, Finarelli and Clyde (2004) included 200 morphological (craniodental and postcranial) characters in a cladistic analysis for 13 fossil and 5 extant hominoid genera. The fossil groups encompassed taxa across the entire superfamily Hominoidea and not just the hominins (i.e. they also included Miocene apes, such as *Graecopithecus* and *Kenyapithecus*). The clades recovered were highly unstable and none of them found bootstrap support at the 70% confidence level.

As noted by Sanderson (1995), loss of resolution in a bootstrap tree is not in itself an undesirable event when homoplasy is present in a dataset, because it decreases the probability of Type II errors (accepting that a group is monophyletic when it is not). In other words, 'no clade' is better than a strongly supported 'false clade'. What the studies described above demonstrate is that very little is still known about hominin relationships and therefore current phylogenies for the hominins should be treated cautiously (Collard and Wood, 2000; Curnoe, 2003; Hawks, 2004).

Lastly, the final set of analyses showed that sexual dimorphism may play an important role in the reconstruction of hominoid relationships. The implications of this for hominin phylogenetics are significant. The pattern and degree of sexual dimorphism in fossil hominins is a longstanding debate in palaeoanthropology. The amount of dimorphism present in the hypodigm of hominin species is generally higher than the level observed in modern humans. Exact randomisation methods have shown that the fossils from Hadar, Maka and Laetoli, assigned to the species *Australopithecus afarensis*, display a range of sexual dimorphism in the jaws and limb bones that is at least as extreme as the ones observed in extant gorillas and orangutans (Richmond and Jungers, 1995). It has been proposed that this variation is in fact indicative of the presence of more than one species in the hypodigm of this taxon. A recent review of the fossils from Kanapoi and Allia Bay in Kenya, assigned to the species *Australopithecus anamensis*, also showed that the level of body size dimorphism present in this taxon is at least as high as that found in *A. afarensis* (Ward et al., 2001). Plio-Pleistocene hominins were more dimorphic than later species and a progressive decrease in the level of sexual dimorphism occurred in the human lineage (Frayer and Wolpoff, 1985). Even within the genus *Homo* earlier species were more

dimorphic than more recent ones. For example, early *Homo* species show a degree of sex differences intermediate between australopithecines and modern humans. Similarly, the morphology of the mandible of *H. heidelbergensis* from Atapuerca in Spain is considerably more dimorphic than that of modern humans (Rosas et al., 2002).

The high degree of sexual dimorphism in fossil taxa may thus become a confounding variable in cladistic analyses of the hominins. One of the problems, of course, is that the sex of the specimens recovered is often very difficult to assess in the hominin fossil record due to the poor preservation of many specimens.

8.6 Conclusion

Hominoid craniodental datasets often produce cladograms that are inconsistent with the consensus molecular phylogeny for this group of primates. The latter is highly supported and generally considered to be accurate. This is problematic for phylogenetic analyses of fossil taxa because these are largely based on this type of data. The aim of this project was to test the hypothesis that osseous characters related to nerves and vessels produce accurate phylogenies for the hominoids. For this purpose, parsimony and bootstrap tests were carried out on a dataset composed of this type of data. The cladograms produced were then compared to the consensus molecular phylogeny for the hominoids, which is widely considered to be accurate; they were also compared to cladograms obtained from a dataset of standard craniometric characters. The hypothesis was deemed to be supported if the trees

yielded by the nerve- and vessel-related dataset were compatible with the molecular tree. The results showed that unlike standard craniodental characters, nerve- and vessel-related traits generate strongly supported clades that are more consistent with the hominoid molecular phylogeny. Overall, the results indicated that cranial characters related to nerves and vessels may be a better focus for hominoid phylogenetic studies than standard craniodental characters. I concur with Hawks (2004) when he states that a major problem in hominin cladistics is the lack of suitable samples to subject to character analysis before the application of parsimony analysis. Character analysis is the "detailed decision-making process that determines which characters are important enough to include, how they should be scored [...], whether they are correlated [...], and so on" (Hawks, 2004: 216). My ability to carry out a thorough character analysis in this study was strongly due to the availability of large samples for extant hominoids.

Three other important findings also emerged from this project. First, cladistic analyses are strongly influenced by methodological choices such as coding method, outgroup selection and taxonomic level. Parsimony analyses yielded minimum-length trees that differed considerably from each other depending on these parameters. In terms of outgroup choice, this study supports Colless' (1989) view that a number of taxa, or groups of taxa, should be used as outgroups and then a consensus of the results should be produced. In terms of coding methods, procedures that are conceptually sound, such as the segment and the divergence methods, always outperformed less rigorous methods, such as the binary and Baum's methods. Thus, whenever possible the former procedures should be the preferred choice.

A major point of interest is the fact that bootstrap tests were less affected than parsimony tests by the methodological issues described above and produced consensus cladograms that were consistent with each other and with the well-supported molecular phylogeny for the hominoids. This is important because if bootstrapping overcomes the problems associated with methodological choices, then this technique should become a standard practise in hominin phylogenetic studies. Relying on bootstrapped phylogenies may come with the cost of obtaining only partially resolved cladograms. However, keeping in mind that the generation of reliable phylogenetic hypotheses is crucial for comparative studies and for understanding adaptation, a partially resolved cladogram is more desirable than a strongly supported, inaccurate cladogram.

Second, sexual dimorphism seems to introduce some level of homoplasy in the datasets. This is problematic for the hominin fossil record because fossil species display an amount of sexual dimorphism at least as high as extant hominoids. Interestingly, analyses based solely on female specimens were considerably more successful at recovering the correct phylogeny for the hominoids than analyses based only on male specimens. If this holds for the fossil hominins too, then analyses based only on female specimens should be preferred to mixed-sex analyses. The caveat here is that sexing fossil specimens is not always straight-forward due to the fragmentary nature of the material.

Third, non-phylogenetic character correlations appear to be a source of error in the recovery of hominoid phylogenetic hypotheses. However, the shortcomings of the statistical techniques available for studying correlations among metric and discrete

variables do not allow a confident assessment of the extent of this phenomenon and its impact on phylogenetic analyses. This study supports Collard and Wood (2001:170) contention that "too little is known about the issue of character correlation at the moment to use it as a justification for abandoning the use of multiple craniodental characters in cladistic analyses of hominins and other primates". The development of techniques for detecting correlated evolution in mixed (i.e. continuous and discrete) datasets should be viewed as an important area of future research.

This study showed that soft-tissue linked cranial characters are more reliable for recovering the phylogenetic relationships of extant hominoids than standard craniodental traits. It follows that these characters should be a better focus for studies of hominin phylogeny than standard craniodental traits.

BIBLIOGRAPHY

Ackermann, R. R. and Cheverud, J.M., 2002. Discerning evolutionary processes in patterns of tamarin (genus *Saguinus*) craniofacial variation. American Journal of Physical Anthropology 117, 260-271.

Aiello, L.C., 1992. Allometry and the analysis of size and shape in human evolution. Journal of Human Evolution 22, 127-147.

Aiello, L. and Collard, M., 2001. Our newest oldest ancestor? Nature 410, 526-527.

Anderson, J.E., 1967. Skeletal anomalies as genetic indicators. In: Brothwell, D.R. (Ed.), Skeletal Biology of Earlier Human Populations. Pergamon Press, London, pp. 135-147.

Andrews, P. and Cronin, J.E., 1982. The relationships of *Sivapithecus* and *Ramapithecus* and the evolution of the orangutan. Nature 297, 541-546.

Andrews, P. and Martin, L., 1987. Cladistic relationships of extant and fossil hominoids. Journal of Human Evolution 16, 101-118.

Andrews, P., 1985. Family group systematics and evolution among catarrhine primates. In: Delson, E. (Ed.) Ancestors: the Hard Evidence. Alan R. Liss, New York, pp. 14-22.

Andrews, P., 1987. Aspects of hominoid phylogeny. In: Patterson, C. (Ed.), Molecules and Morphology in Evolution: Conflict or Compromise? Cambridge University Press, Cambridge, pp. 23-53.

Andrews, P., 1988. A phylogenetic analysis of the Primates. In: Benton, M. (Ed.), The Phylogeny and Classification of the Tetrapods: Mammals. Volume 2. Clarendon Press, Oxford, pp. 143-175.

Andrews, P., 1992. Evolution and environment in the Hominoidea. Nature 360, 641-646.

Ansorge, H., 2001. Assessing non-metric skeleton characters as a morphological tool. Zoology 104, 268-277.

Archie, J.W., 1985. Methods for coding variable morphological features for numerical taxonomic analysis. Systematic Zoology 34, 326-345.

Asfaw, B., White, T., Lovejoy, O., Latimer, B., Simpson, S. and Suwa, G., 1999. *Australopithecus garhi*: A new species of early hominid from Ethiopia. Science 284, 629-635.

Ashlock, P.D., 1974. The uses of cladistics. Annual Review of Ecology and Systematics 5, 81-99.

Ashton, E.H. and Zuckerman, S., 1950. The infraorbital foramen in the hominoidea. Proceedings of the Zoological Society of London 131, 471-485.

Bailey, W.J., Hayasaka, K., Skinner, C.G., Kehoe, S., Sieu, L.C., Slightom, J.L. and Goodman, M., 1992. Re-examination of the African hominoid trichotomy with additional sequences from the primate β-globin gene cluster. Molecular Phylogenetics and Evolution 1, 97-135.

Banks, S.J. and Collard, M., 2004. Reconstructing human behavioural evolution through phylogenetic analyses of extant hominoid behaviour. American Journal of Physical Anthropology 123 (S38), 59. Abstract.

Barriel, V., 1994. Les relations de parenté au sein des Hominoidea et la place de *Pan paniscus*: comparaison et analyse méthodologique des phylogénies morphologiques et moleculaires. Ph.D. Dissertation, University of Bordeaux I.

Barriel, V., 1997. *Pan paniscus* and hominoid phylogeny: morphological data, molecular data and total evidence. Folia Primatologica 68, 50-56.

Barriel, V., Darlu, P. and Tassy, O., 1993. Mammalian phylogeny and conflicts between morphological and molecular data. Annales des Sciences Naturelles. 12ème Serie. Zoologie et Biologie Animale 14, 157-171.

Baum, B.R., 1988. A simple procedure for establishing discrete characters from measurement data, applicable to cladistics. Taxon 37, 63-70.

Begun, D.R., 1992. Miocene fossil hominids and the chimp-human clade. Science 257, 1929-1933.

Begun, D.R., 1994. Relations among the great apes and humans: new interpretations based on the fossil great ape *Dryopithecus*. Yearbook of Physical Anthropology 37, 11-64.

Begun, D.R., Ward, C.V. and Rose, M.D., 1997. Events in hominoid evolution. In: Begun, D.R., Ward, C.V., Rose, M.D. (Eds.), Function, Phylogeny and Fossils: Miocene Hominoid Evolution and Adaptations. Plenum Press, New York, pp. 389-415.

Benefit, B.R. and McCrossin, M.L., 1997. Earliest known Old World monkey skull. Nature 388, 368-371.

Benfer, R.A., 1970. Associations among cranial traits. American Journal of Physical Anthropology 32, 463-464.

Benveniste, R.E. and Todaro, G.J., 1976. Evolution of type C viral genes: evidence for an Asian origin of man. Nature 261, 101-108.

Berge, J.K. and Bergman, R.A., 2001. Variations in size and in symmetry of foramina of the human skull. Clinical Anatomy 14, 406-413.

Bermúdez de Castro, J.M., Arsuaga, J.L., Carbonell, E., Rosas, A., Martínez, I. and Mosquera, M., 1997. A hominid from the Lower Pleistocene of Atapuerca, Spain: possible ancestor to Neandertals and modern humans. Science 276, 1392-1395.

Berry, A.C. and Berry, R.J., 1967. Epigenetic variation in the human cranium. Journal of Anatomy 10, 361-379.

Berry, A.C. and Berry, R.J., 1971. Epigenetic polymorphism in the primate skeleton. In: Chiarelli, A.B. (Ed.), Comparative Genetics in Monkeys, Apes and Humans. Academic Press, London, pp. 13-41.

Berry, R.J., 1967. The biology of non-metrical variation in mice and men. In: Brothwell, D.R. (Ed.), The Skeletal Biology of Earlier Human Populations. Pergamon Press, London or Oxford, pp. 103-133.

Boyd, G.I. 1934. The emissary foramina of the cranium in primates. Anatomy 69, 113-117.

Boyd, G.I., 1930. The emissary foramina of the cranium in man and the anthropoids. Anatomy 65, 108-121.

Braga, J. and Boesch, C., 1997a. Further data about venous channels in South African Plio-Pleistocene hominids. Journal of Human Evolution 33, 423-447.

Braga, J. and Boesch, C., 1997b. The "radiator" bias. A reply to Falk and Gage. Journal of Human Evolution 33, 503-506.

Braga, J., 1993. Ossification du processus styloide chez les Pongidés. Comptes Rendues de l'Académie des Sciences de Paris, t. 317, serie II, 273-277.

Braga, J., 1995. Définition de certains caractères discrets craniens chez *Pongo*, *Gorilla* et *Pan*. Perspectives taxonomiques et phylogénétiques. Ph.D. Dissertation, University of Bordeaux I.

Braga, J., 1996a. Emissary canals in the hominoidea and their phylogenetic significance. Folia Primatologica 65, 144-153.

Braga, J., 1996b. Nouvelles données sur l'insertion antérieure du septum nasal des grands singes africains. Applications en paléoanthropologie. Comptes Rendues de l'Académie des Sciences de Paris, t. 322, serie II, 1087-1092.

Braga, J., 2001. Cranial discrete variation in the great apes: new prospects in palaeoprimatology. In: De Bonis, L., Koufos, G.D., Andrews, P. (Eds.), Hominoid Evolution and Climatic Change in Europe. Volume 2. Phylogeny of the Neogene Hominoid Primates of Eurasia. Cambridge University Press, Cambridge, pp. 151-190.

Brown, P., Sutikna, T., Morwood, M. J. et al., 2004. A new small-bodied hominin from the Late Pleistocene of Flores, Indonesia. Nature 431, 1055-1061.

Brown, W.M., Prager, E.M., Wang, A. and Wilson, A.C., 1982. Mitochondrial DNA sequences of primates: tempo and mode of evolution. Journal of Molecular Evolution 18, 225-239.

Brunet, M., Guy, F., Pilbeam, D. et al., 2002. A new hominid from the Upper Miocene of Chad, Central Africa. Nature 418, 145-151.

Butynski, T.M., 2002. The guenons: an overview of diversity and taxonomy. In: Glenn, M.E., Cords, M. (Eds.), The Guenons. Diversity and Adaptation in African Monkeys. Kluwer Academic/Plenum Publishers, pp. 3-13.

Caccone, A. and Powell, J.R., 1989. DNA divergence among hominoids. Evolution 43, 925-942.

Cameron, D.W. and Groves, C.P., 2004. Bones, Stones and Molecules: Out of Africa and Human Origins. Elsevier Academic Press.

Cela-Conde, C.J. and Altaba, C.R., 2002. Multiplying genera versus moving species: a new taxonomic proposal for the family Hominidae. South African Journal of Science 98, 229-232.

Chamberlain, A.T. and Wood, B.A., 1987. Early hominid phylogeny. Journal of Human Evolution 16, 119-133.

Ciochon, R., 1983. Hominoid cladistics and the ancestry of modern apes and humans: a summary statement. In: Ciochon, R., Corruccini, R.S. (Eds.), New Interpretations of Ape and Human Ancestry. Plenum Press, New York, pp. 783-843.

Clark, C. and Curran, D.J.,1986. Outgroup analysis, homoplasy, and global parsimony: a response to Maddison, Donoghue, and Maddison. Systematic Zoology 35, 422-426.

Collard M., Gibbs S. and Wood B.A., 2001. Phylogenetic utility of higher primate postcranial morphology. American Journal of Physical Anthropology 32 (Supplement), 52.

Collard, M. and Aiello, L.C., 2000. From forelimbs to two legs. Nature 404, 339-340.

Collard, M. and Elton, S., 2002. Phylogenetic utility of papionin postcranial morphology. American Journal of Physical Anthropology 34 (Supplement), 56. Abstract.

Collard, M. and O'Higgins, P., 2001. Ontogeny and homoplasy in the papionin monkey face. Evolution and Development 3, 322-331.

Collard, M. and Wood, B., 2001. Homoplasy and the early hominid masticatory system: inferences from analyses of extant hominoids and papionins. Journal of Human Evolution 41, 167-194.

Collard, M. and Wood, B.A., 2000. Reliability of craniodental evidence in fossil catarrhine phylogenetics. Proceedings of the National Academy of Science USA 96, 5003-5006.

Collard, M., 1998. Morphological evolution of the hominoids and papionins: Implications for palaeoanthropological cladistics. Ph.D. Dissertation, University of Liverpool.

Collard, M., Lieberman, D.E. and Wood, B.A. Hominid homoiology: an assessment of the impact of phenotypic plasticity on phylogenetic analyses of humans and their fossil relatives. Journal of Human Evolution, in press.

Colless, D.H., 1985. On the status of outgroups in phylogenetics. Systematic Zoology 34, 364-366.

Conte, R.A., Samonte, R.V. and Verma, R.S., 1998. Evolutionary divergence of the oncogenes GLI, HST and INT2. Heredity 81, 10-13.

Corruccini, R.S. and McHenry, H.M., 2001. Knuckle-walking hominid ancestors. Journal of Human Evolution 40, 507-511.

Corruccini, R.S., 1978. Comparative osteometrics of the hominoid wrist joint, with special reference to knuckle-walking. Journal of Human Evolution 7, 307-321.

Corruccini, R.S., 1992. Bootstrap approaches to estimating confidence intervals from molecular dissimilarities and resultant trees. Journal of Human Evolution 23, 481-493.

Corruccini, R.S., 1994. How certain are hominoid phylogenies? The role of confidence intervals in cladistics. In: Corruccini, R.S., Ciochon, R.L. (Eds.),

Integrative Approaches to the Past: Palaeoanthropological Advances in Honour of F. Clark Howell. Prentice Hall, Enselwood Cliffs, NT, pp. 167-183.

Creel, N., 1986. Size and phylogeny in hominoid primates. Systematic Zoology 35, 81-94.

Curnoe, D. and Thorne, A., 2003. Number of ancestral human species: a molecular perspective. Homo 53, 201-224.

Curnoe, D., 2001. Early *Homo* from southern Africa: a cladistic perspective. South African Journal of Science 97, 186-190.

Curnoe, D., 2003. Problems with the use of cladistic analysis in palaeoanthropology. Homo 53, 225-234.

Czelusniak, J., Goodman, M., 1995. Hominoid phylogeny estimated by model selection using goodness of fit significance tests. Molecular Phylogenetics and Evolution 4, 283-290.

Dainton, M. and Macho, G.A., 1999. Did knuckle walking evolve twice? Journal of Human Evolution 36, 171-194.

Deinard, A. and Kidd, K., 1999. Evolution of a HOXB6 intergenic region within the great apes and humans. Journal of Human Evolution 36, 687-703.

Deinard, A., Sirugo, G. and Kidd, K., 1998. Hominoid phylogeny: inferences from a sub-terminal minisatellite analysed by repeat expansion detection (RED). Journal of Human Evolution 35, 313-317.

Disotell, T.R., 2000. Molecular systematics of the Cercopithecidae. In: Whitehead, P.F., Jolly, C. (Eds.), Old World Monkeys. Cambridge University Press, pp. 29-56.

Djian, P. and Green, H., 1989. Vectorial expansion of the involucrin gene and the relatedness of the hominoids. Proceedings of the National Academy of Sciences of the United States of America 86, 8447-8451.

Donoghue, M.J. and Cantino, P.D., 1984. The logic and limitations of the outgroup substitution approach to cladistic analysis. Systematic Botany 9, 192-202.

Dupain, J. and Van Elsacker, L., 2001. The status of the bonobo (*Pan paniscus*) in the Democratic Republic of Congo. In: Galdikas, B.M.F., Briggs, N.E., Sheeran, L.K., Shapiro, G.L., Goodall, J. (Eds.), All Apes Great and Small, Volume 1: African Apes. Kluwer Academic/Plenum Publishers, New York, pp. 57-74.

Eckhardt, R.B. and Protsch von Zieten, R.R., 1992. Apes and apomorphies: the anterior nasal spine as a projection of cladistic conceptions. Zeitschrift für Morphologie und Anthropologie 79, 95-101.

Falk, D. and Conroy, G., 1983. The cranial venous sinus system in *Australopithecus afarensis*. Nature 306, 779-781.

Falk, D., 1986. Evolution of cranial blood drainage in hominids: enlarged occipital/marginal sinuses and emissary foramina. American Journal of Physical Anthropology 70, 311-324.

Falk, D., 1993. Meningeal arterial patterns in the great apes: implications for hominid vascular evolution. American Journal of Physical Anthropology 92, 81-97.

Falsetti, A.B., Jungers, W.L. and Cole III, T.M., 1993. Morphometrics of the Callitrichid forelimb: a case study in size and shape. International Journal of Primatology, 14: 551-572,

Farris, J.S., 1982. Outgroups and parsimony. Systematic Zoology 31, 328-334.

Farris, J.S., 1989. The retention index and homoplasy index. Systematic Zoology 38, 406-407.

Felsenstein, J., 1983. Parsimony in systematics: Biological and statistical issues. Annual Review of Ecology and Systematics 14, 313-333.

Felsenstein, J., 1985a. Phylogenies and the comparative method. American Naturalist 125, 1-15.

Felsenstein, J., 1985b. Confidence limits on phylogenies: An approach using the bootstrap. Evolution 39, 783-791.

Finarelli, J.A. and Clyde, W.C., 2004. Reassessing hominoid phylogeny: Evaluating congruence in the morphologic and temporal data. Paleobiology 30, 614-651.

Fitch, W.M. and Atchley, W.R., 1987. Divergence in inbred strains of mice: a comparison of three different types of data. In: Patterson, C. (Ed.) Molecules and Morphology in Evolution: Conflict or Compromise? Cambridge University Press, Cambridge, pp. 203-216.

Forey, P.L., 1990. Cladistics. In Briggs, D.E., Crowther, P.R. (Eds.) Palaeobiology a Synthesis. Blackwell Scientific Publication, Oxford, pp. 430-434.

Fox, D.L., Fisher, D.C. and Leighton, L.R., 1999. Reconstructing phylogeny with and without temporal data. Science 284, 1816-1819.

Frayer, D.H., Wolpoff, M.H., Thorne, A.G., Smith, F.H. and Pope, G., 1993. Theories of modern human origin: The palaeontological test. American Anthropologist 95, 14-50.

Frayer, D.W. and Wolpoff, M.H., 1985. Sexual dimorphism. Annual Review of Anthropology 14, 429-473.

Garner, K.J. and Ryder, O.A., 1996. Mitochondrial DNA diversity in gorillas. Molecular Phylogenetics and Evolution 6, 39-48.

Gebo, D. L., MacLatchy, L., Kityo, R., Deino, A., Kingston, J. and Pilbeam, D., 1997. A hominoid genus from the early Miocene of Uganda. Science 276, 401-404.

Gee, H., 2001. Return to the planet of the apes. Nature 412, 131-132.

Gibbs, S., Collard, M. and Wood, B., 2000. Soft-tissue characters in higher primate phylogenetics. Proceedings of the National Academy of Science USA 97, 11130-11132.

Gibbs, S., Collard, M. and Wood, B., 2002. Soft-tissue anatomy of the extant hominoids: a review and phylogenetic analysis. Journal of Anatomy 200, 3-49.

Gittleman, J.L. and Kot, M., 1990. Adaptation and a null model for estimating phylogenetic effects. Systematic Zoology 39, 227-241.

Goldman, N., 1988. Methods for discrete coding of variable morphological features for numerical analysis. Cladistics 4, 59-71.

Goodman, M., 1962. Immunochemistry of the primates and primate evolution. Annuals of the NY Academy of Sciences 102, 219-234.

Goodman, M., 1963. Serological analysis of recent hominoids. Human Biology 35, 377-436.

Goodman, M., Bailey, W.J., Hayasaka, K., Stanhope, M.J., Slightom, J.L. and Czelusniak, J., 1994. Molecular evidence on primate phylogeny from DNA sequences. American Journal of Physical Anthropology 94, 3-24.

Goodman, M., Braunitzer, G., Stanzi A. and Schrank, B., 1983. Evidence on human origins from haemoglobins of African apes. Nature 303, 546-548.

Goodman, M., Koop, B.F., Czelusniak, J., Fitch, D.H.A., Tagle, D.A. and Slightom, J.L., 1989. Molecular phylogeny of the family of apes and humans. Genome 31, 316-335.

Goodman, M., McConkey, E.H. and Page, S.L., 2002. Reconstructing human evolution in the age of genomic exploration. In: Harcourt, C.S., Sherwood,

B.R. (Eds.), New Perspectives in Primate Evolution and Behaviour. Westbury Academic and Scientific Publishing, pp. 47-70.

Goodman, M., Porter, C.A., Czelusniak, J., Page, S.L., Schneider, H., Shoshani, J., Gunnell, G. and Groves, C.P., 1998, Toward a phylogenetic classification of primates based on DNA evidence complemented by fossil evidence. Molecular Phylogenetics and Evolution 9, 585-598.

Gray, H., 1999. Gray's Anatomy. Elsevier, London.

Groves, C. P., 1989. A Theory of Human and Primate Evolution. Oxford University Press, New York.

Groves, C.P. and Paterson, J.D., 1991. Testing hominoid phylogeny with the PHYLIP program. Journal of Human Evolution 20, 167-183.

Groves, C.P., 1986. Systematics of the great apes. In: Swindler, D.R., Erwin, J. (Eds.) Comparative Primate Biology: Systematic, Evolution and Anatomy. Vol.1. A. R. Liss, New York, pp. 187-217.

Groves, C.P., 1987. A review of J. H. Schwartz's "The Red Ape: Orangutans and human origins", published 1987 by Houghton Mifflin, Boston. Journal of Human Evolution 16, 537-542.

Groves, C.P., 2000. Phylogeny of the Cercopithecoidea. In: Whitehead, P.F., Jolly, C.J. (Eds.), Old World Monkeys. Cambridge University Press, Cambridge, pp. 77-98.

Groves, C.P., 2001. Primate Taxonomy. Smithsonian Institution Press, Washington and London.

Gruneberg, H., 1952. Genetical studies on the skeleton of the mouse. IV. Quasi-continuous variations. Journal of Genetics 51, 95-114.

Gruneberg, H., 1963. The pathology of development. Blackwell, Oxford.

Haile-Selassie, Y., 2001. Late Miocene hominids from the Middle Awash, Ethiopia. Nature 412, 178-181.

Hall, C.R., Wu, Y., Shaffer, L.G. and Hecht, J.T., 2001. Familial case of Potocki-Shaffer syndrome associated with microdeletion of EXT2 and ALX4. Clinical Genetics 60, 356-359.

Hanihara, T. and Ishida, H., 2001. Frequency variations of discrete cranial traits in major human populations. I. Supernumerary ossicle variations. Journal of Anatomy 198, 609-706.

Hanihara, T. and Ishida, H., 2001. Frequency variations of discrete cranial traits in major human populations. II. Hypostotic variations. Journal of Anatomy 198, 707-26.

Hanihara, T. and Ishida, H., 2001. Frequency variations of discrete cranial traits in major human populations. III. Hyperostotic variations. Journal of Anatomy 199, 251-72.

Hanihara, T. and Ishida, H., 2001. Frequency variations of discrete cranial traits in major human populations. IV. Vessel and nerve related variations. Journal of Anatomy 199, 273-87.

Harrison, T., 1993. Cladistic concepts and the species problem in hominoid evolution. In: Kimbel, W.H., Martin, L.B. (Eds.), Species, Species Concepts and Primate Evolution. Plenum Press, New York, pp. 345-371.

Hartman, S.E., 1988. A cladistic analysis of hominoid molars. Journal of Human Evolution 17, 489-502.

Hartman, S.E., 1989. Stereophotogrammetric analysis of occlusal morphology of extant hominoid molars: phenetics and function. American Journal of Physical Anthropology 80,145-166.

Harvey, P.H. and Pagel, M., 1991. The Comparative Method in Evolutionary Biology. Oxford University Press.

Hauser, G. and De Stefano, G.F., 1989. Epigenetic Variants of the Human Skull. Schweizerbart, Stuttgart.

Hawks, J., 2004. How much can cladistics tell us about hominid relationships? American Journal of Physical Anthropology 125, 207-219.

Hennig, W., 1966. Phylogenetic Systematics. University of Illinois Press, Urbana.

Hillis, D.M, and Bull, J.J., 1993. An empirical test of bootstrapping as a method for assessing confidence in phylogenetic analysis. Systematic Biology 42, 182-192.

Hillis, D.M., Bull, J.J., White, M.E., Badget, M.R. and Molineux, I.J., 1992. Experimental phylogenetics: a generation of a known phylogeny. Science 255, 589-592.

Horai, S., Hayasaka, K., Kondo, R., Tsugane, K. and Takahata, N., 1995. Recent African origin of modern humans revealed by complete sequences of hominoid mitochondrial DNAs. Proceedings of the National Academy of Science USA 92, 532-536.

Horai, S., Satta, Y., Hayasaka, K., Kondo, R., Inoue, T., Ishida, T., Hayashi, S. and Takahata, N., 1995. Man's place in hominoidea revealed by mitochondrial DNA genealogy. Journal of Molecular Evolution 35, 32-43.

Jungers, W.L., Falsetti, A.B. and Wall, C.E., 1995. Shape, relative size, and size-adjustments in morphometrics. Yearbook of Physical Anthropology 38, 137-161.

Keller, M.P., Seifried, B.A. and Chance, P.F., 1999. Molecular evolution of the CMT1A-REP region: a human- and chimpanzee-specific repeat. Molecular Biology and Evolution 16, 1019-1026.

Kitching, I.J., Forey, P.L., Humphries, C.J. and Williams, D.M., 1998. Cladistics. Oxford University Press, Oxford.

Klinger, H.P., Hamerton, J.L., Mutton, D. and Lang, E., 1963. The chromosomes of the Hominoidea. In: Washburn, S.L. (Ed.), Classification and Human Evolution. Aldine, Chicago, pp. 235-242.

Kluge, A.G., 1983. Cladistics and the classification of the great apes. In: Ciochon, R.L., Corruccini, R.S. (Eds.), New Interpretations of Ape and Human Ancestry. Plenum Press, New York, pp. 151-177.

Kluge, A.G., 1989. A concern for evidence and a phylogenetic hypothesis of relationships among *Epicrates* (Boidae, Serpentes). Systematic Zoology 38, 7-25.

Kluge, A.G., 1998. Total evidence or taxonomic congruence: cladistics or consensus classification. Cladistics 14, 151-158.

Köhler, M. and Moya-Sola, S., 1999. A finding of Oligocene primates on the European continent. Proceedings of the National Academy of Science USA 96, 14664-14667.

Koop, B.F., Goodman, M., Xu, P., Chan, K. and Slightom, J.L., 1986. Primate n-globin DNA sequences and man's place among the great apes. Nature 319, 234-238.

Koop, B.F., Siemieniak, D., Slightom, J.L., Goodman, M., Dunbar, J., Wright, P.C. and Simons, E.L., 1989. *Tarsius* delta and beta globin genes: conversions, evolution and systematic implications. Journal of Biology and Chemistry 264, 68-79.

Leakey, M.G., Fiebel, C.S., McDougall I. and Walker, A.C., 1995. New four-million-year-old hominid species from Kanapoi and Allia Bay, Kenya. Nature 376, 565-571.

Leakey, M.G., Spoor, F., Brown, F.H., Gathogo, P.N., Kiarie, C., Leakey, L.N. and McDougall, I., 2001. New hominin genus from eastern Africa shows diverse middle Pliocene lineages. Nature 410, 433-440.

Lewis, O.J., 1989. Functional Morphology of the Evolving Hand and Foot. Oxford University Press, Oxford.

Lieberman, D.E., 1995. Testing hypotheses about recent human evolution from skulls. Current Anthropology 36, 159-178.

Lieberman, D.E., 1996. How and why humans grow thin skulls: experimental evidence for systemic cortical robusticity. American Journal of Physical Anthropology 101, 217-236.

Lieberman, D.E., 1997. Making behavioral and phylogenetic inferences from hominid fossils: considering the developmental influence of mechanical forces. Annual Review of Anthropology 26, 185-210.

Lieberman, D.E., 1999. Homology and hominid phylogeny: problems and potential solutions. Evolutionary Anthropology 7, 142-151.

Lieberman, D.E., 2001. Another face in our family tree. Nature 410, 419-420.

Lieberman, D.E., Ross, C.R. and Ravosa, M., 2000. The primate cranial base: ontogeny, function and integration. Yearbook of Physical Anthropology 43, 117-169.

Lieberman, D.E., Wood, B.A. and Pilbeam, D.R., 1996. Homoplasy and early *Homo*: an analysis of the evolutionary relationships of *H. habilis sensu stricto* and *H. rudolfensis*. Journal of Human Evolution 30, 97-120.

Lindenfors, P. and Tullberg, B.S., 1998. Phylogenetic analyses of primate size evolution: the consequences of sexual selection. Biological Journal of the Linnean Society 64, 413-447.

Lockwood, C.A. and Fleagle, J.G., 1999. The recognition and evaluation of homoplasy in primate and human evolution. Yearbook of Physical Anthropology 42, 189-232.

Lockwood, C.A., Kimbel, W.H. and Lynch, J.M., 2004. Morphometrics and hominoid phylogeny: Support for a chimpanzee-human clade and differentiation among great ape subspecies. Proceedings of the National Academy of Sciences, USA 101, 4356-4360.

Lovejoy, C.O., Cohn, M.J. and White T.D., 1999. Morphological analysis of the mammalian postcranium: a developmental perspective. Proceedings of the National Academy of Sciences USA 96, 13247-13252.

Lovejoy, C.O., Meindl, R.S., Ohman, J.C., Heiple, K.G. and White T.D., 2002. The Maka femur and its bearing on the antiquity of human walking: applying contemporary concepts of morphogenesis to the human fossil record. American Journal of Physical Anthropology 119, 97-133.

Luker, J., McNamara, T. and Sandy, J., 1998. Holes in the head: parietal foramina, a developmental anomaly seen during a routine orthodontic assessment. International Journal of Paediatric Dentistry 8, 209-211.

Lycett, S.J., and Collard, M., 2005. Do homoiologies impede phylogenetic analyses of the fossil hominids? An assessment based on extant papionin craniodental morphology. Journal of Human Evolution 49, 618-642.

Maddison, W.P. and Maddison, D.R., 2001. MacClade: Analysis of Phylogeny and Character Evolution, Version 4.03. Sinauer, Sunderland, MA.

Maddison, W.P., Donohue, M.J. and Maddison, D.R., 1984. Outgroup analysis and parsimony. Systematic Zoology 33, 83-103.

Mann, A. and Weiss, M., 1996. Hominoid phylogeny and taxonomy: a consideration of the molecular and fossil evidence in an historical perspective. Molecules, Phylogeny and Evolution 5, 169-181.

Marks, J., 1983. Hominoid cytogenetics and evolution. Yearbook of Physical Anthropology 26, 131-159.

Marks, J., 1993. Hominoid heterochromatin: terminal C-bands as a complex genetic trait linking chimpanzee and gorilla. American Journal of Physical Anthropology 90, 237-246.

Marshall, J.T. and Sugardjito, J., 1986. Gibbon systematics. In: Swindler, D. R. and Erwin, J. (Eds.), Comparative Primate Biology. Vol. 1: Systematics, Evolution, and Anatomy. Alan R. Liss, New York, pp. 137-185.

Martin, L., 1986. Relationships among extant and extinct great apes and humans. In: Wood, B., Martin, L., Andrews, P. (Eds.) Major Topics in Primate and Human Evolution. Cambridge University Press, Cambridge, pp.161-187.

Martin, R.D., 1993. Allometric aspects of skull morphology in *Theropithecus*. In: Jablonski, N.G. (Ed.) Theropithecus: The Rise and Fall of a Primate Genus. Cambridge University Press, Cambridge, pp.273-298.

Masters, J.C. and Brothers, D.J., 2002. Lack of congruence between morphological and molecular data in reconstructing the phylogeny of the Galagonidae. American Journal of Physical Anthropology 117, 79-93.

McCollum, M.A. and Sharpe, P.T., 2001. Developmental genetics and early hominid craniodental evolution. Bioessays 23, 481-493.

McCollum, M.A., 1999. The robust australopithecine face: a morphogenetic perspective. Science 284, 301-305.

McCracken, K.G., Harshman, J., McClellan, D.A. and Afton, A.D., 1999. Data set incongruence and correlated character evolution: an example of functional convergence in the hind-limbs of stifftail diving ducks. Systematic Biology 48, 683-714.

Mickevich, M.F., 1978. Taxonomic congruence. Systematic Zoology 27, 143-158.

Miller, D.A., 1977. Evolution of primate chromosomes. Science 198, 1116-11124

Mirazón Lahr, M. and Foley, R., 2004. Human evolution writ small. Nature 431, 1043-1044.

Miyamoto, M.M. and Fitch, W.M., 1995. Testing species phylogenies and phylogenetic methods with congruence. Systematic Biology 44, 64-76.

Mohammadali, K., Eladari, M.E. and Galibert, F., 1995. Gorilla and orangutan C-MYC nucleotide-sequences: inferences on hominoid phylogeny. Journal of Molecular Evolution 41, 262-276.

Morwood, M.J., Soejono, R.P., Roberts, R.G. et al., 2004. Archaeology and age of a new hominin from Flores in eastern Indonesia. Nature 431, 1087-1091.

Msuya, C.P. and Harrison, T., 1996. The circumorbital foramina in primates: a phylogenetic perspective. Darmstädter Beiträge zur Naturgeschichte 6, 103-109.

Nadal-Roberts, M. and Collard, M., 2005. Impact of methodological choices on assessments of the reliability of primate phylogenetic hypotheses. Folia Primatologica 76, 207-221.

Nixon, K.C. and Carpenter, J.M., 1993. On outgroups. Cladistics 9, 413-426.

Nomina Anatomica, 1989. International anatomical nomenclature committee. Churchill Livingstone, Edinburgh.

Nowak, R.M., 1999. Walker's Primates of the World. Johns Hopkins University Press, Baltimore and London.

Nunn, C.L. and Barton, R.A., 2001. Comparative methods for studying primate adaptation and allometry. Evolutionary Anthropology 10, 81-98.

O'Higgins, P. and Collard, M., 2002. Sexual dimorphism and facial growth in papionin monkeys. Journal of Zoology 257, 255-272.

Oates, J.F. and Davies, A.G., 1994. What are the colobines?. In: Davies, A.G., Oates, J.F. (Eds.), Colobine Monkeys: their Ecology, Behaviour and Evolution. Cambridge University Press, Cambridge, pp. 1-9.

Oates, J.F., Davies, A.G. and Delson, E., 1994. The diversity of living colobines. In: Davies, A.G., Oates, J.F. (Eds.), Colobine Monkeys: their Ecology, Behaviour and Evolution. Cambridge University Press, Cambridge, pp. 45-73.

O'Keefe, F.R. and Wagner, P.J., 2001. Deriving and testing hypotheses of correlated character evolution using character compatibility. Systematic Biology 50, 657-675.

Oxnard, C.E., 1984. The Order of Man: a Biomathematical Anatomy of Primates. Yale University Press, New Haven.

Page, S.L. and Goodman, M., 2001. Catarrhine phylogeny: noncoding DNA evidence for a diphyletic origin of the Mangabeys and for a human-chimpanzee clade. Molecular Phylogenetics and Evolution 18, 14-25.

Pagel, M.D., 1992. A method for the analysis of comparative data. Journal of Theoretical Biology 156, 431-442.

Patterson, F.G.P. and Matevia, M.L., 2001. The status of gorillas worldwide. In: Galdikas, B.M.F., Briggs, N.E., Sheeran, L.K., Shapiro, G.L., Goodall, J. (Eds.), All Apes Great and Small, Volume 1: African Apes. Kluwer Academic/Plenum Publishers, New York, pp. 151-163.

Penin, X., Berge, C. and Baylac, M., 2002. Ontogenetic study of the skull in modern humans and the common chimpanzee: neotenic hypothesis reconsidered with a tridimensional procrustes analysis. American Journal of Physical Anthropology 118, 50-62.

Perrinpecontal, P., Gouy, M., Nigon, V.M. and Trabuchet, G., 1992. Evolution of the primate beta-globin gene region, nucleotide sequence of the delta-beta-globin intergenic region of *Gorilla* and phylogenetic relationships between African apes and man. Journal of Molecular Evolution 34, 17-30.

Pilbeam, D. and Young, N., 2004. Hominoid evolution: synthesizing disparate data. Comptes Rendus Palevol 3, 305-321.

Pilbeam, D., 1996. Genetic and morphological records of the Hominoidea and hominid origins: a synthesis. Molecules, Phylogeny and Evolution 5, 155-168.

Pilbeam, D., 2000. Hominoid systematics: the soft evidence. Proceedings of the National Academy of Science USA 97, 10684-10686.

Plavcan, J.M., 2002. Taxonomic variation in the patterns of craniofacial dimorphism in primates. Journal of Human Evolution 42, 579-608.

Pleijel, F., 1995. On character coding for phylogenetic reconstruction. Cladistics 11, 309-315.

Prat, S., 2003. Origine et taxonomie des premiers représentants du genre *Homo*. Ph.D. Dissertation, University of Bordeaux I.

Purvis, A., 1995. A composite estimate of primate phylogeny. Philosophical Transactions: Biological Sciences 348, 405-421.

Purvis, A., Gittleman, J.L. and Luh, H., 1994. Truth or consequences: effects of phylogenetic accuracy on two comparative methods. Journal of Theoretical Biology 167, 293-300.

Rae, T.C., 1997. The early evolution of the hominoid face. In: Begun, D., Ward, C., Rose, M. (Eds.), Function, Phylogeny, and Fossils: Miocene Hominoid Evolution and Adaptations. Plenum Press, New York, pp. 59-77.

Rasheed, B.K.A., Whisenant, E.C., Fernandez, R., Ostrer, H. and Bhatnagar, Y.M., 1991. A Y-chromosomal DNA fragment is conserved in human and chimpanzee. Molecular Biology and Evolution 8, 416-432.

Relethford, J.H., 1994. Craniometric variation among modern human populations. American Journal of Physical Anthropology 95, 53-62.

Richmond, B.G. and Jungers, W.L., 1995. Size variation and sexual dimorphism in *A. afarensis* and living hominoids. Journal of Human Evolution 29, 229-245.

Richmond, B.G. and Strait, D.S., 2000. Evidence that humans evolved from a knuckle-walking ancestor. Nature 404, 382-385.

Richmond, B.G. and Strait, D.S., 2001. Knuckle-walking hominid ancestor: a reply to Corruccini and McHenry. Journal of Human Evolution 40, 513-520

Röhrer-Ertl, O., 1999. The influence of sample selection on results in empirical studies and heuristics. In: Koppe, T., Nagai, H., Alt, K.W. (Eds.), The paranasal sinuses of higher primates. Development, Function and Evolution. Quintessence, London, pp. 227-234.

Rosas, A., Bastir, M., Martínez Maza, C., and Bermúdez de Castro, J.M., 2002. Sexual dimorphism in the Atapuerca-SH hominids. The evidence from the mandibles. Journal of Human Evolution 42, 451-474.

Rosenberger, A.L., Strasser, E. and Delson, E., 1985. Anterior dentition of *Notharctus* and the Adapid-Anthropoid hypothesis. Folia Primatologica 44, 15-39.

Ruano, G., Rogers, J., Ferguson-Smith, A. and Kidd, K., 1992. DNA sequence polymorphism within hominoid species exceeds the number of phylogenetically informative characters for a HOX2 locus. Molecular Biology and Evolution 9, 575-586.

Ruvolo, M., 1994. Molecular evolutionary processes and conflicting gene trees: the hominoid case. American Journal of Physical Anthropology 94, 89-113.

Ruvolo, M., 1997. Molecular phylogeny of the hominoids: inferences from multiple independent DNA sequence data sets. Molecular Biology and Evolution 14, 248-265.

Sanderson, M.J., 1995. Objections to bootstrapping phylogenies: a critique. Systematic Biology 44, 299-320.

Sarich, V., 1971. A molecular approach to the question of human origins. In: Dolhinow, P., Sarich, V. (Eds.), Background for Man. Little, Brown, Boston, pp. 60-81.

Sarich, V.M. and Wilson, A.C., 1967. Immunological timescale for hominoid evolution. Science 158, 1200-1203.

Satta, Y., Klein J., and N. Takahata., 2000. DNA archives and our nearest relative: The trichotomy problem revisited. Molecular Phylogenetics and Evolution 14, 259-275.

Schwartz, J.H., 1983. Palatine fenestrae, the orangutan and hominoid evolution. Primates 24, 231-240.

Schwartz, J.H., 1984a. The evolutionary relationships of man and orangutans. Nature 308: 501-505.

Schwartz, J.H., 1984b. Hominoid evolution: a review and a reassessment. Current Anthropology 25, 655-672.

Schwartz, J.H., 1986. Primate systematics and a classification of the order. In: Swindler, D.R., Erwin, J. (Eds.), Comparative Primate Biology: Systematics, Evolution and Anatomy. A. R. Liss, New York, pp. 1-41.

Schwartz, J.H., 1987. The Red Ape: Orangutans and Human Origins. Houghton Mifflin, Boston.

Senut, B., Pickford, M., Gommery, D., Mein, P., Cheboi, K. and Coppens, Y., 2001. First hominid from the Miocene (Lukeino formation, Kenya). Comptes Rendues de l'Académie des Sciences de Paris, Sciences de la Terre et des planètes 0, 1-9.

Serdoz, D., 2001. Hominoid Phylogeny: an analysis using population genetic techniques and craniometric data. Unpublished M.Sci. Dissertation. University College London.

Shea, B.T. and Inouye, S.E., 1993. Knuckle-walking ancestors. Science 259, 293-294.

Shoshani, J., Groves, C.P., Simons, E.L. and Gunnell, G.F., 1996. Primate phylogeny: morphological vs molecular results. Molecular Phylogenetics and Evolution 5, 102-154.

Sibley, C.G. and Ahlquist, J.E., 1984. The phylogeny of hominoid primates as indicated by DNA-DNA hybridisation. Journal of Molecular Evolution 20, 2-15.

Sibley, C.G. and Ahlquist, J.E., 1987. DNA hybridization evidence of hominoid phylogeny: results from an expanded dataset. Journal of Molecular Evolution 26, 99-121.

Sibley, C.G., Comstock, J.A. and Ahlquist, J.E., 1990. DNA hybridisation evidence of hominoid phylogeny: a reanalysis of the data. Journal of Molecular Evolution 30, 202-236.

Siegel, S. and Castellan, N.J.Jr., 1988. Non Parametric Statistics for the Behavioral Sciences. McGraw-Hill International Editions, New York.

Skelton, R.R. and McHenry, H.M., 1992. Evolutionary relationships among early hominids. Journal of Human Evolution 23, 309-349.

Skelton, R.R. and McHenry, H.M., 1998. Trait list bias and a reappraisal of early hominid phylogeny. Journal of Human Evolution 34, 109-113.

Skelton, R.R., McHenry, H.M. and Drawhorn, G.M., 1986. Phylogenetic analysis of early hominids. Current Anthropology 27, 21-43.

Smith, A.B., 1994. Systematics and the Fossil Record. Blackwell, London.

Smith, E.N. and Gutberlet, R.L., 2001. Generalized frequency coding: a method of preparing polymorphic multistate characters for phylogenetic analysis. Systematic Biology 50, 156-169.

Sneath, P.H.A. and Sokal, R.R., 1973. Numerical Taxonomy. Freeman, San Francisco.

Sober, E., 1983. Parsimony in systematics: philosophical issues. Annual Review of Ecology and Systematics 14, 335-357.

Stanyon, R. and Chiarelli, B., 1982. Phylogeny of the Hominoidea: the chromosomal evidence. Journal of Human Evolution 11, 493-504.

Strait, D.S. 2001. Integration, phylogeny and the hominid cranial base. American Journal of Physical Anthropology 114, 273-297.

Strait, D.S. and Grine, F.E., 1998. Trait list bias? A reply to Skelton and McHenry. Journal of Human Evolution 34, 115-118.

Strait, D.S. and Grine, F.E., 1999. Cladistics and early hominid phylogeny. Science 285, 1210.

Strait, D.S. and Grine, F.E., 1999. Cladistics and early hominid phylogeny. Science 285, 1210.

Strait, D.S. and Grine, F.E., 2004. Inferring hominoid and early hominid phylogeny using craniodental characters: the role of fossil taxa. Journal of Human Evolution 47, 399-452.

Strait, D.S. and Wood, B.A., 1999. Early hominid biogeography. Proceedings of the National Academy of Sciences, USA 96, 9196-9200.

Strait, D.S., Grine, F.E. and Moniz, M.A., 1997. A reappraisal of early hominid phylogeny. Journal of Human Evolution 32, 17-82.

Stringer, C., 1987a. A numerical cladistic analysis for the genus *Homo*. Journal of Human Evolution 16, 135-146.

Stringer, C.B., 1987b. A numerical cladistic analysis for the genus *Homo*. Journal of Human Evolution 16, 135-146.

Susman, R.L. and Stern, J., 1991. Locomotor behaviour in early hominids: epistemology and fossil evidence. In: Coppens, Y., Senut, B. (Eds.), Origine(s) de la Bipédie chez les Hominidés. CNRS, Paris, pp. 121-131.

Suzuki, H., Kawamoto, Y., Takenaka, O., Munechika, I., Hori, H. and Sakurai, S., 1994. Phylogenetic relationships among *Homo sapiens* and related species based on restriction site variations in RDNA spacers. Biochemical Genetics 32, 257-269.

Swofford, D.L., 1998. PAUP*. Phylogenetic Analysis Using Parsimony (*and Other Methods). Version 4.0. Sinauer Associates, Sunderland, Massachusetts.

Tattersall, I. and Eldredge, N., 1977. Fact, theory and fantasy in human paleontology. American Scientist 65, 204-211.

Templeton, A., 1983. Phylogenetic inference from restriction endonuclease cleavage site maps with particular reference to the evolution of humans and the apes. Evolution 37, 221-244.

Thiele, K., 1993. The Holy Grail of the perfect character: the cladistic treatment of morphometric data. Cladistics 9, 275-304.

Thoma, A., 1977. Variations anatomiques et parenté taxonomique chez les Hominoidea. Comptes Rendues de l'Académie des Sciences de Paris, t. 284, serie D, 2507-2510

Thoma, A., 1978. Quasi-kontinuierliche Variabilität und genetische Einheitlichkeit der Hominoidea. Zeitschrift für Morphologie und Anthropologie 69, 7-15.

Thoma, A., 1979. Further studies on quasi-continuous variations in Hominoidea. Zeitschrift für Morphologie und Anthropologie 70, 104-110.

Thoma, A., 1981. The pattern of quasi-continuous variation in *Homo sapiens.* Journal of Human Evolution 10, 303-310.

Thorpe, R.S., 1984. Coding morphometric characters for constructing distance Wagner networks. Evolution 38, 244-255.

Tobias, P.V. and Falk, D., 1988. Evidence of a dual pattern of cranial venous sinuses on the endocranial cast of Taung (*Australopithecus africanus*). American Journal of Physical Anthropology 76, 309-312.

Trinkaus, E., 1990. Cladistics and the hominid fossil record. American Journal of Physical Anthropology 83,1-11.

Tuttle, R.H., 1969. Knuckle-walking and the problem of human origins. Science 166, 953-961.

Uchida, A., 1998. Design of the mandibular molar in the extant great apes and Miocene fossil hominoids. American Journal of Physical Anthropology 106 (Supplement), 119-126.

Ueda, S., Watanabe, Y., Saitou, N., Omoto, K., Hayashida, H., Miyata, T., Hisajima, H. and Honjo, T., 1989. Nucleotide sequences of immunoglobulin-epsilon pseudogenes in man and apes and their phylogenetic relationships. Journal of Molecular Biology 205, 85-90.

Verheyen, W.N., 1962. Contribution à la craniologie comparée des primates. Les genres *Colobus* Illiger 1811 et *Cercopithecus* Linne 1758. Musée Royal de l'Afrique Centrale: Tervuren, Belgique. Annales, Serie IN 8, Sciences Zoologiques n 105.

Viguier, B., 2002. Is the morphological disparity of lemur skulls (Primates) controlled by phylogeny and/or environmental constraints? Biological Journal of the Linnean Society 76, 577-590.

Ward, C.V., Leakey, M.D. and Walker, A., 2001. Morphology of *A. anamensis* from Kanapoi and Allia Bay, Kenya. Journal of Human Evolution 41, 255-368.

Watrous, L.E. and Wheeler, Q.D., 1981. The outgroup comparison method of character analysis. Systematic Zoology 30, 1-11.

White, T.D., Suwa, G. and Asfaw, B., 1994. *Australopithecus ramidus*, a new species of early hominid from Aramis, Ethiopia. Nature 371, 306-312.

Wiens, J.J., 1993. Phylogenetic systematics of the tree lizards (genus *Urosaurus*). Herpetologica 49, 399-420.

Wiens, J.J., 1995. Polymorphic characters in phylogenetic systematics. Systematic Biology 44, 482-500.

Wiens, J.J., 1998. Testing phylogenetic methods with tree congruence: phylogenetic analysis of polymorphic morphological characters in phrynosomatid lizards. Systematic Biology 47, 427-444.

Wiens, J.J., 2001. Character analysis in morphological phylogenetics: problems and solutions. Systematic Biology 50, 689-699.

Wildman, D. E., Uddin, M., Liu, G., Grossman, L. and Goodman, M. 2003. Implications of natural selection in shaping 99.4% nonsynonymous DNA identity between humans and chimpanzees: Enlarging genus *Homo*. Proceedings of the National Academy of Science USA 100, 7181-7188.

Wood, B. and Collard, M., 1999. The human genus. Science 284, 65-71.

Wood, B. and Richmond, B.G., 2000. Human evolution: taxonomy and paleobiology. Journal of Anatomy 196, 19-60.

Wood, B., 1991. Koobi Fora Research Project Vol. 4: Hominid Cranial Remains. Clarendon Press, Oxford.

Wood, B., 1992a. Early hominid species and speciation. Journal of Human Evolution 22, 351-365.

Wood, B., 1992b. Origin and evolution of the genus *Homo*. Nature 355, 783-790.

Wood, B., 2000. Investigating human evolutionary history. Journal of Anatomy 197, 3-17.

Wood, B., 2002. Hominid revelations from Chad. Nature 418, 133-135.

Wood, B.A. and Chamberlain, A.T., 1987. The nature and affinities of the robust Australopithecines: a review. Journal of Human Evolution 16, 625-641.

Wood, B.A., 1988. Are 'robust' australopithecines a monophyletic group? In: Grine, F.E. (Ed.), Evolutionary History of the "Robust" Australopithecines. Aldine de Gruyter, New York, pp. 269-284.

Yoder, A.D., 1994. Relative position of the Cheirogaleidae in strepsirhine phylogeny: a comparison of morphological and molecular methods and results. American Journal of Physical Anthropology 94, 25-46.

Yunis, J.J. and Prakash, O., 1982. The origin of man: a chromosomal pictorial legacy. Science 215, 1525-1530.

Zeitoun, V., 1996. Le tubercule préglenoide des *Homo erectus*. Implication phylogénétique. Comptes Rendues de l'Académie des Sciences de Paris, t. 322, serie IIa, 997-1003.

Zuckerkandl, E., Jones, R.T. and Pauling L., 1960. A comparison of animal hemoglobins by tryptic peptide pattern analysis. Proceedings of the National Academy of Sciences USA 46, 1349-1360.

Appendix I. LIST OF SPECIMENS

The specimens listed in this appendix are grouped by genus. For each specimen I included:

1. a specimen number,
2. the catalogue number, as appeared on the specimen label,
3. the sex, as listed in the museum catalogues,
4. the museum collection to which the specimen belongs,
5. the species, as listed in the museum catalogues, and where possible the subspecies,
6. the locality where the specimen was collected, as appeared in the museum catalogues.

Abbreviations

M= Male
F= Female
?= Unknown
NHM= Natural History Museum, London
MRAC= Royal Museum of Central Africa, Tervuren
IMAZ= Anthropological Institute and Museum, University of Zurich
ZSCM= Zoology State Collection, Munich
SCAP= State Collection of Anthropology and Palaeoanatomy, Munich
Duckworth= Duckworth Laboratory, Cambridge

Genus *Gorilla*

Specimen	Catalogue	Sex	Museum	Species	Subspecies	Locality
3	AS760	M	IMAZ	*G. gorilla*	*G. gorilla gorilla*	Cameroon
9	AS1691	F	IMAZ	*G. gorilla*	*G. g. gorilla*	French Cameroon
13	AS1604	M	IMAZ	*G. gorilla*	*G. g. gorilla*	French Congo
29	PAL11	M	IMAZ	*G. gorilla*	*G. g. gorilla*	?
36	5563	F	IMAZ	*G. gorilla*	*G. g. gorilla*	Gabon
37	6594	F	IMAZ	*G. gorilla*	*G. g. gorilla*	French Cameroon
39	7117	M	IMAZ	*G. gorilla*	*G. g. gorilla*	?
42	10769	M	IMAZ	*G. gorilla*	*G. g. gorilla*	?
43	7692	M	IMAZ	*G. gorilla*	*G. g. gorilla*	?
44	7488	F	IMAZ	*G. gorilla*	*G. g. gorilla*	?
45	6600	F	IMAZ	*G. gorilla*	*G. g. gorilla*	?
52	6680	M	IMAZ	*G. gorilla*	*G. g. gorilla*	Cameroon
53	6896	F	IMAZ	*G. gorilla*	*G. g. gorilla*	Spanish Guinea
106	RG807	F	MRAC	*G. gorilla*	*G. gorilla graueri*	Baraka, forest Sibatwa
107	RG804	M	MRAC	*G. gorilla*	*G. g. graueri*	Baraka, forest Sibatwa
108	RG998	M	MRAC	*G. gorilla*	*G. g. graueri*	Baraka, forest Sibatwa
109	RG999	M	MRAC	*G. gorilla*	*G. g. graueri*	Baraka, forest Sibatwa
110	RG813	F	MRAC	*G. gorilla*	*G. g. graueri*	Baraka, forest Sibatwa
111	RG833	F	MRAC	*G. gorilla*	*G. g. graueri*	Baraka, forest Sibatwa
112	RG14769	F	MRAC	*G. gorilla*	*G. g. graueri*	Shabunda region
113	RG14615	F	MRAC	*G. gorilla*	*G. g. graueri*	Lubero
114	RG26206	M	MRAC	*G. gorilla*	*G. g. graueri*	Bukavu?
115	RG17770	M	MRAC	*G. gorilla*	*G. g. graueri*	Lubutu
192	RG8608	M	MRAC	*G. gorilla*	*G. gorilla beringei*	mt Karissimbi
193	RG2263	F	MRAC	*G. gorilla*	*G. g. beringei*	Virunga

194	RG2257	M	MRAC	*G. gorilla*	*G. g. beringei*	Virunga
195	RG8187	M	MRAC	*G. gorilla*	*G. gorilla rex-pygmaerum*	Luofo
196	RG20085	M	MRAC	*G. gorilla*	*G. g. rex-pygmaerum*	Butembo MGL
197	RG15356	F	MRAC	*G. gorilla*	*G. g. rex-pygmaerum*	Ibatsero, terr. Lubero
198	RG15354	F	MRAC	*G. gorilla*	*G. g. rex-pygmaerum*	Ibatsero, terr. Lubero

Genus *Pan*

Specimen	Catalogue No	Sex	Museum	Species	Subspecies	Locality
1	AS53	M	IMAZ	*P. troglodytes*	*P.t.troglodytes*	?
7	AS1586	F	IMAZ	*P. troglodytes*	*P.t.troglodytes*	Cameroon
11	AS918	M	IMAZ	*P. troglodytes*	*P.t.troglodytes*	Cameroon
28	AS1745	F	IMAZ	*P. troglodytes*	*P.t.troglodytes*	?
38	AS6533	F	IMAZ	*P. troglodytes*	*P.t.troglodytes*	Liberia
40	AS1223	M	IMAZ	*P. troglodytes*	*P.t.troglodytes*	?
71	RG888	M	MRAC	*P. paniscus*		Kasai District
72	RG13201	F	MRAC	*P. paniscus*		Lingomo (Ikela), 350m
73	RG11149	M	MRAC	*P. paniscus*		Djolu (Lulonga?)
74	RG26945	M	MRAC	*P. paniscus*		Banalia?
75	RG26989	F	MRAC	*P. paniscus*		Banalia?
76	RG29066	F	MRAC	*P. paniscus*		Lubutu
77	RG28712	M	MRAC	*P. paniscus*		?
78	RG27699	M	MRAC	*P. paniscus*		Ponthierville, Congo
79	RG27698	F	MRAC	*P. paniscus*		Ponthierville, Congo
80	RG27696	M	MRAC	*P. paniscus*		Ponthierville, Congo
81	RG29036	M	MRAC	*P. paniscus*		?

82	RG29037	M	MRAC	*P. paniscus*		?
83	RG29047	M	MRAC	*P. paniscus*		Dongo, Yahuma
84	RG29040	F	MRAC	*P. paniscus*		Wamba, near Balangala
85	RG29045	F	MRAC	*P. paniscus*		Dongo, Yahuma
86	RG29052	M	MRAC	*P. paniscus*		Batiamoyowa, near Ponthierville
87	RG29050	M	MRAC	*P. paniscus*		Road Stanleyville, Yatolema
88	RG29059	F	MRAC	*P. paniscus*		Dongo, Oshwe (Kasai)
90	RG29063	M	MRAC	*P. paniscus*		Bolobo
91	RG29060	F	MRAC	*P. paniscus*		Dongo, Oshwe (Kasai)
92	RG29065	F	MRAC	*P. paniscus*		Djeka, Katako Kombe
93	84036M4	F	MRAC	*P. paniscus*		Yahuma, Yahuma
94	84036M10	F	MRAC	*P. paniscus*		?
95	84036M9	M	MRAC	*P. paniscus*		?
96	88041M3	F	MRAC	*P. paniscus*		Babusoko
99	88041M2	M	MRAC	*P. paniscus*		Babusoko
102	RG29034	F	MRAC	*P. paniscus*		?
103	RG29035	F	MRAC	*P. paniscus*		?
104	RG21697	F	MRAC	*P. paniscus*		?
105	RG11353	M	MRAC	*P. paniscus*		Chefferie Baolongo, Lopori
116	RG31489	M	MRAC	*P. troglodytes*	*P.t.verus*	Regio Tappi
117	RG31490	F	MRAC	*P. troglodytes*	*P.t.verus*	Regio Tappi
178	RG928	F	MRAC	*P. troglodytes*	*P.t.schweinfurthii*	Uele'
179	RG1048	F	MRAC	*P. troglodytes*	*P.t.schweinfurthii*	Uele'
180	RG2297	M	MRAC	*P. troglodytes*	*P.t.schweinfurthii*	Mawambi
181	RG4188	F	MRAC	*P. troglodytes*	*P.t.schweinfurthii*	Poko
182	RG8369	M	MRAC	*P. troglodytes*	*P.t.schweinfurthii*	Koteli
183	RG10448	F	MRAC	*P. troglodytes*	*P.t.schweinfurthii*	Buta

184	RG11362	M	MRAC	*P. troglodytes*	*P.t.schweinfurthii*	Moba
185	RG10447	M	MRAC	*P. troglodytes*	*P.t.schweinfurthii*	Buta
186	RG14219	M	MRAC	*P. troglodytes*	*P.t.schweinfurthii*	Budjala
187	RG27265	F	MRAC	*P. troglodytes*	*P.t.schweinfurthii*	Babundji, Ponthierville
188	RG27697	M	MRAC	*P. troglodytes*	*P.t.schweinfurthii*	Regio Digba, Terr Ango
189	Z4202	F	MRAC	*P. troglodytes*	*P.t.schweinfurthii*	?
190	RG35122	M	MRAC	*P. troglodytes*	*P.t.verus*	N. of Central Provence
191	RG35123	M	MRAC	*P. troglodytes*	*P.t.verus*	N. of Central Province
220	1968.7.5.8	M	NHM	*P. troglodytes*	*P.t.verus*	?
221	1924.8.6.1	M	NHM	*P. troglodytes*	*P.t.troglodytes*	?
222	1939.3363	M	NHM	*P. troglodytes*	*P.t.troglodytes*	?
223	1864.12.1.7	F	NHM	*P. troglodytes*	*P.t.troglodytes*	?
224	1939.3378	F	NHM	*P. troglodytes*	*P.t.troglodytes*	?
225	1901.8.9.10	M	NHM	*P. troglodytes*	*P.t.schweinfurthii*	?
226	1883.7.28.18	F	NHM	*P. troglodytes*	*P.t.troglodytes*	?
227	1939.3385	M	NHM	*P. troglodytes*	*P.t.troglodytes*	?

Genus *Homo*

Specimen	Catalogue	Sex	Museum	Species	Locality	Notes
5	AS25	M	IMAZ	*H. sapiens*	?	?
10	AS215	F	IMAZ	*H. sapiens*	?	?
14	AS216	M	IMAZ	*H. sapiens*	?	?
33	AS2191	F	IMAZ	*H. sapiens*	Africa	Negro
34	AS1207	M	IMAZ	*H. sapiens*	Africa	Negro
35	PAL98	F	IMAZ	*H. sapiens*	Africa	Negro

55	18.B.III.1	M	IMAZ	*H. sapiens*	Asia	Java
56	38.B.III.21	F	IMAZ	*H. sapiens*	Asia	Sumatra
57	19.B.III.2	M	IMAZ	*H. sapiens*	Asia	Malaysia
58	22.B.III.5	F	IMAZ	*H. sapiens*	Asia	Malaysia
59	838.B.I.205	M	IMAZ	*H. sapiens*	Europe	Romania
60	839.B.I.206	F	IMAZ	*H. sapiens*	Europe	Estonia
61	30.B.III.13	F	IMAZ	*H. sapiens*	Asia	Malaysia
62	27.B.III.10	M	IMAZ	*H. sapiens*	Asia	China
63	4549.AI.43	M	IMAZ	*H. sapiens*	?	?
64	4456.BV.108	F	IMAZ	*H. sapiens*	Maori	New Zealand
65	849.B.I.216	M	IMAZ	*H. sapiens*	Europe	Finland
66	1830BII218	M	IMAZ	*H. sapiens*	Africa	Herero
67	5665BII240	F	IMAZ	*H. sapiens*	Africa	Herero
68	5664BII239	F	IMAZ	*H. sapiens*	Africa	Herero
69	847.B.I.214	M	IMAZ	*H. sapiens*	Europe	Russia
70	846.B.I.213	M	IMAZ	*H. sapiens*	Europe	Russia
288	1735	M	Duckworth	*H. sapiens*	Africa	Somalia
289	AF15.0.5	M	Duckworth	*H. sapiens*	Africa	Somalia
290	AF15.0.9	F	Duckworth	*H. sapiens*	Africa	Somalia
291	AF23.0.36	M	Duckworth	*H. sapiens*	Africa	Haya
292	5	M	Duckworth	*H. sapiens*	Australia	Australia
293	2160	F	Duckworth	*H. sapiens*	Australia	Australia
294	2117	M	Duckworth	*H. sapiens*	Australia	Australia (South)
295	2132	F	Duckworth	*H. sapiens*	Australia	Australia (West)
296	2143	F	Duckworth	*H. sapiens*	Australia	Australia
297	9	M	Duckworth	*H. sapiens*	Australia	Australia
298	OC3.0.3	F	Duckworth	*H. sapiens*	Australia	Australia (Queensland)

299	2122	M	Duckworth	*H. sapiens*	Australia	Australia (South)
300	2154	M	Duckworth	*H. sapiens*	Australia	Australia (Queensland)
301	2137	M	Duckworth	*H. sapiens*	Australia	Australia
302	1177	F	Duckworth	*H. sapiens*	Europe	Finland
303	1247	M	Duckworth	*H. sapiens*	Europe	France
304	1049	F	Duckworth	*H. sapiens*	Europe	Austria
305	1155	M	Duckworth	*H. sapiens*	Europe	Czech Rep.
306	836	F	Duckworth	*H. sapiens*	Europe	UK
307	1203	F	Duckworth	*H. sapiens*	Asia	India
308	1704	F	Duckworth	*H. sapiens*	Asia	India
309	1703	F	Duckworth	*H. sapiens*	Asia	India
310	1218	M	Duckworth	*H. sapiens*	Asia	India
311	AF23.0.34	F	Duckworth	*H. sapiens*	Africa	Haya
312	AF23.0.32	M	Duckworth	*H. sapiens*	Africa	Haya
313	AF23.0.112	F	Duckworth	*H. sapiens*	Africa	Haya

Genus *Pongo*

Specimen	Catalogue	Sex	Museum	Species	Subspecies	Locality
22	AS1561	M	IMAZ	*P. pygmaeus*	*P. pygmaeus pygmaeus*	Borneo
23	AS1564	F	IMAZ	*P. pygmaeus*	*P. pygmaeus abelii*	Sumatra
24	AS1565	F	IMAZ	*P. pygmaeus*	*P. p. abelii*	Sumatra
27	AS1684	M	IMAZ	*P. pygmaeus*	*P. p. pygmaeus*	Borneo
32	AS1986	M	IMAZ	*P. pygmaeus*	*P. p. pygmaeus*	W-Borneo
118	1981/27	M	SCAP	*P. pygmaeus*	*P. p. pygmaeus*	W-Borneo
119	1981/25	M	SCAP	*P. pygmaeus*	*P. p. pygmaeus*	W-Borneo

120	1981/33	F	SCAP	*P. pygmaeus*	*P. p. pygmaeus*	W-Borneo
121	1981/28	F	SCAP	*P. pygmaeus*	*P. p. pygmaeus*	W-Borneo
122	1981/47	F	SCAP	*P. pygmaeus*	*P. p. pygmaeus*	W-Borneo
123	1981/45	M	SCAP	*P. pygmaeus*	*P. p. pygmaeus*	W-Borneo
124	1981/64	M	SCAP	*P. pygmaeus*	*P. p. pygmaeus*	W-Borneo
125	1981/62	M	SCAP	*P. pygmaeus*	*P. p. pygmaeus*	W-Borneo
126	1981/69	M	SCAP	*P. pygmaeus*	*P. p. pygmaeus*	W-Borneo
127	1981/70	M	SCAP	*P. pygmaeus*	*P. p. pygmaeus*	W-Borneo
128	1981/68	M	SCAP	*P. pygmaeus*	*P. p. pygmaeus*	W-Borneo
129	1981/78	F	SCAP	*P. pygmaeus*	*P. p. pygmaeus*	W-Borneo
130	1981/75	F	SCAP	*P. pygmaeus*	*P. p. pygmaeus*	W-Borneo
131	1981/74	F	SCAP	*P. pygmaeus*	*P. p. pygmaeus*	W-Borneo
132	1981/88	F	SCAP	*P. pygmaeus*	*P. p. pygmaeus*	W-Borneo
133	1981/90	F	SCAP	*P. pygmaeus*	*P. p. pygmaeus*	W-Borneo
134	1981/247	M	SCAP	*P. pygmaeus*	*P. p. abelii*	Sumatra
135	1981/248	F	SCAP	*P. pygmaeus*	*P. p. abelii*	Sumatra
145	1913/1467	F	ZSCM	*P. pygmaeus*	*P. p. abelii*	Sumatra
146	1913/1469	F	ZSCM	*P. pygmaeus*	*P. p. abelii*	Sumatra
147	1913/1465	M	ZSCM	*P. pygmaeus*	*P. p. abelii*	Sumatra
148	1913/1452	F	ZSCM	*P. pygmaeus*	*P. p. abelii*	Sumatra
161	1955/228	F	ZSCM	*P. pygmaeus*	*P. p. abelii*	Sumatra
162	1963/234	M	ZSCM	*P. pygmaeus*	*P. p. abelii*	Sumatra
163	1913/1466	M	ZSCM	*P. pygmaeus*	*P. p. abelii*	Sumatra
219	1980/346	F	NHM	*P. pygmaeus*	*P. p. abelii*	Sumatra

Genus *Hylobates*

Specimen	Catalogue No	Sex	Museum	Species	Locality
4	AS1532	M	IMAZ	*H. lar*	Thailand
8	AS1559	F	IMAZ	*H. lar*	Thailand
12	AS1538	M	IMAZ	*H. lar*	Thailand
18	AS1574	F	IMAZ	*H. lar*	Thailand
20	AS265	M	IMAZ	*S. syndactylus*	Sumatra
21	AS183	F	IMAZ	*S. syndactylus*	Sumatra
25	AS1579	F	IMAZ	*H. lar*	Thailand
26	AS1578	M	IMAZ	*H. lar*	Thailand
49	AS1738	M	IMAZ	*S. syndactylus*	?
50	AS1992	M	IMAZ	*S. syndactylus*	Malaysia
51	AS1734	M	IMAZ	*S. syndactylus*	Sumatra
136	1981/260	M	SCAP	*S. syndactylus*	W-Borneo
137	1981/259	M	SCAP	*S. syndactylus*	Sumatra
138	1981/307	M	SCAP	*S. syndactylus*	W-Borneo
139	1981/253	M	SCAP	*S. syndactylus*	W-Borneo
140	1981/251	M	SCAP	*S. syndactylus*	W-Borneo
141	1981/256	F	SCAP	*H. moloch*	N-Sarawak
142	1981/266	M	SCAP	*H. moloch*	W-Borneo
143	1981/275	M	SCAP	*H. moloch*	W-Borneo
144	1981/279	F	SCAP	*H. moloch*	W-Borneo
149	1981/280	F	SCAP	*H. moloch*	W-Borneo
150	1981/292	F	SCAP	*H. moloch*	W-Borneo
151	1981/284	M	SCAP	*H. moloch*	W-Borneo
152	1981/329	F	SCAP	*H. moloch*	W-Borneo
153	1981/326	M	SCAP	*H. moloch*	W-Borneo

154	1981/301	M	SCAP	*H. moloch*	W-Borneo
155	1981/293	F	SCAP	*H. moloch*	W-Borneo
156	1981/321	F	SCAP	*H. moloch*	W-Borneo
157	1981/314	F	SCAP	*H. moloch*	W-Borneo
158	1981/302	M	SCAP	*H. moloch*	W-Borneo
159	1981/311	M	SCAP	*H. moloch*	W-Borneo
160	1981/303	F	SCAP	*H. moloch*	W-Borneo
164	1904/21	F	ZSCM	*S. syndactylus*	Sumatra
165	1906/84a	M	ZSCM	*S. syndactylus*	Sumatra
166	1981/412	F	SCAP	*H. moloch*	N-Sarawak
167	1981/351	F	SCAP	*H. moloch*	W-Borneo
168	1908/3561	F	ZSCM	*S. syndactylus*	Sumatra
169	1964/231	F	ZSCM	*S. syndactylus*	Sumatra
170	1908/432	M	ZSCM	*S. syndactylus*	Sumatra
171	1981/317	M	SCAP	*H. moloch*	W-Borneo
172	1981/364	F	SCAP	*H. moloch*	N-Sarawak
173	1907/693	M	ZSCM	*S. syndactylus*	W-Borneo
174	1908/433	M	ZSCM	*S. syndactylus*	Sumatra
175	1908/434	M	ZSCM	*S. syndactylus*	Sumatra
176	1905/56	M	ZSCM	*S. syndactylus*	Sumatra
177	1905/60	F	ZSCM	*S. syndactylus*	Sumatra
199	ZD1920/1.26.2	F	NHM	*S. syndactylus*	Sumatra
200	ZD1881.3.15.1	M	NHM	*S. syndactylus*	Sumatra
201	ZD1920.1.26.1	M	NHM	*S. syndactylus*	Sumatra
202	ZD1919.11.12.1	M	NHM	*S. syndactylus*	Sumatra
203	ZD1906.10.4.1	M	NHM	*S. syndactylus*	Malaysia
204	ZD1867.4.12.5	M	NHM	*S. syndactylus*	?

205	ZD1919.11.12.2	F	NHM	*S. syndactylus*	Sumatra
206	ZD1938.11.30.5	F	NHM	*S. syndactylus*	Sumatra
207	ZD1955.1481	M	NHM	*S. syndactylus*	Malaya
212	1955.1494	M	NHM	*H. lar*	Thailand
213	1955.1489	M	NHM	*H. lar*	Malaya
214	1924.9.2.6	F	NHM	*H. lar*	Burma
215	1955.1497	M	NHM	*H. lar*	Thailand

Genus *Papio*

Specimen	Catalogue No	Sex	Museum	Species	Locality
248	1931.2.1.3	M	NHM	*P. ursinus*	SW-Africa
249	1906.5.12.2	F	NHM	*P. ursinus*	S-Africa
250	1927.2.11.3	M	NHM	*P. ursinus*	Mozambique
251	1908.1.1.2	F	NHM	*P. ursinus*	Mozambique
252	1955.1130	M	NHM	*P. ursinus*	Zambia
253	1927.2.11.4	F	NHM	*P. ursinus*	Mozambique
254	1925.1.2.1	M	NHM	*P. ursinus*	SW-Africa
255	1934.11.1.2	F	NHM	*P. ursinus*	S-Africa
256	1905.5.7.37	M	NHM	*P. ursinus*	S-Africa
257	1908.7.19.1	M	NHM	*P. ursinus*	Rhodesia
258	1964.2174	F	NHM	*P. anubis*	Ethiopia
259	1908.8.9.42	F	NHM	*P. anubis*	Uganda
260	1930.12.1.1	M	NHM	*P. anubis*	Uganda
261	1902.9.2.1	M	NHM	*P. anubis*	Sudan
262	1930.12.1.2	F	NHM	*P. anubis*	Uganda

263	1934.11.20.1	M	NHM	*P. anubis*	Ethiopia
264	1914.3.8.2	F	NHM	*P. anubis*	Sudan
265	1901.8.9.23	F	NHM	*P. anubis*	Kenya
266	1922.12.19.6	M	NHM	*P. anubis*	Zaire
267	1939.1035	F	NHM	*P. anubis*	?

Genus *Cercopithecus*

Specimen	Catalogue No	Sex	Museum	Species	Locality
41	6812	F	IMAZ	*C. aethiops*	?
228	1956.266	M	NHM	*C. aethiops*	Ghana
229	1956.264	F	NHM	*C. aethiops*	Ghana
230	1967.1146	M	NHM	*C. aethiops*	Ethiopia
231	1967.1148	F	NHM	*C. aethiops*	Ethiopia
232	1977.2768	M	NHM	*C. aethiops*	W-Africa
233	1911.2.12.1	F	NHM	*C. aethiops*	Sudan
234	1924.8.7.1	M	NHM	*C. aethiops*	Ethiopia
235	1954.757	F	NHM	*C. aethiops*	Uganda
236	1930.3.6.1	M	NHM	*C. aethiops*	Uganda
237	1972.27	F	NHM	*C. aethiops*	Kenya
238	1981.53	M	NHM	*C. mona*	Ghana
239	1956.388	F	NHM	*C. mona*	Ghana
240	1967.1714	M	NHM	*C. mona*	Cameroon
241	1948.469	M	NHM	*C. mona*	Cameroon
242	1948.460	F	NHM	*C. mona*	Cameroon
243	1948.466	F	NHM	*C. mona*	Cameroon

244	1938.7.7.9	M	NHM	*C. mona*	Cameroon
245	1966.6352	F	NHM	*C. mona*	Cameroon
246	1948.470	M	NHM	*C. mona*	Cameroon
247	1932.8.1.9	F	NHM	*C. mona*	Cameroon

Genus *Colobus*

Specimen	Catalogue No	Sex	Museum	Species	Locality
54	6057	M	IMAZ	*C. polykomos*	?
268	1956.344	F	NHM	*C. polykomos*	Ivory Coast
269	1956.343	F	NHM	*C. polykomos*	Ivory Coast
270	1971.2359	M	NHM	*C. polykomos*	Ivory Coast
271	1956.359	M	NHM	*C. polykomos*	Ghana
272	1956.346	F	NHM	*C. polykomos*	Ivory Coast
273	1956.349	M	NHM	*C. polykomos*	Ghana
274	1956.361	F	NHM	*C. polykomos*	Togo
275	1956.352	F	NHM	*C. polykomos*	Ghana
276	1935.10.22.5	F	NHM	*C. polykomos*	Ghana
277	1971.2367	M	NHM	*C. polykomos*	Ghana
278	1969.374	M	NHM	*C. angolensis*	Uganda
279	1902.1.2.20	F	NHM	*C. angolensis*	Kenya
280	1969.372	M	NHM	*C. angolensis*	Uganda
281	1930.11.11.9	M	NHM	*C. angolensis*	Zaire
282	1929.5.14.24	F	NHM	*C. angolensis*	Uganda
283	1951.364	F	NHM	*C. angolensis*	Tanganyka
284	1937.8.18.1	M	NHM	*C. angolensis*	Tanganyka

285	1938.4.21.2	F	NHM	*C. angolensis*	Tanganyka
286	1927.3.1.3	F	NHM	*C. angolensis*	Zaire
287	1927.3.1.2	M	NHM	*C. angolensis*	Zaire

Appendix II. CHARACTER DESCRIPTION

1. Accessory infraorbital foramen (IOF). This character scores the presence of one or more accessory foramina (*foramen infraorbitale accessorium*). The infraorbital foramen (*foramen infraorbitale*) is the external opening of the infraorbital canal that transmits the infraorbital nerve and vessels from the orbit to the face. It is located on the external surface of the maxilla, below the orbital margin. Accessory infraorbital foramina transmit accessory branches of the infraorbital nerve and vessels. The character states were scored as follows: accessory infraorbital foramina absent (0) and present (1) (Plate I-a).

2. Zygomatico-temporal foramen (ZTF). The zygomatico-temporal foramen (*foramen zygomaticotemporale*) transmits the zygomatico-temporal nerve from the orbit. It is generally located on the posteromedial temporal surface of the zygomatic near the base of the frontal process. It can be absent, single or multiple. This character scores the presence of one or more foramina: zygomatico-temporal foramina absent (0) and present (1) (Plate I-b).

3. Zygomatico-facial foramen (ZFF). The zygomatico-facial foramen (*foramen zygomaticofaciale*) transmits the zygomatico-facial nerve and vessels from the orbit to the face. It is located on the anterolateral surface of the zygomatic bone near the orbital border. The number of foramina is variable. This character scores the presence of one or more foramina: zygomatico-facial foramina absent (0) and present (1) (Plate I-c).

4. Posterior ethmoid foramen (PEF). The posterior ethmoid foramen (*foramen ethmoidale posterius*) transmits the posterior ethmoidal vessels to the anterior cranial fossa at the lateral edge of the cribriform plate. It is located posteriorly on the medial

wall of the orbit, on or near the fronto-ethmoid suture. This character scores the presence of one or more posterior ethmoid foramina: posterior ethmoid foramina absent (0) and present (1) (Plate I-d).

5. Mastoid foramen (MaF). This foramen (*foramen mastoideum*) transmits an emissary vein from the sigmoid sinus and a small dural branch of the occipital artery. The foramen can be absent, single or multiple. This character scores the presence of one or more foramina: mastoid foramina absent (0) and present (1) (Plate I-e).

6. Infraorbital notch (ION). This notch is an inconstant feature that appears on the lower margin of the orbit. I have never encountered its description in the literature so I could not find out what nerves and/or vessels it transmits. However, due to its anatomical position, I hypothesise that it carries branches of the infraorbital nerve and vessels from the orbit to the face. This character scores the presence of a notch: inferior orbital margin notch absent (0) and present (1) (Plate I-g).

7. Infraorbital bridge (IOB). Sometimes a spine forms over the inferior orbital margin notch to form a more or less complete bridge. This character scores the presence of a complete bridge: inferior orbital margin bridge absent (0) and present (1) (Plate I-c).

8. Infraorbital canal internal opening, anterior (ICIO). The orbital opening of the infraorbital canal is located on the orbit floor in variable positions. This character scores the position of this opening as anterior and close to the orbital margin (0) or away from the orbital margin (1) (Plate I-f).

9. Infraorbital groove (IOG). This groove (*sulcus infraorbitale*) on the orbital floor carries the infraorbital nerve and vessels. It sinks into the orbital floor to become the infraorbital canal, opening at the infraorbital foramen. This character scores the presence of a groove: infraorbital groove absent (0) and present (1) (Plate I-f).

10. Supralacrimal structures (SLGB). These structures are located on the medial wall of the orbit at the level of, or slightly above, the lacrimal bone. They generally occur in the form of an antero-posteriorly directed groove, sometimes covered by a bony bridge to form a short canal. I have never come across these features in the literature I have studied so its function is unknown. However, due to its proximity to the anterior ethmoid foramen I suspect that it transmits branches of the nasociliary nerve and ethmoid vessels. This character scores the presence of a supralacrimal groove or bridge: supralacrimal structures absent (0) and present (1).

11. Supraorbital notch (SON). This feature (*incisura supraorbitale*) transmits the supraorbital nerve and vessels (artery) and it is usually located on the upper border of the orbit. The number, position and size of notches are variable. This character scores the presence of a notch: supraorbital notch absent (0) and present (1) (Plate I-h).

12. Supraorbital foramen (SOF). The supraorbital notch can develop to form a complete foramen (*foramen supraorbitale*). Also in this case the number, position and size of foramina are variable. This character scores the presence of a complete foramen: supraorbital foramen absent (0) and present (1) (Plate I-h).

13. Zygomatico-temporal foramen position 1, sutural ($ZTFP_1b$). Zygomatico-temporal foramina are located on the zygomatico-frontal suture, on the zygomatic bone or on the frontal bone. This character scores occurrence of foramina on the suture as absent (0) or present (1) (Plate I-b).

14. Zygomatico-temporal foramen position 1, zygomatic ($ZTFP_1c$). This character scores the occurrence of zygomatico-temporal foramina on the frontal process of the zygomatic bone as absent (0) or present (1) (Plate I-b,o).

15. Zygomatico-temporal foramen position 1, frontal ($ZTFP_1a$). This character scores the occurrence of zygomatico-temporal foramina on the zygomatic process of the frontal bone as absent (0) or present (1) (Plate I-b).

16. Zygomatico-temporal foramen position 2, posterior bar ($ZTFP_2b$). Zygomatico-temporal foramina are located either on the anterior aspect of the orbital bar or on the posterior aspect of the orbital bar. This characters scores the occurrence of foramina on the posterior aspect of the orbital bar as absent (0) or present (1) (Plate I-b).

17. Zygomatico-temporal foramen position 2, anterior bar ($ZTFP_2$). This character scores the occurrence of zygomatico-temporal foramina on the anterior aspect of the orbital bar as absent (0) or present (1) (Plate I-b).

18. Zygomatico-orbital foramen position, sutural (ZOFPb). The orbital openings of the zygomatico-temporal canals are named here zygomatico-orbital foramina. The position of these openings can be on the frontal bone, on the suture or on the zygomatic bone. This character scores the occurrence of zygomatico-orbital foramina on the suture as absent (0) or present (1) (Plate I-f).

19. Zygomatico-orbital foramen position, frontal (ZOFPa). This characters scores the occurrence of zygomatico-orbital foramina on the frontal bone as absent (0) or present (1) (Plate I-f).

20. Zygomatico-orbital foramen position, zygomatic (ZOFPc). This characters scores the occurrence of zygomatico-orbital foramina on the zygomatic bone as absent (0) or present (1) (Plate I-f).

21. Zygomatico-facial notch (ZFN). This notch (*incisura zygomaticofaciale*) appears on the lateral margin of the orbit, on the zygomatic bone. It can be considered as an

incomplete zygomatico-facial foramen. This character scores the presence of a notch: zygomatico-facial notch absent (0) and present (1).

22. Zygomatico-facial foramen position, zygomatic (ZFFPc). The zygomatico-facial foramina are located on the corpus of the zygomatic bone, or on the spheno-frontal process of the zygomatic bone. This character scores the occurrence of zygomatico-facial foramina on the spheno-frontal process of the zygomatic bone as absent (0) or present (1) (Plate I-c).

23. Zygomatico-facial foramen position, corpus (ZFFPa,b). This character scores the occurrence of zygomatico-facial foramina on the corpus of the zygomatic bone as absent (0) or present (1) (Plate I-c).

24. Anterior ethmoid foramen position, sutural (AEFP). This foramen (*foramen ethmoidale anterius*) transmits the nasociliary nerve and the anterior ethmoidal vessels to the anterior cranial fossa at the lateral edge of the cribriform plate. It is located on, or close to, the fronto-ethmoid suture. This character was scored as extra-sutural (0) or sutural (1) (Plate I-d).

25. Foramen rotundum (FRo). This foramen transmits the maxillary nerve V^2. It is located in the greater wing of the sphenoid behind the medial end of the superior orbital fissure. Originally part of the superior orbital fissure, it is secondarily separated and this separation can be complete or incomplete. This character scores the presence of a complete foramen rotundum: foramen rotundum incomplete (0) foramen rotundum complete (1) (Plate I-z).

26. Occipital foramen (OcF). The occipital foramen (*foramen occipitale*, *sensu* Boyd, 1938) is an emissary foramen in the region of the inion, close to or on the mid-line: occipital foramen absent (0) and present (1) (Plate I-ae).

27. Posterior ethmoid foramen position, sutural (PEFPb). The posterior ethmoid foramen occurs either on the fronto-ethmoidal suture or on the frontal bone. This character scores the position of the posterior ethmoid foramen on the suture as absent (0) or present (1) (Plate I-d).

28. Superior orbital fissure (SOFi). This character scores the presence of a slightly to well-developed superior orbital fissure as absent (0) or present (1) (Plate I-z).

29. Posterior ethmoid foramen position, frontal (PEFPa). This character scores the position of the posterior ethmoid foramen on the frontal bone as absent (0) or present (1) (Plate I-d).

30. Middle meningeal arteries emissaries (MMAE). This character scores the presence of the middle meningeal artery emissaries as absent (0) or present (1) (Plate I-ag).

31. Mastoid foramen position, sutural (MaFPb). This foramen is located near the posterior margin of the petromastoid part of the temporal bone. The external opening can occur on the mastoid bone, the occipital bone, or the suture in between. This character scores the presence of mastoid foramina on the mastoid-occipital suture as absent (0) or present (1) (Plate I-e).

32. Mastoid foramen position, mastoid (MaFPa). This character scores the presence of mastoid foramina on the mastoid bone as absent (0) or present (1) (Plate I-e).

33. Mastoid foramen position, occipital (MaFPc). This character scores the presence of mastoid foramina on the occipital bone as absent (0) or present (1) (Plate I-e).

34. Stylomastoid bridge (SMB). This bridge is an inconstant feature that occurs on the posterolateral margin of the stylomastoid foramen. I have never encountered its description in the literature so its function seems to be unknown. However, due to its

position I suggest that it encloses any of the neural or venous parts that pass through the stylomastoid foramen (*foramen stylomastoideum*). The latter transmits the facial nerve VII and stylomastoid branch of the posterior auricular artery. The foramen also contains the stylomastoid artery. This character scores the presence of a complete bridge: stylomastoid bridge absent (0) and present (1) (Plate I-r).

35. Stylomastoid foramen position (SMFP). The position of the stylomastoid foramina was scored as anterior (0) or posterior (1) with respect to the biporionic line on a plane perpendicular to the orbital plane (Plate I-aj).

36. Parietal foramen, parietal (PaF_1). This foramen (*foramen parietale*) transmits a vein from the sagittal sinus and a branch of the occipital artery. It is usually, but not always located on the parietal bones, posteriorly and close to the sagittal plane. However it can also occur on the mid-parietal suture and on the occipital bone. This character scores the occurrence of parietal foramina on the parietal bones as absent (0) or present (1) (Plate I-i).

37. Parietal foramen, sutural (PaF_2). This character scores the occurrence of parietal foramina on the mid-parietal suture as absent (0) or present (1) (Plate I-i).

38. Parietal foramen, occipital (PaF_3). This character scores the occurrence of parietal foramina on the occipital bone as absent (0) or present (1) (Plate I-i).

39. Carotid canal position, posterior to the biporionic line ($CaCP_1$). The position of the carotid canal was scored as anterior (0) or posterior (1) relative to the biporionic line (Plate I-aj).

40. Carotid canal, position relative to Basion ($CaCP_2$). This character scores the position of the carotid canal relative to a plane parallel to the orbital plane and through Basion. It was scored as on the plane (0) or not on the plane (1) (Plate I-aj).

41. Infraorbital foramen size (IOFSz). By 'size of a foramen' I refer to the surface area of the external orifice of the main foramen. This was computed by approximating the shape of the foramen to the shape of an ellipse. For this purpose, two measurements were taken: the maximum diameter on the short axis (D) and the length of the diameter perpendicular to it (L). The area was then calculated using the well-known formula for the area of an ellipse:

$$Area = \left(\frac{\pi}{4}\right) \times L \times D$$

Diameters up to 1.3mm were measured using graduated fishing wires and guitar strings. These ranged from 0.1 to 1.3mm. Diameters bigger than 1.3 mm were measured using the internal digital callipers. This character evaluates the size of the main infraorbital foramen.

42. Zygomatico-temporal foramen size (ZTFSz). This character calculates the area of the main zygomatico-temporal foramen.

43. Zygomatico-facial foramen size (ZFFSz). This character calculates the area of the main zygomatico-facial foramen.

44. Mastoid foramen size (MaFSz). This character calculates the area of the main mastoid foramen.

45. Stylomastoid foramen size (SMFSz). This character calculates the area of the stylomastoid foramen.

46. Carotid canal size (CaCSz). This character calculates the area of the carotid canal.

47. Jugular foramen length (JuFL). In the case of the jugular foramen, it was not possible to estimate the surface area of the external orifice of a canal due to the irregular shape of the foramen. Therefore, only one measurement was taken to

quantify its 'length'. This measurement is defined as the chord distance from the margins of the jugular notch on the occipital bone.

48. Hypoglossal canal size (HyCSz). This character calculates the area of the hypoglossal canal.

49. Foramen ovale size (FOvSz). This character calculates the area of the foramen ovale.

50. Greater palatine foramen size (GPFSz). This character calculates the area of the greater palatine foramen.

51. Lesser palatine foramen size (LPFSz). This character calculates the area of the main lesser palatine foramen.

52. Mental foramen size (MeFSz). This character calculates the area of the main mental foramen.

53. Mandibular foramen size (MbFSz). This character calculates the area of the mandibular foramen.

54. Infraorbital foramen position, minimum distance from zygomaxillary suture ($IOFP_1$). This is the first of three variables used to quantify the position of the infraorbital foramen. It measures the minimum distance of the foramen from the zygomaxillary suture. The shape of this suture is variable within and across species, so this measurement may not be a very good representative of the 'average' distance of the foramen to the suture. With this in mind another variable was introduced and this is described next (Plate I-al).

55. Infraorbital foramen position, transverse distance from zygomaxillary suture ($IOFP_2$). This variable measures the distance of the most lateral point on the foramen to the zygomaxillary suture orienting the callipers on a plane perpendicular to the orbital plane (Plate I-al).

56. Mandibular foramen position, distance to Gonion ($MbFP_1$). This foramen (*foramen mandibulae*) transmits the inferior alveolar nerve V^3 and inferior alveolar vessels. It is located on the internal surface of the mandibular ramus. This character measures the chord distance from the mandibular foramen to Gonion.

57. Foramen magnum size (FMaSz). This character calculates the area of the foramen magnum (Plate I-am).

58. Incisive canal diameter (InCL). In this case, it was not possible to estimate the surface area of the external orifice of a canal due to the irregular shape of the foramen. Therefore only one measurement was taken to quantify its 'length'. This measurement is defined as the maximum width of the incisive foramen parallel to the sagittal plane.

59. Mental foramen position ($MeFP_1$). The height of the main mental foramen on the mandibular corpus was expressed as the percentage ratio of two measurements: the height of the mandibular corpus holding the callipers on a plane perpendicular to the alveolar process through the mental foramen (H_C); the minimum distance of the superior border of the foramen from the alveolar process on the same plane (H_M) (Plate I-an). The position of the foramen was then calculated as:

$$MeFP_1 = \frac{H_M}{H_C} \times 100$$

60. Incisive canal position (InCP). This variable quantifies the position of the incisive foramen on the palate. Two measurements were taken: the chord distance of the most posterior point of the foramen to the palatomaxillary suture on the midline (D_S); the chord distance of the same point on the foramen margin to Supradentale (D_I) (Plate I-aj). The position of the incisive canal was then expressed as:

$$InCP = \frac{D_I}{D_S} \times 100$$

61. Infraorbital foramen, position ($IOFP_3$). This is the last of the three variables used to quantify the position of the infraorbital foramen on the maxilla. It describes the height of the largest infraorbital foramen along the body of the maxilla. Two measurements were taken following Ashton and Zuckerman (1958): the distance of the superior border of the external foramen to the lower border of the orbit measured holding the callipers in a direction parallel to the sagittal plane (H_O); the distance of the inferior border of the external foramen to the alveolar process holding the callipers in a direction parallel to the sagittal plane (H_A) (Plate I-k). The position of the infraorbital foramen is then expressed as the percentage ratio of H_O to H_A:

$$IOFP_3 = \frac{H_O}{H_A} \times 100$$

62. Infrajugular process expression (IJPE). This process is the most constant protuberance in the petrous part of the temporal bone, and it divides the jugular foramen into an anterior and a posterior part. This character scores the presence of a moderately and strongly expressed process: infrajugular process absent (0) and present (1) (Plate I-k).

63. Hypoglossal canal divisions (HyC). The hypoglossal canal (*canalis hypoglossi*) transmits the hypoglossal nerve (XII) and the meningeal branch of the ascending pharyngeal artery. It is located anteriorly and above the occipital condyles. This canal can be single or divided into multiple canals. The division of the hypoglossal canals can be complete (laminar) or partial (spinal). The divisions were scored as absent (0) i.e. single canal, or present (1) i.e. multiple canals (Plate I-k).

64. Intermediate condylar canal (ICC). The intermediate condylar canal (*canalis condylaris intermedius*) is an osseous canal of variable diameter and length located on the exocranial surface of the occipital, lateral to the occipital condyle. Its anterior opening is located near the anterior opening of the hypoglossal canal, while its

posterior opening is near the condylar canal or the condylar fossa. This character scores the presence of a partial or complete canal: intermediate condylar canal absent (0), partial or complete canal present (1) (Plate I-s,w).

65. Condylar canal (CoC). The condylar canal (*canalis condylaris*) is an inconstant canal that transmits a sigmoid emissary vein. The inner aperture is located at the end of the sigmoid sinus groove; the external opening is situated on the floor of the condylar fossa. This character scores the presence of a canal: condylar canal absent (0) and present (1).

66. Condylar canal, jugular opening (CoCO). The condylar canal can open into the jugular foramen (Braga, 1995). This character scores the position of the internal opening of the condylar canal: opening on the sigmoid sinus groove (0) and opening in the jugular foramen (1).

67. Craniopharyngeal canal (CPC). The craniopharyngeal canal (*canalis craniopharyngeus*) transmits vessels between the mucose of the fornix pharyngis and the hypophyseal fossa, but also some nerves connected to the dura mater. The endocranial opening is in the pituitary fossa, while the exocranial opening can be found in the region where the external base of the cranium forms the roof of the pharyngeal cavity. This character scores the presence of a canal: craniopharyngeal canal absent (0) and present (1) (Plate I-p).

68. Marginal foramen (MgF). This structure (*foramen marginale*) is formed when a groove that runs towards the lateral margin of the tympanic plate is converted into a foramen by a bony bridge. It transmits a small branch of the auricolo-temporal nerve. This character scores the presence of a marginal foramen: marginal foramen absent (0) and present (1).

69. Foramen ovale (FOv). The foramen ovale (also known as *foramen venosum*) transmits the mandibular nerve (V^3), an accessory meningeal artery, and often the lesser petrosal nerve. It is located on the greater wing of the sphenoid, posterior to the foramen rotundum. It can appear as several different variants. Here, only its complete morphology, with a fully formed lateral wall, was scored as present (1). All other morphologies were scored as absent (0) (Plate I-j,y,ad).

70. Foramen ovale, position (FOvP). The position of the foramen ovale was scored as extra-sutural (0) or sutural (1). The suture in consideration is the sphenotemporal suture (Plate I-ae).

71. Median basilar canal (MBC). The median basilar canal (*canalis basilaris medianus*) pierces the posterior portion of the basilar part of the occipital bone. It allows the passage of an emissary vein (Braga, 1995). This character scores the presence of a median basilar canal: canal absent (0) and present (1).

72. Jugular bridging (JuB). The jugular foramen transmits the inferior petrosal sinus and the sigmoid sinus to the internal jugular vein, the glossopharyngeal nerve (IX), the vagus nerve (X), the spinal accessory nerve (XI), the meningeal branch of occipital artery, the meningeal branch of ascending pharyngeal artery and the ascending pharyngeal artery. It is located at the posterior end of the petro-occipital suture and it is a large irregular hiatus between the occipital and petrous bones. Its long axis is directed anteromedially. Its anterior part contains the inferior petrosal sinus, its intermediate part the glossopharyngeal, vagus and accessory nerves and its posterior part the internal jugular vein. Protuberances of various sizes and shapes can project from the basilar part of the occipital bone and petrous part of the temporal bone, more or less deep into the foramen jugulare. These protuberances can form bony bridges more or less complete across the foramen (*ponticuli foraminis*

jugularis). This character scores the presence of these bridges. This character scores the presence of partial or complete bony bridges across the jugular foramen: jugular bridging absent (0) and present (1) (Plate I-t).

73. Foramen magnum shape, round (FMaS). This character scores the shape of the foramen magnum as: not round (0) and round (1) (Plate I-am).

74. Foramen magnum position, posterior to stylomastoids ($FMaP_2$). The position of the foramen magnum was scored relative to a line through the stylomastoid foramina as anterior to/on the line (0) or posterior to the line (1), on a plane perpendicular to the orbital plane (Plate I-aj).

75. Foramen magnum position, posterior to biporionic line ($FMaP_1$). The position of the foramen magnum was scored relative to the biporionic line as anterior to/on the line (0) or posterior to the line (1), on a plane perpendicular to the orbital plane (Plate I-aj).

76. Innominate canal (InF). This is an inconstant canal that appears posteromedial to the foramen ovale. When present it transmits the lesser petrous nerve. This character scores the presence of an innominate canal: canal absent (0) and present (1).

77. Foramen spinosum (FSp). The foramen spinosum (also *foramen petrosum*) transmits middle meningeal vessels and a recurrent branch of nerve (V^3). It is located posterolateral to the foramen ovale. It manifests itself in many different forms, with more or less complete walls. This character was scored as incomplete (0) when it presented partially developed walls, or complete (1) when it showed fully developed walls (Plate I-j,y,ad).

78. Foramen of Vesalius (FVe). This foramen forms from the anterior margin of the foramen ovale and it transmits either the whole or part of the venous portion of the foramen ovale. Its expression is variable in the degree of separation from the oval

foramen. This character scores a fully formed foramen of Vesalius as present (1). All other morphologies were scored as absent (0) (Plate I-ab).

79. Pterygo-spinous bridge (PSB). This bridge (*ponticulus pterygospinosus*) derives from secondary ossification of the pterygo-spinous ligament, which extends from the sphenoid spine to the pterygospinous process, on the posterior border of the lateral pterygoid lamina. The bridge can be more or less complete. Here it was scored as absent (0) when absent or incomplete, and present (1) when complete (Plate I-l).

80. Pterygo-alar bridge (PAB). This bridge (*ponticulus pterygoalari*) derives from secondary ossification of the pterygo-alar ligament, which extends from the sphenoid wing to the pterygospinous process, on the posterior border of the lateral pterygoid lamina. The bridge can be more or less complete. Here it was scored as absent (0) when absent or incomplete, and present (1) when complete.

81. Foramen spinosum position (FSpP). The position of the foramen spinosum was scored as extra-sutural (0) or sutural (1). The suture in consideration is the sphenotemporal suture (Plate I-j).

82. Foramen lacerum (FLa). This foramen transmits the internal carotid artery and accompanying sympathetic and venous plexuses. It is a short canal completely traversed by meningeal branches of the ascending pharyngeal artery. This character scores the presence of a foramen lacerum: foramen lacerum absent (0) and present (1) (Plate I-j,y).

83. Squamosal foramen (RAC_2). Inconstant foramen that perforates the temporal squama above the posterior root of the zygomatic arch, transmitting a vessel from the petro-squamous sinus. This character scores the presence of a squamosal foramen: squamosal foramen absent (0) and present (1).

84. Postglenoid foramen (RAC_1). Inconstant foramen located anterior to the external acoustic meatus in the line of fusion of the temporal squama and tympanic part. It transmits a vessel from the petro-squamous sinus. This character scores the presence of a postglenoid foramen: postglenoid foramen absent (0) and present (1) (Plate I-af).

85. Greater palatine foramen position (GPFP). This foramen (*foramen palatinum majus*) transmits the greater palatine nerve (V^2) and descending palatine vessels. It is located near the lateral palatal border close to the palatomaxillary suture. This character scores the position of the greater palatine foramen as extra-sutural (0) or sutural (1) (Plate I-ah).

86. Palatine crests (PCr). These are bony spicules on the palatine bone that mark the passage of palatine nerves and vessels. This character scores the presence of palatine crests: palatine crests absent (0) and present (1).

87. Lesser palatine foramina (LPF). These foramina pierce the palatine pyramidal process and transmit the lesser palatine nerve (V^2) and lesser palatine vessels. This character scores the presence of lesser palatine foramina: lesser palatine foramina absent (0) and present (1) (Plate I-ah).

88. Lesser palatine foramen position (LPFP). The position of the main lesser palatine foramen was also scored as extra-sutural (0) or sutural (1) (Plate I-ah).

89. Accessory mental foramen (MeF). The mental foramen (*foramen mentale*) transmits the mental nerve (V^3) and mental vessels. It is located on the external surface of the mandibular corpus. This character scores the presence of an accessory mental foramen: accessory foramen absent (0) and present (1) (Plate I-x).

90. Mandibular foramen position ($MbFP_2$). The position of the mandibular foramen was also scored as below (0) or above (1) the dental row.

91. Serres canal (SeC). This feature is generally located behind and slightly below the mandibular foramen. It transmits the basal mandibular vein. This character scores the presence of a Serres canal: canal absent (0) and present (1) (Plate I-v).

92. Molar foramen (MoF). This foramen (*foramen molare*) is situated antero-superior to the mandibular foramen. It represents a separate neurovascular canal for the third molar. This character scores the presence of a foramen: molar foramen absent (0) and present (1).

93. Retromolar foramen (RMF). Located in the retromolar fossa, the *foramen retromolare* transmits neurovascular bundles. This character scores the presence of a retromolar foramen: retromolar foramen absent (0) and present (1).

94. Robinson canal (RoC). Located in the retromolar triangle, this foramen transmits an artery and a nerve for the alveolar region of the third molar. This character scores the presence of a Robinson canal: Robinson canal absent (0) and present (1) (Plate I-u).

95. Mylohyoid bridge (MyB). The mylohyoid bridge (*ponticulus mylohyoideus)* is a bony formation that transforms the mylohyoid groove into a canal of variable length. This canal serves for the passage of the mylohyoid nerve (a muscular branch of the inferior alveolar nerve). It is located on the posterior surface of the mandible, on the mandibular ramus. The character scores the presence of a bridge: Mylohyoid bridge absent (0) and present (1).

96. Clinoidescaroticum foramen (CSF). This foramen transmits the internal carotid artery as it leaves the cavernous sinus. It is formed when the anterior clinoid process is connected to the middle clinoid process by a thin osseous bar, completing a foramen around the internal carotid artery. Its morphology can be more or less complete. Here only complete foramina were scored as present (1). All other variants

were scored as absent (0). This trait is located inside the cranium so it was observed inserting a dental mirror into the skull from the foramen magnum.

97. Posterior clinoid foramen (PCF). This foramen is formed when an osseous bar joints the posterior clinoid process with the basilar part of the occipital bone. It can exist in various forms. Here only the complete morphology was scored as present (1). All other variants were scored as absent (0). I have never encountered the description of this structure in the literature so I don't know its function.

98. Inferior orbital fissure foramen (IFF). The inferior orbital fissure (*fissura orbitalis inferior*) transmits maxillary nerve (V^2), zygomatic nerve, infraorbital vessels and communicating branch from inferior ophtalmic vein. Sometimes a foramen is formed at the lateral end of the fissure on the orbit floor. I have been unable to determine the function of this foramen. However, from its location I can speculate that it forms around some of the nerves and vessels transmitted through the inferior orbital fissure. This character scores the presence of a complete foramen: inferior orbital fissure foramen absent (0) and present (1) (Plate I-if).

99. Mental foramen position relative to P_3 ($MeFP_2$). The position of the mental foramen relative to the lower third premolar was scored as not under P_3 (0) or under P_3 (1) (Plate I-ai).

100. Incisive canal, single or double (InC). This canal (*canalis incisiva*) transmits the nasopalatine nerve and the descending septal artery. It is located anteriorly on the palatal process of the maxilla. It can be single or multiple. This character was scored as: incisive canal multiple (0) and single (1) (Plate I-n,aa).

101. Palatine fenestrae (PFn). These are two large openings on the palatal process of the maxilla that connect the oral cavity with the nasal cavity (Schwartz, 1983). They

transmit the nasopalatine nerve and vessels. This character scores the presence of palatine fenestrae: palatine fenestrae absent (0) and present (1) (Plate I-m).

102. Stylomastoid foramen shape, round (SMFS). This character scores the shape of the stylomastoid foramen as: not round (0) and round (1).

103. Infraorbital foramen shape, round (IOFS). This character scores the shape of the infraorbital foramen as: not round (0) and round (1).

104. Carotid canal shape, round (CaCS). This character scores the shape of the carotid canal as: not round (0) and round (1).

105. Greater palatine foramen shape, round (GPFS). This character scores the shape of the greater palatine foramen as: not round (0) and round (1).

106. Mental foramen shape, tear-shaped (MeFS). This character scores the shape of the mental foramen as: not tear-shaped (0) and tear-shaped (1).

107. Zygomaticotemporal foramen shape, round (ZTFS). This character scores the shape of the zygomaticotemporal foramen as: not round (0) and round (1).

108. Mastoid foramen shape, round (MaFS). This character scores the shape of the mastoid foramen as: not round (0) and round (1).

109. Lesser palatine foramen shape, round (LPFS). This character scores the shape of the lesser palatine foramen as: not round (0) and round (1).

110. Mandibular foramen shape, round (MbFS). This character scores the shape of the mandibular foramen as: not round (0) and round (1).

111. Zygomaticofacial foramen shape, round (ZFFS). This character scores the shape of the zygomaticofacial foramen as: not round (0) and round (1).

112. Supragenial bridge (SGB). This is a bony bridge located superior to the mental spine in the internal surface of the mandibular body. This character scores the presence of a complete bridge: supragenial bridge absent (0) and present (1).

Plate I – PHOTOS OF CHARACTERS

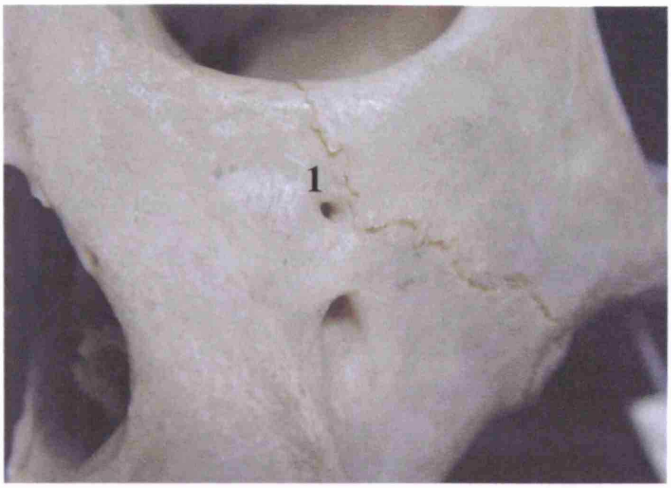

Plate I-a

Character 1 – Accessory infraorbital foramen (present)

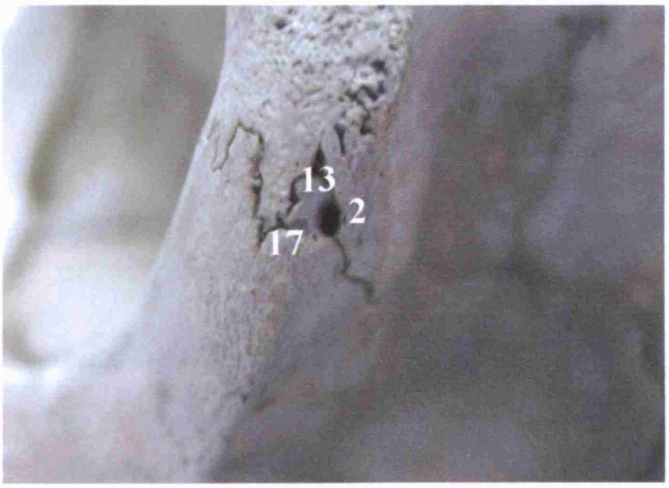

Plate I-b

Character 2 – Zygomatico-temporal foramen (present)
Character 13 – Zygomatico-temporal foramen, sutural
Character 17 – Zygomatico-temporal foramen on bar

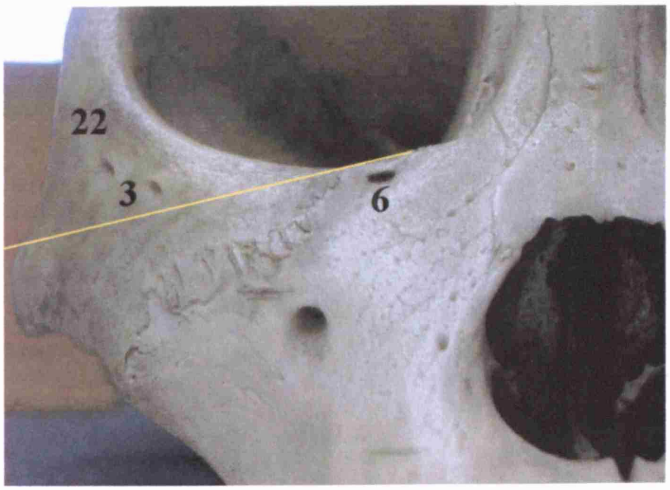

Plate I-c

Character 3 – Zygomatico-facial foramina (present)
Character 6 – Infraorbital bridge (present)
Character 22 – Zygomatico-facial foramen, zygomatic

Plate I-d

Character 4 – Posterior ethmoid foramen (present)
Character 24 – Anterior ethmoid foramen (extra-sutural)
Character 27 – Posterior ethmoid foramen sutural

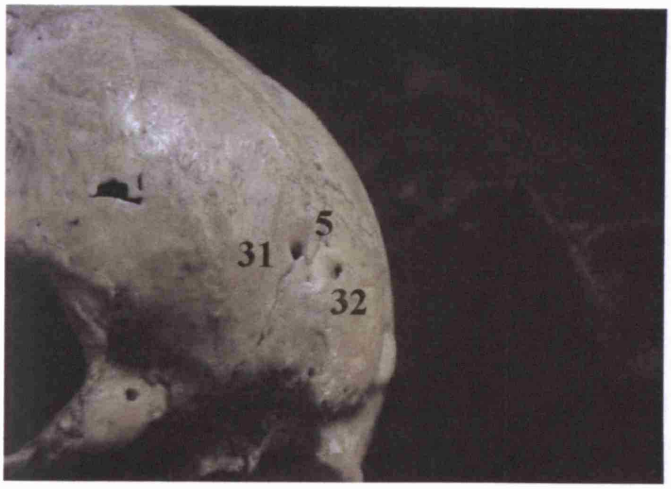

Plate I-e

Character 5 – Mastoid foramina (present)
Character 31 – Mastoid foramen, sutural
Character 32 – Mastoid foramen, mastoid

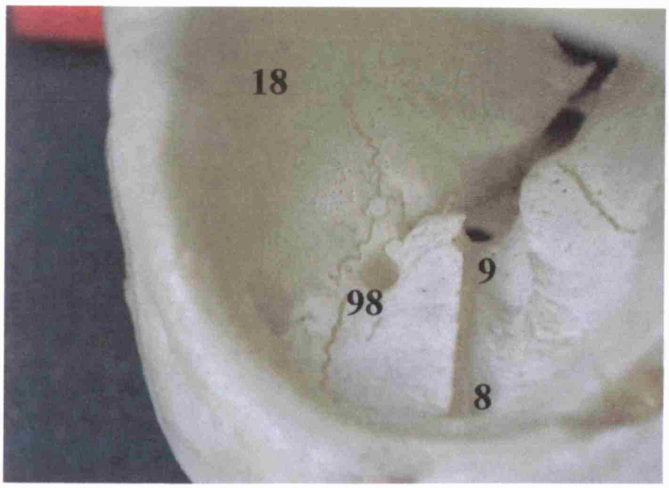

Plate I-f

Character 8 – Infraorbital canal, anterior internal opening
Character 9 – Infraorbital groove (present)
Character 18 – Zygomatico-orbital foramen, sutural
Character 98 – Inferior orbital fissure foramen

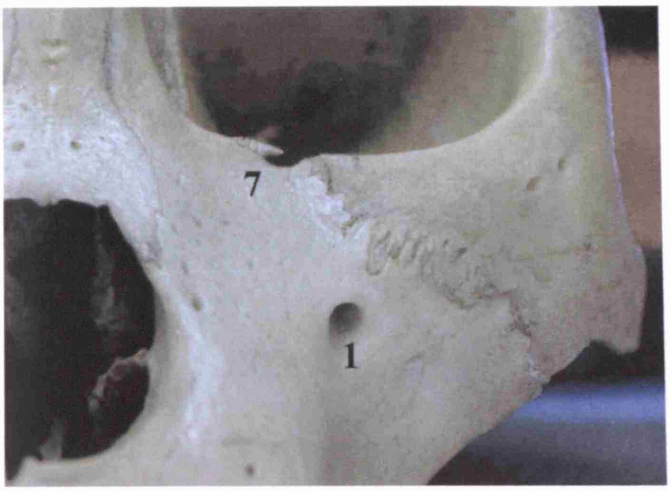

Plate I-g

Character 1- Accessory infraorbital foramen (absent)
Character 7 – Infraorbital notch

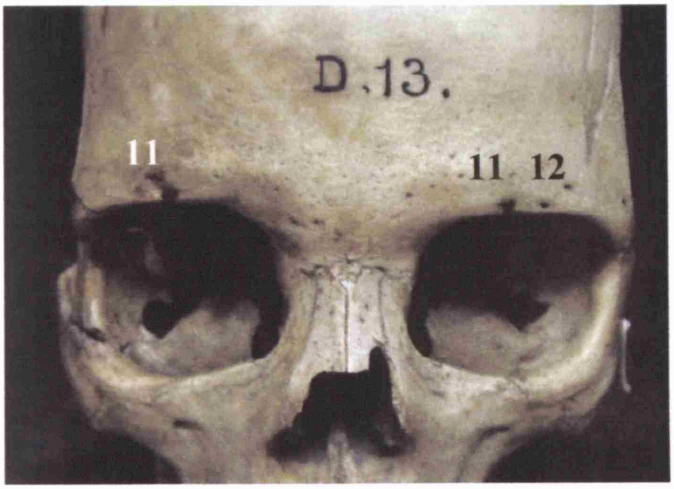

Plate I-h

Character 11 – Supraorbital notch
Character 12 – Supraorbital foramen

Plate I-i

Character 36 – Parietal foramen

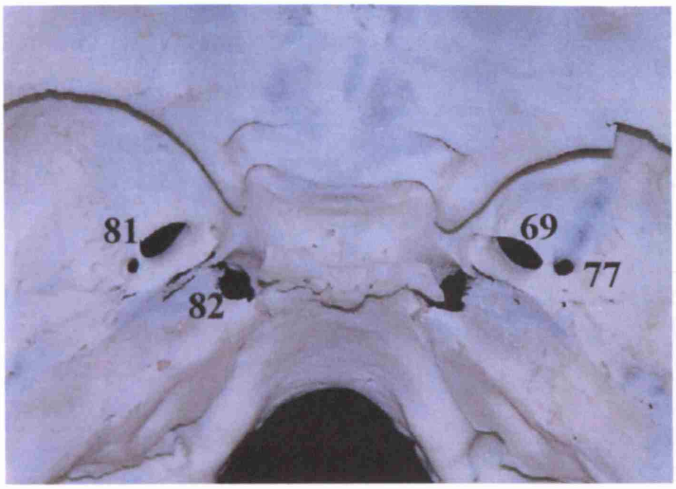

Plate I-j

Character 69 – Foramen ovale, complete medial wall
Character 77 – Foramen spinosum, complete medial wall
Character 81 – Foramen spinosum position
Character 82 – Foramen lacerum (present)

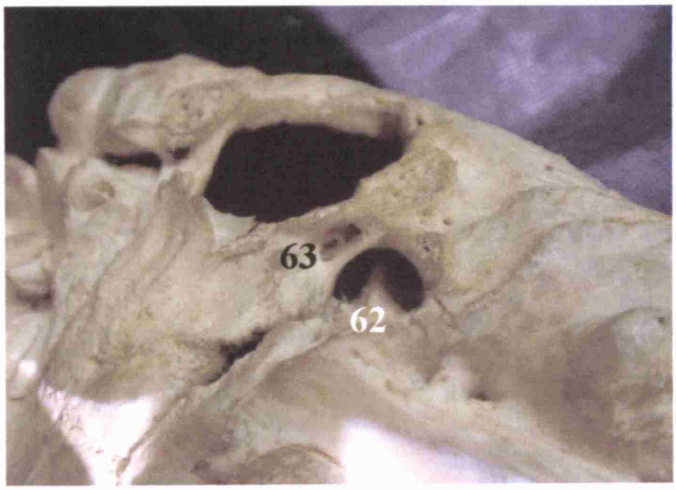

Plate I-k

Character 62 – Infrajugular process expression
Character 63 – Hypoglossal canal divisions (present)

Plate I-l

Character 79 – Pterygospinous bridge

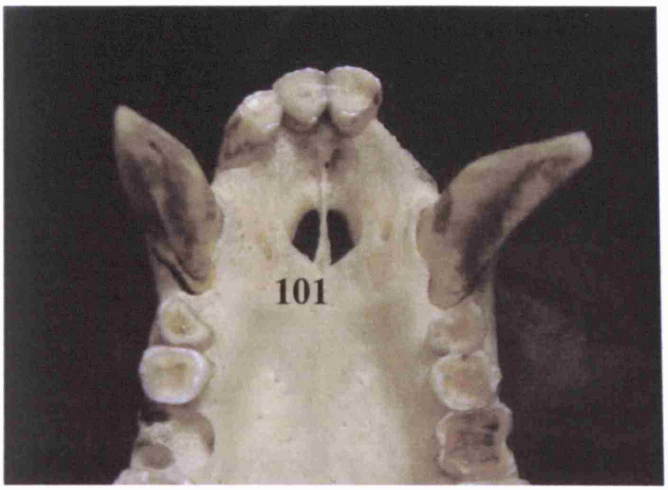

Plate I-m

Character 101 – Palatine fenestrae

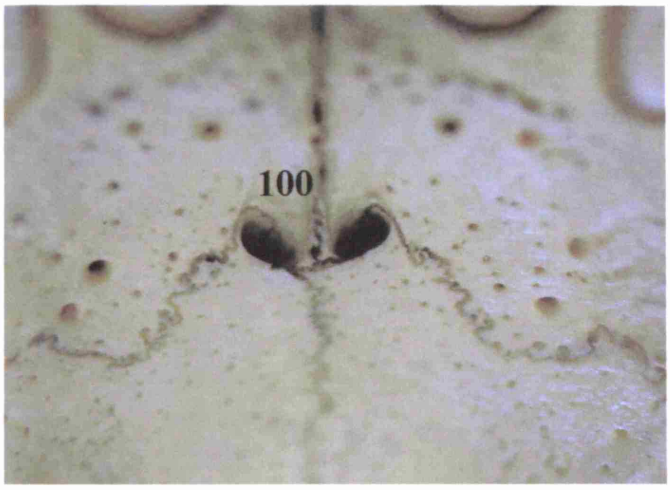

Plate I-n

Character 100 – Incisive canal (double)

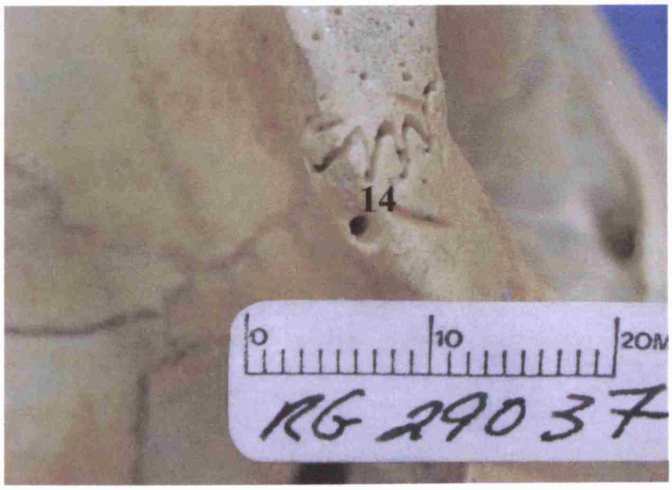

Plate I-o

Character 14 – Zygomatico-temporal foramen, zygomatic

Plate I-p

Character 67 – Craniopharyngeal canal (present)

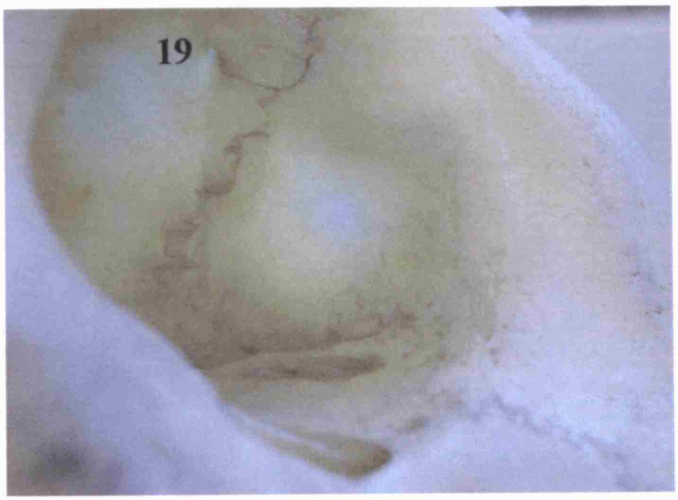

Plate I-q

Character 19 – Zygomatico-orbital foramen,frontal

Plate I-r

Character 34 – Stylomastoid bridge (present)

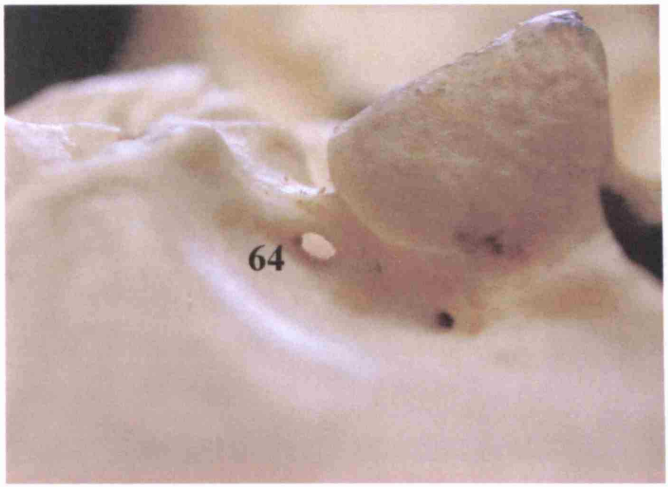

Plate I-s

Character 64 – Intermediate condylar canal (present)

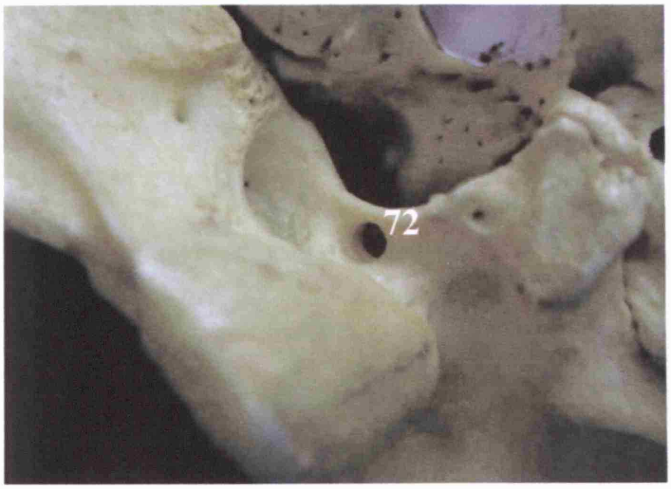

Plate I-t

Character 72 – Jugular bridging (present)

Plate I-u

Character 94 – Robinson canal (present)

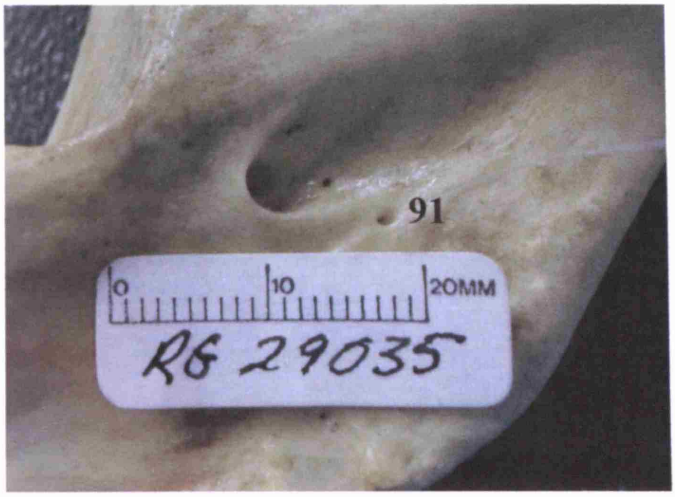

Plate I-v

Character 91– Serres canal

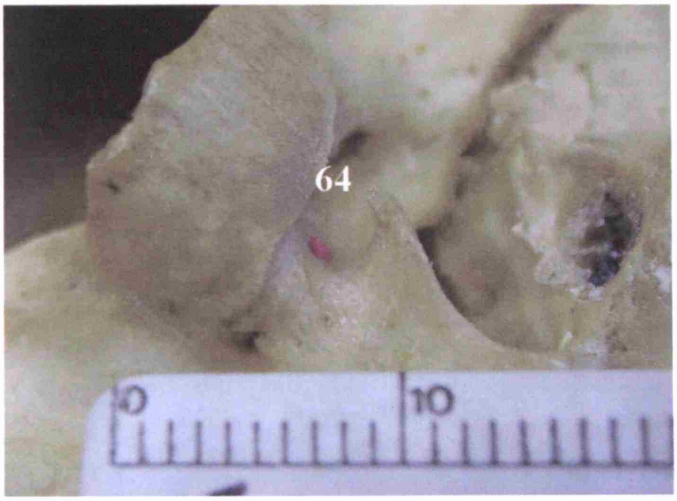

Plate I-w

Character 64– Intermediate condylar canal (present))

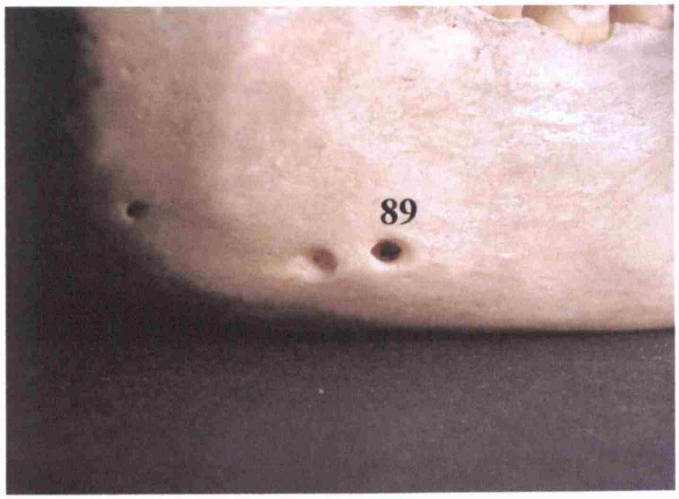

Plate I-x

Character 89– Accessory mental foramen (present)

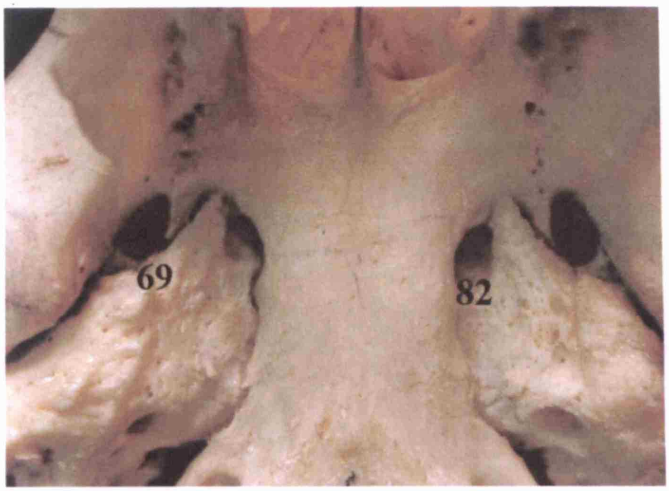

Plate I-y

Character 69 – Foramen ovale, incomplete medial wall
Character 82 – Foramen lacerum (present)

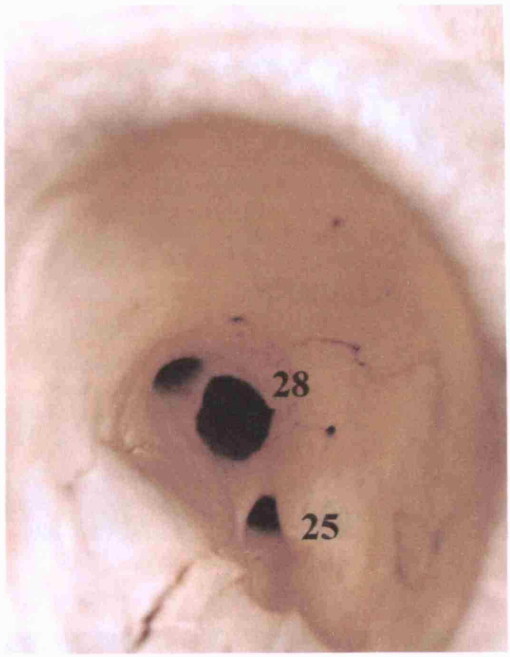

Plate I-z

Character 25 – Foramen rotundum (present)
Character 28 – Superior orbital fissure (absent)

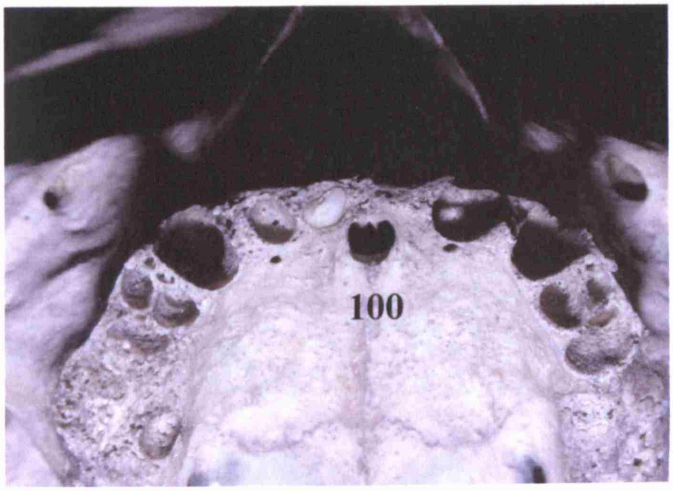

Plate I-aa

Character 100 – Incisive canal (single)

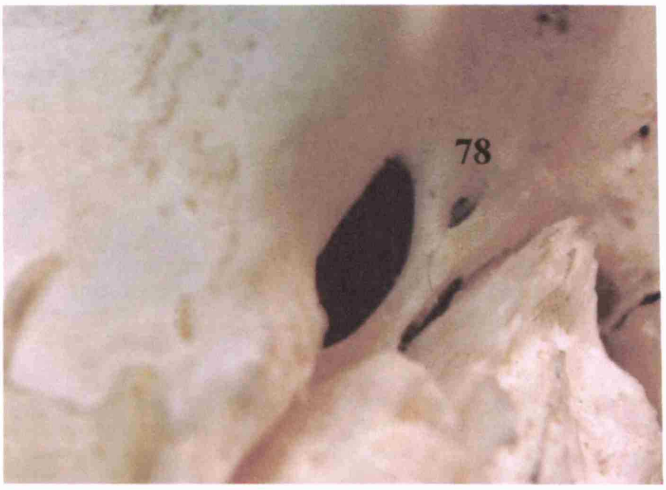

Plate I-ab

Character 78 – Foramen of Vesalius (present)

Plate I-ac

Character 70 – Foramen Ovale, sutural

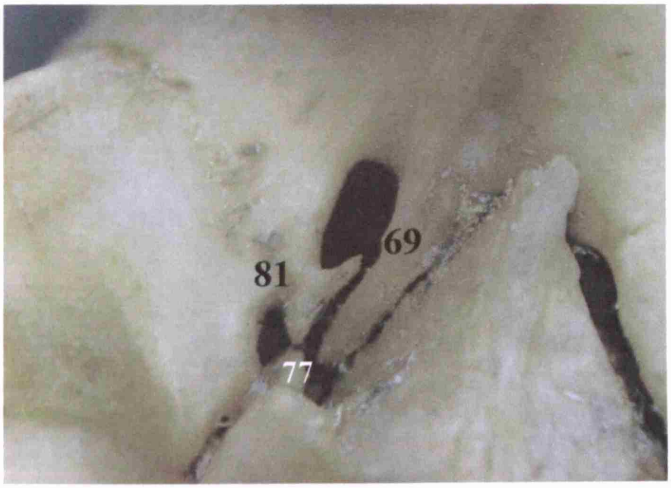

Plate I-ad

Character 69 – Foramen Ovale, incomplete medial wall
Character 77 – Foramen spinosum, incomplete medial wall
Character 81 – Foramen spinosum, sutural

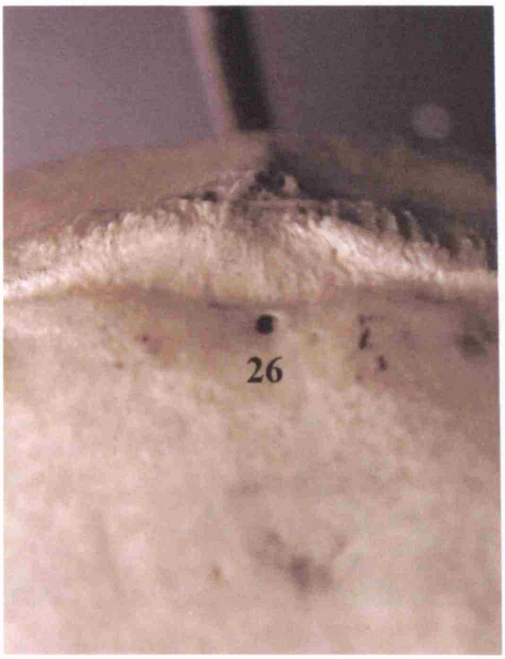

Plate I-ae

Character 26 – Occipital foramen (present)

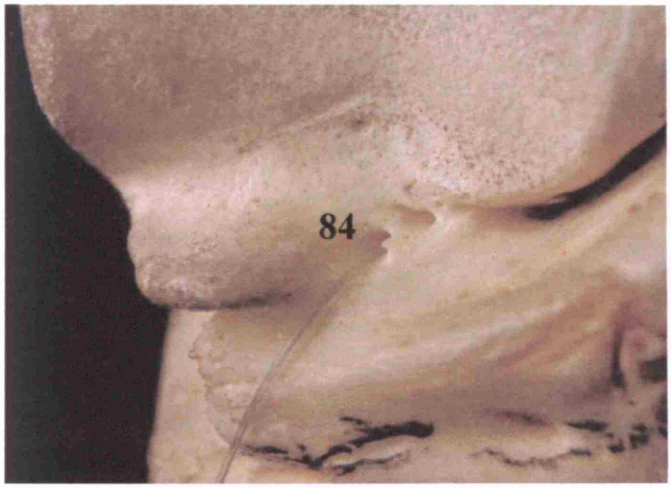

Plate I-af

Character 84 – Postglenoid foramen

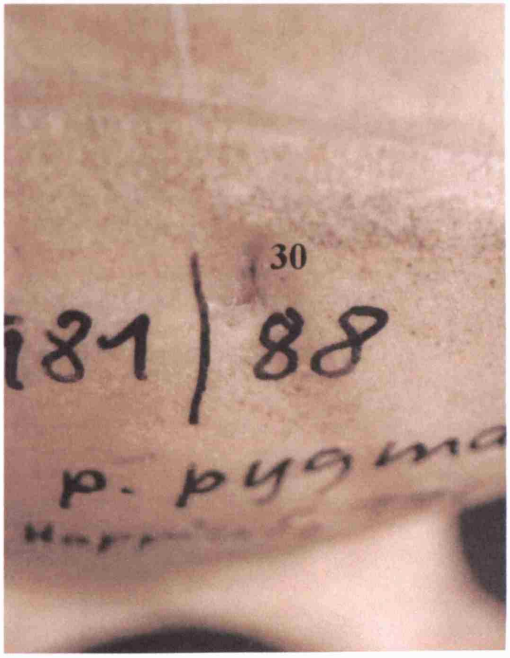

Plate I-ag

Character 30 – MMAE (present)

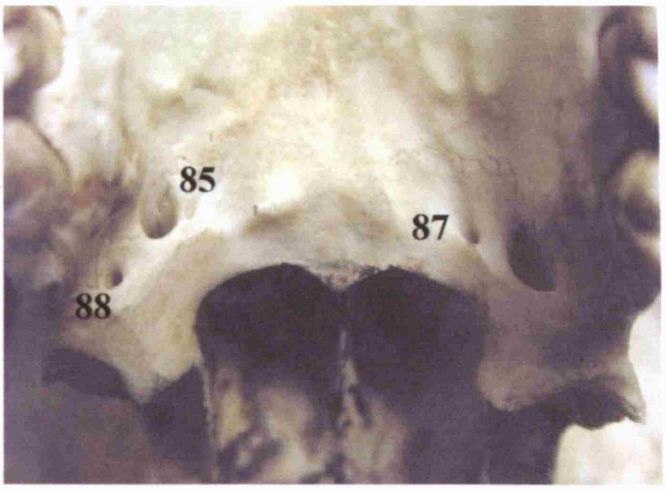

Plate I-ah

Character 85 – Greater palatine foramen position, sutural
Character 87 – Lesser palatine foramen (present)
Character 88 – Lesser palatine foramen position, sutural

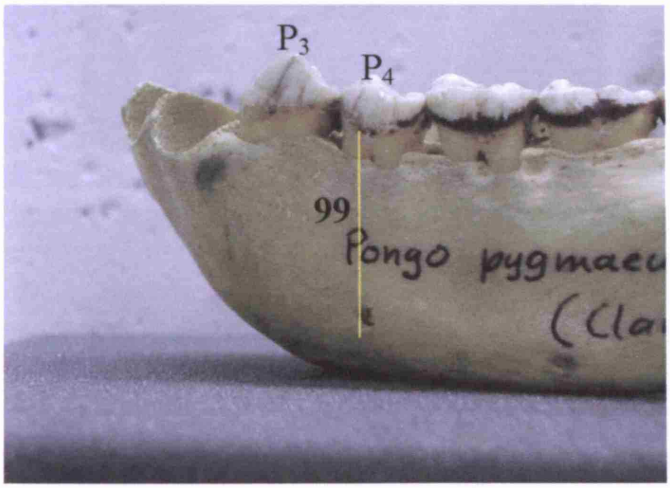

Plate I-ai

Character 99 – Mental foramen under P_3 (other)

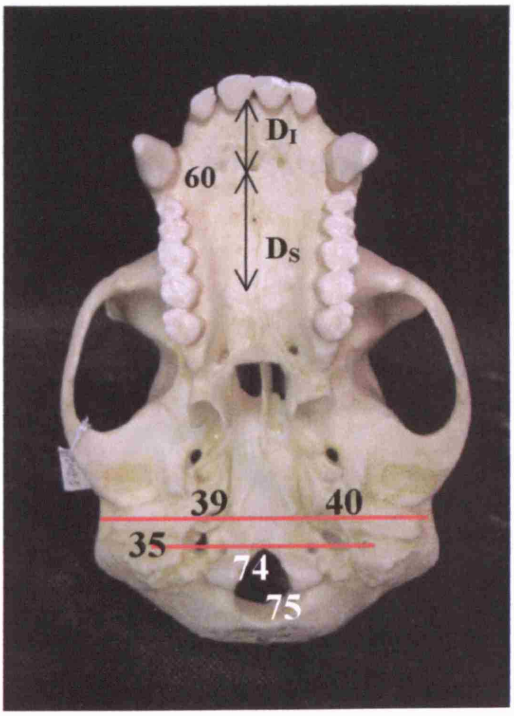

Plate I-aj

Character 35 – Stylomastoid foramen position, posterior to biporionic line
Character 39 – Carotid canal position, posterior to biporionic line (other)
Character 40 – Carotid canal position, at level with Basion
Character 60 – Incisive canal position
Character 74 – Foramen Magnum position, posterior to stylomastoids
Character 75 – Foramen Magnum position, posterior to biporionic line

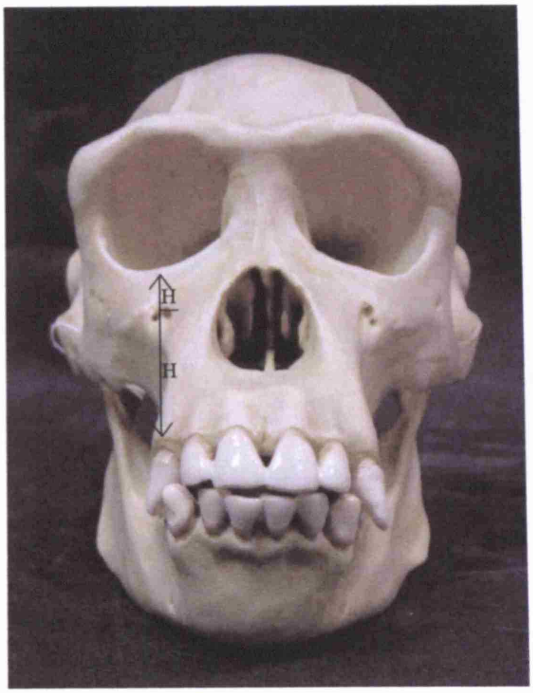

Plate I-ak

Character 61 –
Infraorbital foramen
position ($IOFP_3$)

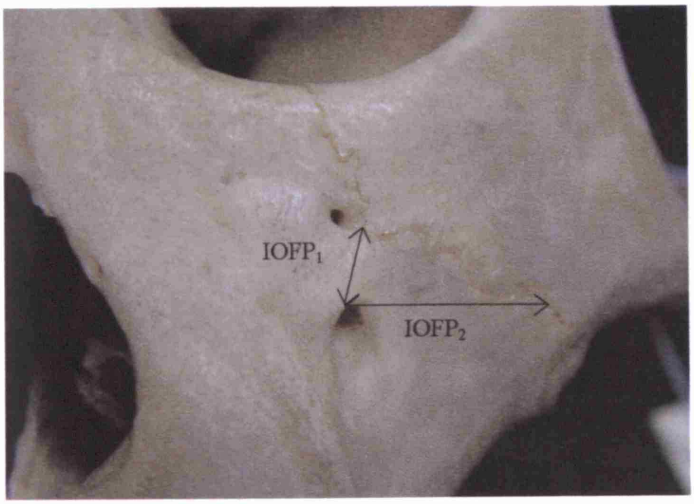

Plate I-al

Character 54 – $IOFP_1$,
minimum sutural distance
Character 55 – $IOFP_2$,
transverse sutural distance

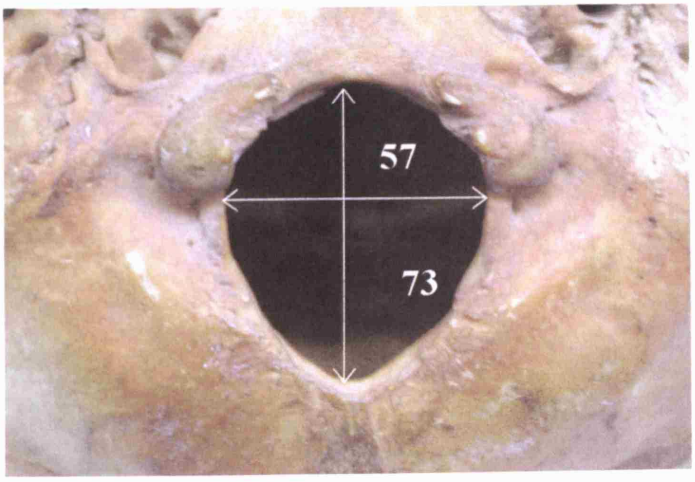

Plate I-am

Character 57 – Foramen
Magnum Size
Character 73 – Foramen
Magnum shape (non-round)

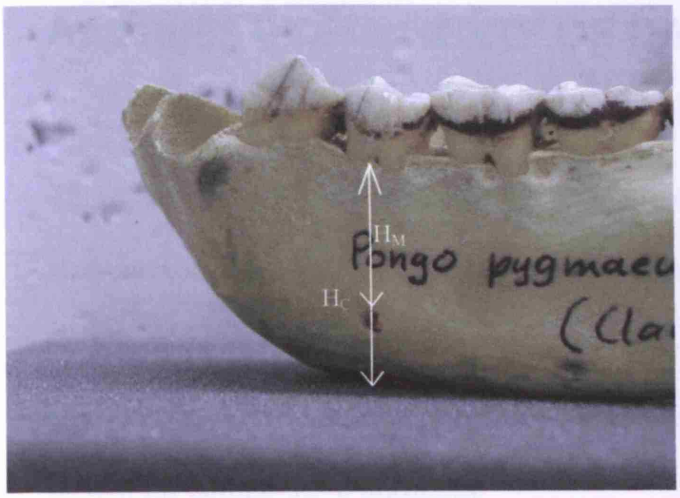

Plate I-an

Character 59 – Mental foramen position

Appendix III. SUMMARY OF DATA

This appendix is divided into two parts. The first part (Appendix IIIa) summarises the size-corrected, metric variables included in this study. For each variable, I included the mean value, the standard deviation (S.D.), the minimum value and the range. I also presented the plots of the mean values (with a 95% confidence limit) across genera for comparative purposes.

The second part (Appendix IIIb) summarises the frequency values of the non-metric binary traits included in the analyses. For each variable I listed the number of cases for each character state and the percentage of occurrence of the trait.

Appendix IIIa. Summary table for the metric variables included in this study (size-corrected, multiplied by 100).

Taxon		ZFFSz	CaCSz	JuFL	MeFSz	IOFP1	IOFP2	MbFP1	FMaSz	InCL	MeFP1	InCP	IOFP3
Gorilla	Mean	.1372	12.2223	37.0962	7.5233	32.4648	62.1099	114.3361	64.9336	16.3370	54.7939	65.5824	44.7026
	N	60	60	60	60	60	60	58	27	30	60	30	59
	S.D.	.74664	1.68575	4.83401	1.93765	8.62161	17.07709	18.34317	5.36875	4.31918	4.87329	21.06024	7.56083
	Min	.00	8.83	26.41	4.60	13.67	28.39	77.91	53.37	11.19	45.57	42.37	27.94
	Range	4.40	8.14	21.90	9.44	36.80	74.26	88.42	23.94	20.04	19.58	119.63	32.56
Pan	Mean	3.3467	12.6062	38.6858	6.6650	13.7930	34.3828	67.2232	94.9560	10.9995	58.0679	60.4968	39.9978
	N	116	118	116	120	120	120	120	57	60	118	59	120
	S.D	.68848	1.21878	4.27084	.90147	3.62372	6.74665	10.49601	27.73306	2.24044	4.52779	17.15604	8.16937
	Min	2.10	9.30	29.48	4.91	5.47	22.52	41.90	53.05	6.99	44.81	40.07	20.20
	Range	3.20	6.13	20.99	4.93	17.74	30.20	54.57	93.94	9.22	25.37	119.45	44.50
Homo	Mean	2.2958	17.9316	48.1876	6.8551	15.9318	37.5930	63.4185	86.3435	10.8481	48.5252	59.9799	26.0362
	N	94	94	95	94	96	96	96	48	48	96	48	96
	S.D.	1.57121	2.24295	6.10968	1.28999	4.73125	8.31210	11.36745	6.56944	3.32492	5.34313	38.80881	6.01682
	Min	.00	13.22	33.36	4.38	7.13	19.09	36.76	72.83	4.16	30.76	34.58	12.84
	Range	5.60	11.58	34.81	6.31	20.25	42.48	52.28	28.53	14.70	32.49	250.28	29.52
Pongo	Mean	4.5089	10.7140	31.4849	7.3381	22.9398	36.3819	97.7172	65.2969	5.5519	62.4294	78.9460	25.6135
	N	62	62	62	62	62	62	61	31	30	62	31	62
	S.D.	1.03336	1.17797	4.75882	1.46319	6.14412	11.64245	16.87231	7.02902	1.42558	4.81664	12.65622	4.92394
	Min	2.40	8.63	19.94	4.38	11.93	17.51	73.48	49.50	2.99	53.61	58.45	16.59
	Range	4.60	5.95	24.07	7.69	26.27	44.44	71.39	28.45	5.26	22.14	48.76	19.63
Hylobates	Mean	4.7452	11.9754	36.1717	5.2395	27.2955	32.9292	76.3569	65.9410	20.5347	62.2710	70.2501	25.6373
	N	118	118	118	118	118	118	118	59	59	118	59	118
	S.D.	1.62055	1.39895	4.73847	1.29223	8.14661	9.59139	14.42754	5.77931	3.71505	4.33164	21.51702	11.53699

	Min	.00	8.82	28.52	2.66	7.06	9.88	51.64	55.25	11.27	51.29	38.06	12.86
	Range	8.86	6.97	28.41	8.46	37.57	48.29	65.88	26.13	16.74	23.64	124.38	91.33
Papio	Mean	4.9400	12.4920	38.3607	7.0672	48.0869	54.4528	98.4598	69.0196	40.8863	73.2792	72.7666	39.4254
	N	40	40	40	40	38	38	40	20	20	40	20	40
	S.D.	1.58340	1.62951	5.30262	3.14862	14.35314	16.17560	11.22048	5.44435	9.16639	6.18224	10.89303	9.53668
	Min	.00	9.65	29.45	4.19	17.71	20.41	77.52	58.43	12.26	59.51	50.49	24.55
	Range	7.47	6.31	23.69	16.94	60.00	70.28	45.21	22.08	45.34	24.92	42.18	41.74
Cercopithecus	Mean	3.1522	10.1333	32.0272	5.1804	24.1539	31.4538	63.1194	58.4580	31.9768	78.3795	86.0224	21.5688
	N	42	42	42	42	42	42	41	21	21	41	21	42
	S.D.	1.36267	1.12468	3.28496	1.75839	7.10141	7.61267	7.58526	3.52679	4.39211	3.68933	15.96905	6.11107
	Min	.00	8.02	26.54	2.96	14.67	21.47	45.40	50.45	22.37	70.90	68.34	12.24
	Range	5.25	4.54	12.49	8.33	33.23	30.03	31.22	12.05	17.72	14.73	59.39	22.80
Colobus	Mean	2.3367	10.5167	31.3083	4.7999	21.4489	34.7667	99.4586	60.6187	31.6075	68.4513	70.9105	17.2793
	N	41	41	42	41	42	42	42	21	20	42	20	42
	S.D.	1.38522	1.06333	6.77161	.81970	7.87449	11.88930	20.09209	4.75502	6.67004	4.48018	12.16574	3.71850
	Min	.00	8.67	14.90	3.34	5.94	9.30	51.49	52.85	13.52	61.29	55.38	10.92
	Range	5.25	4.34	27.04	3.22	31.15	53.27	73.87	21.29	26.80	17.07	40.24	15.52

For each metric variable, the genus mean value of the size-corrected measurements, the number of cases (N), the standard deviation (S.D.), the minimum value (Min) and the range are provided.

43: Zygomaticofacial foramen size (ZFFSz)

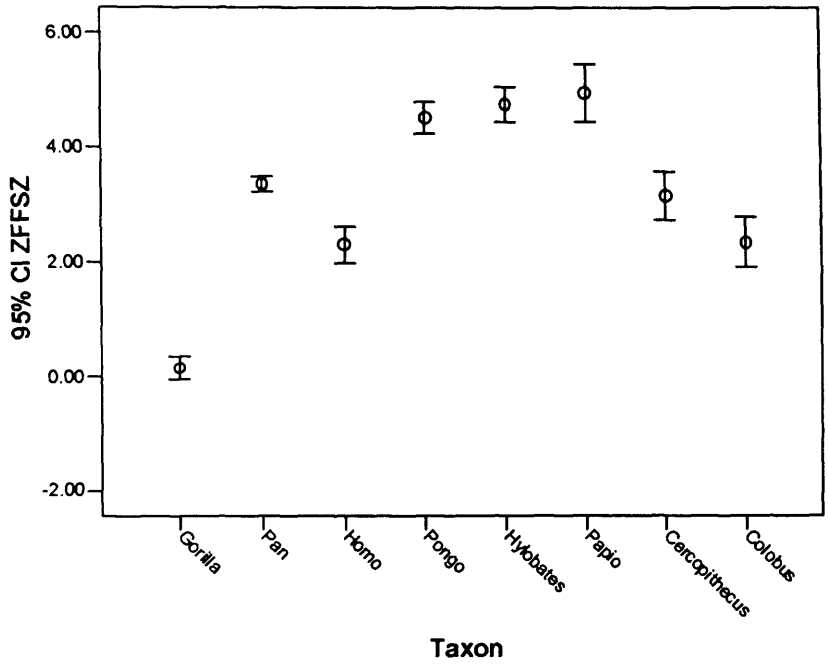

46: Carotid canal size (CaCSz)

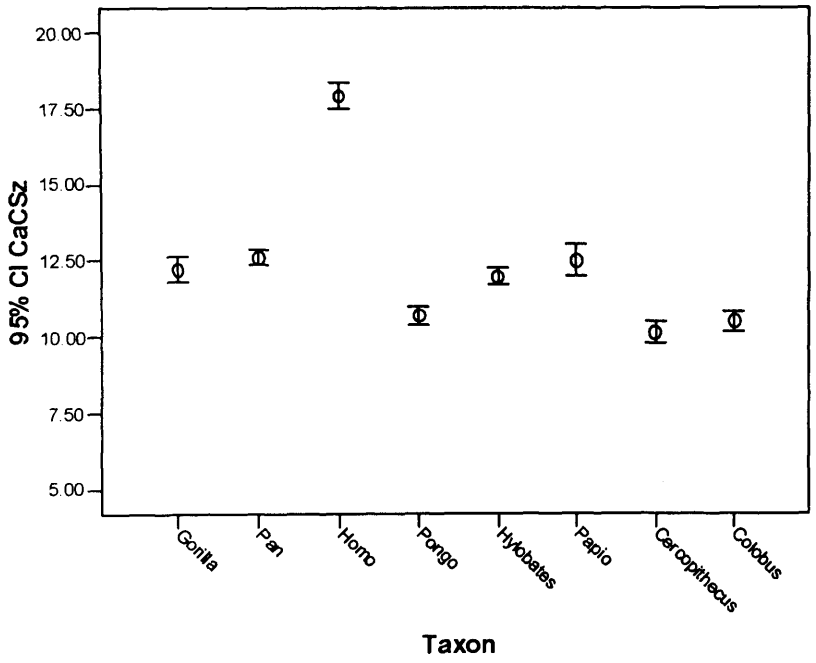

47: Jugular foramen length (JuFL)

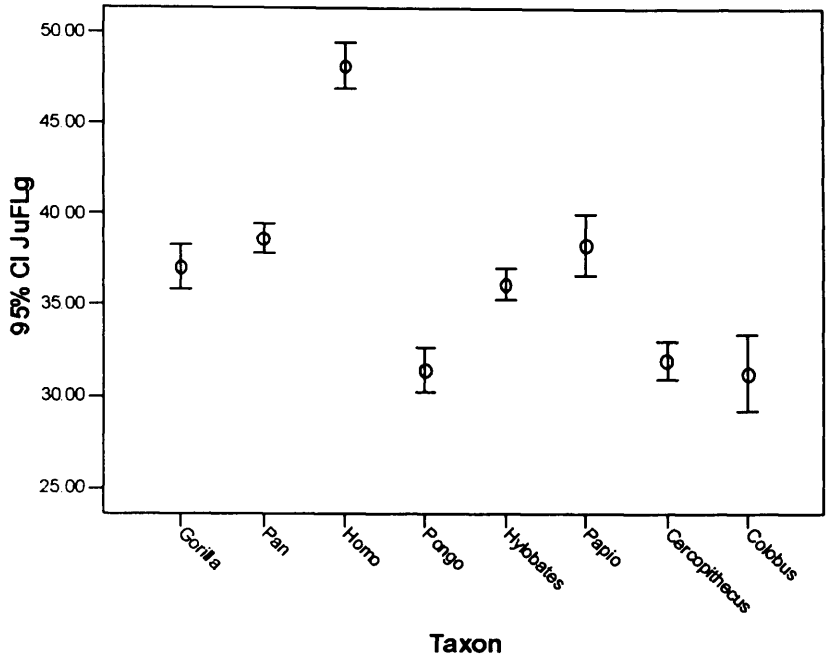

52: Mental foramen size (MeFSz)

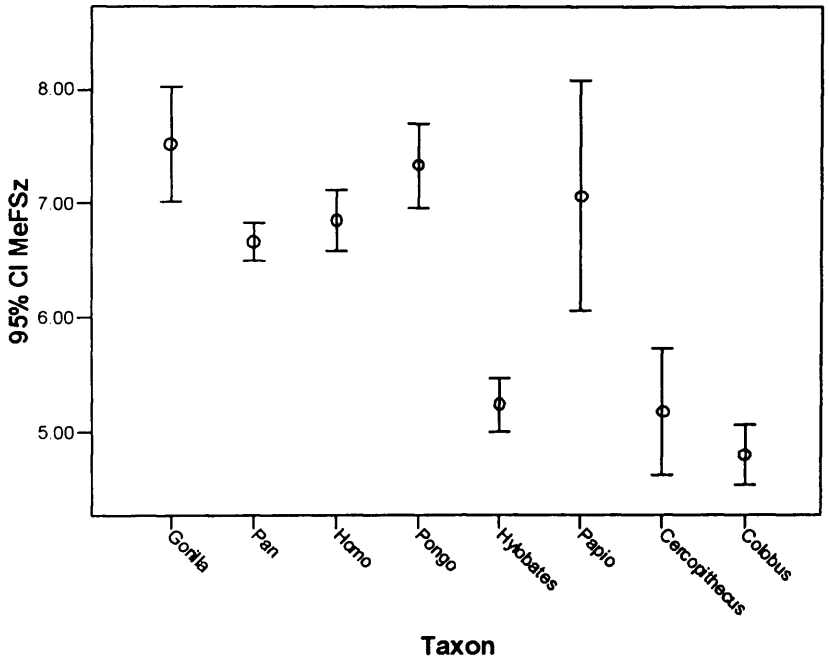

54: Infraorbital foramen position, minimum sutural distance (IOFP1)

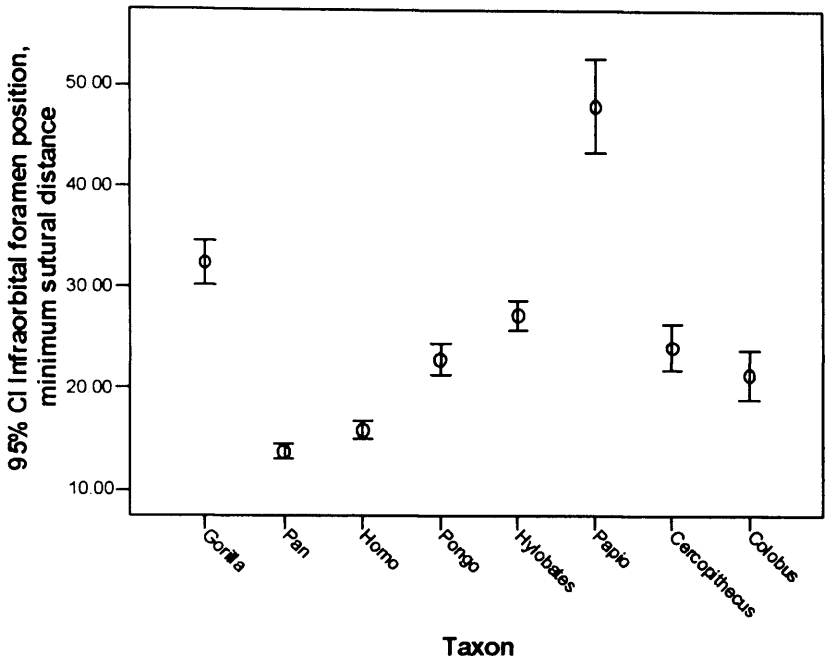

55: Infraorbital foramen position, transverse sutural distance (IOFP2)

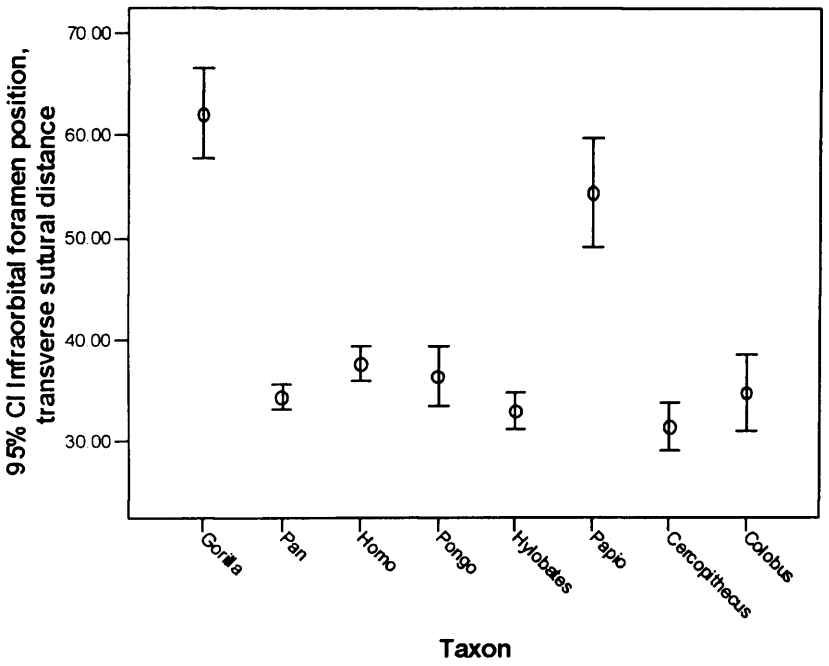

56: Gonion (MbFP1)

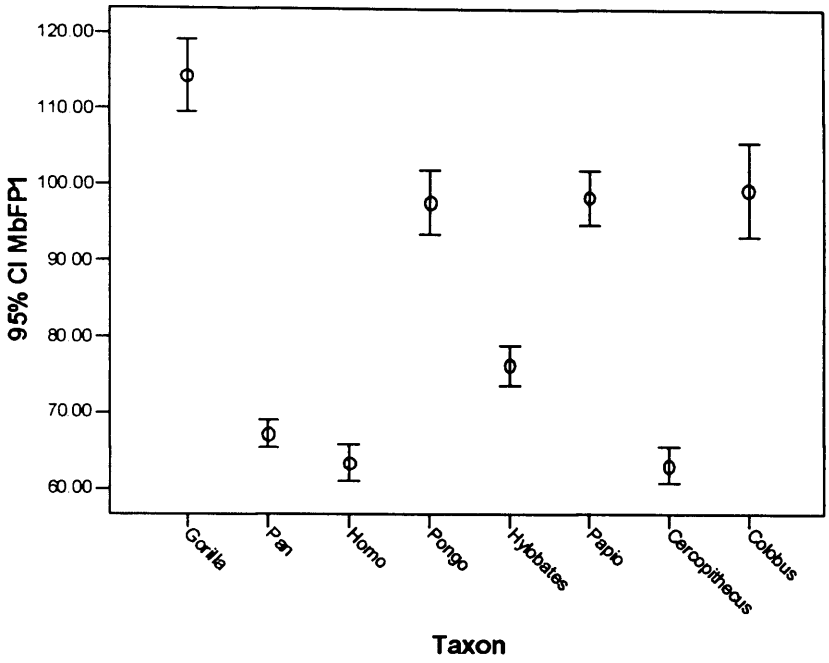

57: Foramen Magnum size (FMaSz)

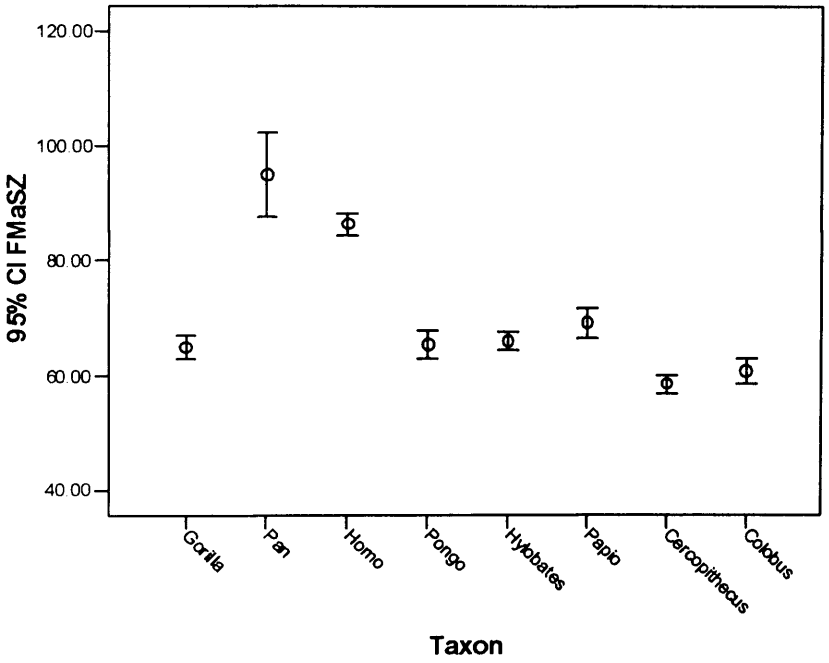

58: Incisive canal diameter (lnCL)

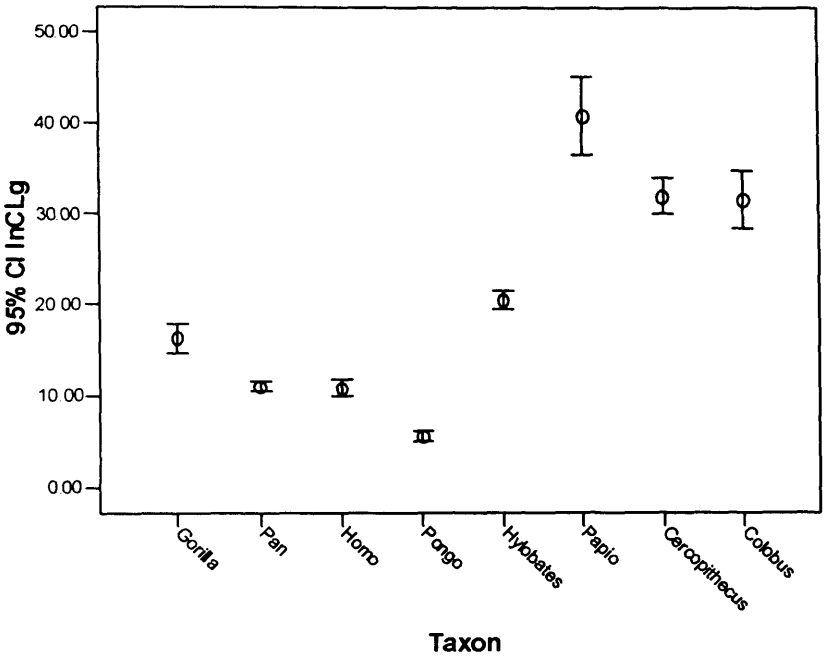

59: Mental foramen position (MeFP1)

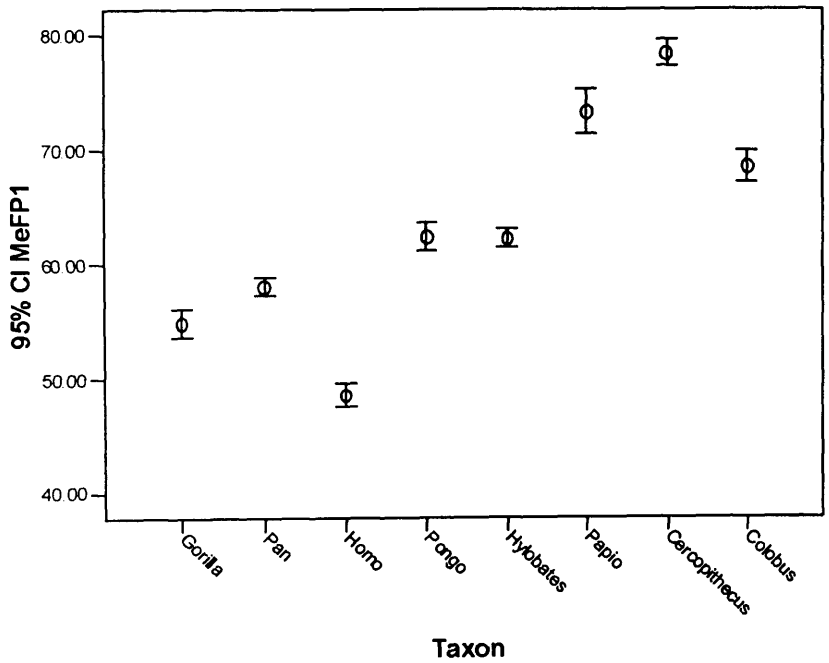

60: Incisive canal position (InCP)

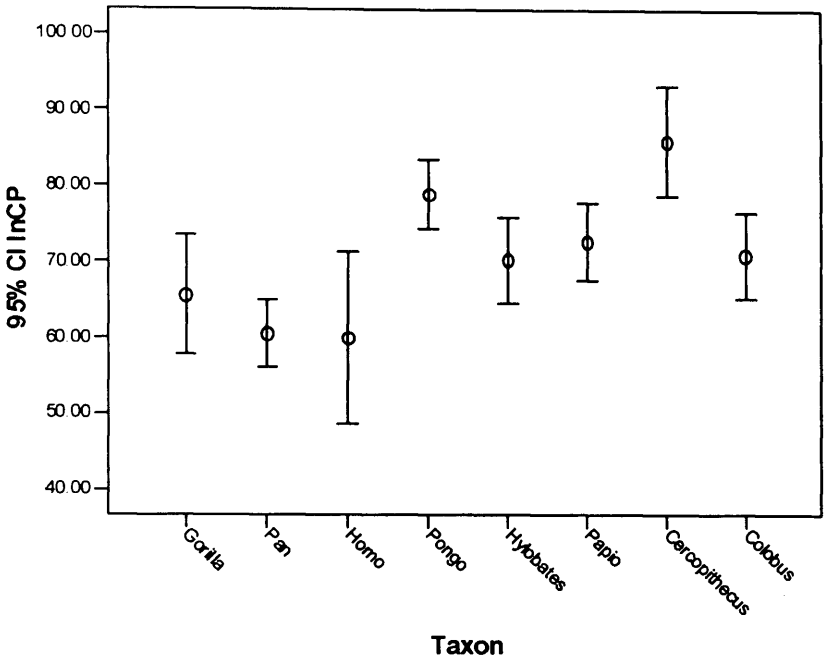

61: Infraorbital foramen position (IOFP3)

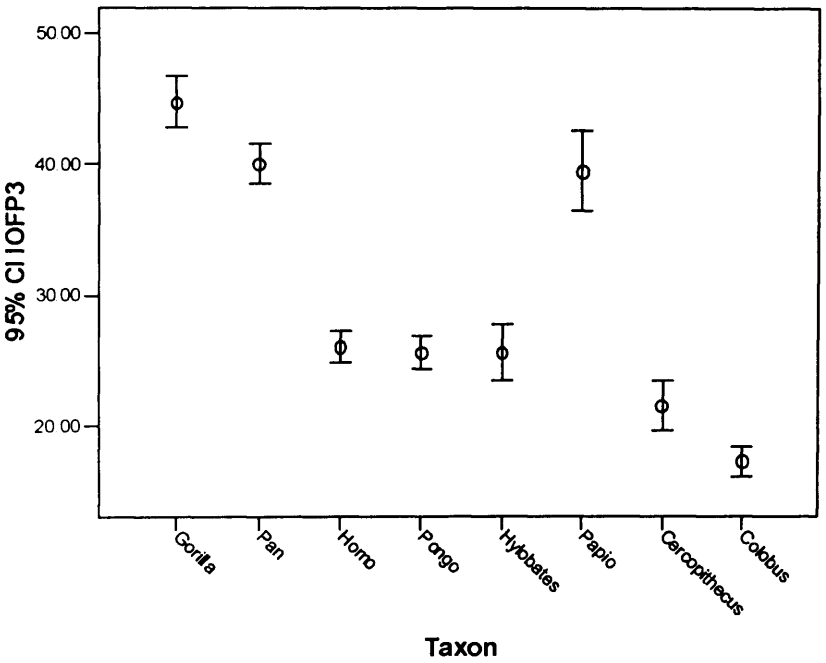

Appendix IIIb. Summary tables of the frequency of occurrence of non-metric variables.

1: Accessory infraorbital foramina (IOF)

			Taxa							
			Gorilla	Pan	Homo	Pongo	Hylobates	Papio	Cercopithecus	Colobus
Accessory infraorbital foramina	Absent	Count	18	53	87	4	48	0	0	0
		% within Taxa	30.0%	44.2%	90.6%	6.5%	40.7%	.0%	.0%	.0%
	Present	Count	42	67	9	58	70	40	42	42
		% within Taxa	70.0%	55.8%	9.4%	93.5%	59.3%	100.0%	100.0%	100.0%
Total		Count	60	120	96	62	118	40	42	42
		% within Taxa	100.0%	100.0%	100.0%	100.0%	100.0%	100.0%	100.0%	100.0%

2: Zygomatico-temporal foramina (ZTF)

			Taxa							
			Gorilla	Pan	Homo	Pongo	Hylobates	Papio	Cercopithecus	Colobus
Zygomatico-temporal foramina	Absent	Count	0	4	13	61	9	0	2	0
		% within Taxa	.0%	3.3%	13.5%	98.4%	7.6%	.0%	4.8%	.0%
	Present	Count	60	116	83	1	109	40	40	42
		% within Taxa	100.0%	96.7%	86.5%	1.6%	92.4%	100.0%	95.2%	100.0%
Total		Count	60	120	96	62	118	40	42	42
		% within Taxa	100.0%	100.0%	100.0%	100.0%	100.0%	100.0%	100.0%	100.0%

3: Zygomatico-facial foramina (ZFF)

			Taxa							
			Gorilla	Pan	Homo	Pongo	Hylobates	Papio	Cercopithecus	Colobus
Zygomatico-facial foramina	Absent	Count	58	0	28	0	1	2	2	4
		% within Taxa	96.7%	.0%	29.2%	.0%	.8%	5.0%	4.8%	9.5%
	Present	Count	2	120	68	62	117	38	40	38
		% within Taxa	3.3%	100.0%	70.8%	100.0%	99.2%	95.0%	95.2%	90.5%
Total		Count	60	120	96	62	118	40	42	42
		% within Taxa	100.0%	100.0%	100.0%	100.0%	100.0%	100.0%	100.0%	100.0%

4: Posterior ethmoid foramen (PEF)

			Taxa							
			Gorilla	Pan	Homo	Pongo	Hylobates	Papio	Cercopithecus	Colobus
Posterior ethmoid foramen	Absent	Count	32	14	4	0	76	17	42	20
		% within Taxa	53.3%	11.8%	4.2%	.0%	64.4%	43.6%	100.0%	47.6%
	Present	Count	28	105	92	62	42	22	0	22
		% within Taxa	46.7%	88.2%	95.8%	100.0%	35.6%	56.4%	.0%	52.4%
Total		Count	60	119	96	62	118	39	42	42
		% within Taxa	100.0%	100.0%	100.0%	100.0%	100.0%	100.0%	100.0%	100.0%

5: Mastoid foramen (MaF)

			Taxa							
			Gorilla	Pan	Homo	Pongo	Hylobates	Papio	Cercopithecus	Colobus
Mastoid foramen	Absent	Count	39	79	32	7	23	2	3	8
		% within Taxa	65.0%	65.8%	33.3%	11.3%	19.5%	5.0%	7.1%	19.0%
	Present	Count	21	41	64	55	95	38	39	34
		% within Taxa	35.0%	34.2%	66.7%	88.7%	80.5%	95.0%	92.9%	81.0%
Total		Count	60	120	96	62	118	40	42	42
		% within Taxa	100.0%	100.0%	100.0%	100.0%	100.0%	100.0%	100.0%	100.0%

6: Infraorbital bridge (IOB)

			Taxa							
			Gorilla	Pan	Homo	Pongo	Hylobates	Papio	Cercopithecus	Colobus
Infraorbital bridge	Absent	Count	60	107	94	62	114	40	42	42
		% within Taxa	100.0%	89.2%	97.9%	100.0%	96.6%	100.0%	100.0%	100.0%
	Present	Count	0	13	2	0	4	0	0	0
		% within Taxa	.0%	10.8%	2.1%	.0%	3.4%	.0%	.0%	.0%
Total		Count	60	120	96	62	118	40	42	42
		% within Taxa	100.0%	100.0%	100.0%	100.0%	100.0%	100.0%	100.0%	100.0%

7: Infraorbital notch (ION)

			Taxa							
			Gorilla	Pan	Homo	Pongo	Hylobates	Papio	Cercopithecus	Colobus
Infraorbital notch	Absent	Count	55	91	90	62	84	39	42	41
		% within Taxa	91.7%	75.8%	93.8%	100.0%	71.2%	97.5%	100.0%	97.6%
	Present	Count	5	29	6	0	34	1	0	1
		% within Taxa	8.3%	24.2%	6.3%	.0%	28.8%	2.5%	.0%	2.4%
Total		Count	60	120	96	62	118	40	42	42
		% within Taxa	100.0%	100.0%	100.0%	100.0%	100.0%	100.0%	100.0%	100.0%

8: Infraorbital canal, anterior opening (ICIO)

			Taxa							
			Gorilla	Pan	Homo	Pongo	Hylobates	Papio	Cercopithecus	Colobus
Infraorbital canal, anterior opening	Close to orbital margin	Count	34	120	7	10	118	40	40	42
		% within Taxa	65.4%	100.0%	7.8%	19.2%	100.0%	100.0%	95.2%	100.0%
	Away from orbital margin	Count	18	0	83	42	0	0	2	0
		% within Taxa	34.6%	.0%	92.2%	80.8%	.0%	.0%	4.8%	.0%
Total		Count	52	120	90	52	118	40	42	42
		% within Taxa	100.0%	100.0%	100.0%	100.0%	100.0%	100.0%	100.0%	100.0%

9: Infraorbital groove (IOG)

			Taxa							
			Gorilla	Pan	Homo	Pongo	Hylobates	Papio	Cercopithecus	Colobus
Infraorbital groove	Absent	Count	1	0	26	3	114	2	38	42
		% within Taxa	1.9%	.0%	30.2%	5.6%	96.6%	5.0%	90.5%	100.0%
	Present	Count	53	120	60	51	4	38	4	0
		% within Taxa	98.1%	100.0%	69.8%	94.4%	3.4%	95.0%	9.5%	.0%
Total		Count	54	120	86	54	118	40	42	42
		% within Taxa	100.0%	100.0%	100.0%	100.0%	100.0%	100.0%	100.0%	100.0%

10: Supralacrimal structures (SLGB)

			Taxa							
			Gorilla	Pan	Homo	Pongo	Hylobates	Papio	Cercopithecus	Colobus
Supralacrimal structures	Absent	Count	34	91	60	54	117	38	36	42
		% within Taxa	56.7%	75.8%	63.8%	87.1%	99.2%	95.0%	85.7%	100.0%
	Present	Count	26	29	34	8	1	2	6	0
		% within Taxa	43.3%	24.2%	36.2%	12.9%	.8%	5.0%	14.3%	.0%
Total		Count	60	120	94	62	118	40	42	42
		% within Taxa	100.0%	100.0%	100.0%	100.0%	100.0%	100.0%	100.0%	100.0%

11: Supraorbital notches (SON)

			Taxa							
			Gorilla	Pan	Homo	Pongo	Hylobates	Papio	Cercopithecus	Colobus
Supraorbital notches	Absent	Count	36	92	19	55	67	0	15	39
		% within Taxa	60.0%	76.7%	19.8%	88.7%	56.8%	.0%	35.7%	92.9%
	Present	Count	24	28	77	7	51	40	27	3
		% within Taxa	40.0%	23.3%	80.2%	11.3%	43.2%	100.0%	64.3%	7.1%
Total		Count	60	120	96	62	118	40	42	42
		% within Taxa	100.0%	100.0%	100.0%	100.0%	100.0%	100.0%	100.0%	100.0%

12: Supraorbital foramina (SOF)

			Taxa							
			Gorilla	Pan	Homo	Pongo	Hylobates	Papio	Cercopithecus	Colobus
Supraorbital foramina	Absent	Count	59	119	75	62	114	40	42	42
		% within Taxa	98.3%	99.2%	78.1%	100.0%	96.6%	100.0%	100.0%	100.0%
	Present	Count	1	1	21	0	4	0	0	0
		% within Taxa	1.7%	.8%	21.9%	.0%	3.4%	.0%	.0%	.0%
Total		Count	60	120	96	62	118	40	42	42
		% within Taxa	100.0%	100.0%	100.0%	100.0%	100.0%	100.0%	100.0%	100.0%

13: Zygomatico-temporal foramen sutural ($ZTFP_1b$)

			Taxa							
			Gorilla	Pan	Homo	Pongo	Hylobates	Papio	Cercopithecus	Colobus
Zygomatico-temporal foramen sutural	Absent	Count	33	70	93	62	100	13	11	26
		% within Taxa	55.0%	58.3%	96.9%	100.0%	87.0%	32.5%	26.2%	61.9%
	Present	Count	27	50	3	0	15	27	31	16
		% within Taxa	45.0%	41.7%	3.1%	.0%	13.0%	67.5%	73.8%	38.1%
Total		Count	60	120	96	62	115	40	42	42
		% within Taxa	100.0%	100.0%	100.0%	100.0%	100.0%	100.0%	100.0%	100.0%

14: Zygomatico-temporal foramen zygomatic ($ZTFP_2b$)

			Taxa							
			Gorilla	Pan	Homo	Pongo	Hylobates	Papio	Cercopithecus	Colobus
Zygomatico-temporal foramen zygomatic	Absent	Count	44	43	15	61	17	27	35	15
		% within Taxa	73.3%	35.8%	15.6%	98.4%	14.8%	67.5%	83.3%	35.7%
	Present	Count	16	77	81	1	98	13	7	27
		% within Taxa	26.7%	64.2%	84.4%	1.6%	85.2%	32.5%	16.7%	64.3%
Total		Count	60	120	96	62	115	40	42	42
		% within Taxa	100.0%	100.0%	100.0%	100.0%	100.0%	100.0%	100.0%	100.0%

15: Zygomatico-temporal foramen frontal ($ZTFP_1a$)

			Taxa							
			Gorilla	Pan	Homo	Pongo	Hylobates	Papio	Cercopithecus	Colobus
Zygomatico-temporal foramen frontal	Absent	Count	24	102	96	62	114	40	40	42
		% within Taxa	40.0%	85.0%	100.0%	100.0%	99.1%	100.0%	95.2%	100.0%
	Present	Count	36	18	0	0	1	0	2	0
		% within Taxa	60.0%	15.0%	.0%	.0%	.9%	.0%	4.8%	.0%
Total		Count	60	120	96	62	115	40	42	42
		% within Taxa	100.0%	100.0%	100.0%	100.0%	100.0%	100.0%	100.0%	100.0%

16: Zygomatico-temporal foramen on plate ($ZTFP_2b$)

			Taxa							
			Gorilla	Pan	Homo	Pongo	Hylobates	Papio	Cercopithecus	Colobus
Zygomatico-temporal foramen on plate	Absent	Count	5	19	13	62	58	40	29	27
		% within Taxa	8.9%	16.1%	13.5%	100.0%	52.3%	100.0%	69.0%	64.3%
	Present	Count	51	99	83	0	53	0	13	15
		% within Taxa	91.1%	83.9%	86.5%	.0%	47.7%	.0%	31.0%	35.7%
Total		Count	56	118	96	62	111	40	42	42
		% within Taxa	100.0%	100.0%	100.0%	100.0%	100.0%	100.0%	100.0%	100.0%

17: Zygomatico-temporal foramen on bar ($ZTFP_2a$)

			Taxa							
			Gorilla	Pan	Homo	Pongo	Hylobates	Papio	Cercopithecus	Colobus
Zygomatico-temporal foramen on bar	Absent	Count	42	79	95	61	45	0	15	14
		% within Taxa	75.0%	66.9%	99.0%	98.4%	40.5%	.0%	35.7%	33.3%
	Present	Count	14	39	1	1	66	40	27	28
		% within Taxa	25.0%	33.1%	1.0%	1.6%	59.5%	100.0%	64.3%	66.7%
Total		Count	56	118	96	62	111	40	42	42
		% within Taxa	100.0%	100.0%	100.0%	100.0%	100.0%	100.0%	100.0%	100.0%

18: Zygomatico-orbital foramen sutural ($ZOFP_b$)

			Taxa							
			Gorilla	Pan	Homo	Pongo	Hylobates	Papio	Cercopithecus	Colobus
Zygomatico-orbital foramen sutural	Absent	Count	46	22	82	61	110	29	22	2
		% within Taxa	82.1%	18.3%	85.4%	98.4%	96.5%	72.5%	52.4%	4.8%
	Present	Count	10	98	14	1	4	11	20	40
		% within Taxa	17.9%	81.7%	14.6%	1.6%	3.5%	27.5%	47.6%	95.2%
Total		Count	56	120	96	62	114	40	42	42
		% within Taxa	100.0%	100.0%	100.0%	100.0%	100.0%	100.0%	100.0%	100.0%

19: Zygomatico-orbital foramen frontal (ZOFPa)

			Taxa							
			Gorilla	Pan	Homo	Pongo	Hylobates	Papio	Cercopithecus	Colobus
Zygomatico-orbital foramen frontal	Absent	Count	5	89	96	62	114	11	22	40
		% within Taxa	8.9%	74.2%	100.0%	100.0%	100.0%	27.5%	52.4%	95.2%
	Present	Count	51	31	0	0	0	29	20	2
		% within Taxa	91.1%	25.8%	.0%	.0%	.0%	72.5%	47.6%	4.8%
Total		Count	56	120	96	62	114	40	42	42
		% within Taxa	100.0%	100.0%	100.0%	100.0%	100.0%	100.0%	100.0%	100.0%

20: Zygomatico-orbital foramen zygomatic (ZOFPc)

			Taxa							
			Gorilla	Pan	Homo	Pongo	Hylobates	Papio	Cercopithecus	Colobus
Zygomatico-orbital foramen zygomatic	Absent	Count	56	119	27	62	12	40	42	42
		% within Taxa	100.0%	99.2%	28.1%	100.0%	10.5%	100.0%	100.0%	100.0%
	Present	Count	0	1	69	0	102	0	0	0
		% within Taxa	.0%	.8%	71.9%	.0%	89.5%	.0%	.0%	.0%
Total		Count	56	120	96	62	114	40	42	42
		% within Taxa	100.0%	100.0%	100.0%	100.0%	100.0%	100.0%	100.0%	100.0%

21: Zygomatico-facial notch (ZFN)

			Taxa							
			Gorilla	Pan	Homo	Pongo	Hylobates	Papio	Cercopithecus	Colobus
Zygomatico-facial notch	Absent	Count	60	120	92	53	84	40	42	35
		% within Taxa	100.0%	100.0%	100.0%	85.5%	72.4%	100.0%	100.0%	83.3%
	Present	Count	0	0	0	9	32	0	0	7
		% within Taxa	.0%	.0%	.0%	14.5%	27.6%	.0%	.0%	16.7%
Total		Count	60	120	92	62	116	40	42	42
		% within Taxa	100.0%	100.0%	100.0%	100.0%	100.0%	100.0%	100.0%	100.0%

22: Zygomatico-facial foramen on zygomatic (ZFFPc)

			Taxa							
			Gorilla	Pan	Homo	Pongo	Hylobates	Papio	Cercopithecus	Colobus
Zygomatico-facial foramen on zygomatic	Absent	Count	59	8	59	0	9	2	11	7
		% within Taxa	98.3%	6.7%	61.5%	.0%	7.6%	5.0%	26.2%	16.7%
	Present	Count	1	112	37	62	109	38	31	35
		% within Taxa	1.7%	93.3%	38.5%	100.0%	92.4%	95.0%	73.8%	83.3%
Total		Count	60	120	96	62	118	40	42	42
		% within Taxa	100.0%	100.0%	100.0%	100.0%	100.0%	100.0%	100.0%	100.0%

23: Zygomatico-facial foramen on corpus (ZFFPa,b)

			Taxa							
			Gorilla	Pan	Homo	Pongo	Hylobates	Papio	Cercopithecus	Colobus
Zygomatico-facial foramen on corpus	Absent	Count	59	62	46	61	74	40	29	31
		% within Taxa	98.3%	51.7%	47.9%	98.4%	62.7%	100.0%	69.0%	73.8%
	Present	Count	1	58	50	1	44	0	13	11
		% within Taxa	1.7%	48.3%	52.1%	1.6%	37.3%	.0%	31.0%	26.2%
Total		Count	60	120	96	62	118	40	42	42
		% within Taxa	100.0%	100.0%	100.0%	100.0%	100.0%	100.0%	100.0%	100.0%

24: Anterior ethmoid foramen, sutural (AEFP)

			Taxa							
			Gorilla	Pan	Homo	Pongo	Hylobates	Papio	Cercopithecus	Colobus
Anterior ethmoid foramen, sutural	Extra sutural	Count	30	62	34	24	94	39	34	33
		% within Taxa	54.5%	53.0%	35.4%	38.7%	79.7%	100.0%	81.0%	78.6%
	Sutural	Count	25	55	62	38	24	0	8	9
		% within Taxa	45.5%	47.0%	64.6%	61.3%	20.3%	.0%	19.0%	21.4%
Total		Count	55	117	96	62	118	39	42	42
		% within Taxa	100.0%	100.0%	100.0%	100.0%	100.0%	100.0%	100.0%	100.0%

25: Foramen rotundum (FRo)

			Taxa							
			Gorilla	Pan	Homo	Pongo	Hylobates	Papio	Cercopithecus	Colobus
Foramen rotundum	Incomplete	Count	0	19	0	0	22	0	0	4
		% within Taxa	.0%	16.0%	.0%	.0%	19.3%	.0%	.0%	9.5%
	Complete	Count	60	100	96	62	92	40	42	38
		% within Taxa	100.0%	84.0%	100.0%	100.0%	80.7%	100.0%	100.0%	90.5%
Total		Count	60	119	96	62	114	40	42	42
		% within Taxa	100.0%	100.0%	100.0%	100.0%	100.0%	100.0%	100.0%	100.0%

26: Occipital foramen (OcF)

			Taxa							
			Gorilla	Pan	Homo	Pongo	Hylobates	Papio	Cercopithecus	Colobus
Occipital foramen	Absent	Count	30	59	45	31	55	20	21	21
		% within Taxa	100.0%	98.3%	93.8%	100.0%	93.2%	100.0%	100.0%	100.0%
	Present	Count	0	1	3	0	4	0	0	0
		% within Taxa	.0%	1.7%	6.3%	.0%	6.8%	.0%	.0%	.0%
Total		Count	30	60	48	31	59	20	21	21
		% within Taxa	100.0%	100.0%	100.0%	100.0%	100.0%	100.0%	100.0%	100.0%

27: Posterior ethmoid foramen, sutural (PEFPb)

			Taxa							
			Gorilla	Pan	Homo	Pongo	Hylobates	Papio	Cercopithecus	Colobus
Posterior ethmoid foramen, sutural	Absent	Count	41	32	23	6	78	39	42	41
		% within Taxa	71.9%	26.9%	24.0%	10.0%	66.1%	100.0%	100.0%	97.6%
	Present	Count	16	87	73	54	40	0	0	1
		% within Taxa	28.1%	73.1%	76.0%	90.0%	33.9%	.0%	.0%	2.4%
Total		Count	57	119	96	60	118	39	42	42
		% within Taxa	100.0%	100.0%	100.0%	100.0%	100.0%	100.0%	100.0%	100.0%

28: Superior orbital fissure (SOFi)

			Taxa							
			Gorilla	Pan	Homo	Pongo	Hylobates	Papio	Cercopithecus	Colobus
Superior orbital fissure	Absent	Count	52	10	0	8	39	30	2	17
		% within Taxa	86.7%	8.5%	.0%	12.9%	33.1%	75.0%	4.8%	40.5%
	Present	Count	8	108	96	54	79	10	40	25
		% within Taxa	13.3%	91.5%	100.0%	87.1%	66.9%	25.0%	95.2%	59.5%
Total		Count	60	118	96	62	118	40	42	42
		% within Taxa	100.0%	100.0%	100.0%	100.0%	100.0%	100.0%	100.0%	100.0%

29: Posterior ethmoid foramen, frontal (PEFPa)

			Taxa							
			Gorilla	Pan	Homo	Pongo	Hylobates	Papio	Cercopithecus	Colobus
Posterior ethmoid foramen, frontal	Absent	Count	47	97	69	53	115	17	42	20
		% within Taxa	82.5%	81.5%	71.9%	85.5%	97.5%	43.6%	100.0%	47.6%
	Present	Count	10	22	27	9	3	22	0	22
		% within Taxa	17.5%	18.5%	28.1%	14.5%	2.5%	56.4%	.0%	52.4%
	Total	Count	57	119	96	62	118	39	42	42
		% within Taxa	100.0%	100.0%	100.0%	100.0%	100.0%	100.0%	100.0%	100.0%

30: Middle meningeal artery emissaries (MMAE)

			Taxa							
			Gorilla	Pan	Homo	Pongo	Hylobates	Papio	Cercopithecus	Colobus
Middle meningeal artery emissaries	Absent	Count	60	118	94	60	118	36	40	42
		% within Taxa	100.0%	98.3%	97.9%	96.8%	100.0%	90.0%	95.2%	100.0%
	Present	Count	0	2	2	2	0	4	2	0
		% within Taxa	.0%	1.7%	2.1%	3.2%	.0%	10.0%	4.8%	.0%
	Total	Count	60	120	96	62	118	40	42	42
		% within Taxa	100.0%	100.0%	100.0%	100.0%	100.0%	100.0%	100.0%	100.0%

31: Mastoid foramen position, sutural (MaFPb)

			Taxa							
			Gorilla	Pan	Homo	Pongo	Hylobates	Papio	Cercopithecus	Colobus
Mastoid foramen position, sutural	Absent	Count	54	107	68	43	48	7	7	11
		% within Taxa	90.0%	89.2%	70.8%	69.4%	40.7%	17.5%	16.7%	26.2%
	Present	Count	6	13	28	19	70	33	35	31
		% within Taxa	10.0%	10.8%	29.2%	30.6%	59.3%	82.5%	83.3%	73.8%
	Total	Count	60	120	96	62	118	40	42	42
		% within Taxa	100.0%	100.0%	100.0%	100.0%	100.0%	100.0%	100.0%	100.0%

32: Mastoid foramen position, mastoid (MaFPa)

			Taxa							
			Gorilla	Pan	Homo	Pongo	Hylobates	Papio	Cercopithecus	Colobus
Mastoid foramen position, mastoid	Absent	Count	45	91	56	26	91	36	38	38
		% within Taxa	75.0%	75.8%	58.3%	41.9%	77.1%	90.0%	90.5%	90.5%
	Present	Count	15	29	40	36	27	4	4	4
		% within Taxa	25.0%	24.2%	41.7%	58.1%	22.9%	10.0%	9.5%	9.5%
	Total	Count	60	120	96	62	118	40	42	42
		% within Taxa	100.0%	100.0%	100.0%	100.0%	100.0%	100.0%	100.0%	100.0%

33: Mastoid foramen position, occipital (MaFPc)

			Taxa							
			Gorilla	Pan	Homo	Pongo	Hylobates	Papio	Cercopithecus	Colobus
Mastoid foramen position, occipital	Absent	Count	60	119	93	62	116	36	42	42
		% within Taxa	100.0%	99.2%	96.9%	100.0%	98.3%	90.0%	100.0%	100.0%
	Present	Count	0	1	3	0	2	4	0	0
		% within Taxa	.0%	.8%	3.1%	.0%	1.7%	10.0%	.0%	.0%
	Total	Count	60	120	96	62	118	40	42	42
		% within Taxa	100.0%	100.0%	100.0%	100.0%	100.0%	100.0%	100.0%	100.0%

34: Stylomastoid bridge (SMB)

			Taxa							
			Gorilla	Pan	Homo	Pongo	Hylobates	Papio	Cercopithecus	Colobus
Stylomastoid bridge	Absent	Count	52	67	83	54	111	29	34	40
		% within Taxa	86.7%	56.3%	88.3%	87.1%	94.1%	72.5%	81.0%	95.2%
	Present	Count	8	52	11	8	7	11	8	2
		% within Taxa	13.3%	43.7%	11.7%	12.9%	5.9%	27.5%	19.0%	4.8%
	Total	Count	60	119	94	62	118	40	42	42
		% within Taxa	100.0%	100.0%	100.0%	100.0%	100.0%	100.0%	100.0%	100.0%

35: Stylomastoid bridge, posterior to biporion (SMFP)

			Taxa							
			Gorilla	Pan	Homo	Pongo	Hylobates	Papio	Cercopithecus	Colobus
Stylomastoid bridge, posterior to biporion	Absent	Count	0	0	0	0	0	20	0	0
		% within Taxa	.0%	.0%	.0%	.0%	.0%	50.0%	.0%	.0%
	Present	Count	60	119	94	62	118	20	42	42
		% within Taxa	100.0%	100.0%	100.0%	100.0%	100.0%	50.0%	100.0%	100.0%
Total		Count	60	119	94	62	118	40	42	42
		% within Taxa	100.0%	100.0%	100.0%	100.0%	100.0%	100.0%	100.0%	100.0%

36: Parietal foramen, parietal (PaF_1)

			Taxa							
			Gorilla	Pan	Homo	Pongo	Hylobates	Papio	Cercopithecus	Colobus
Parietal foramen, parietal	Absent	Count	59	115	50	62	115	39	42	41
		% within Taxa	98.3%	99.1%	52.1%	100.0%	97.5%	97.5%	100.0%	97.6%
	Present	Count	1	1	46	0	3	1	0	1
		% within Taxa	1.7%	.9%	47.9%	.0%	2.5%	2.5%	.0%	2.4%
Total		Count	60	116	96	62	118	40	42	42
		% within Taxa	100.0%	100.0%	100.0%	100.0%	100.0%	100.0%	100.0%	100.0%

37: Parietal foramen, sutural (PaF_2)

			Taxa							
			Gorilla	Pan	Homo	Pongo	Hylobates	Papio	Cercopithecus	Colobus
Parietal foramen, sutural	Absent	Count	13	51	43	23	44	19	21	21
		% within Taxa	43.3%	87.9%	89.6%	74.2%	88.0%	95.0%	100.0%	100.0%
	Present	Count	17	7	5	8	6	1	0	0
		% within Taxa	56.7%	12.1%	10.4%	25.8%	12.0%	5.0%	.0%	.0%
	Total	Count	30	58	48	31	50	20	21	21
		% within Taxa	100.0%	100.0%	100.0%	100.0%	100.0%	100.0%	100.0%	100.0%

38: Parietal foramen, occipital (PaF_3)

			Taxa							
			Gorilla	Pan	Homo	Pongo	Hylobates	Papio	Cercopithecus	Colobus
Parietal foramen, occipital	Absent	Count	30	58	48	31	49	20	21	21
		% within Taxa	100.0%	100.0%	100.0%	100.0%	83.1%	100.0%	100.0%	100.0%
	Present	Count	0	0	0	0	10	0	0	0
		% within Taxa	.0%	.0%	.0%	.0%	16.9%	.0%	.0%	.0%
	Total	Count	30	58	48	31	59	20	21	21
		% within Taxa	100.0%	100.0%	100.0%	100.0%	100.0%	100.0%	100.0%	100.0%

39: Carotid canal, posterior to biporion ($CaCP_1$)

			Taxa							
			Gorilla	Pan	Homo	Pongo	Hylobates	Papio	Cercopithecus	Colobus
Carotid canal, posterior to biporion	Anterior	Count	30	44	96	12	0	40	38	35
		% within Taxa	50.0%	37.0%	100.0%	19.4%	.0%	100.0%	90.5%	83.3%
	Posterior	Count	30	75	0	50	118	0	4	7
		% within Taxa	50.0%	63.0%	.0%	80.6%	100.0%	.0%	9.5%	16.7%
Total		Count	60	119	96	62	118	40	42	42
		% within Taxa	100.0%	100.0%	100.0%	100.0%	100.0%	100.0%	100.0%	100.0%

40: Carotid canal, position relative to basion ($CaCP_2$)

			Taxa							
			Gorilla	Pan	Homo	Pongo	Hylobates	Papio	Cercopithecus	Colobus
Carotid canal, position relative to basion	On plane	Count	58	119	74	62	118	38	42	42
		% within Taxa	100.0%	100.0%	77.1%	100.0%	100.0%	95.0%	100.0%	100.0%
	Not on plane	Count	0	0	22	0	0	2	0	0
		% within Taxa	.0%	.0%	22.9%	.0%	.0%	5.0%	.0%	.0%
Total		Count	58	119	96	62	118	40	42	42
		% within Taxa	100.0%	100.0%	100.0%	100.0%	100.0%	100.0%	100.0%	100.0%

62: Infraugular process expression (IJPE)

			Taxa							
			Gorilla	Pan	Homo	Pongo	Hylobates	Papio	Cercopithecus	Colobus
Infraugular process expression	Absent	Count	1	8	0	10	18	11	2	8
		% within Taxa	1.7%	6.8%	.0%	16.1%	15.3%	27.5%	4.8%	20.0%
	Present	Count	59	110	94	52	100	29	40	32
		% within Taxa	98.3%	93.2%	100.0%	83.9%	84.7%	72.5%	95.2%	80.0%
Total		Count	60	118	94	62	118	40	42	40
		% within Taxa	100.0%	100.0%	100.0%	100.0%	100.0%	100.0%	100.0%	100.0%

63: Hypoglossal canal divisions (HyC)

			Taxa							
			Gorilla	Pan	Homo	Pongo	Hylobates	Papio	Cercopithecus	Colobus
Hypoglossal canal divisions	Absent	Count	45	57	8	43	59	35	20	11
		% within Taxa	77.6%	48.7%	8.3%	69.4%	50.0%	87.5%	47.6%	26.2%
	Present	Count	13	60	88	19	59	5	22	31
		% within Taxa	22.4%	51.3%	91.7%	30.6%	50.0%	12.5%	52.4%	73.8%
Total		Count	58	117	96	62	118	40	42	42
		% within Taxa	100.0%	100.0%	100.0%	100.0%	100.0%	100.0%	100.0%	100.0%

64: Intermediate condylar canal (ICC)

			Taxa							
			Gorilla	Pan	Homo	Pongo	Hylobates	Papio	Cercopithecus	Colobus
Intermediate condylar canal	Absent	Count	55	105	49	61	118	40	42	39
		% within Taxa	94.8%	88.2%	51.0%	98.4%	100.0%	100.0%	100.0%	92.9%
	Partial or complete	Count	3	14	47	1	0	0	0	3
		% within Taxa	5.2%	11.8%	49.0%	1.6%	.0%	.0%	.0%	7.1%
Total		Count	58	119	96	62	118	40	42	42
		% within Taxa	100.0%	100.0%	100.0%	100.0%	100.0%	100.0%	100.0%	100.0%

65: Condylar canal (CoC)

			Taxa							
			Gorilla	Pan	Homo	Pongo	Hylobates	Papio	Cercopithecus	Colobus
Condylar canal	Absent	Count	46	66	35	61	116	39	42	40
		% within Taxa	79.3%	57.9%	36.5%	98.4%	98.3%	97.5%	100.0%	95.2%
	Present	Count	12	48	61	1	2	1	0	2
		% within Taxa	20.7%	42.1%	63.5%	1.6%	1.7%	2.5%	.0%	4.8%
Total		Count	58	114	96	62	118	40	42	42
		% within Taxa	100.0%	100.0%	100.0%	100.0%	100.0%	100.0%	100.0%	100.0%

66: Condylar canal internal opening, jugular (CoCO)

			Taxa							
			Gorilla	Pan	Homo	Pongo	Hylobates	Papio	Cercopithecus	Colobus
Condylar canal internal opening, jugular	Sigmoid sinus groove	Count	52	102	40	61	118	40	42	42
		% within Taxa	89.7%	89.5%	41.7%	98.4%	100.0%	100.0%	100.0%	100.0%
	Jugular foramen	Count	6	12	56	1	0	0	0	0
		% within Taxa	10.3%	10.5%	58.3%	1.6%	.0%	.0%	.0%	.0%
Total		Count	58	114	96	62	118	40	42	42
		% within Taxa	100.0%	100.0%	100.0%	100.0%	100.0%	100.0%	100.0%	100.0%

67: Craniopharyngeal canal (CPC)

			Taxa							
			Gorilla	Pan	Homo	Pongo	Hylobates	Papio	Cercopithecus	Colobus
Craniopharyngeal canal	Absent	Count	19	43	48	26	56	20	21	20
		% within Taxa	65.5%	79.6%	100.0%	83.9%	94.9%	100.0%	100.0%	100.0%
	Present	Count	10	11	0	5	3	0	0	0
		% within Taxa	34.5%	20.4%	.0%	16.1%	5.1%	.0%	.0%	.0%
Total		Count	29	54	48	31	59	20	21	20
		% within Taxa	100.0%	100.0%	100.0%	100.0%	100.0%	100.0%	100.0%	100.0%

68: Marginal foramen (MgF)

			Taxa							
			Gorilla	Pan	Homo	Pongo	Hylobates	Papio	Cercopithecus	Colobus
Marginal foramen	Absent	Count	45	109	65	62	115	35	35	38
		% within Taxa	75.0%	91.6%	67.7%	100.0%	97.5%	87.5%	83.3%	90.5%
	Present	Count	15	10	31	0	3	5	7	4
		% within Taxa	25.0%	8.4%	32.3%	.0%	2.5%	12.5%	16.7%	9.5%
Total		Count	60	119	96	62	118	40	42	42
		% within Taxa	100.0%	100.0%	100.0%	100.0%	100.0%	100.0%	100.0%	100.0%

69: Foramen ovale, complete medial wall (FOv)

			Taxa							
			Gorilla	Pan	Homo	Pongo	Hylobates	Papio	Cercopithecus	Colobus
Foramen ovale, complete medial wall	Other	Count	0	12	3	22	25	40	42	41
		% within Taxa	.0%	10.0%	3.1%	35.5%	21.2%	100.0%	100.0%	100.0%
	Complete	Count	60	108	93	40	93	0	0	0
		% within Taxa	100.0%	90.0%	96.9%	64.5%	78.8%	.0%	.0%	.0%
Total		Count	60	120	96	62	118	40	42	41
		% within Taxa	100.0%	100.0%	100.0%	100.0%	100.0%	100.0%	100.0%	100.0%

70: Foramen ovale, sutural (FOvP)

			Taxa							
			Gorilla	Pan	Homo	Pongo	Hylobates	Papio	Cercopithecus	Colobus
Foramen ovale, sutural	Extra sutural	Count	49	68	96	28	107	37	42	39
		% within Taxa	81.7%	58.1%	100.0%	45.2%	90.7%	92.5%	100.0%	95.1%
	Suture	Count	11	49	0	34	11	3	0	2
		% within Taxa	18.3%	41.9%	.0%	54.8%	9.3%	7.5%	.0%	4.9%
Total		Count	60	117	96	62	118	40	42	41
		% within Taxa	100.0%	100.0%	100.0%	100.0%	100.0%	100.0%	100.0%	100.0%

71: Median basilar canal (MBC)

			Taxa							
			Gorilla	Pan	Homo	Pongo	Hylobates	Papio	Cercopithecus	Colobus
Median basilar canal	Absent	Count	28	59	45	31	59	20	21	21
		% within Taxa	93.3%	100.0%	93.8%	100.0%	100.0%	100.0%	100.0%	100.0%
	Present	Count	2	0	3	0	0	0	0	0
		% within Taxa	6.7%	.0%	6.3%	.0%	.0%	.0%	.0%	.0%
Total		Count	30	59	48	31	59	20	21	21
		% within Taxa	100.0%	100.0%	100.0%	100.0%	100.0%	100.0%	100.0%	100.0%

72: Jugular bridging (JuB)

			Taxa							
			Gorilla	Pan	Homo	Pongo	Hylobates	Papio	Cercopithecus	Colobus
Jugular bridging	Absent	Count	58	97	83	58	110	40	38	39
		% within Taxa	96.7%	80.8%	86.5%	93.5%	93.2%	100.0%	90.5%	92.9%
	Present	Count	2	23	13	4	8	0	4	3
		% within Taxa	3.3%	19.2%	13.5%	6.5%	6.8%	.0%	9.5%	7.1%
Total		Count	60	120	96	62	118	40	42	42
		% within Taxa	100.0%	100.0%	100.0%	100.0%	100.0%	100.0%	100.0%	100.0%

73: Foramen magnum, round (FMaS)

			Taxa							
			Gorilla	Pan	Homo	Pongo	Hylobates	Papio	Cercopithecus	Colobus
Foramen magnum, round	Absent	Count	25	50	46	31	40	19	15	17
		% within Taxa	92.6%	83.3%	95.8%	100.0%	67.8%	95.0%	71.4%	81.0%
	Present	Count	2	10	2	0	19	1	6	4
		% within Taxa	7.4%	16.7%	4.2%	.0%	32.2%	5.0%	28.6%	19.0%
Total		Count	27	60	48	31	59	20	21	21
		% within Taxa	100.0%	100.0%	100.0%	100.0%	100.0%	100.0%	100.0%	100.0%

74: Foramen magnum, posterior to stylomastoid ($FMaP_2$)

			Taxa							
			Gorilla	Pan	Homo	Pongo	Hylobates	Papio	Cercopithecus	Colobus
Foramen magnum, posterior to stylomastoid	Absent	Count	16	46	47	8	49	20	19	20
		% within Taxa	55.2%	78.0%	97.9%	25.8%	84.5%	100.0%	90.5%	95.2%
	Present	Count	13	13	1	23	9	0	2	1
		% within Taxa	44.8%	22.0%	2.1%	74.2%	15.5%	.0%	9.5%	4.8%
Total		Count	29	59	48	31	58	20	21	21
		% within Taxa	100.0%	100.0%	100.0%	100.0%	100.0%	100.0%	100.0%	100.0%

75: Foramen magnum, relative to biporionic ($FMaP_1$)

			Taxa							
			Gorilla	Pan	Homo	Pongo	Hylobates	Papio	Cercopithecus	Colobus
Foramen magnum, realtive to biporionic	Anterior	Count	1	0	39	0	0	20	3	0
		% within Taxa	3.3%	.0%	81.3%	.0%	.0%	100.0%	14.3%	.0%
	Posterior	Count	29	60	9	31	59	0	18	21
		% within Taxa	96.7%	100.0%	18.8%	100.0%	100.0%	.0%	85.7%	100.0%
Total		Count	30	60	48	31	59	20	21	21
		% within Taxa	100.0%	100.0%	100.0%	100.0%	100.0%	100.0%	100.0%	100.0%

76: Innominate canal (InF)

			Taxa							
			Gorilla	Pan	Homo	Pongo	Hylobates	Papio	Cercopithecus	Colobus
Innominate canal	Absent	Count	57	107	91	61	116	40	42	41
		% within Taxa	95.0%	89.2%	94.8%	98.4%	98.3%	100.0%	100.0%	100.0%
	Present	Count	3	13	5	1	2	0	0	0
		% within Taxa	5.0%	10.8%	5.2%	1.6%	1.7%	.0%	.0%	.0%
Total		Count	60	120	96	62	118	40	42	41
		% within Taxa	100.0%	100.0%	100.0%	100.0%	100.0%	100.0%	100.0%	100.0%

77: Foramen spinosum, complete median wall (FSp)

			Taxa							
			Gorilla	Pan	Homo	Pongo	Hylobates	Papio	Cercopithecus	Colobus
Foramen spinosum, complete median wall	Other	Count	21	51	27	46	113	35	41	41
		% within Taxa	35.0%	42.5%	28.1%	74.2%	95.8%	87.5%	97.6%	100.0%
	Complete	Count	39	69	69	16	5	5	1	0
		% within Taxa	65.0%	57.5%	71.9%	25.8%	4.2%	12.5%	2.4%	.0%
Total		Count	60	120	96	62	118	40	42	41
		% within Taxa	100.0%	100.0%	100.0%	100.0%	100.0%	100.0%	100.0%	100.0%

78: Foramen of Vesalius (FVe)

			Taxa							
			Gorilla	Pan	Homo	Pongo	Hylobates	Papio	Cercopithecus	Colobus
Foramen of Vesalius	Other	Count	51	105	49	56	116	39	42	41
		% within Taxa	85.0%	87.5%	51.0%	90.3%	98.3%	100.0%	100.0%	97.6%
	Complete	Count	9	15	47	6	2	0	0	1
		% within Taxa	15.0%	12.5%	49.0%	9.7%	1.7%	.0%	.0%	2.4%
Total		Count	60	120	96	62	118	39	42	42
		% within Taxa	100.0%	100.0%	100.0%	100.0%	100.0%	100.0%	100.0%	100.0%

79: Pterygospinous bridge (PSB)

			Taxa							
			Gorilla	Pan	Homo	Pongo	Hylobates	Papio	Cercopithecus	Colobus
Pterygospinous bridge	Other	Count	20	95	73	56	49	18	0	0
		% within Taxa	33.3%	79.2%	76.0%	90.3%	41.5%	45.0%	.0%	.0%
	Complete	Count	40	25	23	6	69	22	42	42
		% within Taxa	66.7%	20.8%	24.0%	9.7%	58.5%	55.0%	100.0%	100.0%
Total		Count	60	120	96	62	118	40	42	42
		% within Taxa	100.0%	100.0%	100.0%	100.0%	100.0%	100.0%	100.0%	100.0%

80: Pterygoalar bridge (PAB)

			Taxa							
			Gorilla	Pan	Homo	Pongo	Hylobates	Papio	Cercopithecus	Colobus
Pterygoalar bridge	Other	Count	60	118	58	61	117	7	27	22
		% within Taxa	100.0%	98.3%	60.4%	98.4%	99.2%	17.5%	64.3%	52.4%
	Complete	Count	0	2	38	1	1	33	15	20
		% within Taxa	.0%	1.7%	39.6%	1.6%	.8%	82.5%	35.7%	47.6%
Total		Count	60	120	96	62	118	40	42	42
		% within Taxa	100.0%	100.0%	100.0%	100.0%	100.0%	100.0%	100.0%	100.0%

81: Foramen spinosum, sutural (FSpP)

			Taxa							
			Gorilla	Pan	Homo	Pongo	Hylobates	Papio	Cercopithecus	Colobus
Foramen spinosum, sutural	Extra sutural	Count	46	43	96	32	117	28	24	41
		% within Taxa	76.7%	36.8%	100.0%	52.5%	99.2%	71.8%	57.1%	100.0%
	Sutural	Count	14	74	0	29	1	11	18	0
		% within Taxa	23.3%	63.2%	.0%	47.5%	.8%	28.2%	42.9%	.0%
Total		Count	60	117	96	61	118	39	42	41
		% within Taxa	100.0%	100.0%	100.0%	100.0%	100.0%	100.0%	100.0%	100.0%

82: Foramen lacerum (FLa)

			Taxa							
			Gorilla	Pan	Homo	Pongo	Hylobates	Papio	Cercopithecus	Colobus
Foramen lacerum	Absent	Count	58	97	0	4	115	39	36	34
		% within Taxa	96.7%	80.8%	.0%	6.5%	97.5%	97.5%	85.7%	81.0%
	Present	Count	2	23	96	58	3	1	6	8
		% within Taxa	3.3%	19.2%	100.0%	93.5%	2.5%	2.5%	14.3%	19.0%
	Total	Count	60	120	96	62	118	40	42	42
		% within Taxa	100.0%	100.0%	100.0%	100.0%	100.0%	100.0%	100.0%	100.0%

83: Squamosal foramen (RaC_2)

			Taxa							
			Gorilla	Pan	Homo	Pongo	Hylobates	Papio	Cercopithecus	Colobus
Squamosal foramen	Absent	Count	60	119	96	61	118	34	42	42
		% within Taxa	100.0%	100.0%	100.0%	98.4%	100.0%	85.0%	100.0%	100.0%
	Present	Count	0	0	0	1	0	6	0	0
		% within Taxa	.0%	.0%	.0%	1.6%	.0%	15.0%	.0%	.0%
	Total	Count	60	119	96	62	118	40	42	42
		% within Taxa	100.0%	100.0%	100.0%	100.0%	100.0%	100.0%	100.0%	100.0%

84: Postglenoid foramen (RaC1)

			Taxa							
			Gorilla	Pan	Homo	Pongo	Hylobates	Papio	Cercopithecus	Colobus
Postglenoid foramen	Absent	Count	59	119	96	57	115	2	36	28
		% within Taxa	98.3%	100.0%	100.0%	91.9%	97.5%	5.0%	85.7%	70.0%
	Present	Count	1	0	0	5	3	38	6	12
		% within Taxa	1.7%	.0%	.0%	8.1%	2.5%	95.0%	14.3%	30.0%
Total		Count	60	119	96	62	118	40	42	40
		% within Taxa	100.0%	100.0%	100.0%	100.0%	100.0%	100.0%	100.0%	100.0%

85: Greater palatine foramen, sutural (GPFP)

			Taxa							
			Gorilla	Pan	Homo	Pongo	Hylobates	Papio	Cercopithecus	Colobus
Greater palatine foramen, sutural	Extra sutural	Count	0	0	15	0	44	0	0	10
		% within Taxa	.0%	.0%	15.6%	.0%	39.3%	.0%	.0%	23.8%
	Sutural	Count	60	119	81	62	68	40	42	32
		% within Taxa	100.0%	100.0%	84.4%	100.0%	60.7%	100.0%	100.0%	76.2%
Total		Count	60	119	96	62	112	40	42	42
		% within Taxa	100.0%	100.0%	100.0%	100.0%	100.0%	100.0%	100.0%	100.0%

86: Palatine crests (PCr)

			Taxa							
			Gorilla	Pan	Homo	Pongo	Hylobates	Papio	Cercopithecus	Colobus
Palatine crests	Absent	Count	34	82	38	23	8	32	35	42
		% within Taxa	100.0%	71.9%	40.4%	44.2%	6.8%	80.0%	83.3%	100.0%
	Present	Count	0	32	56	29	110	8	7	0
		% within Taxa	.0%	28.1%	59.6%	55.8%	93.2%	20.0%	16.7%	.0%
	Total	Count	34	114	94	52	118	40	42	42
		% within Taxa	100.0%	100.0%	100.0%	100.0%	100.0%	100.0%	100.0%	100.0%

87: Lesser palatine foramen (LPF)

			Taxa							
			Gorilla	Pan	Homo	Pongo	Hylobates	Papio	Cercopithecus	Colobus
Lesser palatine foramen	Absent	Count	2	5	4	42	47	36	21	25
		% within Taxa	3.3%	4.2%	4.2%	67.7%	40.2%	90.0%	50.0%	59.5%
	Present	Count	58	114	92	20	70	4	21	17
		% within Taxa	96.7%	95.8%	95.8%	32.3%	59.8%	10.0%	50.0%	40.5%
	Total	Count	60	119	96	62	117	40	42	42
		% within Taxa	100.0%	100.0%	100.0%	100.0%	100.0%	100.0%	100.0%	100.0%

88: Lesser palatine foramen, sutural (LPFP)

			Taxa							
			Gorilla	Pan	Homo	Pongo	Hylobates	Papio	Cercopithecus	Colobus
Lesser palatine foramen, sutural	Absent	Count	31	70	41	52	93	36	28	38
		% within Taxa	51.7%	58.8%	42.7%	83.9%	79.5%	90.0%	66.7%	90.5%
	Present	Count	29	49	55	10	24	4	14	4
		% within Taxa	48.3%	41.2%	57.3%	16.1%	20.5%	10.0%	33.3%	9.5%
Total		Count	60	119	96	62	117	40	42	42
		% within Taxa	100.0%	100.0%	100.0%	100.0%	100.0%	100.0%	100.0%	100.0%

89: Accessory mental foramen (MeF)

			Taxa							
			Gorilla	Pan	Homo	Pongo	Hylobates	Papio	Cercopithecus	Colobus
Accessory mental foramen	Absent	Count	37	120	92	44	112	0	16	35
		% within Taxa	61.7%	100.0%	95.8%	71.0%	94.9%	.0%	38.1%	83.3%
	Present	Count	23	0	4	18	6	40	26	7
		% within Taxa	38.3%	.0%	4.2%	29.0%	5.1%	100.0%	61.9%	16.7%
Total		Count	60	120	96	62	118	40	42	42
		% within Taxa	100.0%	100.0%	100.0%	100.0%	100.0%	100.0%	100.0%	100.0%

90: Mandibular foramen position, above dental row ($MbFP_2$)

			Taxa							
			Gorilla	Pan	Homo	Pongo	Hylobates	Papio	Cercopithecus	Colobus
Mandibular foramen position, above dental row	Below dental row	Count	1	106	61	1	95	39	40	7
		% within Taxa	1.7%	88.3%	63.5%	1.6%	81.9%	97.5%	95.2%	16.7%
	Above dental row	Count	59	14	35	61	21	1	2	35
		% within Taxa	98.3%	11.7%	36.5%	98.4%	18.1%	2.5%	4.8%	83.3%
Total		Count	60	120	96	62	116	40	42	42
		% within Taxa	100.0%	100.0%	100.0%	100.0%	100.0%	100.0%	100.0%	100.0%

91: Serres canal (SeC)

			Taxa							
			Gorilla	Pan	Homo	Pongo	Hylobates	Papio	Cercopithecus	Colobus
Serres canal	Absent	Count	50	100	77	61	103	40	42	42
		% within Taxa	86.2%	83.3%	80.2%	98.4%	87.3%	100.0%	100.0%	100.0%
	Present	Count	8	20	19	1	15	0	0	0
		% within Taxa	13.8%	16.7%	19.8%	1.6%	12.7%	.0%	.0%	.0%
Total		Count	58	120	96	62	118	40	42	42
		% within Taxa	100.0%	100.0%	100.0%	100.0%	100.0%	100.0%	100.0%	100.0%

92: Molar foramen (MoF)

			Taxa							
			Gorilla	Pan	Homo	Pongo	Hylobates	Papio	Cercopithecus	Colobus
Molar foramen	Absent	Count	25	78	76	59	86	38	40	29
		% within Taxa	43.1%	65.0%	79.2%	95.2%	72.9%	95.0%	95.2%	69.0%
	Present	Count	33	42	20	3	32	2	2	13
		% within Taxa	56.9%	35.0%	20.8%	4.8%	27.1%	5.0%	4.8%	31.0%
Total		Count	58	120	96	62	118	40	42	42
		% within Taxa	100.0%	100.0%	100.0%	100.0%	100.0%	100.0%	100.0%	100.0%

93: Retromolar foramen (RMF)

			Taxa							
			Gorilla	Pan	Homo	Pongo	Hylobates	Papio	Cercopithecus	Colobus
Retromolar foramen	Absent	Count	57	120	92	62	118	40	42	40
		% within Taxa	96.6%	100.0%	95.8%	100.0%	100.0%	100.0%	100.0%	95.2%
	Present	Count	2	0	4	0	0	0	0	2
		% within Taxa	3.4%	.0%	4.2%	.0%	.0%	.0%	.0%	4.8%
Total		Count	59	120	96	62	118	40	42	42
		% within Taxa	100.0%	100.0%	100.0%	100.0%	100.0%	100.0%	100.0%	100.0%

94: Robinson canal (RoC)

			Taxa							
			Gorilla	Pan	Homo	Pongo	Hylobates	Papio	Cercopithecus	Colobus
Robinson canal	Absent	Count	59	120	87	62	113	40	42	42
		% within Taxa	100.0%	100.0%	90.6%	100.0%	95.8%	100.0%	100.0%	100.0%
	Present	Count	0	0	9	0	5	0	0	0
		% within Taxa	.0%	.0%	9.4%	.0%	4.2%	.0%	.0%	.0%
Total		Count	59	120	96	62	118	40	42	42
		% within Taxa	100.0%	100.0%	100.0%	100.0%	100.0%	100.0%	100.0%	100.0%

95: Mylohyoid bridge (MyB)

			Taxa							
			Gorilla	Pan	Homo	Pongo	Hylobates	Papio	Cercopithecus	Colobus
Mylohyoid bridge	Absent	Count	40	120	78	62	118	40	42	42
		% within Taxa	67.8%	100.0%	81.3%	100.0%	100.0%	100.0%	100.0%	100.0%
	Present	Count	19	0	18	0	0	0	0	0
		% within Taxa	32.2%	.0%	18.8%	.0%	.0%	.0%	.0%	.0%
Total		Count	59	120	96	62	118	40	42	42
		% within Taxa	100.0%	100.0%	100.0%	100.0%	100.0%	100.0%	100.0%	100.0%

96: Clinoidescaroticum foramen (CSF)

			Taxa							
			Gorilla	Pan	Homo	Pongo	Hylobates	Papio	Cercopithecus	Colobus
Clinoidescaroticum foramen	Other	Count	43	105	66	15	87	24	36	36
		% within Taxa	71.7%	89.7%	70.2%	25.0%	76.3%	63.2%	85.7%	85.7%
	Complete	Count	17	12	28	45	27	14	6	6
		% within Taxa	28.3%	10.3%	29.8%	75.0%	23.7%	36.8%	14.3%	14.3%
Total		Count	60	117	94	60	114	38	42	42
		% within Taxa	100.0%	100.0%	100.0%	100.0%	100.0%	100.0%	100.0%	100.0%

97: Posterior clinoid foramen (PCF)

			Taxa							
			Gorilla	Pan	Homo	Pongo	Hylobates	Papio	Cercopithecus	Colobus
Posterior clinoid foramen	Other	Count	36	57	84	10	31	14	36	21
		% within Taxa	60.0%	48.7%	87.5%	16.9%	27.7%	35.0%	85.7%	50.0%
	Complete	Count	24	60	12	49	81	26	6	21
		% within Taxa	40.0%	51.3%	12.5%	83.1%	72.3%	65.0%	14.3%	50.0%
Total		Count	60	117	96	59	112	40	42	42
		% within Taxa	100.0%	100.0%	100.0%	100.0%	100.0%	100.0%	100.0%	100.0%

98: Inferior orbital fissure foramen (IFF)

			Taxa							
			Gorilla	Pan	Homo	Pongo	Hylobates	Papio	Cercopithecus	Colobus
Inferior orbital fissure foramen	Absent	Count	34	47	94	48	117	37	42	37
		% within Taxa	100.0%	39.2%	97.9%	92.3%	99.2%	92.5%	100.0%	88.1%
	Present	Count	0	73	2	4	1	3	0	5
		% within Taxa	.0%	60.8%	2.1%	7.7%	.8%	7.5%	.0%	11.9%
Total		Count	34	120	96	52	118	40	42	42
		% within Taxa	100.0%	100.0%	100.0%	100.0%	100.0%	100.0%	100.0%	100.0%

99: Mental foramen under P3 ($MeFP_2$)

			Taxa							
			Gorilla	Pan	Homo	Pongo	Hylobates	Papio	Cercopithecus	Colobus
Mental foramen under P3	Posterior to P3	Count	24	111	91	58	14	12	40	33
		% within Taxa	41.4%	92.5%	94.8%	93.5%	11.9%	31.6%	95.2%	80.5%
	Under P3	Count	34	9	5	4	104	26	2	8
		% within Taxa	58.6%	7.5%	5.2%	6.5%	88.1%	68.4%	4.8%	19.5%
Total		Count	58	120	96	62	118	38	42	41
		% within Taxa	100.0%	100.0%	100.0%	100.0%	100.0%	100.0%	100.0%	100.0%

100: Single incisive canal (InC)

			Taxa							
			Gorilla	Pan	Homo	Pongo	Hylobates	Papio	Cercopithecus	Colobus
Single incisive canal	Multiple	Count	18	0	5	2	52	20	21	21
		% within Taxa	60.0%	.0%	10.4%	6.5%	88.1%	100.0%	100.0%	100.0%
	Single	Count	12	60	43	29	7	0	0	0
		% within Taxa	40.0%	100.0%	89.6%	93.5%	11.9%	.0%	.0%	.0%
Total		Count	30	60	48	31	59	20	21	21
		% within Taxa	100.0%	100.0%	100.0%	100.0%	100.0%	100.0%	100.0%	100.0%

101: Palatine fenestrae (PFn)

			Taxa							
			Gorilla	Pan	Homo	Pongo	Hylobates	Papio	Cercopithecus	Colobus
Palatine fenestrae	Absent	Count	30	60	48	31	24	0	0	0
		% within Taxa	100.0%	100.0%	100.0%	100.0%	42.1%	.0%	.0%	.0%
	Present	Count	0	0	0	0	33	20	21	21
		% within Taxa	.0%	.0%	.0%	.0%	57.9%	100.0%	100.0%	100.0%
Total		Count	30	60	48	31	57	20	21	21
		% within Taxa	100.0%	100.0%	100.0%	100.0%	100.0%	100.0%	100.0%	100.0%

102: Stylomastoid foramen, round (SMFS)

			Taxa							
			Gorilla	Pan	Homo	Pongo	Hylobates	Papio	Cercopithecus	Colobus
Stylomastoid foramen, round	Other	Count	54	85	73	55	104	38	36	26
		% within Taxa	90.0%	71.4%	77.7%	88.7%	88.9%	95.0%	85.7%	61.9%
	Round	Count	6	34	21	7	13	2	6	16
		% within Taxa	10.0%	28.6%	22.3%	11.3%	11.1%	5.0%	14.3%	38.1%
Total		Count	60	119	94	62	117	40	42	42
		% within Taxa	100.0%	100.0%	100.0%	100.0%	100.0%	100.0%	100.0%	100.0%

103: Infraorbital foramen, round (IOFS)

			Taxa							
			Gorilla	Pan	Homo	Pongo	Hylobates	Papio	Cercopithecus	Colobus
Infraorbital foramen, round	Other	Count	51	70	83	46	114	38	31	36
		% within Taxa	85.0%	58.3%	86.5%	74.2%	96.6%	95.0%	73.8%	85.7%
	Round	Count	9	50	13	16	4	2	11	6
		% within Taxa	15.0%	41.7%	13.5%	25.8%	3.4%	5.0%	26.2%	14.3%
Total		Count	60	120	96	62	118	40	42	42
		% within Taxa	100.0%	100.0%	100.0%	100.0%	100.0%	100.0%	100.0%	100.0%

104: Carotid canal, round (CaCS)

			Taxa							
			Gorilla	Pan	Homo	Pongo	Hylobates	Papio	Cercopithecus	Colobus
Carotid canal, round	Other	Count	39	86	96	39	85	23	17	29
		% within Taxa	65.0%	72.3%	100.0%	62.9%	72.0%	57.5%	40.5%	69.0%
	Round	Count	21	33	0	23	33	17	25	13
		% within Taxa	35.0%	27.7%	.0%	37.1%	28.0%	42.5%	59.5%	31.0%
Total		Count	60	119	96	62	118	40	42	42
		% within Taxa	100.0%	100.0%	100.0%	100.0%	100.0%	100.0%	100.0%	100.0%

105: Greater palatine foramen, round (GPFS)

			Taxa							
			Gorilla	Pan	Homo	Pongo	Hylobates	Papio	Cercopithecus	Colobus
Greater palatine foramen, round	Other	Count	57	119	94	62	101	40	40	42
		% within Taxa	95.0%	100.0%	97.9%	100.0%	85.6%	100.0%	95.2%	100.0%
	Round	Count	3	0	2	0	17	0	2	0
		% within Taxa	5.0%	.0%	2.1%	.0%	14.4%	.0%	4.8%	.0%
Total		Count	60	119	96	62	118	40	42	42
		% within Taxa	100.0%	100.0%	100.0%	100.0%	100.0%	100.0%	100.0%	100.0%

106: Mental foramen, tear-shaped (MeFS)

			Taxa							
			Gorilla	Pan	Homo	Pongo	Hylobates	Papio	Cercopithecus	Colobus
Mental foramen, tear-shaped	Other	Count	52	83	95	60	114	38	40	42
		% within Taxa	86.7%	69.2%	99.0%	96.8%	96.6%	95.0%	95.2%	100.0%
	Tear-shaped	Count	8	37	1	2	4	2	2	0
		% within Taxa	13.3%	30.8%	1.0%	3.2%	3.4%	5.0%	4.8%	.0%
Total		Count	60	120	96	62	118	40	42	42
		% within Taxa	100.0%	100.0%	100.0%	100.0%	100.0%	100.0%	100.0%	100.0%

107: Zygomatico-temporal foramen, round (ZTFS)

			Taxa							
			Gorilla	Pan	Homo	Pongo	Hylobates	Papio	Cercopithecus	Colobus
Zygomatico-temporal foramen, round	Other	Count	5	11	6	0	1	0	4	0
		% within Taxa	8.3%	9.2%	6.3%	.0%	.9%	.0%	9.5%	.0%
	Round	Count	55	109	90	62	115	40	38	42
		% within Taxa	91.7%	90.8%	93.8%	100.0%	99.1%	100.0%	90.5%	100.0%
Total		Count	60	120	96	62	116	40	42	42
		% within Taxa	100.0%	100.0%	100.0%	100.0%	100.0%	100.0%	100.0%	100.0%

108: Mastoid foramen, round (MaFS)

			Taxa							
			Gorilla	Pan	Homo	Pongo	Hylobates	Papio	Cercopithecus	Colobus
Mastoid foramen, round	Other	Count	59	118	84	59	108	39	42	42
		% within Taxa	98.3%	98.3%	87.5%	95.2%	92.3%	97.5%	100.0%	100.0%
	Round	Count	1	2	12	3	9	1	0	0
		% within Taxa	1.7%	1.7%	12.5%	4.8%	7.7%	2.5%	.0%	.0%
Total		Count	60	120	96	62	117	40	42	42
		% within Taxa	100.0%	100.0%	100.0%	100.0%	100.0%	100.0%	100.0%	100.0%

109: Lesser palatine foramen, round (LPFS)

			Taxa							
			Gorilla	Pan	Homo	Pongo	Hylobates	Papio	Cercopithecus	Colobus
Lesser palatine foramen, round	Other	Count	56	109	94	57	104	40	39	41
		% within Taxa	96.6%	92.4%	97.9%	91.9%	89.7%	100.0%	92.9%	97.6%
	Round	Count	2	9	2	5	12	0	3	1
		% within Taxa	3.4%	7.6%	2.1%	8.1%	10.3%	.0%	7.1%	2.4%
Total		Count	58	118	96	62	116	40	42	42
		% within Taxa	100.0%	100.0%	100.0%	100.0%	100.0%	100.0%	100.0%	100.0%

110: Mandibular foramen, round (MbFS)

			Taxa							
			Gorilla	Pan	Homo	Pongo	Hylobates	Papio	Cercopithecus	Colobus
Mandibular foramen, round	Other	Count	57	113	83	59	111	38	42	40
		% within Taxa	98.3%	94.2%	86.5%	95.2%	96.5%	95.0%	100.0%	95.2%
	Round	Count	1	7	13	3	4	2	0	2
		% within Taxa	1.7%	5.8%	13.5%	4.8%	3.5%	5.0%	.0%	4.8%
Total		Count	58	120	96	62	115	40	42	42
		% within Taxa	100.0%	100.0%	100.0%	100.0%	100.0%	100.0%	100.0%	100.0%

111: Zygomatic-facial foramen, round (ZFFS)

			Taxa							
			Gorilla	Pan	Homo	Pongo	Hylobates	Papio	Cercopithecus	Colobus
Zygomatico-facial foramen, round	Other	Count	60	106	90	62	101	38	32	35
		% within Taxa	100.0%	89.8%	93.8%	100.0%	86.3%	95.0%	76.2%	83.3%
	Round	Count	0	12	6	0	16	2	10	7
		% within Taxa	.0%	10.2%	6.3%	.0%	13.7%	5.0%	23.8%	16.7%
Total		Count	60	118	96	62	117	40	42	42
		% within Taxa	100.0%	100.0%	100.0%	100.0%	100.0%	100.0%	100.0%	100.0%

112: Supragenial bridge (SGB)

			Taxa							
			Gorilla	Pan	Homo	Pongo	Hylobates	Papio	Cercopithecus	Colobus
Supragenial bridge	Absent	Count	29	60	48	29	58	19	21	20
		% within Taxa	100.0%	100.0%	100.0%	93.5%	98.3%	95.0%	100.0%	95.2%
	Present	Count	0	0	0	2	1	1	0	1
		% within Taxa	.0%	.0%	.0%	6.5%	1.7%	5.0%	.0%	4.8%
	Total	Count	29	60	48	31	59	20	21	21
		% within Taxa	100.0%	100.0%	100.0%	100.0%	100.0%	100.0%	100.0%	100.0%

Appendix IV. DATA MATRICES

In this appendix, I included the data matrices used to test Hypothesis 1a (Main Hypothesis). See Chapter 5 for explanation.

Analysis 1a.1a

	IOF	ZTF	ZFF	PEF	MaF	IOB	ION	ICIO	IOG	SLGB	SON	SOF	ZTFP	ZTFP	ZTFP	ZTFP2b	ZTFP2a	ZTIPb
Gorilla	A	5	E	9	D	8	9	4	3	1	7	8	6	A	0	2	9	8
Pan	A	5	4	3	D	3	1	A	2	5	B	8	6	5	3	2	9	1
Homo	E	A	C	2	9	8	9	1	8	2	3	0	D	1	9	2	D	8
Pongo	3	E	4	1	4	8	9	1	4	7	C	8	D	E	9	D	D	D
Hylobates	A	6	4	A	4	8	1	A	C	C	7	8	A	1	9	8	4	D
Papio	3	5	5	8	4	7	9	A	3	A	0	8	1	A	9	D	0	7
Cercopithecus	3	6	5	E	4	7	9	A	C	7	3	8	1	A	8	8	4	5
Colobus	3	5	8	9	5	7	9	A	C	C	D	8	6	5	9	8	4	1

	ZTIPa	ZTIPc	ZFN	ZFFPc	ZFFPd	AEFP	Fro	OcF	PEFPb	SOFi	PEFPa	MMAE	MaFPb	MaFPa	MaFPc	SMB	SMFP	PaF1
Gorilla	0	9	A	E	C	4	5	7	7	D	7	8	D	8	8	8	6	8
Pan	6	9	A	4	3	4	C	7	3	4	7	7	D	9	8	1	6	8
Homo	B	2	A	C	1	1	4	7	3	1	7	7	9	2	7	9	6	0
Pongo	B	9	2	3	C	3	4	7	0	4	7	7	9	1	8	8	6	8
Hylobates	B	0	2	4	5	A	C	7	7	9	D	6	5	9	7	A	6	8
Papio	2	9	A	4	C	E	5	7	C	D	1	9	2	9	4	5	E	8
Cercopithecus	4	9	A	9	5	A	5	7	C	3	D	7	2	9	7	7	6	8
Colobus	B	9	2	6	6	A	9	7	C	9	1	7	3	9	7	9	6	8

	PaF2	PaF3	CaCP1	CaCP2	IOFSZ	ZTFSZ	ZFFSZ	MaFSZ	SMFSZ	CaCSZ	JuFLg	HyCSZ	FOvSZ	GPFSZ	LPFSZ	MeFSZ	MbFSZ	ZMSmind
Gorilla	0	8	5	8	3	5	E	9	4	2	6	5	2	1	4	1	2	2
Pan	8	8	5	8	3	4	B	B	3	3	4	4	5	4	2	5	7	9
Homo	8	8	D	0	0	B	9	1	0	0	0	0	0	6	1	5	5	C
Pongo	6	8	2	8	7	C	0	3	5	6	A	8	5	6	A	1	5	6
Hylobates	8	3	0	8	8	B	3	8	B	A	9	A	E	A	A	B	C	6
Papio	8	7	C	8	9	0	3	2	8	8	4	4	6	1	A	6	0	0
Cercopithecus	9	7	A	8	E	A	B	9	E	E	C	D	B	D	A	C	C	8
Colobus	9	7	9	8	C	4	A	B	B	C	C	D	B	D	A	D	C	8

	ZMStvd	Go	FMaSZ	InCLg	MeFpos	InCpos	IOFpos	IJPE	HyC	ICC	CoC	CoCO	CPC	MgF	Fov	FOvP	MBC	JuB
Gorilla	0	0	3	8	C	9	0	3	C	8	4	7	2	4	1	7	7	8
Pan	5	5	5	A	A	C	3	6	6	5	2	7	5	8	3	1	7	3
Homo	6	D	0	B	E	E	8	2	0	0	0	0	A	2	2	C	7	6
Pongo	8	4	3	C	7	2	8	9	C	9	A	8	6	D	7	1	7	8
Hylobates	A	8	A	8	7	7	8	9	6	A	A	A	9	B	7	8	7	8
Papio	2	4	8	0	2	5	3	B	C	8	A	8	8	6	C	8	7	9
Cercopithecus	C	C	D	3	0	1	C	6	5	9	A	8	8	5	C	A	7	7
Colobus	9	4	D	3	4	6	E	A	3	7	A	8	8	7	C	9	7	7

	FMaS	FMaP2	FMaP1	InF	FSp	Fve	PSB	PAB	FSpP	Fla	RaC2	RaC1	GPFP	PCr	LPF	LPFP	MeF	MbFP
Gorilla	8	3	5	7	2	5	6	B	6	B	8	A	4	D	2	3	5	1
Pan	6	7	4	6	3	5	C	B	1	6	8	B	4	C	2	4	D	B
Homo	9	B	D	7	1	0	B	4	C	0	8	B	B	3	2	1	C	6
Pongo	B	0	5	7	7	7	D	B	3	2	8	7	4	3	A	A	6	1
Hylobates	3	8	4	8	B	B	6	B	C	C	8	A	D	0	7	A	B	A
Papio	8	9	D	7	A	A	6	0	5	B	0	0	4	8	E	B	0	C
Cercopithecus	5	9	7	7	B	A	1	4	5	8	8	4	4	8	9	6	2	B
Colobus	6	9	5	7	B	8	1	4	C	6	8	3	C	D	A	B	7	4

	SeC	MoF	RMF	RoC	MyB	CSF	PCF	IFF	MeFPos2	InC	PFn	SMFS	IOFS	CaCS	GPFS	MeFS	ZTFS	MaFS
Gorilla	3	0	7	8	1	7	8	8	3	6	B	9	7	7	7	5	8	8
Pan	3	4	7	8	9	C	7	0	A	1	B	3	2	7	8	0	9	8
Homo	3	6	7	4	1	7	D	9	B	3	B	5	7	E	8	9	7	3
Pongo	B	C	7	8	9	0	2	8	A	2	B	9	5	7	8	8	5	7
Hylobates	3	5	7	7	9	7	2	9	0	B	6	A	D	7	2	9	4	7
Papio	B	C	7	7	9	5	4	8	3	B	2	A	A	6	8	8	7	7
Cercopithecus	B	C	7	7	9	9	D	8	A	B	2	8	5	1	7	8	9	8
Colobus	B	5	7	7	9	9	7	6	9	B	2	2	7	7	8	9	7	8

	LPFS	MbFS	ZFFS	SGB
Gorilla	7	8	B	7
Pan	7	7	5	7
Homo	8	4	8	7
Pongo	7	7	B	7
Hylobates	6	8	5	7
Papio	7	7	8	7
Cercopithecus	7	6	3	7
Colobus	7	7	5	7

Analysis 1a.1b

	IOF	ZTF	ZFF	PEF	MaF	IOB	ION	ICIO	IOG	SLGB	SON	SOF	ZTFP	ZTFP	ZTFP	ZTFP2b	ZTFP2a	ZTIPb
Gorilla	1	1	0	1	1	0	1	1	1	1	1	0	1	1	1	1	1	1
Pan	1	1	1	1	1	1	1	0	1	1	1	0	1	1	1	1	1	1
Homo	1	1	1	1	1	0	1	1	1	1	1	1	0	1	0	1	0	1
Pongo	1	0	1	1	1	0	0	1	1	1	1	0	0	0	0	0	0	0
Hylobates	1	1	1	1	1	0	1	0	0	0	1	0	1	1	0	1	1	0
Papio	1	1	1	1	1	0	0	0	1	0	1	0	1	1	0	0	1	1
Cercopithecus	1	1	1	0	1	0	0	0	1	1	1	0	1	1	0	1	1	1
Colobus	1	1	1	1	1	0	0	0	0	0	1	0	1	1	0	1	1	1

	ZTIPa	ZTIPc	ZFN	ZFFPc	ZFFPd	AEFP	Fro	OcF	PEFPb	SOFi	PEFPa	MMAE	MaFPb	MaFPa	MaFPc	SMB	SMFP	PaF1
Gorilla	1	0	0	0	0	1	1	0	1	1	1	0	1	1	0	1	1	0
Pan	1	0	0	1	1	1	1	0	1	1	1	0	1	1	0	1	1	0
Homo	0	1	0	1	1	1	1	1	1	1	1	0	1	1	0	1	1	1
Pongo	0	0	1	1	0	1	1	0	1	1	1	0	1	1	0	1	1	0
Hylobates	0	1	1	1	1	1	1	1	1	1	0	0	1	1	0	1	1	0
Papio	1	0	0	1	0	0	1	0	0	1	1	1	1	1	1	1	1	0
Cercopithecus	1	0	0	1	1	1	1	0	0	1	0	0	1	1	0	1	1	0
Colobus	0	0	1	1	1	1	1	0	0	1	1	0	1	1	0	0	1	0

	PaF2	PaF3	CaCP1	CaCP2	IOFSZ	ZTFSZ	ZFFSZ	MaFSZ	SMFSZ	CaCSZ	JuFLg	HyCSZ	FOvSZ	GPFSZ	LPFSZ	MeFSZ	MbFSZ	ZMSmind
Gorilla	1	0	1	0	1	1	0	0	1	1	0	1	1	1	1	1	1	1
Pan	1	0	1	0	1	1	1	0	1	1	1	1	1	1	1	1	1	0
Homo	1	0	0	1	1	0	0	1	1	1	1	1	1	1	1	1	1	0
Pongo	1	0	1	0	1	0	1	1	1	0	0	0	1	1	0	1	1	0
Hylobates	1	1	1	0	0	0	1	0	0	0	0	0	0	0	0	0	0	1
Papio	0	0	0	0	0	1	1	1	1	0	0	1	1	1	0	1	1	1
Cercopithecus	0	0	1	0	0	0	0	0	0	0	0	0	0	0	0	0	0	0
Colobus	0	0	1	0	0	1	0	0	0	0	0	0	0	0	0	0	0	0

	ZMStvd	Go	FMaSZ	InCLg	MeFpos	InCpos	IOFpos	IJPE	HyC	ICC	CoC	CoCO	CPC	MgF	Fov	FOvP	MBC	JuB
Gorilla	1	1	1	1	0	0	1	1	1	1	1	1	1	1	1	1	1	0
Pan	0	0	1	0	0	0	1	1	1	1	1	1	1	1	1	1	0	1
Homo	0	0	1	0	0	0	0	1	1	1	1	1	0	1	1	0	1	1
Pongo	0	1	1	0	1	1	0	1	1	0	0	0	1	0	1	1	0	1
Hylobates	0	0	0	1	1	0	0	1	1	0	0	0	1	0	1	1	0	1
Papio	1	1	0	1	1	1	1	1	1	0	0	0	0	1	0	1	0	0
Cercopithecus	0	0	0	1	1	1	0	1	1	0	0	0	0	1	0	0	0	1
Colobus	0	1	0	1	1	1	0	1	1	1	0	0	0	1	0	0	0	1

	FMaS	FMaP2	FMaP1	InF	FSp	Fve	PSB	PAB	FSpP	Fla	RaC2	RaC1	GPFP	PCr	LPF	LPFP	MeF	MbFP
Gorilla	1	1	1	0	1	1	1	0	1	0	0	0	1	0	1	1	1	1
Pan	1	1	1	1	1	1	1	0	1	1	0	0	1	1	1	1	0	1
Homo	0	0	1	1	1	1	1	1	0	1	0	0	1	1	1	1	0	1
Pongo	0	1	1	0	1	1	1	0	1	1	0	1	1	1	1	1	1	1
Hylobates	1	1	1	0	0	0	1	0	0	0	0	0	1	1	1	1	1	1
Papio	0	0	0	0	1	0	1	1	1	0	1	1	1	1	1	1	1	0
Cercopithecus	1	1	1	0	0	0	1	1	1	1	0	1	1	1	1	1	1	0
Colobus	1	0	1	0	0	0	1	1	0	1	0	1	1	0	1	1	1	1

	SeC	MoF	RMF	RoC	MyB	CSF	PCF	IFF	MeFPos2	InC	PFn	SMFS	IOFS	CaCS	GPFS	MeFS	ZTFS	MaFS
Gorilla	1	1	0	0	1	1	1	0	1	1	0	1	1	1	0	1	1	0
Pan	1	1	0	0	0	1	1	1	1	1	0	1	1	1	0	1	1	0
Homo	1	1	0	1	1	1	1	0	1	1	0	1	1	0	0	0	1	1
Pongo	0	0	0	0	0	1	1	1	1	1	0	1	1	1	0	0	1	0
Hylobates	1	1	0	0	0	1	1	0	1	1	1	1	0	1	1	0	1	1
Papio	0	0	0	0	0	1	1	1	1	0	1	0	0	1	0	0	1	0
Cercopithecus	0	0	0	0	0	1	1	0	0	0	1	1	1	1	0	0	1	0
Colobus	0	1	0	0	0	1	1	1	1	0	1	1	1	1	0	0	1	0

	LPFS	MbFS	ZFFS	SGB
Gorilla	0	0	0	0
Pan	1	1	1	0
Homo	0	1	1	0
Pongo	1	0	0	1
Hylobates	1	0	1	0
Papio	0	0	0	0
Cercopithecus	1	0	1	0
Colobus	0	0	1	0

Analysis 1a.1c

	IOF	ZTF	ZFF	PEF	MaF	IOB	ION	ICIO	IOG	SLGB	SON	SOF	ZTFP	ZTFP	ZTFP	ZTFP2b	ZTFP2a	ZTIPb
Gorilla	4	6	1	3	2	1	6	6	7	8	4	6	6	3	8	8	3	4
Pan	2	5	7	6	1	8	7	1	8	6	3	5	5	5	7	6	4	7
Homo	1	2	2	7	3	6	5	8	4	7	7	8	2	7	1	7	1	3
Pongo	5	1	7	8	6	1	1	7	5	4	2	1	1	1	1	1	2	1
Hylobates	3	3	6	2	4	7	8	1	2	2	5	7	3	8	5	5	5	2
Papio	6	6	4	5	8	1	4	1	6	3	8	1	7	4	1	1	8	5
Cercopithecus	6	4	5	1	7	1	1	5	3	5	6	1	8	2	6	3	6	6
Colobus	6	6	3	4	5	1	3	1	1	1	1	1	4	6	1	4	7	8

	ZTIPa	ZTIPc	ZFN	ZFFPc	ZFFPd	AEFP	Fro	OcF	PEFPb	SOFi	PEFPa	MMAE	MaFPb	MaFPa	MaFPc	SMB	SMFP	PaF1
Gorilla	8	1	1	1	3	5	4	1	4	1	4	1	1	6	1	5	2	4
Pan	5	6	1	6	7	6	2	6	6	6	5	4	2	5	5	8	2	3
Homo	1	7	1	2	8	8	4	7	7	8	6	5	3	7	7	3	2	8
Pongo	1	1	6	8	2	7	4	1	8	5	3	6	4	8	1	4	2	1
Hylobates	1	8	8	5	6	3	1	8	5	4	2	1	5	4	6	2	2	7
Papio	7	1	1	7	1	1	4	1	1	2	8	8	7	3	8	7	1	6
Cercopithecus	6	1	1	3	5	2	4	1	1	7	1	7	8	1	1	6	2	1
Colobus	4	1	7	4	4	4	3	1	3	3	7	1	6	1	1	1	2	5

	PaF2	PaF3	CaCP1	CaCP2	IOFSZ	ZTFSZ	ZFFSZ	MaFSZ	SMFSZ	CaCSZ	JuFLg	HyCSZ	FOvSZ	GPFSZ	LPFSZ	MeFSZ	MbFSZ	ZMSmind
Gorilla	8	1	5	1	7	5	1	4	6	7	5	5	7	7	6	8	7	7
Pan	6	1	6	1	6	7	5	1	7	6	7	7	4	5	7	4	4	1
Homo	4	1	1	8	8	2	4	8	8	8	8	8	8	4	8	6	6	2
Pongo	7	1	7	1	5	1	8	6	5	5	2	4	6	6	1	7	5	4
Hylobates	5	8	8	1	4	4	6	5	3	3	4	3	1	3	2	3	1	6
Papio	3	1	1	7	3	8	7	7	4	4	6	6	5	8	3	5	8	8
Cercopithecus	1	1	3	1	1	3	3	3	1	1	3	1	2	1	5	2	2	5
Colobus	1	1	4	1	2	6	2	2	2	2	1	2	3	2	4	1	3	3

	ZMStvd	Go	FMaSZ	InCLg	MeFpos	InCpos	IOFpos	IJPE	HyC	ICC	CoC	CoCO	CPC	MgF	Fov	FOvP	MBC	JuB
Gorilla	8	8	7	4	2	3	8	7	2	5	6	6	8	7	8	6	8	2
Pan	3	3	5	3	3	2	7	5	5	7	7	7	7	3	6	7	1	8
Homo	6	2	8	2	1	1	5	8	8	8	8	8	1	8	7	1	7	7
Pongo	5	5	6	1	5	7	3	3	3	4	2	5	6	1	4	8	1	3
Hylobates	2	4	3	5	4	4	4	4	4	1	3	1	5	2	5	5	1	4
Papio	7	6	4	8	7	6	6	1	1	1	4	1	1	5	1	4	1	1
Cercopithecus	1	1	1	7	8	8	2	6	6	1	1	1	1	6	1	1	1	6
Colobus	4	7	2	6	6	5	1	2	7	6	5	1	1	4	1	3	1	5

	FMaS	FMaP2	FMaP1	InF	FSp	Fve	PSB	PAB	FSpP	Fla	RaC2	RaC1	GPFP	PCr	LPF	LPFP	MeF	MbFP
Gorilla	4	7	4	6	7	7	6	1	4	3	1	3	4	1	8	7	6	7
Pan	5	6	5	8	6	6	2	4	8	6	1	1	4	5	6	6	1	3
Homo	2	2	2	7	8	8	3	6	1	8	1	1	3	7	7	8	2	5
Pongo	1	8	5	4	5	5	1	3	7	7	7	5	4	6	2	3	5	8
Hylobates	8	5	5	5	3	3	5	2	3	2	1	4	1	8	5	4	3	4
Papio	3	1	1	1	4	1	4	8	5	1	8	8	4	4	1	2	8	1
Cercopithecus	7	4	3	1	2	1	7	5	6	4	1	6	4	3	4	5	7	2
Colobus	6	3	5	1	1	4	7	7	1	5	1	7	2	1	3	1	4	6

	SeC	MoF	RMF	RoC	MyB	CSF	PCF	IFF	MeFPos2	InC	PFn	SMFS	IOFS	CaCS	GPFS	MeFS	ZTFS	MaFS
Gorilla	6	8	6	1	8	5	3	1	6	5	1	2	5	5	7	7	3	3
Pan	7	7	1	1	1	1	5	8	4	8	1	7	8	2	1	8	2	3
Homo	8	4	7	8	7	6	1	4	2	6	1	6	3	1	5	2	4	8
Pongo	4	2	1	1	1	8	8	6	3	7	1	4	6	6	1	3	6	6
Hylobates	5	5	1	7	1	4	7	3	8	4	5	3	1	3	8	4	5	7
Papio	1	3	1	1	1	7	6	5	7	1	6	1	2	7	1	6	6	5
Cercopithecus	1	1	1	1	1	2	2	1	1	1	6	5	7	8	6	5	1	1
Colobus	1	6	8	1	1	2	4	7	5	1	6	8	4	4	1	1	6	1

	LPFS	MbFS	ZFFS	SGB
Gorilla	4	2	1	1
Pan	6	7	5	1
Homo	2	8	4	1
Pongo	7	5	1	8
Hylobates	8	3	6	5
Papio	1	6	3	7
Cercopithecus	5	1	8	1
Colobus	3	4	7	6

Analysis 1a.1d

	IOF	ZTF	ZFF	PEF	MaF	IOB	ION	ICIO	IOG	SLGB	SON	SOF	ZTFP	ZTFP	ZTFP	ZTFP2b	ZTFP2a	ZTIPb
Gorilla	H	Q	0	B	8	0	2	8	Q	A	A	0	B	6	F	N	6	4
Pan	E	Q	Q	N	8	2	6	0	Q	6	5	0	A	G	3	M	8	L
Homo	2	M	H	Q	G	0	1	P	H	9	L	5	0	M	0	M	0	3
Pongo	P	0	Q	Q	N	0	0	L	P	3	2	0	0	0	0	0	0	0
Hylobates	E	P	Q	9	L	0	7	0	0	0	A	0	3	M	0	C	E	0
Papio	Q	Q	P	E	P	0	0	0	P	1	Q	0	G	8	0	0	Q	6
Cercopithecus	Q	P	P	0	P	0	0	1	2	3	G	0	J	4	1	7	G	C
Colobus	Q	Q	N	D	L	0	0	0	0	0	1	0	9	G	0	9	G	P

	ZTIPa	ZTIPc	ZFN	ZFFPc	ZFFPd	AEFP	Fro	OcF	PEFPb	SOFi	PEFPa	MMAE	MaFPb	MaFPa	MaFPc	SMB	SMFP	PaF1
Gorilla	N	0	0	0	0	B	Q	0	7	3	4	0	2	6	0	3	Q	0
Pan	6	0	0	P	C	B	M	0	J	P	4	0	2	6	0	B	Q	0
Homo	0	J	0	9	D	G	Q	1	K	Q	7	0	7	A	0	3	Q	C
Pongo	0	0	3	Q	0	F	Q	0	N	M	3	0	7	E	0	3	Q	0
Hylobates	0	N	7	P	9	5	L	1	8	G	0	0	E	5	0	1	Q	0
Papio	J	0	0	P	0	0	Q	0	0	6	E	2	L	2	2	6	C	0
Cercopithecus	C	0	0	J	7	4	Q	0	0	P	0	1	L	2	0	4	Q	0
Colobus	1	0	4	L	6	5	N	0	0	E	D	0	J	2	0	1	Q	0

	PaF2	PaF3	CaCP1	CaCP2	IOFSZ	ZTFSZ	ZFFSZ	MaFSZ	SMFSZ	CaCSZ	JuFLg	HyCSZ	FOvSZ	GPFSZ	LPFSZ	MeFSZ	MbFSZ	ZMSmind
Gorilla	E	0	C	0	L	H	0	2	L	G	A	C	M	Q	F	Q	K	G
Pan	3	0	F	0	L	K	H	0	L	D	C	F	E	H	P	H	D	0
Homo	2	0	0	5	Q	9	B	L	Q	Q	Q	Q	Q	H	Q	J	H	3
Pongo	6	0	L	0	D	0	Q	K	J	B	1	9	K	J	0	P	H	A
Hylobates	3	4	Q	0	C	A	K	A	5	6	9	7	0	A	1	3	0	D
Papio	1	0	0	1	B	Q	M	Q	F	9	C	D	J	Q	0	D	Q	Q
Cercopithecus	0	0	2	0	0	A	C	7	0	0	2	0	5	0	2	1	2	B
Colobus	0	0	4	0	6	G	8	6	5	2	0	3	4	2	2	0	4	8

	ZMStvd	Go	FMaSZ	InCLg	MeFpos	InCpos	IOFpos	IJPE	HyC	ICC	CoC	CoCO	CPC	MgF	Fov	FOvP	MBC	JuB
Gorilla	Q	Q	H	D	D	G	B	Q	5	1	5	2	8	6	Q	4	1	0
Pan	3	3	F	8	E	F	A	P	C	3	A	2	5	2	N	A	0	4
Homo	6	0	Q	7	C	F	6	Q	P	C	F	E	0	8	Q	0	1	3
Pongo	4	J	H	0	F	K	6	M	7	0	0	0	4	0	G	D	0	1
Hylobates	1	7	7	G	F	H	6	M	C	0	0	0	1	0	K	2	0	1
Papio	K	J	B	Q	J	J	9	J	3	0	0	0	0	3	0	1	0	0
Cercopithecus	0	0	0	M	K	M	5	P	D	0	0	0	0	4	0	0	0	2
Colobus	2	J	2	M	H	H	4	L	J	1	1	0	0	2	0	1	0	1

	FMaS	FMaP2	FMaP1	InF	FSp	Fve	PSB	PAB	FSpP	Fla	RaC2	RaC1	GPFP	PCr	LPF	LPFP	MeF	MbFP
Gorilla	0	B	Q	1	G	3	G	0	5	0	0	0	Q	0	Q	C	9	Q
Pan	4	5	Q	2	E	3	5	0	F	4	0	0	Q	7	Q	A	0	3
Homo	1	0	4	1	J	C	6	A	0	Q	0	0	M	F	Q	E	1	9
Pongo	0	J	Q	0	6	2	2	0	B	P	0	2	Q	E	8	4	7	Q
Hylobates	8	3	Q	0	1	0	E	0	0	0	0	0	F	P	F	5	1	4
Papio	1	0	0	0	3	0	D	L	7	0	3	P	Q	5	2	2	Q	0
Cercopithecus	7	2	M	0	0	0	Q	9	A	3	0	3	Q	4	C	8	F	1
Colobus	4	1	Q	0	0	0	Q	C	0	4	0	7	K	0	A	2	4	L

	SeC	MoF	RMF	RoC	MyB	CSF	PCF	IFF	MeFPos2	InC	PFn	SMFS	IOFS	CaCS	GPFS	MeFS	ZTFS	MaFS
Gorilla	3	E	0	0	8	7	A	0	E	A	0	2	3	8	1	3	P	0
Pan	4	8	0	0	0	2	C	F	1	Q	0	7	A	7	0	7	N	0
Homo	5	5	1	2	4	7	3	0	1	N	0	5	3	0	0	0	P	3
Pongo	0	1	0	0	0	J	L	2	1	P	0	2	6	9	0	0	Q	1
Hylobates	3	6	0	1	0	6	J	0	2	3	E	2	0	7	3	0	Q	2
Papio	0	1	0	0	0	9	G	1	H	0	Q	1	1	A	0	1	Q	0
Cercopithecus	0	1	0	0	0	3	3	0	1	0	Q	3	6	E	1	1	N	0
Colobus	0	7	1	0	0	3	C	3	4	0	Q	9	3	7	0	0	Q	0

	LPFS	MbFS	ZFFS	SGB
Gorilla	0	0	0	0
Pan	2	1	2	0
Homo	0	3	1	0
Pongo	2	1	0	1
Hylobates	2	0	3	0
Papio	0	1	1	1
Cercopithecus	1	0	6	0
Colobus	0	1	4	1

Analysis 1a.2a

	IOF	ZTF	ZFF	PEF	MaF	IOB	ION	ICIO	IOG	SLGB	SON	SOF	ZTFP	ZTFP	ZTFP	ZTFP2b	ZTFP2a	ZTIPb
Gorilla	6	3	A	8	9	6	7	4	3	1	5	6	3	7	0	2	5	4
Pan	6	3	3	3	9	1	1	8	2	4	9	6	3	4	2	2	5	0
Homo	A	7	8	2	6	6	7	1	8	2	2	0	9	1	7	2	9	4
Pongo	1	A	3	1	2	6	7	1	4	6	9	6	9	A	7	9	9	9
Hylobates	6	4	3	9	2	6	1	8	A	9	5	6	6	1	7	6	2	9
Papio	1	3	3	7	2	5	7	8	3	8	0	6	0	7	7	9	0	4

	ZTIPa	ZTIPc	ZFN	ZFFPc	ZFFPd	AEFP	Fro	OcF	PEFPb	SOFi	PEFPa	MMAE	MaFPb	MaFPa	MaFPc	SMB	SMFP	PaF1
Gorilla	0	7	7	A	8	4	3	5	7	9	5	6	9	6	6	6	4	6
Pan	4	7	7	3	2	4	9	5	3	3	5	5	9	7	6	1	4	6
Homo	8	2	7	8	1	1	3	5	3	0	5	5	5	2	5	7	4	0
Pongo	8	7	1	3	8	3	3	5	0	3	5	5	5	1	6	6	4	6
Hylobates	8	0	1	3	3	8	9	5	7	6	A	6	2	7	5	7	4	6
Papio	2	7	7	3	8	A	3	5	A	9	0	3	0	7	2	3	A	6

	PaF2	PaF3	CaCP1	CaCP2	IOFSZ	ZTFSZ	ZFFSZ	MaFSZ	SMFSZ	CaCSZ	JuFLg	HyCSZ	FOvSZ	GPFSZ	LPFSZ	MeFSZ	MbFSZ	ZMSmind
Gorilla	0	6	5	6	3	4	A	7	4	2	6	5	2	1	4	1	2	2
Pan	6	6	5	6	3	3	7	9	3	3	4	4	5	4	2	5	7	9
Homo	6	6	9	0	0	8	8	1	0	0	0	0	0	6	1	5	5	8
Pongo	6	6	2	6	7	8	0	3	5	6	8	8	5	6	8	1	5	4
Hylobates	6	1	0	6	8	8	3	7	A	A	9	A	A	A	8	A	A	6
Papio	6	5	9	6	9	0	3	2	8	8	4	4	6	1	8	6	0	0

	ZMStvd	Go	FMaSZ	InCLg	MeFpos	InCpos	IOFpos	IJPE	HyC	ICC	CoC	CoCO	CPC	MgF	Fov	FOvP	MBC	JuB
Gorilla	0	0	3	4	8	5	0	2	8	6	4	5	2	2	1	6	5	6
Pan	5	5	5	6	6	8	3	5	3	4	2	5	3	6	3	1	5	1
Homo	5	A	0	7	A	A	8	1	0	0	0	0	8	1	2	A	5	4
Pongo	7	3	3	8	3	1	8	7	8	7	8	6	4	9	7	1	5	6
Hylobates	8	6	A	4	3	4	8	7	3	7	8	8	7	8	7	6	5	6
Papio	2	3	8	0	0	2	3	8	8	6	8	6	6	4	A	6	5	7

	FMaS	FMaP2	FMaP1	InF	FSp	Fve	PSB	PAB	FSpP	Fla	RaC2	RaC1	GPFP	PCr	LPF	LPFP	MeF	MbFP
Gorilla	6	3	3	5	2	4	2	7	5	8	6	6	3	A	2	2	3	1
Pan	4	5	3	4	3	4	8	7	1	4	6	7	3	7	2	3	9	8
Homo	6	9	9	5	1	0	7	2	9	0	6	7	8	3	2	1	8	4
Pongo	7	0	3	5	7	5	9	7	2	2	6	4	3	3	8	8	3	1
Hylobates	1	6	3	6	9	9	2	7	9	8	6	6	A	0	6	8	7	7
Papio	6	7	9	5	8	8	2	0	4	8	0	0	3	7	A	8	0	9

	SeC	MoF	RMF	RoC	MyB	CSF	PCF	IFF	MeFPos2	InC	PFn	SMFS	IOFS	CaCS	GPFS	MeFS	ZTFS	MaFS
Gorilla	3	0	5	6	1	5	7	6	3	6	7	6	5	4	5	4	6	6
Pan	3	3	5	6	7	A	6	0	8	1	7	1	1	4	6	0	7	6
Homo	3	5	5	2	1	5	A	6	8	3	7	3	5	A	6	7	5	3
Pongo	9	9	5	6	7	0	2	6	8	2	7	6	3	4	6	6	4	5
Hylobates	3	4	5	5	7	5	2	6	0	9	2	7	9	4	1	7	3	5
Papio	9	9	5	5	7	5	3	6	3	9	0	7	7	4	6	6	5	5

	LPFS	MbFS	ZFFS	SGB
Gorilla	5	6	7	5
Pan	5	5	3	5
Homo	6	3	5	5
Pongo	5	5	7	5
Hylobates	4	6	3	5
Papio	5	5	5	5

Analysis 1a.2b

	IOF	ZTF	ZFF	PEF	MaF	IOB	ION	ICIO	IOG	SLGB	SON	SOF	ZTFP	ZTFP	ZTFP	ZTFP2b	ZTFP2a	ZTIPb
Gorilla	1	1	0	1	1	0	1	1	1	1	1	0	1	1	1	1	1	1
Pan	1	1	1	1	1	1	1	0	1	1	1	0	1	1	1	1	1	1
Homo	1	1	1	1	1	0	1	1	1	1	1	1	0	1	0	1	0	1
Pongo	1	0	1	1	1	0	0	1	1	1	1	0	0	0	0	0	0	0
Hylobates	1	1	1	1	1	0	1	0	0	0	1	0	1	1	0	1	1	0
Papio	1	1	1	1	1	0	0	0	1	0	1	0	1	1	0	0	1	1

	ZTIPa	ZTIPc	ZFN	ZFFPc	ZFFPd	AEFP	Fro	OcF	PEFPb	SOFi	PEFPa	MMAE	MaFPb	MaFPa	MaFPc	SMB	SMFP	PaF1
Gorilla	1	0	0	0	0	1	1	0	1	1	1	0	1	1	0	1	1	0
Pan	1	0	0	1	1	1	1	0	1	1	1	0	1	1	0	1	1	0
Homo	0	1	0	1	1	1	1	1	1	1	1	0	1	1	0	1	1	1
Pongo	0	0	1	1	0	1	1	0	1	1	1	0	1	1	0	1	1	0
Hylobates	0	1	1	1	1	1	1	1	1	1	0	0	1	1	0	1	1	0
Papio	1	0	0	1	0	0	1	0	0	1	1	1	1	1	1	1	1	0

	PaF2	PaF3	CaCP1	CaCP2	IOFSZ	ZTFSZ	ZFFSZ	MaFSZ	SMFSZ	CaCSZ	JuFLg	HyCSZ	FOvSZ	GPFSZ	LPFSZ	MeFSZ	MbFSZ	ZMSmind
Gorilla	1	0	1	0	1	1	0	0	1	1	0	0	1	1	1	1	1	1
Pan	1	0	1	0	1	1	1	0	1	0	0	0	1	1	1	1	1	0
Homo	1	0	0	1	1	0	0	1	1	1	1	1	1	1	1	1	1	0
Pongo	1	0	1	0	0	0	1	1	1	0	0	0	1	1	0	1	1	0
Hylobates	1	1	1	0	0	0	1	0	0	0	0	0	0	0	0	0	0	1
Papio	0	0	0	0	0	1	1	1	1	0	0	0	1	1	0	0	1	1

	ZMStvd	Go	FMaSZ	InCLg	MeFpos	InCpos	IOFpos	IJPE	HyC	ICC	CoC	CoCO	CPC	MgF	Fov	FOvP	MBC	JuB
Gorilla	1	1	1	1	0	0	1	1	1	1	1	1	1	1	1	1	1	0
Pan	0	0	0	0	0	0	1	1	1	1	1	1	1	1	1	1	0	1
Homo	0	0	1	0	0	0	0	1	1	1	1	1	0	1	1	0	1	1
Pongo	0	1	1	0	1	1	0	1	1	0	0	0	1	0	1	1	0	1
Hylobates	0	0	0	1	1	1	0	1	1	0	0	0	1	0	1	1	0	1
Papio	1	1	0	1	1	1	1	1	1	0	0	0	0	1	0	1	0	0

	FMaS	FMaP2	FMaP1	InF	FSp	Fve	PSB	PAB	FSpP	Fla	RaC2	RaC1	GPFP	PCr	LPF	LPFP	MeF	MbFP
Gorilla	1	1	1	0	1	1	1	0	1	0	0	0	1	0	1	1	1	1
Pan	1	1	1	1	1	1	1	0	1	1	0	0	1	1	1	1	0	1
Homo	0	0	1	1	1	1	1	1	0	1	0	0	1	1	1	1	0	1
Pongo	0	1	1	0	1	1	1	0	1	1	0	1	1	1	1	1	1	1
Hylobates	1	1	1	0	0	0	1	0	0	0	0	0	1	1	1	1	1	1
Papio	0	0	0	0	1	0	1	1	1	0	1	1	1	1	1	1	1	0

	SeC	MoF	RMF	RoC	MyB	CSF	PCF	IFF	MeFPos2	InC	PFn	SMFS	IOFS	CaCS	GPFS	MeFS	ZTFS	MaFS
Gorilla	1	1	0	0	1	1	1	0	1	1	0	1	1	1	0	1	1	0
Pan	1	1	0	0	0	1	1	1	1	1	0	1	1	1	0	1	1	0
Homo	1	1	0	1	1	1	1	0	1	1	0	1	1	0	0	0	1	1
Pongo	0	0	0	0	0	1	1	1	1	1	0	1	1	1	0	0	1	0
Hylobates	1	1	0	0	0	1	1	0	1	1	1	1	0	1	1	0	1	1
Papio	0	0	0	0	0	1	1	1	1	0	1	0	0	1	0	0	1	0

	LPFS	MbFS	ZFFS	SGB
Gorilla	0	0	0	0
Pan	1	1	1	0
Homo	0	1	1	0
Pongo	1	0	0	1
Hylobates	1	0	1	0
Papio	0	0	0	0

Analysis 1a.2c

	IOF	ZTF	ZFF	PEF	MaF	IOB	ION	ICIO	IOG	SLGB	SON	SOF	ZTFP	ZTFP	ZTFP	ZTFP2b	ZTFP2a	ZTIPb
Gorilla	4	5	1	2	2	1	4	4	5	6	3	4	5	2	6	6	3	4
Pan	2	4	5	4	1	6	5	1	6	4	2	3	4	4	5	4	4	6
Homo	1	2	2	5	3	4	3	6	2	5	5	6	2	5	1	5	1	3
Pongo	5	1	5	6	5	1	1	5	3	3	1	1	1	1	1	1	2	1
Hylobates	3	3	4	1	4	5	6	1	1	1	4	5	3	6	4	3	5	2
Papio	6	5	3	3	6	1	2	1	4	2	6	1	6	3	1	1	6	5

	ZTIPa	ZTIPc	ZFN	ZFFPc	ZFFPd	AEFP	Fro	OcF	PEFPb	SOFi	PEFPa	MMAE	MaFPb	MaFPa	MaFPc	SMB	SMFP	PaF1
Gorilla	6	1	1	1	3	3	3	1	2	1	3	1	1	4	1	4	2	3
Pan	4	4	1	4	5	4	2	4	4	5	4	3	2	3	3	6	2	2
Homo	1	5	1	2	6	6	3	5	5	6	5	4	3	5	5	2	2	6
Pongo	1	1	5	6	2	5	3	1	6	4	2	5	4	6	1	3	2	1
Hylobates	1	6	6	3	4	2	1	6	3	3	1	1	5	2	4	1	2	5
Papio	5	1	1	5	1	1	3	1	1	2	6	6	6	1	6	5	1	4

	PaF2	PaF3	CaCP1	CaCP2	IOFSZ	ZTFSZ	ZFFSZ	MaFSZ	SMFSZ	CaCSZ	JuFLg	HyCSZ	FOvSZ	GPFSZ	LPFSZ	MeFSZ	MbFSZ	ZMSmind
Gorilla	6	1	3	1	5	4	1	2	4	5	3	3	5	5	4	6	5	5
Pan	4	1	4	1	4	5	3	1	5	4	5	5	2	3	5	2	2	1
Homo	2	1	1	6	6	2	2	6	6	6	6	6	6	2	6	4	4	2
Pongo	5	1	5	1	3	1	6	4	3	3	1	2	4	4	1	5	3	3
Hylobates	3	6	6	1	2	3	4	3	1	1	2	1	1	1	2	1	1	4
Papio	1	1	1	5	1	6	5	5	2	2	4	4	3	6	3	3	6	6

	ZMStvd	Go	FMaSZ	InCLg	MeFpos	InCpos	IOFpos	IJPE	HyC	ICC	CoC	CoCO	CPC	MgF	Fov	FOvP	MBC	JuB
Gorilla	6	6	5	4	2	3	6	5	2	4	4	4	6	5	6	4	6	2
Pan	2	2	3	3	3	2	5	4	5	5	5	5	5	3	4	5	1	6
Homo	4	1	6	2	1	1	3	6	6	6	6	6	1	6	5	1	5	5
Pongo	3	4	4	1	5	6	1	2	3	3	1	3	4	1	2	6	1	3
Hylobates	1	3	1	5	4	4	2	3	4	1	2	1	3	2	3	3	1	4
Papio	5	5	2	6	6	5	4	1	1	1	3	1	1	4	1	2	1	1

	FMaS	FMaP2	FMaP1	InF	FSp	Fve	PSB	PAB	FSpP	Fla	RaC2	RaC1	GPFP	PCr	LPF	LPFP	MeF	MbFP
Gorilla	4	5	3	4	5	5	6	1	3	3	1	3	3	1	6	5	5	5
Pan	5	4	4	6	4	4	2	4	6	4	1	1	3	3	4	4	1	2
Homo	2	2	2	5	6	6	3	5	1	6	1	1	2	5	5	6	2	4
Pongo	1	6	4	2	3	3	1	3	5	5	5	5	3	4	2	2	4	6
Hylobates	6	3	4	3	1	2	5	2	2	2	1	4	1	6	3	3	3	3
Papio	3	1	1	1	2	1	4	6	4	1	6	6	3	2	1	1	6	1

	SeC	MoF	RMF	RoC	MyB	CSF	PCF	IFF	MeFPos2	InC	PFn	SMFS	IOFS	CaCS	GPFS	MeFS	ZTFS	MaFS
Gorilla	4	6	5	1	6	3	2	1	4	3	1	2	4	4	5	5	2	1
Pan	5	5	1	1	1	1	3	6	3	6	1	6	6	2	1	6	1	1
Homo	6	3	6	6	5	4	1	3	1	4	1	5	3	1	4	1	3	6
Pongo	2	1	1	1	1	6	6	5	2	5	1	4	5	5	1	2	5	4
Hylobates	3	4	1	5	1	2	5	2	6	2	5	3	1	3	6	3	4	5
Papio	1	2	1	1	1	5	4	4	5	1	6	1	2	6	1	4	5	3

	LPFS	MbFS	ZFFS	SGB
Gorilla	3	1	1	1
Pan	4	5	5	1
Homo	2	6	4	1
Pongo	5	3	1	6
Hylobates	6	2	6	4
Papio	1	4	3	5

Analysis 1a.2d

	IOF	ZTF	ZFF	PEF	MaF	IOB	ION	ICIO	IOG	SLGB	SON	SOF	ZTFP	ZTFP	ZTFP	ZTFP2b	ZTFP2a	ZTIPb
Gorilla	H	Q	0	B	8	0	2	8	Q	A	A	0	B	6	F	N	6	4
Pan	E	Q	Q	N	8	2	6	0	Q	6	5	0	A	G	3	M	8	L
Homo	2	M	H	Q	G	0	1	P	H	9	L	5	0	M	0	M	0	3
Pongo	P	0	Q	Q	N	0	0	L	P	3	2	0	0	0	0	0	0	0
Hylobates	E	P	Q	9	L	0	7	0	0	0	A	0	3	M	0	C	E	0
Papio	Q	Q	P	E	P	0	0	0	P	1	Q	0	G	8	0	0	Q	6

	ZTIPa	ZTIPc	ZFN	ZFFPc	ZFFPd	AEFP	Fro	OcF	PEFPb	SOFi	PEFPa	MMAE	MaFPb	MaFPa	MaFPc	SMB	SMFP	PaF1
Gorilla	N	0	0	0	0	B	Q	0	7	3	4	0	2	6	0	3	Q	0
Pan	6	0	0	P	C	B	M	0	J	P	4	0	2	6	0	B	Q	0
Homo	0	J	0	9	D	G	Q	1	K	Q	7	0	7	A	0	3	Q	C
Pongo	0	0	3	Q	0	F	Q	0	N	M	3	0	7	E	0	3	Q	0
Hylobates	0	N	7	P	9	5	L	1	8	G	0	0	E	5	0	1	Q	0
Papio	J	0	0	P	0	0	Q	0	0	6	E	2	L	2	2	6	C	0

	PaF2	PaF3	CaCP1	CaCP2	IOFSZ	ZTFSZ	ZFFSZ	MaFSZ	SMFSZ	CaCSZ	JuFLg	HyCSZ	FOvSZ	GPFSZ	LPFSZ	MeFSZ	MbFSZ	ZMSmind
Gorilla	E	0	C	0	H	H	0	2	K	D	9	7	M	P	F	Q	K	G
Pan	3	0	F	0	H	K	H	0	K	A	C	B	E	C	P	G	D	0
Homo	2	0	0	5	Q	9	B	L	Q	Q	Q	Q	Q	C	Q	H	H	3
Pongo	6	0	L	0	5	0	Q	K	G	7	0	3	K	E	0	P	H	A
Hylobates	3	4	Q	0	2	A	K	A	0	0	8	0	0	0	1	0	0	D
Papio	1	0	0	1	0	Q	M	Q	D	4	B	9	J	Q	0	C	Q	Q

	ZMStvd	Go	FMaSZ	InCLg	MeFpos	InCpos	IOFpos	IJPE	HyC	ICC	CoC	CoCO	CPC	MgF	Fov	FOvP	MBC	JuB
Gorilla	Q	Q	F	D	D	G	B	Q	5	1	5	2	8	6	Q	4	1	0
Pan	3	3	B	8	E	F	A	P	C	3	A	2	5	2	N	A	0	4
Homo	6	0	Q	7	C	F	6	Q	P	C	F	E	0	8	Q	0	1	3
Pongo	4	J	E	0	F	K	6	M	7	0	0	0	4	0	G	D	0	1
Hylobates	0	7	0	G	F	H	6	M	C	0	0	0	1	0	K	2	0	1
Papio	K	J	6	Q	J	J	9	J	3	0	0	0	0	3	0	1	0	0

	FMaS	FMaP2	FMaP1	InF	FSp	Fve	PSB	PAB	FSpP	Fla	RaC2	RaC1	GPFP	PCr	LPF	LPFP	MeF	MbFP
Gorilla	0	B	Q	1	G	3	G	0	5	0	0	0	Q	0	Q	C	9	Q
Pan	4	5	Q	2	E	3	5	0	F	4	0	0	Q	7	Q	A	0	3
Homo	1	0	4	1	J	C	6	A	0	Q	0	0	M	F	Q	E	1	9
Pongo	0	J	Q	0	6	2	2	0	B	P	0	2	Q	E	8	4	7	Q
Hylobates	8	3	Q	0	1	0	E	0	0	0	0	0	F	P	F	5	1	4
Papio	1	0	0	0	3	0	D	L	7	0	3	P	Q	5	2	2	Q	0

	SeC	MoF	RMF	RoC	MyB	CSF	PCF	IFF	MeFPos2	InC	PFn	SMFS	IOFS	CaCS	GPFS	MeFS	ZTFS	MaFS
Gorilla	3	E	0	0	8	7	A	0	E	A	0	2	3	8	1	3	P	0
Pan	4	8	0	0	0	2	C	F	1	Q	0	7	A	7	0	7	N	0
Homo	5	5	1	2	4	7	3	0	1	N	0	5	3	0	0	0	P	3
Pongo	0	1	0	0	0	J	L	2	1	P	0	2	6	9	0	0	Q	1
Hylobates	3	6	0	1	0	6	J	0	2	3	E	2	0	7	3	0	Q	2
Papio	0	1	0	0	0	9	G	1	H	0	Q	1	1	A	0	1	Q	0

	LPFS	MbFS	ZFFS	SGB
Gorilla	0	0	0	0
Pan	2	1	2	0
Homo	0	3	1	0
Pongo	2	1	0	1
Hylobates	2	0	3	0
Papio	0	1	1	1

Analysis 1a.3a

	IOF	ZTF	ZFF	PEF	MaF	IOB	ION	ICIO	IOG	SLGB	SON	SOF	ZTFP	ZTFP	ZTFP	ZTFP2b	ZTFP2a	ZTIPb
Gorilla	6	3	A	7	9	6	7	4	2	1	5	6	3	7	0	2	5	5
Pan	6	3	3	3	9	1	1	8	1	5	9	6	3	4	3	2	5	0
Homo	A	6	8	2	6	6	7	1	6	2	1	0	9	1	7	2	9	5
Pongo	1	A	3	1	2	6	7	1	3	6	9	6	9	A	7	A	9	9
Hylobates	6	4	3	7	2	6	1	8	9	A	5	6	6	1	7	7	1	9
Cercopithecus	1	4	3	A	2	5	7	8	9	6	1	6	0	7	6	7	1	2

	ZTIPa	ZTIPc	ZFN	ZFFPc	ZFFPd	AEFP	Fro	OcF	PEFPb	SOFi	PEFPa	MMAE	MaFPb	MaFPa	MaFPc	SMB	SMFP	PaF1
Gorilla	0	7	7	A	9	4	3	5	7	A	3	5	9	6	5	6	5	6
Pan	4	7	7	2	3	4	9	5	3	4	3	5	9	7	5	0	5	6
Homo	8	2	7	8	1	1	3	5	3	1	3	5	5	2	5	6	5	0
Pongo	8	7	1	2	9	3	3	5	0	4	3	5	5	1	5	6	5	6
Hylobates	8	0	1	2	4	9	9	5	7	8	9	5	2	7	5	7	5	6
Cercopithecus	2	7	7	6	4	9	3	5	A	3	9	5	0	7	5	5	5	6

	PaF2	PaF3	CaCP1	CaCP2	IOFSZ	ZTFSZ	ZFFSZ	MaFSZ	SMFSZ	CaCSZ	JuFLg	HyCSZ	FOvSZ	GPFSZ	LPFSZ	MeFSZ	MbFSZ	ZMSmind
Gorilla	0	6	5	6	3	2	A	6	4	2	5	4	2	0	4	1	0	0
Pan	6	6	5	6	3	1	7	8	3	3	3	3	5	3	2	5	5	7
Homo	6	6	A	0	0	7	7	0	0	0	0	0	0	4	1	4	3	8
Pongo	5	6	2	6	7	8	0	2	5	6	7	6	4	4	8	1	3	3
Hylobates	6	1	0	6	7	7	2	6	8	8	7	8	A	8	8	9	9	4
Cercopithecus	7	5	8	6	A	6	7	6	A	A	9	A	8	A	8	9	9	5

	ZMStvd	Go	FMaSZ	InCLg	MeFpos	InCpos	IOFpos	IJPE	HyC	ICC	CoC	CoCO	CPC	MgF	Fov	FOvP	MBC	JuB
Gorilla	0	0	3	4	8	5	0	3	9	6	4	5	2	2	1	5	5	6
Pan	5	5	5	6	6	8	2	6	4	3	2	5	3	6	3	1	5	2
Homo	3	9	0	7	A	A	6	2	0	0	0	0	8	2	2	9	5	5
Pongo	5	2	3	8	3	1	6	7	9	7	8	6	4	9	7	1	5	6
Hylobates	7	4	8	4	3	5	6	7	4	7	8	8	7	8	7	6	5	6
Cercopithecus	9	8	A	0	0	1	A	5	4	7	8	6	6	3	A	8	5	5

	FMaS	FMaP2	FMaP1	InF	FSp	Fve	PSB	PAB	FSpP	Fla	RaC2	RaC1	GPFP	PCr	LPF	LPFP	MeF	MbFP
Gorilla	6	3	4	5	2	4	3	7	5	8	5	6	3	A	2	3	3	1
Pan	4	5	3	4	3	4	8	7	1	5	5	7	3	7	2	4	9	8
Homo	7	9	A	5	1	0	7	1	9	0	5	7	8	3	2	1	8	4
Pongo	8	0	4	5	6	5	9	7	2	2	5	3	3	3	9	8	3	1
Hylobates	2	6	3	6	9	9	3	7	9	9	5	6	A	0	7	8	7	8
Cercopithecus	3	7	6	5	9	8	0	1	4	6	5	1	3	7	8	6	0	8

	SeC	MoF	RMF	RoC	MyB	CSF	PCF	IFF	MeFPos2	InC	PFn	SMFS	IOFS	CaCS	GPFS	MeFS	ZTFS	MaFS
Gorilla	3	0	5	6	1	5	5	6	2	6	7	6	5	5	5	4	6	6
Pan	3	3	5	6	7	9	5	0	7	1	7	2	2	5	6	0	7	6
Homo	3	5	5	2	1	5	9	6	7	3	7	4	5	A	6	7	5	2
Pongo	9	9	5	6	7	0	1	6	7	2	7	6	4	5	6	6	3	5
Hylobates	3	4	5	5	7	5	1	6	0	9	2	7	A	5	2	7	2	5
Cercopithecus	9	9	5	5	7	6	9	6	7	9	0	5	4	0	5	6	7	6

	LPFS	MbFS	ZFFS	SGB
Gorilla	5	6	8	5
Pan	5	5	3	5
Homo	6	2	6	5
Pongo	5	5	8	5
Hylobates	4	6	3	5
Cercopithecus	5	6	2	5

Analysis 1a.3b

	IOF	ZTF	ZFF	PEF	MaF	IOB	ION	ICIO	IOG	SLGB	SON	SOF	ZTFP	ZTFP	ZTFP	ZTFP2b	ZTFP2a	ZTIPb
Gorilla	1	1	0	1	1	0	1	1	1	1	1	0	1	1	1	1	1	1
Pan	1	1	1	1	1	1	1	0	1	1	1	0	1	1	1	1	1	1
Homo	1	1	1	1	1	0	1	1	1	1	1	1	0	1	0	1	0	1
Pongo	1	0	1	1	1	0	0	1	1	1	1	0	0	0	0	0	0	0
Hylobates	1	1	1	1	1	0	1	0	0	0	1	0	1	1	0	1	1	0
Cercopithecus	1	1	1	0	1	0	0	0	1	1	1	0	1	1	0	1	1	1

	ZTIPa	ZTIPc	ZFN	ZFFPc	ZFFPd	AEFP	Fro	OcF	PEFPb	SOFi	PEFPa	MMAE	MaFPb	MaFPa	MaFPc	SMB	SMFP	PaF1
Gorilla	1	0	0	0	0	1	1	0	1	1	1	0	1	1	0	1	1	0
Pan	1	0	0	1	1	1	1	0	1	1	1	0	1	1	0	1	1	0
Homo	0	1	0	1	1	1	1	1	1	1	1	0	1	1	0	1	1	1
Pongo	0	0	1	1	0	1	1	0	1	1	1	0	1	1	0	1	1	0
Hylobates	0	1	1	1	1	1	1	1	1	1	0	0	1	1	0	1	1	0
Cercopithecus	1	0	0	1	1	1	1	0	0	1	0	0	1	1	0	1	1	0

	PaF2	PaF3	CaCP1	CaCP2	IOFSZ	ZTFSZ	ZFFSZ	MaFSZ	SMFSZ	CaCSZ	JuFLg	HyCSZ	FOvSZ	GPFSZ	LPFSZ	MeFSZ	MbFSZ	ZMSmind
Gorilla	1	0	1	0	1	1	0	0	1	1	0	1	1	1	1	1	1	1
Pan	1	0	1	0	1	1	1	0	1	1	0	1	1	1	1	1	1	0
Homo	1	0	0	1	1	0	0	1	1	1	1	1	1	1	1	1	1	0
Pongo	1	0	1	0	1	0	1	1	1	0	0	0	1	1	0	1	1	1
Hylobates	1	1	1	0	0	1	1	1	0	0	0	0	0	0	0	0	0	1
Cercopithecus	0	0	1	0	0	1	0	0	0	0	0	0	0	0	0	0	0	1

	ZMStvd	Go	FMaSZ	InCLg	MeFpos	InCpos	IOFpos	IJPE	HyC	ICC	CoC	CoCO	CPC	MgF	Fov	FOvP	MBC	JuB
Gorilla	1	1	1	1	0	0	1	1	1	1	1	1	1	1	1	1	1	0
Pan	0	0	1	0	0	0	1	1	1	1	1	1	1	1	1	1	0	1
Homo	0	0	1	0	0	0	0	1	1	1	1	1	0	1	1	0	1	1
Pongo	0	1	1	0	1	1	0	1	1	0	0	0	1	0	1	1	0	1
Hylobates	0	0	0	1	1	0	0	1	1	0	0	0	1	0	1	1	0	1
Cercopithecus	0	0	0	1	1	1	0	1	1	0	0	0	0	1	0	0	0	1

	FMaS	FMaP2	FMaP1	InF	FSp	Fve	PSB	PAB	FSpP	Fla	RaC2	RaC1	GPFP	PCr	LPF	LPFP	MeF	MbFP
Gorilla	1	1	1	0	1	1	1	0	1	0	0	0	1	0	1	1	1	1
Pan	1	1	1	1	1	1	1	0	1	1	0	0	1	1	1	1	0	1
Homo	0	0	1	1	1	1	1	1	0	1	0	0	1	1	1	1	0	1
Pongo	0	1	1	0	1	1	1	0	1	1	0	1	1	1	1	1	1	1
Hylobates	1	1	1	0	0	0	1	0	0	0	0	0	1	1	1	1	1	1
Cercopithecus	1	1	1	0	0	0	1	1	1	1	0	1	1	1	1	1	1	0

	SeC	MoF	RMF	RoC	MyB	CSF	PCF	IFF	MeFPos2	InC	PFn	SMFS	IOFS	CaCS	GPFS	MeFS	ZTFS	MaFS
Gorilla	1	1	0	0	1	1	1	0	1	1	0	1	1	1	0	1	1	0
Pan	1	1	0	0	0	1	1	1	1	1	0	1	1	1	0	1	1	0
Homo	1	1	0	1	1	1	1	0	1	1	0	1	1	0	0	0	1	1
Pongo	0	0	0	0	0	1	1	1	1	1	0	1	1	1	0	0	1	0
Hylobates	1	1	0	0	0	1	1	0	1	1	1	1	0	1	1	0	1	1
Cercopithecus	0	0	0	0	0	1	1	0	0	0	1	1	1	1	0	0	1	0

	LPFS	MbFS	ZFFS	SGB
Gorilla	0	0	0	0
Pan	1	1	1	0
Homo	0	1	1	0
Pongo	1	0	0	1
Hylobates	1	0	1	0
Cercopithecus	1	0	1	0

Analysis 1a.3c

	IOF	ZTF	ZFF	PEF	MaF	IOB	ION	ICIO	IOG	SLGB	SON	SOF	ZTFP	ZTFP	ZTFP	ZTFP2b	ZTFP2a	ZTIPb
Gorilla	4	6	1	3	2	1	4	4	5	6	3	4	5	3	6	6	3	4
Pan	2	5	5	4	1	6	5	1	6	4	2	3	4	4	5	4	4	6
Homo	1	2	2	5	3	4	3	6	3	5	6	6	2	5	1	5	1	3
Pongo	5	1	5	6	5	1	1	5	4	2	1	1	1	1	1	1	2	1
Hylobates	3	3	4	2	4	5	6	1	1	1	4	5	3	6	3	3	5	2
Cercopithecus	6	4	3	1	6	1	1	3	2	3	5	1	6	2	4	2	6	5

	ZTIPa	ZTIPc	ZFN	ZFFPc	ZFFPd	AEFP	Fro	OcF	PEFPb	SOFi	PEFPa	MMAE	MaFPb	MaFPa	MaFPc	SMB	SMFP	PaF1
Gorilla	6	1	1	1	2	3	3	1	2	1	4	1	1	4	1	4	1	4
Pan	4	4	1	5	5	4	2	4	4	4	5	3	2	3	4	6	1	3
Homo	1	5	1	2	6	6	3	5	5	6	6	4	3	5	6	2	1	6
Pongo	1	1	5	6	1	5	3	1	6	3	3	5	4	6	1	3	1	1
Hylobates	1	6	6	4	4	2	1	6	3	2	2	1	5	2	5	1	1	5
Cercopithecus	5	1	1	3	3	1	3	1	1	5	1	6	6	1	1	5	1	1

	PaF2	PaF3	CaCP1	CaCP2	IOFSZ	ZTFSZ	ZFFSZ	MaFSZ	SMFSZ	CaCSZ	JuFLg	HyCSZ	FOvSZ	GPFSZ	LPFSZ	MeFSZ	MbFSZ	ZMSmind
Gorilla	6	1	3	1	5	5	1	3	4	5	4	4	5	6	4	6	6	6
Pan	4	1	4	1	4	6	4	1	5	4	5	5	3	4	5	3	3	1
Homo	2	1	1	6	6	2	3	6	6	6	6	6	6	3	6	4	5	2
Pongo	5	1	5	1	3	1	6	5	3	3	1	3	4	5	1	5	4	3
Hylobates	3	6	6	1	2	4	5	4	2	2	3	2	1	2	2	2	1	5
Cercopithecus	1	1	2	1	1	3	2	2	1	1	2	1	2	1	3	1	2	4

	ZMStvd	Go	FMaSZ	InCLg	MeFpos	InCpos	IOFpos	IJPE	HyC	ICC	CoC	CoCO	CPC	MgF	Fov	FOvP	MBC	JuB
Gorilla	6	6	5	4	2	3	6	5	1	4	4	4	6	5	6	4	6	1
Pan	3	3	3	3	3	2	5	3	4	5	5	5	5	3	4	5	1	6
Homo	5	2	6	2	1	1	4	6	6	6	6	6	1	6	5	1	5	5
Pongo	4	5	4	1	5	5	2	1	2	3	2	3	4	1	2	6	1	2
Hylobates	2	4	2	5	4	4	3	2	3	1	3	1	3	2	3	3	1	3
Cercopithecus	1	1	1	6	6	6	1	4	5	1	1	1	1	4	1	1	1	4

	FMaS	FMaP2	FMaP1	InF	FSp	Fve	PSB	PAB	FSpP	Fla	RaC2	RaC1	GPFP	PCr	LPF	LPFP	MeF	MbFP
Gorilla	3	5	3	4	5	5	5	1	3	2	1	3	3	1	6	5	5	5
Pan	4	4	4	6	4	4	2	4	6	4	1	1	3	3	4	4	1	2
Homo	2	1	1	5	6	6	3	6	1	6	1	1	2	5	5	6	2	4
Pongo	1	6	4	2	3	3	1	3	5	5	6	5	3	4	1	1	4	6
Hylobates	6	3	4	3	2	2	4	2	2	1	1	4	1	6	3	2	3	3
Cercopithecus	5	2	2	1	1	1	6	5	4	3	1	6	3	2	2	3	6	1

	SeC	MoF	RMF	RoC	MyB	CSF	PCF	IFF	MeFPos2	InC	PFn	SMFS	IOFS	CaCS	GPFS	MeFS	ZTFS	MaFS
Gorilla	4	6	5	1	6	4	3	1	5	3	1	1	3	4	5	5	3	2
Pan	5	5	1	1	1	1	4	6	4	6	1	6	6	2	1	6	2	2
Homo	6	3	6	6	5	5	1	4	2	4	1	5	2	1	3	1	4	6
Pongo	2	2	1	1	1	6	6	5	3	5	1	3	4	5	1	2	6	4
Hylobates	3	4	1	5	1	3	5	3	6	2	5	2	1	3	6	3	5	5
Cercopithecus	1	1	1	1	1	2	2	1	1	1	6	4	5	6	4	4	1	1

	LPFS	MbFS	ZFFS	SGB
Gorilla	2	2	1	1
Pan	4	5	4	1
Homo	1	6	3	1
Pongo	5	4	1	6
Hylobates	6	3	5	5
Cercopithecus	3	1	6	1

Analysis 1a.3d

	IOF	ZTF	ZFF	PEF	MaF	IOB	ION	ICIO	IOG	SLGB	SON	SOF	ZTFP	ZTFP	ZTFP	ZTFP2b	ZTFP2a	ZTIPb
Gorilla	H	Q	0	B	8	0	2	8	Q	A	A	0	B	6	F	N	6	4
Pan	E	Q	Q	N	8	2	6	0	Q	6	5	0	A	G	3	M	8	L
Homo	2	M	H	Q	G	0	1	P	H	9	L	5	0	M	0	M	0	3
Pongo	P	0	Q	Q	N	0	0	L	P	3	2	0	0	0	0	0	0	0
Hylobates	E	P	Q	9	L	0	7	0	0	0	A	0	3	M	0	C	E	0
Cercopithecus	Q	P	P	0	P	0	0	1	2	3	G	0	J	4	1	7	G	C

	ZTIPa	ZTIPc	ZFN	ZFFPc	ZFFPd	AEFP	Fro	OcF	PEFPb	SOFi	PEFPa	MMAE	MaFPb	MaFPa	MaFPc	SMB	SMFP	PaF1
Gorilla	N	0	0	0	0	B	Q	0	7	3	4	0	2	6	0	3	Q	0
Pan	6	0	0	P	C	B	M	0	J	P	4	0	2	6	0	B	Q	0
Homo	0	J	0	9	D	G	Q	1	K	Q	7	0	7	A	0	3	Q	C
Pongo	0	0	3	Q	0	F	Q	0	N	M	3	0	7	E	0	3	Q	0
Hylobates	0	N	7	P	9	5	L	1	8	G	0	0	E	5	0	1	Q	0
Cercopithecus	C	0	0	J	7	4	Q	0	0	P	0	1	L	2	0	4	Q	0

	PaF2	PaF3	CaCP1	CaCP2	IOFSZ	ZTFSZ	ZFFSZ	MaFSZ	SMFSZ	CaCSZ	JuFLg	HyCSZ	FOvSZ	GPFSZ	LPFSZ	MeFSZ	MbFSZ	ZMSmind
Gorilla	E	0	C	0	L	M	0	3	L	G	9	C	M	Q	F	Q	Q	Q
Pan	3	0	F	0	L	Q	H	0	L	D	C	F	E	H	P	H	H	0
Homo	2	0	0	5	Q	B	B	Q	Q	Q	Q	Q	Q	H	Q	J	N	4
Pongo	6	0	L	0	D	0	Q	P	J	B	0	9	K	J	0	P	N	E
Hylobates	3	4	Q	0	C	D	K	D	5	6	8	7	0	A	1	2	0	K
Cercopithecus	0	0	2	0	0	C	C	9	0	0	1	0	5	0	2	0	2	G

	ZMStvd	Go	FMaSZ	InCLg	MeFpos	InCpos	IOFpos	IJPE	HyC	ICC	CoC	CoCO	CPC	MgF	Fov	FOvP	MBC	JuB
Gorilla	Q	Q	H	E	D	G	B	Q	5	1	5	2	8	6	Q	4	1	0
Pan	3	3	F	9	E	F	A	P	C	3	A	2	5	2	N	A	0	4
Homo	6	0	Q	8	C	F	6	Q	P	C	F	E	0	8	Q	0	1	3
Pongo	4	J	H	0	F	K	6	M	7	0	0	0	4	0	G	D	0	1
Hylobates	1	7	7	J	F	H	6	M	C	0	0	0	1	0	K	2	0	1
Cercopithecus	0	0	0	Q	K	M	5	P	D	0	0	0	0	4	0	0	0	2

	FMaS	FMaP2	FMaP1	InF	FSp	Fve	PSB	PAB	FSpP	Fla	RaC2	RaC1	GPFP	PCr	LPF	LPFP	MeF	MbFP
Gorilla	0	B	Q	1	G	3	G	0	5	0	0	0	Q	0	Q	C	9	Q
Pan	4	5	Q	2	E	3	5	0	F	4	0	0	Q	7	Q	A	0	3
Homo	1	0	4	1	J	C	6	A	0	Q	0	0	M	F	Q	E	1	9
Pongo	0	J	Q	0	6	2	2	0	B	P	0	2	Q	E	8	4	7	Q
Hylobates	8	3	Q	0	1	0	E	0	0	0	0	0	F	P	F	5	1	4
Cercopithecus	7	2	M	0	0	0	Q	9	A	3	0	3	Q	4	C	8	F	1

	SeC	MoF	RMF	RoC	MyB	CSF	PCF	IFF	MeFPos2	InC	PFn	SMFS	IOFS	CaCS	GPFS	MeFS	ZTFS	MaFS
Gorilla	3	E	0	0	8	7	A	0	E	A	0	2	3	8	1	3	P	0
Pan	4	8	0	0	0	2	C	F	1	Q	0	7	A	7	0	7	N	0
Homo	5	5	1	2	4	7	3	0	1	N	0	5	3	0	0	0	P	3
Pongo	0	1	0	0	0	J	L	2	1	P	0	2	6	9	0	0	Q	1
Hylobates	3	6	0	1	0	6	J	0	2	3	E	2	0	7	3	0	Q	2
Cercopithecus	0	1	0	0	0	3	3	0	1	0	Q	3	6	E	1	1	N	0

	LPFS	MbFS	ZFFS	SGB
Gorilla	0	0	0	0
Pan	2	1	2	0
Homo	0	3	1	0
Pongo	2	1	0	1
Hylobates	2	0	3	0
Cercopithecus	1	0	6	0

Analysis 1a.4a

	IOF	ZTF	ZFF	PEF	MaF	IOB	ION	ICIO	IOG	SLGB	SON	SOF	ZTFP	ZTFP	ZTFP	ZTFP2b	ZTFP2a	ZTIPb
Gorilla	6	3	A	8	9	6	7	4	2	1	3	6	2	8	0	2	5	5
Pan	6	3	2	3	9	1	1	8	1	4	7	6	2	5	2	2	5	1
Homo	A	7	8	2	5	6	7	1	6	2	0	0	9	1	7	2	9	5
Pongo	1	A	2	1	2	6	7	1	3	5	8	6	9	A	7	A	9	9
Hylobates	6	4	2	8	2	6	1	8	9	9	3	6	6	1	7	7	1	9
Colobus	1	3	6	8	3	5	7	8	9	9	9	6	2	5	7	7	1	1

	ZTIPa	ZTIPc	ZFN	ZFFPc	ZFFPd	AEFP	Fro	OcF	PEFPb	SOFi	PEFPa	MMAE	MaFPb	MaFPa	MaFPc	SMB	SMFP	PaF1
Gorilla	0	7	8	A	9	4	3	5	7	A	5	5	9	6	5	6	5	6
Pan	2	7	8	3	2	4	8	5	3	3	5	5	9	7	5	0	5	6
Homo	7	2	8	8	1	1	2	5	3	0	5	5	5	2	5	6	5	0
Pongo	7	7	2	3	9	3	2	5	0	3	5	5	5	1	5	6	5	6
Hylobates	7	0	2	3	4	9	8	5	7	7	A	5	1	7	5	6	5	6
Colobus	7	7	2	4	5	9	7	5	A	7	0	5	1	7	5	6	5	6

	PaF2	PaF3	CaCP1	CaCP2	IOFSZ	ZTFSZ	ZFFSZ	MaFSZ	SMFSZ	CaCSZ	JuFLg	HyCSZ	FOvSZ	GPFSZ	LPFSZ	MeFSZ	MbFSZ	ZMSmind
Gorilla	0	6	5	6	3	3	A	6	4	2	5	4	2	0	4	1	0	0
Pan	6	6	5	6	3	2	7	8	3	3	3	3	5	3	2	5	5	7
Homo	5	6	A	0	0	8	6	0	0	0	0	0	0	4	1	4	3	8
Pongo	5	6	2	6	7	8	0	2	5	6	7	6	4	4	8	1	3	3
Hylobates	6	1	0	6	7	8	2	5	9	8	7	8	A	8	8	8	9	4
Colobus	7	5	8	6	A	2	8	8	9	A	9	A	8	A	8	A	9	5

	ZMStvd	Go	FMaSZ	InCLg	MeFpos	InCpos	IOFpos	IJPE	HyC	ICC	CoC	CoCO	CPC	MgF	Fov	FOvP	MBC	JuB
Gorilla	0	0	3	4	8	5	0	2	9	6	4	5	2	2	1	6	5	6
Pan	5	5	5	6	6	8	2	5	5	4	2	5	3	6	3	1	5	2
Homo	4	A	0	7	A	A	6	1	0	0	0	0	8	1	2	9	5	5
Pongo	6	3	3	8	3	0	6	7	9	7	8	6	4	9	7	1	5	6
Hylobates	7	6	8	4	3	4	6	7	5	8	8	8	7	7	7	6	5	6
Colobus	6	3	A	0	0	3	A	8	2	5	8	6	6	5	A	7	5	5

	FMaS	FMaP2	FMaP1	InF	FSp	Fve	PSB	PAB	FSpP	Fla	RaC2	RaC1	GPFP	PCr	LPF	LPFP	MeF	MbFP
Gorilla	6	3	4	5	2	5	3	7	4	9	5	6	2	9	2	2	1	1
Pan	4	5	4	4	3	5	8	7	1	5	5	7	2	6	2	3	9	9
Homo	6	9	A	5	1	0	7	1	8	0	5	7	7	3	2	1	8	6
Pongo	8	0	4	5	6	5	9	7	1	2	5	4	2	3	9	8	2	1
Hylobates	2	6	4	6	9	9	3	7	8	9	5	6	9	0	6	8	7	9
Colobus	4	7	4	5	9	6	0	1	8	5	5	0	8	9	9	8	3	4

	SeC	MoF	RMF	RoC	MyB	CSF	PCF	IFF	MeFPos2	InC	PFn	SMFS	IOFS	CaCS	GPFS	MeFS	ZTFS	MaFS
Gorilla	3	0	5	6	1	5	6	6	2	6	7	7	5	4	5	3	6	6
Pan	3	4	5	6	7	9	6	0	7	1	7	2	1	4	6	0	7	6
Homo	3	6	5	2	1	5	A	7	8	3	7	4	5	A	6	7	5	2
Pongo	9	A	5	6	7	0	1	6	7	2	7	7	4	4	6	6	4	5
Hylobates	3	5	5	5	7	5	1	7	0	9	2	8	A	4	1	7	3	5
Colobus	9	5	5	5	7	6	6	4	6	9	0	2	5	4	6	7	5	6

	LPFS	MbFS	ZFFS	SGB
Gorilla	5	6	8	5
Pan	5	5	3	5
Homo	6	3	5	5
Pongo	5	5	8	5
Hylobates	4	6	3	5
Colobus	5	5	3	5

Analysis 1a.4b

	IOF	ZTF	ZFF	PEF	MaF	IOB	ION	ICIO	IOG	SLGB	SON	SOF	ZTFP	ZTFP	ZTFP	ZTFP2b	ZTFP2a	ZTIPb
Gorilla	1	1	0	1	1	0	1	1	1	1	1	0	1	1	1	1	1	1
Pan	1	1	1	1	1	1	1	0	1	1	1	0	1	1	1	1	1	1
Homo	1	1	1	1	1	0	1	1	1	1	1	1	0	1	0	1	0	1
Pongo	1	0	1	1	1	0	0	1	1	1	1	0	0	0	0	0	0	0
Hylobates	1	1	1	1	1	0	1	0	0	0	1	0	1	1	0	1	1	0
Colobus	1	1	1	1	1	0	0	0	0	0	1	0	1	1	0	1	1	1

	ZTIPa	ZTIPc	ZFN	ZFFPc	ZFFPd	AEFP	Fro	OcF	PEFPb	SOFi	PEFPa	MMAE	MaFPb	MaFPa	MaFPc	SMB	SMFP	PaF1
Gorilla	1	0	0	0	0	1	1	0	1	1	1	0	1	1	0	1	1	0
Pan	1	0	0	1	1	1	1	0	1	1	1	0	1	1	0	1	1	0
Homo	0	1	0	1	1	1	1	1	1	1	1	0	1	1	0	1	1	1
Pongo	0	0	1	1	0	1	1	0	1	1	1	0	1	1	0	1	1	0
Hylobates	0	1	1	1	1	1	1	1	1	1	0	0	1	1	0	1	1	0
Colobus	0	0	1	1	1	1	1	0	0	1	1	0	1	1	0	0	1	0

	PaF2	PaF3	CaCP1	CaCP2	IOFSZ	ZTFSZ	ZFFSZ	MaFSZ	SMFSZ	CaCSZ	JuFLg	HyCSZ	FOvSZ	GPFSZ	LPFSZ	MeFSZ	MbFSZ	ZMSmind
Gorilla	1	0	1	0	1	1	0	0	1	1	0	0	1	1	1	1	1	1
Pan	1	0	1	0	1	1	1	0	1	1	1	1	1	1	1	1	1	0
Homo	1	0	0	1	1	0	0	1	1	1	1	1	1	1	1	1	1	0
Pongo	1	0	1	0	0	0	1	1	1	0	0	0	1	1	0	1	1	1
Hylobates	1	1	1	0	0	1	1	1	0	0	0	0	0	0	0	0	0	1
Colobus	0	0	1	0	0	1	0	0	0	0	0	0	0	0	0	0	0	0

	ZMStvd	Go	FMaSZ	InCLg	MeFpos	InCpos	IOFpos	IJPE	HyC	ICC	CoC	CoCO	CPC	MgF	Fov	FOvP	MBC	JuB
Gorilla	1	1	1	1	0	0	1	1	1	1	1	1	1	1	1	1	1	0
Pan	0	0	1	0	1	0	1	1	1	1	1	1	1	1	1	1	0	1
Homo	0	0	1	0	0	0	0	1	1	1	1	1	0	1	1	0	1	1
Pongo	0	1	1	0	1	1	0	1	1	0	0	0	1	0	1	1	0	1
Hylobates	0	0	0	1	1	1	0	1	1	0	0	0	1	0	1	1	0	1
Colobus	0	1	0	1	1	1	0	1	1	1	0	0	0	1	0	0	0	1

	FMaS	FMaP2	FMaP1	InF	FSp	Fve	PSB	PAB	FSpP	Fla	RaC2	RaC1	GPFP	PCr	LPF	LPFP	MeF	MbFP
Gorilla	1	1	1	0	1	1	1	0	1	0	0	0	1	0	1	1	1	1
Pan	1	1	1	1	1	1	1	0	1	1	0	0	1	1	1	1	0	1
Homo	0	0	1	1	1	1	1	1	0	1	0	0	1	1	1	1	0	1
Pongo	0	1	1	0	1	1	1	0	1	1	0	1	1	1	1	1	1	1
Hylobates	1	1	1	0	0	0	1	0	0	0	0	0	1	1	1	1	1	1
Colobus	1	0	1	0	0	0	1	1	0	1	0	1	1	0	1	1	1	1

	SeC	MoF	RMF	RoC	MyB	CSF	PCF	IFF	MeFPos2	InC	PFn	SMFS	IOFS	CaCS	GPFS	MeFS	ZTFS	MaFS
Gorilla	1	1	0	0	1	1	1	0	1	1	0	1	1	1	0	1	1	0
Pan	1	1	0	0	0	1	1	1	1	1	0	1	1	1	0	1	1	0
Homo	1	1	0	1	1	1	1	0	1	1	0	1	1	0	0	0	1	1
Pongo	0	0	0	0	0	1	1	1	1	1	0	1	1	1	0	0	1	0
Hylobates	1	1	0	0	0	1	1	0	1	1	1	1	0	1	1	0	1	1
Colobus	0	1	0	0	0	1	1	1	1	0	1	1	1	1	0	0	1	0

	LPFS	MbFS	ZFFS	SGB
Gorilla	0	0	0	0
Pan	1	1	1	0
Homo	0	1	1	0
Pongo	1	0	0	1
Hylobates	1	0	1	0
Colobus	0	0	1	0

Analysis 1a.4c

	IOF	ZTF	ZFF	PEF	MaF	IOB	ION	ICIO	IOG	SLGB	SON	SOF	ZTFP	ZTFP	ZTFP	ZTFP2b	ZTFP2a	ZTIPb
Gorilla	4	5	1	2	2	1	4	4	5	6	4	4	6	2	6	6	3	4
Pan	2	4	5	4	1	6	5	1	6	4	3	3	5	3	5	4	4	5
Homo	1	2	2	5	3	4	3	6	3	5	6	6	2	5	1	5	1	3
Pongo	5	1	5	6	6	1	1	5	4	3	2	1	1	1	1	1	2	1
Hylobates	3	3	4	1	4	5	6	1	2	2	5	5	3	6	4	3	5	2
Colobus	6	5	3	3	5	1	2	1	1	1	1	1	4	4	1	2	6	6

	ZTIPa	ZTIPc	ZFN	ZFFPc	ZFFPd	AEFP	Fro	OcF	PEFPb	SOFi	PEFPa	MMAE	MaFPb	MaFPa	MaFPc	SMB	SMFP	PaF1
Gorilla	6	1	1	1	2	3	4	1	2	1	3	1	1	4	1	5	1	3
Pan	5	4	1	5	5	4	2	4	4	5	4	4	2	3	4	6	1	2
Homo	1	5	1	2	6	6	4	5	5	6	5	5	3	5	6	3	1	6
Pongo	1	1	4	6	1	5	4	1	6	4	2	6	4	6	1	4	1	1
Hylobates	1	6	6	4	4	1	1	6	3	3	1	1	5	2	5	2	1	5
Colobus	4	1	5	3	3	2	3	1	1	2	6	1	6	1	1	1	1	4

	PaF2	PaF3	CaCP1	CaCP2	IOFSZ	ZTFSZ	ZFFSZ	MaFSZ	SMFSZ	CaCSZ	JuFLg	HyCSZ	FOvSZ	GPFSZ	LPFSZ	MeFSZ	MbFSZ	ZMSmind
Gorilla	6	1	3	1	5	4	1	3	4	5	4	4	5	6	4	6	6	6
Pan	4	1	4	1	4	6	4	1	5	4	5	5	3	4	5	3	3	1
Homo	2	1	1	6	6	2	3	6	6	6	6	6	6	3	6	4	5	2
Pongo	5	1	5	1	3	1	6	5	3	3	2	3	4	5	1	5	4	4
Hylobates	3	6	6	1	2	3	5	4	2	2	3	2	1	2	2	2	1	5
Colobus	1	1	2	1	1	5	2	2	1	1	1	1	2	1	3	1	2	3

	ZMStvd	Go	FMaSZ	InCLg	MeFpos	InCpos	IOFpos	IJPE	HyC	ICC	CoC	CoCO	CPC	MgF	Fov	FOvP	MBC	JuB
Gorilla	6	6	5	4	2	3	6	5	1	3	4	4	6	5	6	4	6	1
Pan	2	2	3	3	3	2	5	4	4	5	5	5	5	3	4	5	1	6
Homo	5	1	6	2	1	1	4	6	6	6	6	6	1	6	5	1	5	5
Pongo	4	4	4	1	5	6	2	2	2	2	1	3	4	1	2	6	1	2
Hylobates	1	3	2	5	4	4	3	3	3	1	2	1	3	2	3	3	1	3
Colobus	3	5	1	6	6	5	1	1	5	4	3	1	1	4	1	2	1	4

	FMaS	FMaP2	FMaP1	InF	FSp	Fve	PSB	PAB	FSpP	Fla	RaC2	RaC1	GPFP	PCr	LPF	LPFP	MeF	MbFP
Gorilla	3	5	2	4	5	5	5	1	4	2	1	3	4	1	6	5	6	5
Pan	4	4	3	6	4	4	2	4	6	4	1	1	4	3	4	4	1	1
Homo	2	1	1	5	6	6	3	5	1	6	1	1	3	5	5	6	2	3
Pongo	1	6	3	2	3	3	1	3	5	5	6	5	4	4	1	2	5	6
Hylobates	6	3	3	3	2	1	4	2	3	1	1	4	1	6	3	3	3	2
Colobus	5	2	3	1	1	2	6	6	1	3	1	6	2	1	2	1	4	4

	SeC	MoF	RMF	RoC	MyB	CSF	PCF	IFF	MeFPos2	InC	PFn	SMFS	IOFS	CaCS	GPFS	MeFS	ZTFS	MaFS
Gorilla	4	6	4	1	6	4	2	1	5	3	1	1	4	5	5	5	2	2
Pan	5	5	1	1	1	1	4	6	3	6	1	5	6	2	1	6	1	2
Homo	6	2	5	6	5	5	1	3	1	4	1	4	2	1	4	2	3	6
Pongo	2	1	1	1	1	6	6	4	2	5	1	3	5	6	1	3	5	4
Hylobates	3	3	1	5	1	3	5	2	6	2	5	2	1	3	6	4	4	5
Colobus	1	4	6	1	1	2	3	5	4	1	6	6	3	4	1	1	5	1

	LPFS	MbFS	ZFFS	SGB
Gorilla	3	1	1	1
Pan	4	5	4	1
Homo	1	6	3	1
Pongo	5	4	1	6
Hylobates	6	2	5	4
Colobus	2	3	6	5

Analysis 1a.4d

	IOF	ZTF	ZFF	PEF	MaF	IOB	ION	ICIO	IOG	SLGB	SON	SOF	ZTFP	ZTFP	ZTFP	ZTFP2b	ZTFP2a	ZTIPb
Gorilla	H	Q	0	B	8	0	2	8	Q	A	A	0	B	6	F	N	6	4
Pan	E	Q	Q	N	8	2	6	0	Q	6	5	0	A	G	3	M	8	L
Homo	2	M	H	Q	G	0	1	P	H	9	L	5	0	M	0	M	0	3
Pongo	P	0	Q	Q	N	0	0	L	P	3	2	0	0	0	0	0	0	0
Hylobates	E	P	Q	9	L	0	7	0	0	0	A	0	3	M	0	C	E	0
Colobus	Q	Q	N	D	L	0	0	0	0	0	1	0	9	G	0	9	G	P

	ZTIPa	ZTIPc	ZFN	ZFFPc	ZFFPd	AEFP	Fro	OcF	PEFPb	SOFi	PEFPa	MMAE	MaFPb	MaFPa	MaFPc	SMB	SMFP	PaF1
Gorilla	N	0	0	0	0	B	Q	0	7	3	4	0	2	6	0	3	Q	0
Pan	6	0	0	P	C	B	M	0	J	P	4	0	2	6	0	B	Q	0
Homo	0	J	0	9	D	G	Q	1	K	Q	7	0	7	A	0	3	Q	C
Pongo	0	0	3	Q	0	F	Q	0	N	M	3	0	7	E	0	3	Q	0
Hylobates	0	N	7	P	9	5	L	1	8	G	0	0	E	5	0	1	Q	0
Colobus	1	0	4	L	6	5	N	0	0	E	D	0	J	2	0	1	Q	0

	PaF2	PaF3	CaCP1	CaCP2	IOFSZ	ZTFSZ	ZFFSZ	MaFSZ	SMFSZ	CaCSZ	JuFLg	HyCSZ	FOvSZ	GPFSZ	LPFSZ	MeFSZ	MbFSZ	ZMSmind
Gorilla	E	0	C	0	K	M	0	3	K	F	A	A	M	Q	F	Q	Q	Q
Pan	3	0	F	0	K	Q	H	0	K	D	C	E	E	H	P	H	H	0
Homo	2	0	0	5	Q	B	B	Q	Q	Q	Q	Q	Q	H	Q	J	N	4
Pongo	6	0	L	0	A	0	Q	P	G	A	1	7	K	J	0	P	N	E
Hylobates	3	4	Q	0	7	D	K	D	0	5	9	5	0	9	1	3	0	K
Colobus	0	0	4	0	0	L	8	7	0	0	0	0	4	0	2	0	5	B

	ZMStvd	Go	FMaSZ	InCLg	MeFpos	InCpos	IOFpos	IJPE	HyC	ICC	CoC	CoCO	CPC	MgF	Fov	FOvP	MBC	JuB
Gorilla	Q	Q	G	F	D	G	B	Q	5	1	5	2	8	6	Q	4	1	0
Pan	3	3	E	9	E	F	A	P	C	3	A	2	5	2	N	A	0	4
Homo	6	0	Q	9	C	F	6	Q	P	C	F	E	0	8	Q	0	1	3
Pongo	4	J	G	0	F	K	6	M	7	0	0	0	4	0	G	D	0	1
Hylobates	0	7	5	J	F	H	6	M	C	0	0	0	1	0	K	2	0	1
Colobus	1	J	0	Q	H	H	4	L	J	1	1	0	0	2	0	1	0	1

	FMaS	FMaP2	FMaP1	InF	FSp	Fve	PSB	PAB	FSpP	Fla	RaC2	RaC1	GPFP	PCr	LPF	LPFP	MeF	MbFP
Gorilla	0	B	Q	1	G	3	G	0	5	0	0	0	Q	0	Q	C	9	Q
Pan	4	5	Q	2	E	3	5	0	F	4	0	0	Q	7	Q	A	0	3
Homo	1	0	4	1	J	C	6	A	0	Q	0	0	M	F	Q	E	1	9
Pongo	0	J	Q	0	6	2	2	0	B	P	0	2	Q	E	8	4	7	Q
Hylobates	8	3	Q	0	1	0	E	0	0	0	0	0	F	P	F	5	1	4
Colobus	4	1	Q	0	0	0	Q	C	0	4	0	7	K	0	A	2	4	L

	SeC	MoF	RMF	RoC	MyB	CSF	PCF	IFF	MeFPos2	InC	PFn	SMFS	IOFS	CaCS	GPFS	MeFS	ZTFS	MaFS
Gorilla	3	E	0	0	8	7	A	0	E	A	0	2	3	8	1	3	P	0
Pan	4	8	0	0	0	2	C	F	1	Q	0	7	A	7	0	7	N	0
Homo	5	5	1	2	4	7	3	0	1	N	0	5	3	0	0	0	P	3
Pongo	0	1	0	0	0	J	L	2	1	P	0	2	6	9	0	0	Q	1
Hylobates	3	6	0	1	0	6	J	0	2	3	E	2	0	7	3	0	Q	2
Colobus	0	7	1	0	0	3	C	3	4	0	Q	9	3	7	0	0	Q	0

	LPFS	MbFS	ZFFS	SGB
Gorilla	0	0	0	0
Pan	2	1	2	0
Homo	0	3	1	0
Pongo	2	1	0	1
Hylobates	2	0	3	0
Colobus	0	1	4	1